Integral Sliding Mode Fault Tolerant Control Schemes with Control Allocation

Thesis submitted for the degree of

Doctor of Philosophy

at the University of Leicester

by

Mirza Tariq Hamayun

B.Sc, M.Sc Electrical and Electronic Engineering

Department of Engineering

Control and Instrumentation Research Group

University of Leicester

June 21, 2013

Abstract

Integral Sliding Mode Fault Tolerant Control Schemes with Control Allocation

Mirza Tariq Hamayun

The key attribute of a Fault Tolerant Control (FTC) system is to maintain overall system stability and acceptable performance in the face of faults and failures within the system. In this thesis new integral sliding mode (ISM) control allocation schemes for FTC are proposed, which have the potential to maintain the nominal fault free performance for the entire system response, in the face of actuator faults and even complete failures of certain actuators. The incorporation of ISM within a control allocation framework uses the measured or estimated values of the actuator effectiveness levels to redistribute the control effort among the healthy actuators to maintain closed-loop stability. This combination allows one controller to be used in both fault free as well as in fault or failure situations. A fault tolerant control allocation scheme which relies on an *a posteri* approach, building on an existing state feedback controller designed using only the primary actuators, is also proposed. Retro-fitting of an ISM scheme to an existing feedback controller is advantageous from an industrial perspective, because fault tolerance can be introduced without changing the existing control loops. To deal with a wider range of operating conditions, the fault tolerant features of ISM are also extended to linear parameter varying systems. A FTC scheme considering only the availability of measured system outputs is also proposed, where now the feedback controller design is based on the estimated states. In each of the ISM fault tolerant schemes proposed, a rigorous closed-loop analysis is carried out to ensure the stability of the sliding motion in the face of faults or failures.. A high fidelity benchmark model of a large transport aircraft is used to demonstrate the efficacy of the new FTC schemes.

Acknowledgments

First of all I want to thank to almighty ALLAH, who is the most merciful, the compassionate, who gave me ability and strength for the accomplishment of this research work;

special thanks to my respected supervisor, Professor Christopher Edwards who always helped me in all the phases of my learning and research;

special gratitude to my respected parents for their support and love ;

thanks to COMSATS Institute of information Technology Pakistan for awarding me scholarship for my PhD study;

thanks to Dr Halim Alwi for helping me in some research issues;

special thanks to my loving wife Attiya Tariq and my kids Mehreen Tariq and Abdur Rafe, who always push me up morally;

Mirza Tariq Hamayun

June 21, 2013

Nomenclature and Abbreviations

Nomenclature

α, β, γ	angle of attack, sideslip and flight path angle (rad)
$B^{\dagger,W}$	weighted right pseudo inverse of B
$B^{\ddagger}$	left pseudo inverse of B
$\mathbb{C}$	field of complex numbers
$\mathbb{R}$	field of real numbers
$\mathscr{R}(B)$	range space of input matrix B
$\subset$	subset
G	Sliding mode matrix
σ	linear switching function
$\mathscr{S}$	sliding surface
$\|.\|$	Euclidean norm for vectors or induced spectral norm for matrices
ρ	nonlinear modulation gain
ν	virtual control input
p, q, r	roll rate, pitch rate and yaw rate (deg/sec)
s	Laplace variable
V_{tas}	true airspeed (m/sec)
$\mathscr{W}$	allowable set of fault or failure
W	actuator effectiveness matrix
ϕ, θ, ψ	roll angle, pitch angle and yaw angle (rad)
h_e, x_e, y_e	geometric earth position with respect to the z (altitude), x and y axis (m)
$\lambda_{min(.)}, \lambda_{max}(.)$	minimum and maximum eigenvalues

Abbreviations

AFTC	Active Fault Tolerant Control
air, aor, ail, aol	aileron inner, outer right and aileron inner, outer left
BRL	Bounded Real Lemma
CA	Control Allocation
CG	Centre of gravity
DI	Dynamic Inversion
DOF	Degree of Freedom
EPR	Engine Pressure Ratio
FDI	Fault Detection and Isolation
FPA	Flight Path Angle
FTC	Fault Tolerant Control
FTLAB	Flight Lab
GARTEUR	Group for Aeronautical Research and Technology in Europe
GS	Gain Scheduling
G(s)	Transfer function
ISM	Integral Sliding Modes
ISMC	Integral Sliding Mode Control
IMM	Interacting Multiple Model
LMI	Linear Matrix Inequallity
LPV	Linear Parameter Varying
LQR	Linear Quadratic Regulator
LTI	Linear Time Invariant
MMST	Multiple Model Switching and Tuning
MPC	Model Predictive Control
MRAC	Model Reference Adaptive Control
PFTC	Passive Fault Tolerant Control
PIM	Pseudo Inverse Method
SMC	Sliding Mode Contol
s.p.d	Symmetric Positive Definite
sp	spoiler
STC	Self Tuning Control
UIO	Unknown Input Observer
VSC	Variable Structure Control
VSCS	Variable Structure Control Systems

Contents

List of Figures

List of Tables

Chapter 1

Introduction

Control is an active research field, and there is always a steady influx of new ideas, concepts and techniques. Control is an essential part of each new technology development, from cell phones to jumbo jets and from washing machines to oil refineries. The objective of some control applications is to hold steady the output (of the process) in the face of unknown disturbances, whilst in others it is tracking a reference signal whilst minimizing the tracking error. To ensure the closed-loop stability of the overall system in the presence of unknown disturbances and in the face of uncertainties which arise as a result of creating an approximate mathematical model for the controller design, is an important part of the control design process. The first systematic study of the stability of systems was given by J.C. Maxwell [48] in 1868, where he stated that *"the stability depends on the roots of a certain characteristic equation having negative real parts"*. Shortly after, A.M. Lyapunov [48] in (1892) started thinking, about, how to prove the stability of motion? This work became the fundamental part of the so-called state variable approach to control theory. Along with stability, issues of operating safety, reliability, performance, cost efficiency and availability of the systems, especially in safety critical plants like aircraft [22], [46] and nuclear reactors, are of great importance [66]. Safety critical systems like aircraft became the basis for the initial research in the field of fault tolerant control systems [136]. Faults or failures in these safety critical systems cannot be totally avoided, however their effects (in terms of human mortality and economic loss) can be mitigated using fault tolerant control schemes.

Fault tolerant control (FTC) systems are an important aspect in safety critical systems and can maintain overall system stability and acceptable performance in the face of faults and failures within the system. One way to achieve a high level of availability, is to ensure a suitable level of redundancy in terms of the key actuators and sensors within the system. In emergency situations this redundancy can be manipulated in a way to achieve fault tolerance. Therefore, as argued in [136], increasing demands for safety, reliability and high system performance, motivated the need for fault tolerant control and has stimulated research in this area. To design fault tolerant controllers many different design paradigms have been proposed in the literature. In the survey paper for example [100], the scattered areas of fault tolerant control research like fault detection and isolation (FDI), robust control, reconfigurable control and fault tolerant control methods are discussed. More recently in [136] the authors have focused on a bibliographical review of existing fault tolerant control and fault detection and isolation techniques.

Design approaches	***References***
Adaptive control	[10, 37, 67, 73]
Control Allocation	[6, 19, 23, 24, 32, 35, 44, 60, 62, 76, 98, 137]
Sliding Mode Control	[6, 30, 41, 62, 105, 106, 118]
Dynamic Inversion	[31, 71]
Multiple Model	[9, 17, 18, 74, 94, 132]
Gain Scheduling	[79]
Linear Parameter Varying	[84, 88, 92, 101, 115],
Model Predictive Control	[72, 82, 89, 91, 112, 130]
H_∞ *robust control*	[67, 87, 124, 129]

Table 1.1: An example of existing control design methodologies in FTC

1.1 Motivation and Challenges

Fault tolerant control systems are designed to maintain the closed-loop performance near to the desired one in the presence of faults or failures. In safety critical systems, redundancy is the key component of FTC design, and can be used in emergency situations to have a safe landing. Nevertheless, when faults have occurred, in some instances the pilots have still managed to land safely: for example on 9 October 2002, the Boeing 747–400 Airline Flight 85 suffered a

lower rudder hardover failure at an altitude of $35,000$ ft (404 people on board including 4 crew members and 14 flight attendants). Due to this failure the rudder deflected left to the maximum position limit causing excessive roll. The crew members managed to land the aircraft safely in Anchorage, Alaska by manipulating the upper rudder and the ailerons together with differential engine thrust [25]. The Kalitta Air Cargo Boeing 747 (5 crew members on board) landed safely in Detroit Metropolitan Airport after losing engine 1 on 20 October 2004. From these incidents it can be inferred that during faults or failures, if some level of redundancy is available, with pilot skill, the faulty or damaged aircraft is still able to fly well enough to ensure a safe landing. One motivation to do research in the area of fault tolerant control (FTC) is its ability to increase the survivability and safety of the safety critical systems.

One of the major hurdles in accepting new ideas in industry, is the requirement to change the whole physical setup. Increasing safety and survivability while maintaining good performance without changing significantly the existing setup can be much more easily accepted. Therefore it is worth exploring techniques which can be retrofitted to an existing design, without altering or removing the existing control loops for fault tolerant control.

In safety critical systems, since the plant operating conditions frequently change and therefore demand methods from the fault tolerant control viewpoint are those which can ensure closed-loop stability over the entire operating regime. Seeking a single control law, which is automatically scheduled as the plant operating conditions change, and maintains closed-loop stability in the entire operating envelope, working in both nominal as well as in fault or failure situations, is challenging.

The objective of this research is to show how the robustness properties of sliding mode control [118], [41]-especially integral sliding modes- can be used in the framework of FTC to provide a suitable solution to the above points to increase the survivability, reliability and stability of safety critical systems. The advantage of using sliding mode based schemes is that actuator faults can be directly handled. However, considering the effects of actuator faults or failures on the closed-loop stability analysis is important and challenging.

The following section explains how the thesis is organized.

1.2 Organization and Contribution of the thesis

The thesis is organized as follows:

In Chapter 2, the definitions and basic terminologies of FTC and some typical types of faults at the sensor, actuator and component level are defined. In addition the difference between a fault and failure is clearly explained. Different types of fault/failure models used in the literature to design fault tolerant schemes against the actuator faults/failures and component faults are discussed. An introduction to FTC is given along with an introduction to different fault tolerant control methods used in the literature based on passive and active approaches. The terminologies used in the fault detection and isolation framework are defined and some of the techniques which can be used for the FDI are also documented.

In Chapter 3, the concept, properties and design principles of sliding mode control are explained. A simple example of a spring-mass-damper system is used to provide insight into the design procedure. Different methods which can be used to implement the sliding mode controller in real practical applications are also given. The concept of integral sliding modes is defined next, with an explanation how it differs from the classical sliding mode control approach explained earlier in the chapter. A detailed procedure for the design of integral sliding mode control laws together with a special choice of sliding surface which helps to mitigate the effects of unmatched uncertainty is explained. The properties of Integral sliding mode control and a simulation example which validates the design is also given. Finally some motivation for the use of integral sliding modes as a candidate for FTC is discussed.

In Chapter 4, a new integral sliding mode FTC scheme is presented, which considers the novel combination of integral sliding modes and a Control Allocation scheme. The design procedure for the integral sliding mode controller is transparent. The concept of a virtual control is also explained, which is then used by the Control Allocation scheme to achieve the demanded actuator position. The proposed FTC scheme uses the estimated actuator effectiveness level

to distribute the control effort among the actuators without reconfiguring the underlying ISM controller. A rigorous closed-loop stability analysis is carried out and it is proved that the proposed scheme can handle some level of error in estimating the actuator effectiveness by the FDI scheme. Furthermore in order to compute the controller parameters such that the closed-loop stability condition (given in the chapter) is satisfied, an LMI synthesis procedure is proposed. The fault tolerant Control Allocation scheme can cope with actuator faults and certain total actuators failure without degrading the desired performance. A benchmark model of a large civil aircraft is used to validate the feasibility of the proposed scheme. The theoretical contribution of this chapter is to consider the novel combination of integral sliding modes with Control Allocation in the framework of FTC, and employing an effective synthesis procedure using LMI optimization, to compute the parameters involved in the control law. The initial results of this chapter were published in [53] and an extended version in the *IEEE Transactions on Automatic Control* [54]. The application of an integral sliding mode FTC scheme on the full nonlinear benchmark model of the large civil aircraft using FTLAB747 is considered in Chapter 5 and was published in [55].

In Chapter 6 an integral sliding mode augmentation scheme is considered in order to introduce fault tolerance at an actuator level. The scheme is based on an *a posteri* approach, building on an existing state feedback controller designed using only the primary actuators. The control allocation scheme is developed based on the idea that if the primary actuators are healthy, the secondary actuator should not be activated, and the secondary actuators should only be activated for fault tolerant purpose if the primary actuators are faulty. The considered FTC approach depends on information about the actuator effectiveness levels to distribute the control signals among the available actuators in the set. The theoretical contribution of this chapter is to consider retrofitting the ideas of integral sliding mode control to an existing control scheme designed using only the primary actuators to induce fault tolerance without the need to remove or alter existing control loops. Possible errors in estimating the actuator effectiveness by the FDI scheme are taken into consideration while a closed-loop stability condition is proposed which must be

satisfied to ensure stability in the case of faults or failures. The efficacy of the proposed scheme is tested by applying it to a nonlinear benchmark model of a large civil aircraft. The results in this chapter were published in [56].

In Chapter 7, the ideas of integral sliding mode control allocation discussed in Chapter 4 are extended for linear parameter varying plants. For the design of the virtual control law, the parameter varying input distribution matrix is factorized into fixed and a matrix with varying components. In this chapter the proposed scheme seeks a single control law which automatically schedules with respect to the varying plant operating conditions, to ensure the closed-loop stability for a wider range of operating conditions. The proposed scheme also depends on information about actuators effectiveness levels for control signal distribution. An effective LMI synthesis procedure is proposed to compute the parameters of the controller, and a rigorous closed-loop stability analysis is undertaken which ensures certain classes of faults or failures can be dealt with in the entire operating envelope (with the assumption that the redundancy is available in the system). A benchmark LPV model of the large civil aircraft is used to demonstrate the efficacy of the FTC scheme. This chapter has been accepted for publication in [58].

Chapter 8 focuses on an output feedback integral sliding mode control allocation scheme in the framework of FTC. This chapter relaxes the assumption made in the early chapters that the full state information is available for the controller design. The chapter also builds on the idea that information about actuators faults/failures is not available to the controller. A direct control allocation scheme is employed in this case to distribute the control signal among the actuators. In order to estimate the plant states an unknown input observer (UIO) is employed and the necessary conditions for the existence of the UIO are included. A rigorous closed-loop stability analysis is carried out and a stability condition is posed in an LMI framework. The controller and the observer gains are computed via LMIs. A benchmark model of a large civil aircraft is used to demonstrate the efficacy of the proposed FTC scheme by considering component faults, together with faults or failures in the actuators channels. The theoretical contribution of this chapter is to consider the output feedback integral sliding modes control allocation in an FTC

framework and proposing an LMI synthesis procedure in order to synthesize the observer gains and the controller parameters which satisfy the closed-loop stability condition. The results of this chapter have been published in [57].

Finally Chapter 9 makes concluding remarks and gives an overview of the research work presented in this thesis. Some ideas through which the current research work can be extended are also given.

Chapter 2

Fault Tolerant Control

Everywhere in our daily life we enjoy the benefits of control–ranging from simple to highly complex applications. Control is used extensively in industry and plays an important role in increasing productivity. It is required to operate safely the systems, where interaction with humans takes place. Particularly in safety critical systems like chemical plants, nuclear reactors, aircraft etc, the reliability and safety of the system is very important. Broadly speaking, control systems which have such capabilities, are termed as Fault Tolerant Control (FTC) systems [100]. In this chapter, different terminologies used in the FTC literature are defined, the notion of faults and failures are distinguished and their classification is explained. The chapter also describes the state of the art in FTC.

2.1 Fault and Failure and their Classification

The term *fault* will first be defined to avoid any confusion. The definition of a *fault* given in this section is in compliance with the definition given in [65].

Fault: "An unexpected change in a system parameter from the acceptable/normal condition, which can degrade system performance." It is a fact that a fault can disturb the normal operation of a system from the desired one, but may be tolerable.

Faults are usually considered to occur very rarely in the system but cannot be totally pre-

vented. However their consequences can sometimes be mitigated by taking appropriate actions. A FTC system, as the name implies, has the potential to tolerate faults in order to maintain the closed-loop performance of the system.

A fault is a sudden event, and can occur in any part of the system. Depending upon the location of occurrence, it can be classified as an actuator fault, a sensor fault and a component fault as can be seen in Figure 2.1.

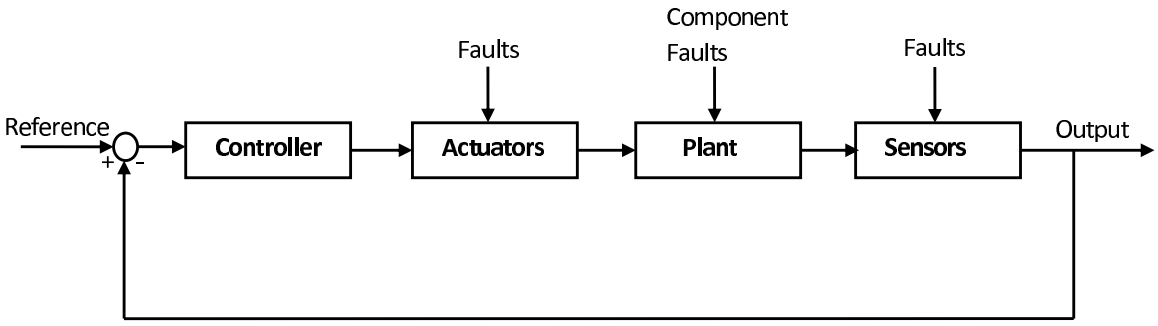

Figure 2.1: Classification of faults (adopted from [121])

Actuator faults: Actuators are the work horses in a control system [138], and represent a linkage/interface between the controller commands and the plant. In Figure 2.3(d), an actuator fault is shown which is termed as a loss in effectiveness, during which time the actuator works with reduced capability as compared to its normal operating condition (when it is fault free) [121]. This means in a post fault condition, the actuator will only be partially effective in achieving the required controller demand, which may affect the overall performance of the system. Actuator faults may occur due to, for instance, a drop in voltage supply, increased resistance, hydraulics leakage etc [121].

Sensor faults: Sensors are used in the control system to measure and convert the physical quantities of interest into an instrument readable form signal (e.g a tachometer measures the speed of a rotating motor shaft and converts it into voltage). A fault in the sensor means an incorrect measurement from the sensor, which in turn can result in a continuous constant offset as compared to the true value [121]. Sensor faults can degrade the feedback system performance even in the presence of a well designed controller. Therefore it is important to detect and isolate sensor faults at an early stage.

Component faults: All faults which do not belong in the category of actuator or sensor faults, can be considered as component faults. A component fault is a very severe type of fault which can occur in the plant components. As a result the input/output dynamical behaviour/properties of the controlled system will be disturbed [16]. Component faults can in turn result in a change in the physical parameters of the system [121], and can reduce the overall performance of the system.

Furthermore, it is important to note that faults can also be classified with respect to their time characteristics i.e. how the fault characteristics change with respect to time. According to [64], [121], the characteristics of faults can change abruptly, incipiently or intermittently with respect to time as can be seen in Figure 2.2. If a fault characteristic changes *abruptly*, it can be

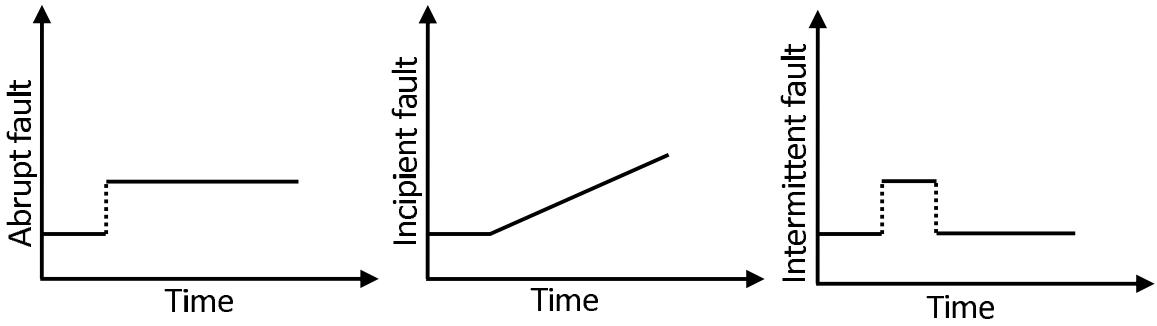

Figure 2.2: Classification of faults with respect to time (adopted from [121])

a very severe situation, as the system stability may also be affected. These types of faults often occur due to hardware damage. On the other hand *incipient faults* represent a scenario whereby the fault characteristics change very slowly, due to slow variations of parameters for instance, and are not severe in nature [121]. However if incipient faults are not attended to for a long time, it can result in a severe situation. *Intermittent faults* occur intermittently with respect to time, and can be due to intermittent contact or damaged wiring in some part of the circuitry.

In the FTC literature, and throughout this thesis, the notion of faults or failures is frequently used and may cause confusion, therefore the difference between them is clearly defined in this chapter in order to avoid any ambiguity.

Difference between fault and failure: Now to distinguish between fault and failure, the term failure is defined in the literature [65], as"A permanent interruption or a complete breakdown of

a component or system to perform a specific function." So a failure is a more serious situation, because the same component or system can not be used any more to perform a task. This means if a failure occurs in a sensor or in an actuator, a different sensor or actuator is required for the continuation of the process. In other words some sort of reconfiguration mechanism is required in the control system to deal with such a situation. For example, in an aircraft, some very severe types of actuator failure, if not promptly detected, can degrade or even destabilize the overall system. Examples are a jam or lock in place failure, a float failure and a runaway/hardover fail-

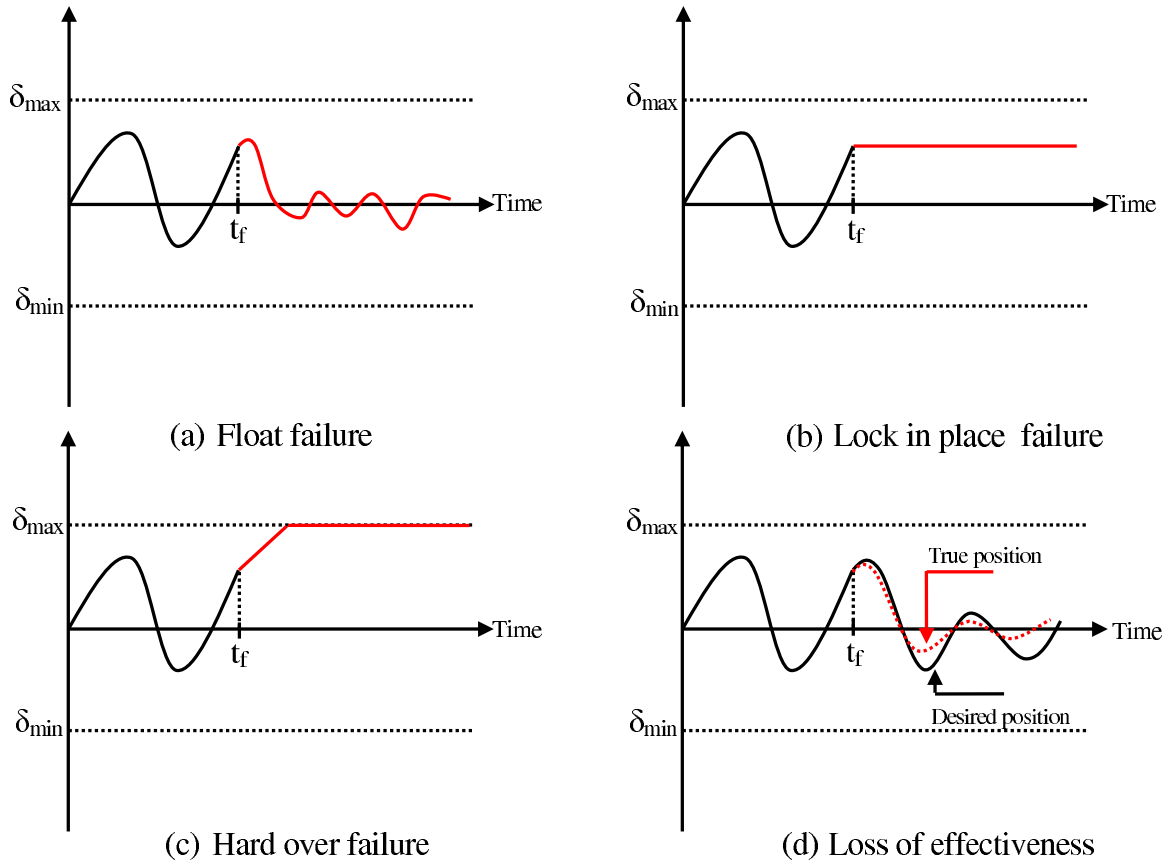

Figure 2.3: Types of actuator failure ((a),(b),(c)) and actuator fault (d)(adopted from [34])

ure as shown in Figure 2.3. In a jam failure, the actuator becomes stuck or jams at some (offset) position due to a lack of lubrication for instance, and does not respond even if a control signal is applied to it. In a float failure, the actuator freely moves and does not provide any desired moment. The runaway/hardover failure is a very destructive type of failure and it causes the actuator to move at its maximum rate limit until a saturation limit is reached. This can be due to a 'wrong

signal' being applied to the actuator. In Figure 2.4, some common types of sensor faults/failures are shown, where the sensor while in the freezing (failure) situation, provides a constant value instead of actual value of the physical state. During the loss of accuracy fault, the sensor does not reflect the actual value of the physical state throughout, whereas a bias fault indicates a constant offset in the measurement. Finally in the drift fault, the offset in the measurement of actual physical state increases with the time. Some common types of faults/failures associated with the actuators and sensors are considered for example in [140], [70], [138], [50], [20], [7].

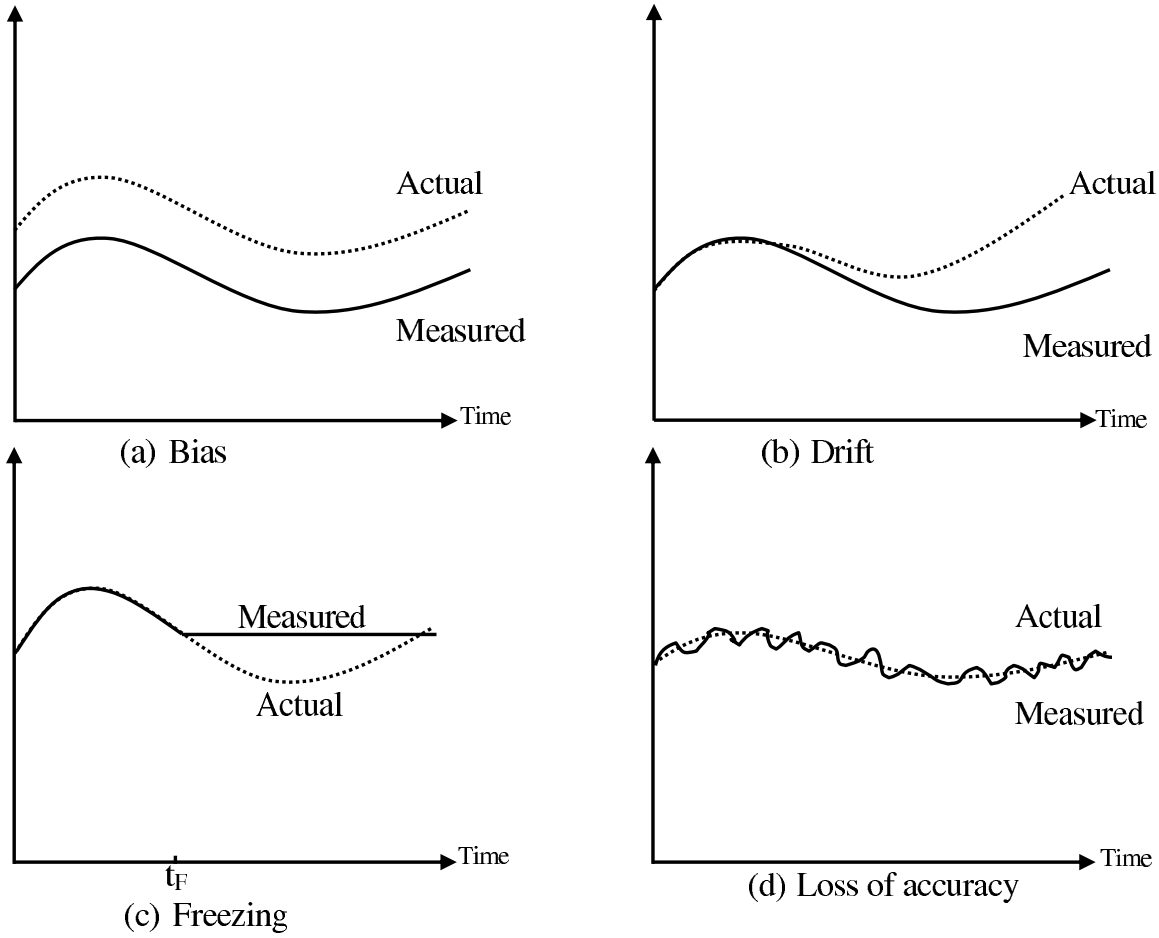

Figure 2.4: Types of sensor failure (a) and sensor faults ((b),(c),(d)) (adopted from [34])

In this thesis, different FTC schemes are proposed which have the potential to deal with faults and failures associated with the actuators, provided that redundant actuators are available. Faults at the component level are also considered, but the sensor faults and failures are not within the scope of this thesis.

2.1.1 Modeling faults and failures

Throughout this thesis, a state space representation of the plant is considered in order to synthesize the fault tolerant controllers. Mathematically a linear time invariant (LTI) uncertain system, subject to actuator faults or failures can be expressed as

$$\dot{x}(t) = Ax(t) + BWu(t) \tag{2.1}$$

where $A \in \mathbb{R}^{n\times n}$, $B \in \mathbb{R}^{n\times m}$ and $W = diag(w_i, \ldots w_m)$ is a diagonal weighting matrix. The scalars $w_i, \ldots w_m$ model the effectiveness level of the actuators. As in [6], if $w_i = 1$, it means that the corresponding i_{th} actuator has no fault and is working perfectly, where as if $1 > w_i > 0$ an actuator fault is present. The situation in which $w_i = 0$, represents a complete loss of effectiveness or failure or a complete breakdown of a particular actuator. Some common types of actuator fault/failure are shown in Figure 2.3. The actuator's fault and failure representation in (2.1), has become the building block for many of the FTC schemes in this thesis because this representation makes the closed-loop stability analysis simple as will be demonstrated in the next chapters. This representation of actuator faults and failures has been used by many other FTC researchers: see for example [96], [114], [134], [69] and [6]. Other fault models used in the literature can be found more recently in [121]. To model the actuator fault/failure, the state space model can be written as [121],

$$\dot{x}(t) = Ax(t) + B\Sigma u(t) + B(I - \Sigma)\bar{u}(t) \tag{2.2}$$

where $\Sigma = \text{diag}[\theta_1, \theta_2, \ldots, \theta_m]$, $\theta_i \in [0 \quad 1]$ and $\bar{u}$ is an uncontrollable offset vector. If $\theta_i = 1$, then the i_{th} actuator is functioning normally, where as if $\theta_i = 0$ then the i_{th} actuator has a failure, i.e the control action from the failed actuator is equal to $\bar{u}(t)$. As a comparison, in model (2.1) the control action from the failed actuator is zero. The values of the diagonal entries θ_i can also take the values between 0 and 1 in order to model a loss in effectiveness actuator fault. It was reported in [121] that the *multiplicative* fault model is a natural way to represent actuator or sensor faults, but general component faults cannot be modeled using a multiplicative fault

model. Equations (2.1)–(2.2) are the examples of multiplicative fault models, where a change in the diagonal entry of W and Σ matrices reflect the effectiveness of a particular column of the B matrix. From equations (2.1)–(2.2), it is clear that faults or failures associated with the actuators, only affect the input distribution matrix B, where as a component fault may introduce changes in the system matrix and can be represented in the following form

$$\dot{x}(t) = (A + \triangle A)x(t) + Bu(t) \tag{2.3}$$

where $\triangle A$ represent change in the system matrix A. Faults and failures of any type are unwanted or undesired events but can not be avoided, however there effects can be mitigated.

2.2 Introduction to Fault Tolerant Control Systems

The need for FTC is increasing rapidly, due to increasing demands for safety, reliability and high system performance in wider engineering applications [136]. FTC systems have the capability to improve the worst case performance and also guarantee an acceptable level of performance of a system even in the presence of faults and failures. The motivation for the early research in the field of fault tolerant control was in the area of flight control systems to improve the reliability and safety of the aircraft [100], [136]. A fault tolerant control system has the capability to maintain some level of acceptable performance or degrade gracefully subsequent to a fault or more specifically *"is a strategy for reliable and highly efficient control law design* [100].

In [136], a FTC system is defined as *"control systems which possess the ability to accommodate component failures automatically. They are capable of maintaining overall system stability and acceptable performance in the event of such failures"*.

From the definitions, it is clear that the main task in achieving fault tolerance is to design a suitable controller which has the ability to maintain overall system stability in fault free as well as in situations when a system becomes faulty. To design such a controller, the system should have redundant control effectors, which can be efficiently used and exploited to achieve

fault tolerance [100], [134]. In case of failure in certain actuators, the control effort can be 'handed over' to healthy actuators to maintain the desired performance or at least some level of acceptable performance. Therefore it is fair to say that redundancy is necessary or is at least a key ingredient in achieving fault tolerance [100], [136]. This redundancy can be the direct replication of the hardware (actuator/sensor) or it can be in the form of dissimilar hardware having similar functionality, which can be used to achieve fault tolerance

Hardware or direct redundancy can provide an effective means of reliable operation. A simple example to explain hardware redundancy is the so-called un-interruptible power supply (UPS), which are used for instance in data centres or in telecommunication equipment where an unexpected power shut can result in the loss of data or information [1], which is not desired in reliable systems. For satisfactory performance and to maintain stability of the system, the usual procedure in fault tolerant control is to replace the faulty sensor/actuator with a healthy one. In safety critical systems such as aircraft abundant actuators and sensors are already provided to deal with unexpected situations [22]. In normal or fault free operation only one hardware component i.e only one actuator is sufficient from control point of view to perform a particular function. To explain it mathematically, consider a linear time invariant system

$$\dot{x}(t) = Ax(t) + Bu(t) \tag{2.4}$$

The input matrix $B \in \mathscr{R}^{n\times m}$ can be partitioned as $B = \begin{bmatrix} B_p & B_s \end{bmatrix}$ where the matrix $B_p \in \mathscr{R}^{n\times l}$ is assumed to be of rank $l < m$ and the pair (A, B_p) is controllable [139]. The matrix B_s constitutes the redundant actuators which can be used in case of fault/failre in the B_p channels.

Redundant sensors or analytical redundancy which is based on the nominal mathematical model of the system can be used to measure the same system state to create a reliable measurement in order to ensure proper controller operation. But in safety critical applications just like aircraft, it is not practical to substitute entirely (sensor) hardware redundancy by analytical redundancy [100]. FTC necessitates the presence of redundancy, and managing the redundancy in a suitable way, is vital.

2.3 Introduction to Fault Detection and Isolation (FDI)

Fault Detection and Isolation (FDI) schemes provide online information about system faults or failures. The fault or failure information provided by the FDI plays an important role in managing the actuator redundancy in an efficient way. On the basis of this information, active FTC methods (as explained in the next section) take the appropriate action to mitigate the effects of these faults/failures. For example the FTC methods proposed in [131], [127] and [5] require knowledge of actuators efficiencies in order to tolerate actuator faults/failures. A typical FDI scheme has three tasks to deal with [100], [136] and are formally defined here as in [65]:

Fault Detection: "*Determination of the faults present in a system and the time of detection*."

Fault Isolation: " *Determination of the kind, location and time of detection of a fault*."

Fault Identification: "*Determination of the size and time-variant behaviour of a fault*."

Fault isolation and *Fault identification* are also referred to as fault diagnosis [136]. The important facet of an FDI scheme is how fast and precisely a fault is detected, isolated and identified, so that prompt action can be taken by the FTC scheme to avoid any abnormality. A detailed discussion on the requirements and merits of FDI and FTC schemes was documented in [135]. Generally FDI schemes in the literature [65], [66], [136] are classified into two categories– *model based* and *model free* FDI schemes. Model based schemes utilize (nominal fault free) mathematical models (analytical redundancy) of the plant for the FDI purposes [135], [136], and can be sub-categorized as residual based FDI schemes and fault estimation based FDI schemes. In residual based FDI schemes, the measurements from the plant sensors are compared with the generated signals from the mathematical model to create residual signals [135]. In the case of no faults, the residuals should vanish or should be very close to zero. The increasing size of residual due to faults or failures can be used for the detection of fault. Residuals are normally used with threshold level to avoid any false alarm due to disturbances or noise signals. The unknown input observer (UIO) based schemes [66] can also be used as a robust (in the sense of decoupling of disturbance signals) residual generators. The idea behind the UIO scheme is *"to make the state estimation error decoupled from the unknown inputs (disturbance signals)"* [66].

Residual based FDI schemes usually provide fault detection capabilities and also the location of the fault [135]. The location of a fault in the system can be inferred by employing a bank of dissimilar residual signals [40]. One possibility is to make each residual sensitive to a particular fault and insensitive to all the others in order to isolate a fault [66]. To demonstrate how an observer works, consider a linear time invariant system as

$$\dot{x}(t) = Ax(t) + Bu(t) \tag{2.5}$$

$$y(t) = Cx(t) \tag{2.6}$$

where $A \in \mathbb{R}^{n\times n}$, $B \in \mathbb{R}^{n\times m}$, $C \in \mathbb{R}^{p\times n}$. In the plant model (2.5)-(2.6) only the measured output $y(t)$ is assumed to be available i.e. all the state variables are not available. In this situation one possibility is to employ a so called full order observer [41] to reconstruct all the state vector. To accomplish this, consider the dynamical system

$$\dot{\hat{x}}(t) = A\hat{x}(t) + Bu(t) - L(y(t) - C\hat{x}(t)) \tag{2.7}$$

where $\hat{x}(t) \in \mathbb{R}^n$ is the estimated state vector and $L \in \mathbb{R}^{n\times p}$ is an observer gain that should be designed such that the matrix $(A+LC)$ is Hurwitz. With a good choice of L, it is possible to ensure the error signal $e(t) := x(t) - \hat{x}(t)$ converge to zero rapidly. The error dynamics associated with the plant (2.5) and the observer in (2.7) can be obtained by using the relation

$$\begin{aligned} \dot{e}(t) &= \dot{x}(t) - \dot{\hat{x}}(t) \\ &= (A+LC)x(t) - (A+LC)\hat{x}(t) \\ &= (A+LC)e(t) \end{aligned} \tag{2.8}$$

If L is designed such that all the eigenvalues of $(A+LC)$ are stable, the error signal will converge to zero asymptotically. However the Luenberger observer in (2.7), in case of unknown inputs or actuator faults for instance, will not be able to force the output estimation error to zero.

Therefore the error dynamics (2.8) will be effected by the unknown input/actuator fault and the error signal $e(t)$ will not converge to zero, which means $\hat{x}(t)$ will not converge to the true state $x(t)$.

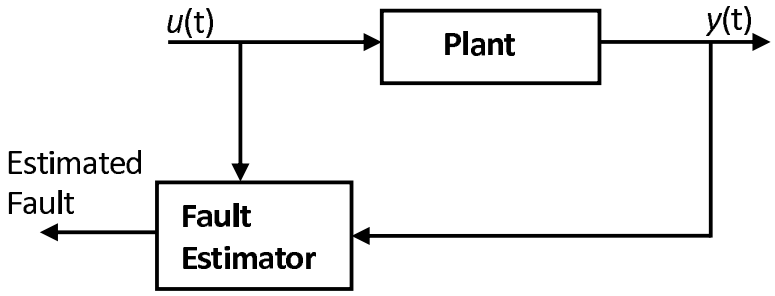

Figure 2.5: Fault estimation based FDI

In certain FTC schemes e.g. [131], [127] and [5], the efficiency level of the actuators (or an estimation of the fault) is also required for the FTC purposes. In order to estimate the actuator efficiency/effectiveness level the schemes proposed for example in [131], [127], [5] can be used. The schemes proposed in [131], [127] used the Kalman filter based approach to estimate the actuator efficiency. The Kalman filter is recursive in nature and is based on a set of mathematical equations which are categorized into two groups: so-called time update equations and measurement update equations [125]. The current estimates of state and error covariance, are used by the time update equations for the *a priori* estimates of state and error covariance for the next time step [125]. These *a priori* estimates of error covariance and state are then used by the measurement update equations together with the output measurement (obtained through the sensors) to compute the Kalman filter gain and to generate *a posteriori* state estimate [125]. The error covariance is updated using the Kalman filter gain for the next cycle and the procedure repeats. The scheme considered in [127], formulated the control effectiveness estimation problem as an augmented state Kalman Filter, where the control effectiveness factors were modeled as the augmented states in the linear plant model.

The actuator effectiveness estimation approach proposed in [5] (details can be found in Section 4.4.1) considered a sliding mode fault reconstruction scheme similar to [40]. The idea behind the scheme in [5] is that the scalars which represent the effectiveness level of the actua-

tors can be estimated from the reconstructed fault signal by introducing a small threshold, when the system error dynamics collapse to zero in finite time.

In certain applications such as passenger aircraft actuator effectiveness can be obtained by using a measurement of the actual actuator deflection compared to the demand. Such information is typically available in many safety critical systems e.g. passenger aircraft [22].

2.4 Fault Tolerant Control Methods

The ultimate objective of a FTC scheme is to provide a desired level of performance in a fault free as well as in failure situation, provided that redundancy is available in the system. The survey papers for example [100], [68], [136] and books [121], [7] provide a bibliographical review of different FTC methods. Depending on the way the problem is tackled, FTC systems can be classified into *passive* fault tolerant control (PFTC) systems and *active* fault tolerant control (AFTC) systems [100], [138], [136], [121]. A block diagram representing the classification of FTC methods is shown in Figure 2.6.

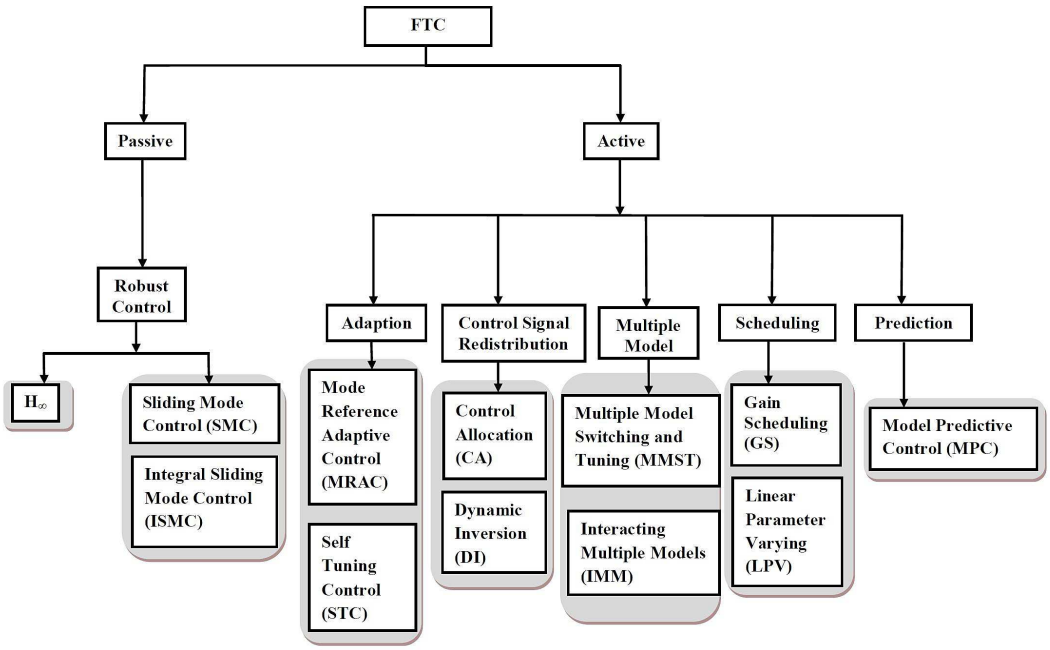

Figure 2.6: Classification of FTC methods (adopted from [121])

2.4.1 Passive Fault Tolerant Control Systems

In PFTC systems the controller is of fixed structure and is designed off-line. PFTC systems are also called reliable control systems in the literature [136]. Due to the fact that PFTC system does not require up to date fault information, the PFTC methods are computationally more attractive [121] . If the uncertainty which acts on the system lies within certain bounds, then a carefully designed *passive* fault tolerant controller can ensure the closed-loop stability, but the PFTC systems can have a limited fault tolerant capability [100], [136].

2.4.1.1 Robust Control

In passive fault tolerant control (PFTC) schemes, the idea is to design a controller using robust control techniques such that the closed-loop system response is robust against certain classes of uncertainties and presumed system faults [43], [100], [136].

H_∞ ***Control***:

H_∞ is a well known technique in the field of robust control, and can take into account the performance and stability requirements [67]. It has applications from the process industry through to aerospace systems [7]. The idea behind H_∞ control is to design a controller which can provide stabilizing properties and minimize the effects of uncertainties and some faults which are known *a priori* and having small effects [67]. Some well known H_∞ controller design methods are H_∞ loop shaping, H_∞ mixed sensitivity and μ synthesis [67]. In the context of FTC, H_∞ optimization technique was used to present an integrated control and diagnosis framework, which was then tested on the nonlinear model of Boeing 747-100/200 [87]. Recently the authors in [124] have reported a mixed H_2/H_∞ approach to design a fault detection observer for LPV systems.

While designing a robust controller, the worst case performance specifications are taken into account, which eventually may lead to a requirement to sacrifice the nominal performance of the system [121]. Faults usually occur very rarely in the system and to sacrifice the nominal performance to obtain robustness against a ceratin class of faults is not appropriate.

2.4.2 Active Fault Tolerant Control Systems

Active fault tolerant control (AFTC) systems on the other hand rely on fault information from the FDI to react appropriately. Specifically AFTC systems, "*react to the system component failures actively, by reconfiguring control actions so that stability and acceptable performance of the entire system can be maintained. In certain circumstances, degraded performance may have to be accepted.*" [136]. A typical AFTC system is represented in Figure 2.7. The structure of an

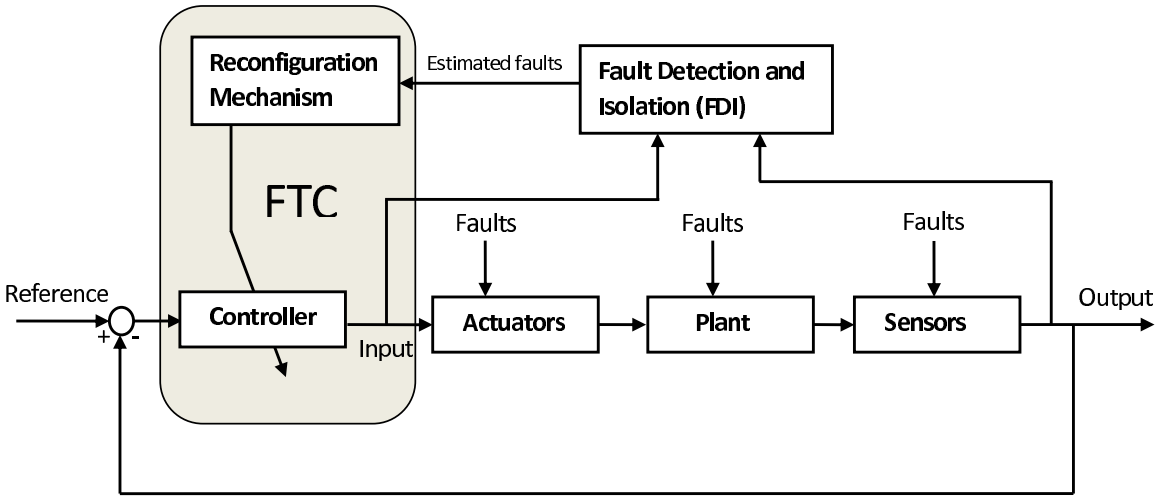

Figure 2.7: Main structure of AFTC systems (adopted from [121])

AFTC system is usually more complex compared to PFTC systems, but it can deal with a wide class of faults [121]. From Figure 2.7, it is clear that there are two aspects which distinguish AFTC systems from PFTC systems. The first one is the FDI scheme and the other one is the reconfiguration mechanism. The reconfiguration mechanism changes the parameters or structure of the controller based on the fault information passed on to it by the FDI unit. It is common practice that FTC and FDI schemes are designed independently i.e. while designing the first the second one is assumed to be perfect and vice versa. Due to the fact that no FDI scheme is perfect [121], it is quite possible that fault information provided by the FDI scheme has some uncertainty and it is important to take such uncertainty into consideration while designing a fault tolerant controller.

In the literature [100], [133], [136], [121], AFTC methods are also classified as *Projection*

based methods, and *online control redesign* methods. In *projection based* methods, one of the pre-computed controllers from a set, which have already been designed off line for different set of faults, is selected depending on the fault information provided by the FDI scheme. In *online control redesign* methods, depending on the fault information provided by the FDI, *the new control scheme is synthesized online* [133]. *Online control redesign* methods are also referred to as *reconfigurable* control or *restructureable* control [121]. In *reconfigurable* control, the controller parameters are computed online depending on the fault information provided by the FDI, where as in *restructureable* control both the structure and controller parameters are computed online [100], [121]. The ultimate goal of a FTC controller design is to minimize the post fault or failure effects, so that the performance is close to the nominal or at least closed-loop stability of the system can be maintained.

2.4.2.1 Adaptation

A carefully designed feedback controller which is designed for a system at a certain operating point, can provide satisfactory performance when the system is functioning around that operating regime. But if the operating conditions keep changing, some sort of adaptation or reconfiguration of the controller is required to cope with these changes. Adaptive control systems, as the name implies, are systems which can adapt to changes in the dynamic characteristics of the process. Formally an adaptive controller is *"a controller with adjustable parameters and a mechanism for adjusting the parameters"* [10]. In [37] an adaptive controller is defined as *"a fixed structure controller, with adjustable parameters"*. Due to its inherent nature of adaptively responding to dynamic changes of the system, adaptive controllers target a significant range of applications from process industries to aerospace [37]. The adaptive control approach is classified into two types: *Indirect adaptive control* and *Direct adaptive control* [37]. In *Indirect adaptive control*, the model is estimated or identified first and then subsequently on the basis of this estimation the controller parameters are computed. In *direct adaptive control* the controller parameters are estimated directly rather than from estimating the model parameters [37], [121].

One of the famous approaches of adaptive control is the Model Reference Adaptive Control (MRAC) whose structure is shown in Figure 2.8. In Figure 2.8, the Reference Model characterises the performance which the plant is required to attain. The output generated by the reference model is compared with the plant output to create the tracking error and the controller parameters are modified accordingly by the Adjustment Mechanism in order to minimize the tracking error [37]. In adaptive control it depends how the problem is formulated as *direct* or *indirect adaptive control*, in case of *direct* approach the controller parameters are estimated directly by using some estimation scheme [121]. For the FTC purposes, the plant model is not

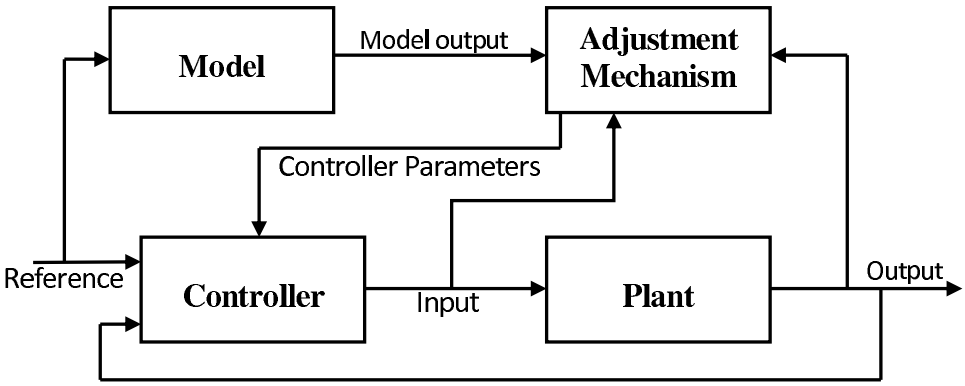

Figure 2.8: Model reference adaptive control system (adopted from [120])

known perfectly due to the faults/failures which may occur, the only objective is to match the dynamics of the plant with the desired dynamics of the reference model.

Another popular approach in the adaptive control family is Self Tuning Control (STC), which requires the online estimation of the plant parameters [37]. A typical STC scheme is shown in Figure 2.9, where it is clear that in the first phase, the plant parameters are estimated by a recursive estimation process, and then subsequently this plant information is used by the control design process to compute the controller parameters. Both schemes (MRAC and STC) mentioned above rely on the certainty equivalence principle (ignoring the uncertainty in the estimated values and treating the estimated values as the true values) [37], [121]. Due to the lack of capability to handle unanticipated faults or sudden change in system dynamics alone [67], a combination with other methods is required such as in [73], a combination of MRAC with multiple model (discussed in the sequel) is considered in order to handle major system changes.

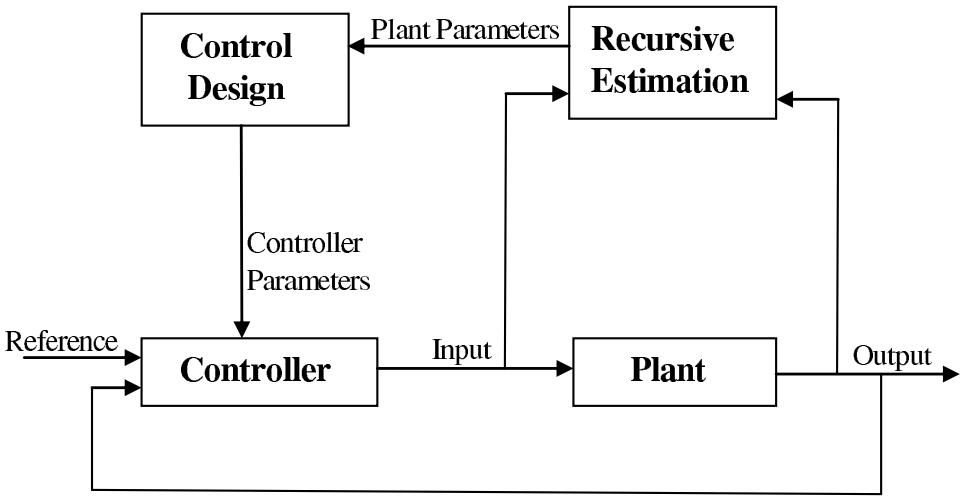

Figure 2.9: Self tuning control system (adopted from [37])

2.4.2.2 Control Allocation

Hardware redundancy (i.e. equipping with more control effectors than axes to control) in safety critical systems for example passenger aircraft [22] and fighter aircraft [46], provides opportunities which can be exploited to design fault tolerant controllers. Control Allocation (CA) has attracted the attention of many FTC researchers because of its ability to handle actuator faults or failures without the need to modify the underlying control law [32], [19], [35], [137]. The advantage of the CA method is that the underlying control law can be designed separately in order to produce the desired control effort and the CA distributes this effort among the available actuators to achieve the required system performance [60], [6]. This feature of CA, allows the control effort by choosing any suitable control paradigm. CA method can also deal with actuator constraints. The work in [38], [19] explicitly uses information about the actuator constraints (rate and position) for CA. The work in [24], [98] described a special structure of CA called daisy chaining where when a control or a set of control effectors are able to generate the commanded moments, then the rest of the control effectors do nothing. In case if the control effectors saturate and are not able to generate the desired moments, it creates an error between the desired moments and that generated by the control effectors, then the next control effector in the set is used to generate only the moments which are lacking due to saturation of the early

control effectors and so on until the desired moments are achieved. To get insight into, how the CA method works, consider a linear model of the plant with redundant actuators, given as in [60]

$$\dot{x}(t) = Ax(t) + Bu(t) \tag{2.9}$$

where $A \in \mathbb{R}^{n\times n}$, $B \in \mathbb{R}^{n\times m}$. Assume that the control input distribution matrix B can be factorized as

$$B = B_v B_u \tag{2.10}$$

where $B_v \in \mathbb{R}^{n\times k}$ and $B_u \in \mathbb{R}^{k\times m}$ and both have *rank* $k < m$ [60]. Substituting (2.10) into (2.9) to get the new system description as follows

$$\dot{x}(t) = Ax(t) + B_v \underbrace{B_u u(t)}_{v(t)} = Ax(t) + B_v v(t)$$

where,

$$v(t) := B_u u(t) \tag{2.11}$$

and therefore

$$u(t) = B_u^{\dagger,W} v(t) \tag{2.12}$$

where $v(t) \in \mathbb{R}^k$ is the virtual control effort [60] and $u(t)$ represents the physical control signals which are directly applied to the actuators. The expression $B_u^{\dagger,W} = WB_u^T(B_uWB_u^T)^{-1}$ is the

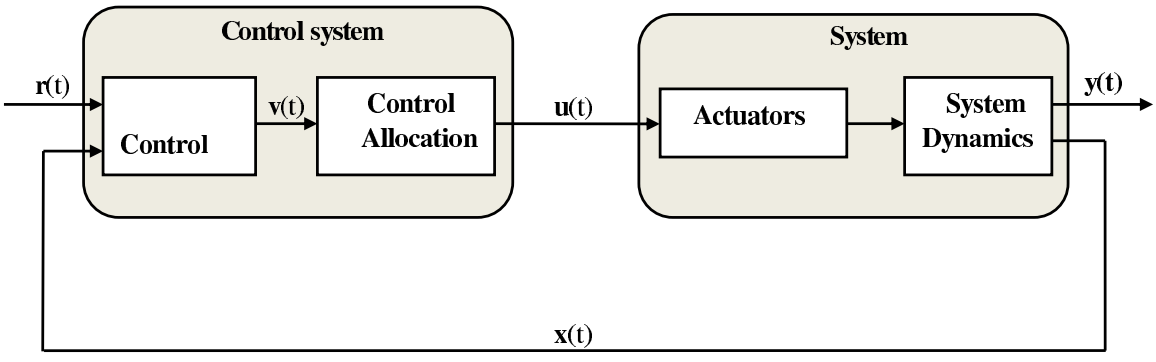

Figure 2.10: Control Allocation scheme (adopted from [59])

weighted right pseudo–inverse of B_u, which provides some design freedom. In order to redistribute the control signals in case of faults or failures, different researchers utilize the design freedom in the pseudo inverse matrix $B^{\dagger}$ in different ways [60], [6]. The structure of the CA scheme is shown in Figure 2.10, which demonstrates that the CA element is not the part of the control law. The virtual control effort $v(t)$ produced by the controller is directly translated into actuators deflections by the CA module.

The benefits of using CA in terms of FTC are exploited in [23], [32] for high performance aircraft. In [99], a comparison of different control allocation methods is made and in [60] optimal control and CA are compared in terms of redistributing a virtual control signal among redundant actuators. In [6], [62] a combination of CA with SMC is considered for FTC. Some recent CA papers in the field of FTC are [76] and [44]. In [78], a modified daisy chaining method is proposed to deal with actuator loss of effectiveness.

2.4.2.3 Sliding Mode Control

Sliding Mode Control is a technique to deal with uncertain systems using the sliding mode concept, and is a particular type of variable structure control (VSC) systems [117]. Sliding mode control (SMC) has a wide range of applications– for example in robotics, process control, vehicle and motion control and aerospace systems [117]. SMC schemes have inherent robustness properties against matched uncertainties (i.e uncertainties which act in the input channels) during a sliding mode. When using sliding mode controllers the closed-loop response of the system is made insensitive to matched disturbances/uncertainties by forcing the system trajectories to slide along the so-called switching surface [118], [41]. The basic concept is to first design a sliding (switching) surface, and then a controller is designed based on this switching surface which induces and maintains the sliding motion on the sliding surface [41]. Due to inherent robustness advantages against matched uncertainties, SMC schemes have the capability to directly deal with actuator faults which can be effectively modeled as matched uncertainties (equation 2.1). A shortcoming of SMC schemes is that failures can not be directly handled, and some sort

of mechanism is required in order to distribute the control effort among the redundant healthy actuators. The work for instance in [106], [62], [105], [4], [30] shows that if there is enough redundancy in the system, SMC can deal with total actuator failures. SMC will be explained in detail in Chapter 3.

2.4.2.4 Control Signal Redistribution

The main goal of a FTC controller design is to achieve performance close to the nominal in the case of actuator faults or failures in the system, and most important of all, to maintain stability of the closed-loop system. One way to deal with this situation is to redistribute the control signals among the healthy actuators. The pseudo inverse method (PIM) is an approach which provides a systematic way for designing such a control strategy [51]. The idea behind the PIM is to design a state feedback gain such that the behavior of the reconfigured system is as close as possible to the nominal one. To explain this, suppose the nominal linear system is given by

$$\dot{x}_p(t) = A_p x_p(t) + B_p u_p(t) \tag{2.13}$$

where, $A_p \in \mathbb{R}^{n\times n}$, $B_p \in \mathbb{R}^{n\times m}$ are the state and input distribution matrices respectively. Let $u_p(t) = K_p x_p(t)$ where, $K_p \in \mathbb{R}^{m\times n}$ is the state feedback gain which has been designed such that the closed-loop system

$$\dot{x}_p(t) = (A_p + B_p K_p) x_p(t) \tag{2.14}$$

is stable and meets the performance specifications. In a post fault/failure scenario suppose that the closed loop dynamics of the faulty system can be represented as

$$\dot{x}_f(t) = (A_f + B_f K_f) x_f(t) \tag{2.15}$$

where, $A_f \in \mathbb{R}^{n\times n}$ and $B_f \in \mathbb{R}^{n\times m}$. Then the desired constant feedback controller K_f can be obtained by equating the closed loop dynamics of the nominal system in (2.14) to that of the

closed loop dynamics of the faulty system in (2.15), i.e.

$$\begin{aligned} A_f + B_f K_f &= A_p + B_p K_p \\ K_f &= B_f^{\ddagger}(A_p - A_f + B_p K_p) \end{aligned} \tag{2.16}$$

where $B_f^{\ddagger}$ denotes the Moore Penrose pseudo inverse of B_f, and provides some degree of freedom, which can be used for redistributing the control signals. In [51], it is argued that the solution to (2.16) does not always guarantee stability of the faulty system. To ensure closed-loop stability, a modified PIM method was proposed in [51], but this method introduces stability constraints while recovering some performance, which can increase the computational burden [121]. In [100], a bank of pre-computed values of K_f for all possible anticipated faults is suggested, and once the fault information is provided by the FDI and the faulty system model (2.15) is obtained, the relevant feedback gain of the system can be modified accordingly. In [100] and [90] the idea of PIM reconfiguration (redistributing the control actions) is presented in order to improve the closed loop stability of the system. In [102], a reconfigurable control law is reported which tries to match the nominal product $B_p u_p$ with the faulty product $B_f u_f$, where B_f is obtained from B_p by eliminating the columns which are effected by the fault. In [110] the problem of PIM and improved PIM was addressed and extended by using a set of admissible reference models.

Dynamic Inversion (DI):

Dynamic inversion (DI) is a method which has a capability to replace the internal dynamics of the system with the desired dynamics. Formally DI is defined as a "*controller synthesis technique by which existing deficient, or undesirable dynamics are canceled and replaced by desirable dynamics*" [31]. The basic concept of DI can be demonstrated mathematically by considering a linear system of the form

$$\dot{x}(t) = Ax(t) + Bu(t) \tag{2.17}$$

To replace the internal system dynamics with that of the desired one, consider the control law as

$$u(t) = B^{-1}(\dot{x}_{des}(t) - Ax(t)) \tag{2.18}$$

where $\dot{x}_{des}(t)$ is the desired response of $\dot{x}(t)$. The main assumption in the design of dynamic inversion controller is that the input matrix B is invertible. In the case when B is non square, the pseudo inverse properties of matrix B can be employed with the assumption that the matrix B is of full rank. According to [36] the desired dynamics $\dot{x}_{des}(t)$ are defined as

$$\dot{x}_{des}(t) = \dot{x}_c(t) + Ke(t) \tag{2.19}$$

where $e(t)$ is the error signal and is defined as $e(t) := x_c(t) - x(t)$ where $x_c(t)$ is the command signal. The design of the controller matrix K is to drive $e(t)$ to zero. Pictorially the process of DI is shown in Figure 2.11. In terms of FTC, DI has the capability to deal with actuator faults

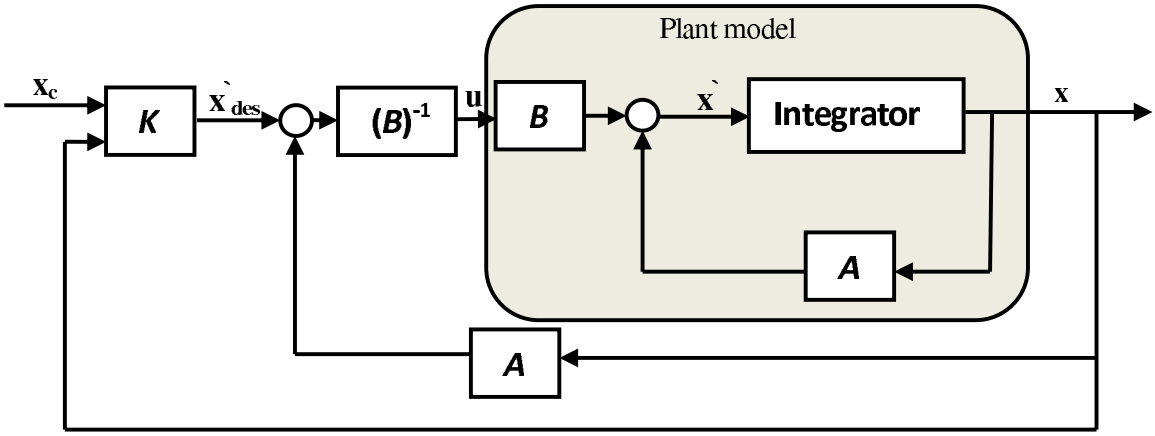

Figure 2.11: Dynamic Inversion Process (adopted from [36])

or failures see for example [71]. In case the model parameters are perfectly known then the undesired dynamics can be completely canceled and replaced by the desired ones. On the other hand if the model parameters are uncertain then the inversion process may cause the stability issues [36]. Typically DI controllers have poor robustness properties since it is assumed that the exact system dynamics are available [31], which is practically not possible due to model

uncertainties. To minimize the effects of model uncertainties, the combination of DI controller with other robust techniques is suggested [31]. In [71] the combined use of DI and MPC is considered for the benchmark model of Boeing 747.

2.4.2.5 Multiple Model

One paradigm to control the dynamical behavior of a nonlinear plant, especially for those where the operating conditions frequently change, is to obtain multiple linear models of the nonlinear plant of interest at different operating conditions, and then to design a suitable controller for each linear model obtained using a linear control theory approach, which can provide a satisfactory performance. The idea is to keep checking during operation which linear model output matches most closely with the current states of the plant [17], and then to activate that model and the corresponding controller. In this way the desired performance can be achieved in the entire operating range.

In terms of FTC, the bank of linear models and the associated controllers should cover all possible sets of faults and failures, in order to cope with such situations. In the case of a fault or failure model that is not in the predesigned set, it may lead to closed-loop instability of the system. The ability of the FDI to provide exact information plays an important role in order to select the correct model and controller pair. Two well known multiple model schemes which can be used for fault tolerant purposes are the Multiple Model Switching and Tuning (MMST) and Interacting Multiple Model (IMM) methods. The MMST scheme was initially proposed to cope with parameter variations which are due to for example to load variations in mechanical systems, and actuator failures in flight control systems [94]. Switching between the controllers to compensate the parameters variations and to maintain the stability while switching, is a crucial part of the MMST scheme [94]. The switching rules and stability issues were discussed in [94]. In [18] the modeling of a control effector failure (float, lock-in-place, hard-over and loss of effectiveness) of an aircraft was documented and a multiple model approach (MMST) was used

to demonstrate the lock-in place failure (horizontal tail). Recently in [9], the concept of using a bank of LQR controllers was proposed to deal with actuator faults governed by an FDI scheme. A similar concept was also considered in [74]. The shortcomings of these schemes are that only the anticipated set of faults and failures can be coped with, multiple faults or failures cannot be handled, and furthermore the number of linear models increase exponentially to address larger systems [121]. However for anticipated faults or failures, MMST scheme provides a fast and promising solution.

The IMM scheme addresses the shortcomings of the MMST scheme by considering a small set of carefully chosen linear models obtained at different operating regime and then designing the controllers for the model set. In the IMM approach, an assumption is made that every possible set of faults/failures can be modeled as a convex combination of the existing predefined model set [121], and the control input is obtained by blending the predefined controllers [132]. In [132], an FDI scheme based on IMM was proposed, and the reconfiguration mechanism was built on predefined controllers which were designed to keep the closed-loop eigenvalues during fault or failure as close as possible to the nominal ones.

2.4.2.6 Scheduling

Gain Scheduling (GS) Control

Gain scheduling (GS) has a wide range of applications from aerospace to process control. Different GS design techniques are discussed in [79]. To design control schemes for nonlinear systems one approach is to create a family of linear models at different operating points in the region of interest, and then to synthesize local controllers which are gain scheduled. In this way well established linear control methods can be used to address and control the nonlinear system. The idea of GS is to compensate the plant parameter variations by varying the controller parameters [10], which means that as the plant operating conditions change the controller parameters change too.

The implementation of the gain scheduling controller can be done by considering the con-

troller parameters as functions of operating conditions or by using lookup tables [10]. Switching between the intermediate operating points may cause unnecessary transients, and may be avoided by creating multiple linear models and then designing particular controllers for each model. For controller scheduling, various ad hoc methods have been proposed, but often these methods do not guarantee acceptable performance (and possibly even stability) other than at the set-points [12]. To calculate the controller parameters for a wide range of operating points could be time consuming and tedious.

Linear Parameter Varying (LPV) Control

Linear parameter varying (LPV) systems are a special class of finite dimensional linear systems, in which the entries of the state space matrices continuously depend on a time varying parameter vector which belongs to a bounded compact set [84]. LPV control schemes are closely related to GS schemes. The LPV methodology resolves many issues associated with the GS method, and ensures performance and closed-loop stability over a wider envelope of operating points. The LPV technique is attractive and appealing for nonlinear plants which can be modelled as time varying systems with state dependent parameters which are measurable online [101].

An LPV system can be defined in state space representation form as [84]

$$\dot{x}(t) = A(\rho)x(t) + B(\rho)u(t) \tag{2.20}$$

$$y(t) = C(\rho)x(t) + D(\rho)u(t) \tag{2.21}$$

where the matrices are of appropriate dimensions and the time varying parameter vector $\rho(t)$ lies in a specified bounded compact set. The matrix entries change according to the parameter vector $\rho(t)$. If the vector $\rho(t)$ is fixed, then the LPV system shown above will become an LTI system. Using LPV techniques, the control law can be automatically scheduled with the operating conditions and guaranteed performance can be proved over a wide operating envelope [12]. For example if all the system states are available, then a suitable state feedback controller $u(t) = -F(\rho)x(t)$ can be designed in order to achieve desired performance and closed-loop

stability of the system

$$\dot{x}(t) = (A(\rho) - B(\rho)F(\rho))x(t)$$

for all the admissible values of $\rho(t)$ in a compact set. LPV methods have attracted much attention in recent years especially for aircraft systems [50]. For LPV systems, several controller synthesis methods have been proposed in recent years in the framework of FTC: the advantages and capabilities of LPV controller synthesis (based on a single quadratic Lyapunov function approach) over gain-scheduling controller designs (based on H_∞ controller synthesis) are discussed and compared in [88] by implementing the two techniques on a high fidelity atmospheric re-entry vehicle. In [115], an output feedback synthesis method using LMIs is presented in order to preserve closed-loop stability in the case of multiple actuator faults. The authors in [101] have explored the combined use of fault estimation and fault compensation for LPV systems. Recently in [92] an active FTC technique was proposed for LPV systems to deal with actuator faults, where actuator faults are identified by using UIO technique by considering them as unknown inputs and a state feedback controller is realized by approximating the LPV system as polytopic system i.e the system whose state space matrices range in a polytope of matrices [92], and tested on a two degree of freedom twin rotor system.

2.4.2.7 Prediction

Model Predictive Control (MPC)

Model predictive control (MPC) is a process specific control, and has become an acceptable standard in the process industry (perhaps after PID) due to its natural capability to deal with constraints and changes in the system dynamics [121]. MPC has numerous applications in the process industry for example petro-chemical and related industries [89].

MPC is based on the dynamical model of the process and an optimization technique, whereby at each sampling time it matches predictive process outputs with the predefined (desired or set point) system trajectory, and creates an optimal control sequence. Then only the first control input in the sequence is actually applied to the plant [89]. Due to the ability of an MPC

controller to handle the constraints i.e. input constraints, state constraints etc, MPC provides a promising basis for FTC [82], [72]. In [82], it is argued that the actuators faults can be easily accommodated in the MPC formulation by modifying the input constraints or by modifying the internal model. In [82] a case study of flight 1862 is considered, where MPC has been used in the framework of FTC. For the FTC purposes, in most of the cases, MPC depends on reliable information from the fault detection and isolation unit in order to update the constraints for the optimization process and to generate new control signals to stabilize the system in the new condition. In [112], to deal with input constraints and actuator failures, an AFTC scheme is proposed for linear systems where multiple MPC controllers are incorporated with the fault detection filter. In [91] a real time implementation of MPC was considered for accommodating actuator and system faults in a three tank system. In that scheme the accommodated MPC controllers were already calculated off-line and each was switched on at the time of the relevant fault. Recently in [130], an actuator FTC scheme was proposed for constrained linear systems, where a bank of MPC controllers (for different possible faults) and state estimators (to match the fault situation) were considered. The scheme uses fault information from the FDI, to activate the appropriate MPC controller.

2.5 Conclusion

In this Chapter a brief introduction to FTC and some common terminologies which are used in the FTC literature have been defined. Typical faults or failures associated with the actuators and sensors were also explained. Redundancy, which is a key criterion in FTC has been defined. A discussion about some FDI schemes was included. Methods which have been used to design fault tolerant controllers using active and passive approaches were also discussed.

In the next Chapter, a SMC scheme will be explained in detail and it will be demonstrated how the closed-loop system response can be made robust against a particular class of uncertainties. A choice of the sliding surface is also discussed which helps not to amplify the unmatched uncertainties (which do not lie in the control input channel) in the sliding mode.

Chapter 3

Integral Sliding Mode Control

The term sliding mode was first used in the literature in the context of relay systems [118]. Sliding mode control (SMC) is a particular class of variable structure control systems (VSCS) [117]. VSCS evolved from work in Russia in the early $1960's$ and spread around the world in the late $1970's$ after the publication of the survey paper by Utkin [116]. VSCS are a class of systems where the control law, as a function of the system state, is deliberately changed (from one structure to another) according to some predefined rules: for example a relay system. A sliding mode is a phase in the closed-loop system response where the plant's state trajectories slide along a sliding surface to the equilibrium point. In sliding mode based schemes, a switching function dictates which structure of the control law is to be used at a particular time instant, depending on the position of the state from the sliding surface. The set of points for which the switching function is zero is called sliding surface. SMC now has become a technical tool to design controllers for uncertain systems and provide robustness properties against matched uncertainties i.e. uncertainties that affect the plant dynamics acting through the input channels [41], because in the so-called sliding mode, the system state trajectories are insensitive to matched uncertainties. However this robustness against external disturbances and parameter variations matched to the control can only be achieved after the occurrence of the sliding mode [41], [118]. Before the occurrence of the sliding mode i.e during the so-called reaching phase, the system is sensitive to external disturbance– even matched ones [118], [119], [28]. In order to eliminate the reaching

phase and to have robustness throughout the entire closed-loop system response (i.e a sliding mode will start from the beginning of the system response) the idea of Integral Sliding Modes (ISM) was initially proposed in [118], [119]. The inherent robustness of sliding mode based schemes make them attractive approaches for practical systems to design controllers, which are robust against external disturbances, model uncertainties and parameter variations.

In this Chapter a step by step design procedure for sliding mode controllers is presented first, and then these ideas are extended to integral sliding modes in order to have a robustness throughout the entire system response. The necessary conditions for the existence of sliding modes are also given. The properties of the system while in the sliding mode are also explained, and are examined through simulations. The design concepts in this Chapter are closely based on [41], [118].

3.1 Introduction

SMC design paradigms [118], [41], [2] have now become mature techniques for the control of uncertain systems to provide effective solutions against parameter changes and model uncertainties. These are attractive features from a practical viewpoint. SMC has appeared to be the most promising robustness technique to handle sudden and large changes in the system dynamics [62] and has many application areas–for example motor control, aircraft and spacecraft control, process control and power systems.

The design of a sliding mode controller comprises two steps. The first step is to design a sliding (switching) surface, on which the sliding motion will take place. The second step is to design a control law, which depends on the choice of the switching function and forces the system state trajectories to reach and slide on the sliding surface ideally. An important condition in the sliding mode literature is to verify the reachability condition, which guarantees the existence of the sliding mode on the sliding surface. An ideal sliding mode can be thought of as the ideal or best performance which can be achieved. Once sliding is achieved and maintained, robustness against matched uncertainties is guaranteed. Details of the design procedures are given in the

next sections.

3.2 Problem statement and equivalent control

In order to explain the design procedure for a system where *full state information* is available, consider an uncertain linear time invariant (LTI) system of the form

$$\dot{x}(t) = Ax(t) + Bu(t) + M\xi(t,x) \tag{3.1}$$

where $A \in \mathbb{R}^{n\times n}$, $B \in \mathbb{R}^{n\times m}$. It is assumed that the matrix B has full rank $rank(B) = m$ [41], where $1 \leq m < n$ and the pair (A,B) is controllable [118], [41]. The matrix $M \in \mathbb{R}^{n\times l}$ is assumed to be known and is in the range space of input distribution matrix B i.e. $\mathscr{R}(M) \subset \mathscr{R}(B)$, therefore it is possible to write $M = BD$ [41], for some $D \in \mathbb{R}^{m\times l}$. The function $\xi(t,x)$ represents an external disturbance or model uncertainty which is unknown but has a known upper bounds for all x and t. Therefore the uncertain system in (3.1) can be rewritten as

$$\dot{x} = Ax(t) + Bu(t) + BD\xi(t,x) \tag{3.2}$$

As a first design step, define a sliding surface as

$$\mathscr{S} = \{x \in \mathbb{R}^n \quad : \quad \sigma(t) = 0\} \tag{3.3}$$

where $\sigma(t)$ is a linear switching function [41] and is defined as

$$\sigma(t) = Gx(t) \tag{3.4}$$

where $G \in \mathbb{R}^{m\times n}$ is a design matrix and is of full rank. Furthermore by design it is assumed that the square matrix GB is nonsingular matrix i.e $\det(GB) \neq 0$. It is important that the sliding motion on the sliding surface should be stable and robust against the uncertainty $\xi(t,x)$. Therefore

in order to analyze the sliding motion associated with the sliding surface (3.3), consider the time derivative of (3.4) given by

$$\dot{\sigma}(t) = G\dot{x}(t) \tag{3.5}$$

Substituting the open-loop dynamical equation (3.2) into (3.5) gives

$$\dot{\sigma}(t) = G\Big(Ax(t) + Bu(t) + BD\xi(t,x)\Big) \tag{3.6}$$

Now it is assumed that the system states are forced to reach the sliding surface at time say t_s, so that after $t \geq t_s$ an ideal sliding motion can be obtained, i.e. during sliding

$$\sigma(t) = \dot{\sigma}(t) = 0 \quad \text{for all} \quad t \geq t_s$$

where the time t_s is termed as reaching phase i.e. the time when the sliding commences. The control vector $u(t)$ such that the time derivative of the vector on the state trajectories equal to zero [118] can be obtained by equating equation (3.6) to zero which yields

$$u_{eq}(t) = -(GB)^{-1}\Big(GAx(t) + GBD\xi(t,x)\Big) \quad \text{for} \quad t \geq t_s \tag{3.7}$$

where the square matrix GB is nonsingular by design. The expression $u_{eq}(t)$ is termed as an equivalent control [118], and is an average control which the control signal must take to maintain the sliding motion on the sliding surface [118] [41]. However it is not the control law which can induce the sliding mode.

Now in order to obtain the expression for the sliding motion (i.e. the motion while the system is

in the sliding mode), substituting the value of $u_{eq}(t)$ from (3.7) into (3.2), yields

$$\begin{aligned}
\dot{x}(t) &= Ax(t) + B\Big(-(GB)^{-1}(GAx(t) + GBD\xi(t,x))\Big) + BD\xi(t,x) \\
&= Ax(t) - B(GB)^{-1}GAx(t) - B(GB)^{-1}GBD\xi(t,x) + BD\xi(t,x) \\
\dot{x}(t) &= \underbrace{(I_n - B(GB)^{-1}G)}_{P_s}Ax(t) + (I_n - B(GB)^{-1}G)BD\xi(t,x) \qquad (3.8)
\end{aligned}$$

Note that the matrix P_s has the property that

$$P_sB = 0 \qquad (3.9)$$

As a result, equation (3.8) can be reduced to

$$\dot{x}(t) = P_sAx(t) \quad \text{for } t \geq t_s \qquad (3.10)$$

From (3.10), it is clear that the effect of the uncertainty $\xi(t,x)$ while in the sliding mode is completely rejected i.e. the reduced order system motion is insensitive to matched uncertainties. Also the stability of the sliding motion (3.10) depends on the choice of sliding surface i.e choice of switching matrix G. The switching matrix G in (3.4) can be designed for example using quadratic minimization approach given in [33] and chapter 4 of [41], which is based on the modified form of a classical linear quadratic *LQR* regulator problem [26].

3.2.1 Sliding Mode Control Laws

The second design step is to design a control law such that the sliding motion on the sliding surface $\mathscr{S}$ can be ensured in finite time and thereafter remains on it. A sliding mode controller typically consists of two parts, a linear part and a nonlinear part and is given by

$$u(t) = u_l(t) + u_n(t) \qquad (3.11)$$

where the nonlinear part is of discontinuous type and is responsible for inducing the sliding motion on the sliding surface $\mathscr{S}$, whereas the linear part which is normally the nominal equivalent control and is responsible to maintain sliding [41]. The specific choice of the sliding mode control law $u(t)$ will be based on the nominal system (i.e the system without uncertainty) and to cope with the uncertainty $\xi(t,x)$ the inherent robustness property against matched ones as demonstrated in the previous section in equation (3.10) will be relied upon. The nominal system associated with (3.2) is

$$\dot{x}(t) = Ax(t) + Bu(t) \tag{3.12}$$

From (3.7), it is clear that the expression for $u_{eq}(t)$ i.e. for the nominal system (3.12) is

$$u_{eq}(t) = -(GB)^{-1}GAx(t) \quad \text{for} \quad t \geq t_s \tag{3.13}$$

A sliding mode controller based on the nominal equivalent control and discontinuous control component is then defined as

$$u(t) = -(GB)^{-1}GAx(t) - \rho(t,x)(GB)^{-1}\frac{\sigma}{\|\sigma\|} \qquad \text{for } \sigma \neq 0 \tag{3.14}$$

where $\frac{\sigma}{\|\sigma\|}$ is a unit vector component [104], [41], and $\rho(t,x)$ is a scalar gain chosen high enough (greater than the size of the uncertainty present in the system) to enforce the sliding motion.

Remark 3.1: For single input systems, the sliding mode controller in (3.14) can be defined as

$$u(t) = -(GB)^{-1}GAx(t) - \rho(t,x)(GB)^{-1}sgn(\sigma) \qquad \text{for } \sigma \neq 0 \tag{3.15}$$

where $sgn(.)$ is the signum function and has the property that $\sigma sgn(\sigma) = |\sigma|$.

3.3 Reachability Problem

In the sliding mode literature the controller $u(t)$ is to be designed such that the reachability condition is satisfied [41] which is a sufficient condition to ensure that at each time instant, the system state trajectories will converge towards the sliding surface. Mathematically this can be expressed for the case of single input systems [41] as

$$\lim_{\sigma \to 0+} \dot{\sigma} < 0 \qquad \lim_{\sigma \to 0-} \dot{\sigma} > 0 \tag{3.16}$$

or in a compact form as

$$\sigma \dot{\sigma} < 0 \tag{3.17}$$

near the sliding surface $\sigma(t) = 0$. A stronger condition which ensures an ideal sliding motion [41] in finite time even in the presence of external disturbance or uncertainty is given by

$$\sigma \dot{\sigma} \leq -\eta |\sigma| \tag{3.18}$$

where η represents a positive design scalar. The expression in (3.18) is often called the η-reachability condition [41].

For multi input systems, the reachability condition in (3.18) will be modified to become

$$\sigma^T \dot{\sigma} \leq -\eta \|\sigma\| \tag{3.19}$$

This is a sufficient condition to show sliding surface $\mathscr{S}$ is attractive .

Finally in order to justify that the controller designed in (3.14) satisfies the η-reachability condition (3.19), substituting the value of (3.14) into (3.6) which gives

$$\begin{aligned} \dot{\sigma}(t) &= GAx(t) + GB\left(-(GB)^{-1}GAx(t) - \rho(t,x)(GB)^{-1}\frac{\sigma}{\|\sigma\|} \right) + GBD\xi(t,x) \\ &= -\rho(t,x)\frac{\sigma}{\|\sigma\|} + GBD\xi(t,x) \end{aligned} \tag{3.20}$$

Pre-multiplying both sides of (3.20) by $\sigma^T(t)$ which gives

$$\sigma^T \dot{\sigma} = -\rho(t,x)\frac{\sigma^T \sigma}{\|\sigma\|} + \sigma^T GBD\xi(t,x) \tag{3.21}$$

By using the property that $\sigma^T \sigma = \|\sigma\|^2$, equation (3.21) becomes

$$\begin{aligned} \sigma^T \dot{\sigma} &= -\rho(t,x)\|\sigma\| + \sigma^T GBD\xi(t,x) \\ &\leq \|\sigma\|(-\rho(t,x) + \|GBD\xi(t,x)\|) \end{aligned} \tag{3.22}$$

For a particular choice of scalar gain $\rho(t,x)$ such that

$$\rho(t,x) \geq \|GBD\xi(t,x)\| + \eta \tag{3.23}$$

the inequality in (3.22) becomes

$$\sigma^T \dot{\sigma} \leq -\eta\|\sigma\| \tag{3.24}$$

From (3.24), it is clear that η-reachability condition is satisfied, which ensures the existence of an ideal sliding motion on the sliding surface $\mathscr{S}$.

3.4 A simple simulation example

In this section, the design procedure for sliding mode controllers discussed in the previous sections are applied to a simulation example to obtain insight into the design procedure.

3.4.1 Spring Mass Damper System

A simple example of a spring-mass-damper system (SMDS) taken from [97] driven by a force $u(t)$ is considered here as shown in Figure 3.1. It is assumed that at $t = 0$ the mass m is pulled down from the equilibrium position, such that $y(0) = 0.1m$ and $\dot{y}(0) = 0.05m/sec$ [97]. The

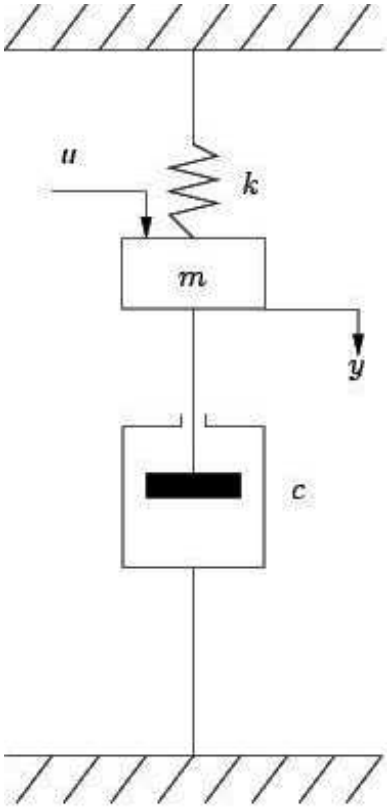

Figure 3.1: Spring Mass Damper System (adopted from [97])

dynamical equation of the mechanical system (Figure 3.1) can be written as

$$m\ddot{y}(t) + c\dot{y}(t) + ky(t) = u(t) \tag{3.25}$$

where k is the spring constant, c is the viscous-friction coefficient and m is the mass. A disturbance signal $asin(y)$ is added into the control input channel to demonstrate the invariance against such a disturbance while in the sliding mode. The values of these constants are chosen as $m = 1$ kg, $c = 3$ N-sec/m, $k = 2$ N/m and $a = 0.1$. In order to write the differential equation (3.25) into state space form, define the state variables as $x_1(t) = y(t)$ and $x_2(t) = \dot{y}(t)$, which represent the position and velocity of the mass m. By taking the time derivative of these state

variables, equation (3.25) can be written in terms of state variables as

$$\dot{x}_1(t) = \dot{y}(t) = x_2(t) \tag{3.26}$$

$$\dot{x}_2(t) = \ddot{y}(t) = -\frac{k}{m}x_1(t) - \frac{c}{m}x_2(t) + \frac{1}{m}(u(t) + asin(x_1(t)) \tag{3.27}$$

Hence, the state space representation of the system in (3.25) is

$$\begin{bmatrix} \dot{x}_1(t) \\ \dot{x}_2(t) \end{bmatrix} = \underbrace{\begin{bmatrix} 0 & 1 \\ -\frac{k}{m} & -\frac{c}{m} \end{bmatrix}}_{A} \underbrace{\begin{bmatrix} x_1(t) \\ x_2(t) \end{bmatrix}}_{x(t)} + \underbrace{\begin{bmatrix} 0 \\ \frac{1}{m} \end{bmatrix}}_{B} (u(t) + asin(x_1(t)) \tag{3.28}$$

By substituting the values for the spring constant k, viscous friction coefficient c, and mass m, it yields

$$\begin{bmatrix} \dot{x}_1(t) \\ \dot{x}_2(t) \end{bmatrix} = \underbrace{\begin{bmatrix} 0 & 1 \\ -2 & -3 \end{bmatrix}}_{A} \begin{bmatrix} x_1(t) \\ x_2(t) \end{bmatrix} + \underbrace{\begin{bmatrix} 0 \\ 1 \end{bmatrix}}_{B} (u(t) + 0.1sin(x_1(t)) \tag{3.29}$$

3.4.2 Simulation objective and SMC design

In the simulation it is assumed that at $t = 0$ the mass m is pulled down from the equilibrium position such that $y(0) = 0.1m$ and $\dot{y}(0) = 0.05m/sec$ [97]. The objective here is to design a sliding mode controller to bring the system back to the equilibrium position from the initial conditions without overshooting in terms of displacement and with a settling time not more than 6 seconds.

Since the first step is to design a sliding surface, so the switching function in (3.4) can be written in terms of states $x_1(t)$ and $x_2(t)$ as

$$\begin{aligned} \sigma(t) &= \begin{bmatrix} G_1 & G_2 \end{bmatrix} \begin{bmatrix} x_1(t) \\ x_2(t) \end{bmatrix} \\ &= G_1x_1(t) + G_2x_2(t) \end{aligned} \tag{3.30}$$

where $G_1 \in \mathbb{R}^{m\times(n-m)}$ and $G_2 \in \mathbb{R}^{m\times m}$ is assumed to be nonsingular i.e. $\det(G_2) \neq 0$. While sliding, the switching function $\sigma(t) = 0$ [118], [41], therefore equation (3.30) can be written as

$$x_2(t) = -\underbrace{G_2^{-1}G_1}_{E} x_1(t) \tag{3.31}$$

where $E \in \mathbb{R}^{m\times(n-m)}$ is the design matrix. It is also clear from (3.31) that once x_1(t) is known, the state $x_2(t)$ can be easily determined, therefore substituting the value of (3.31) into (3.26), the sliding motion is given by

$$\dot{x}_1(t) = -Ex_1(t) \tag{3.32}$$

From (3.32) it is clear that during sliding mode the system behaves as a reduced order i.e. the system's order reduces to the number of control inputs. Now for the design purpose, choosing the value of $G_2 = 1$ which results in $E = G_1$, and hence the switching matrix G takes the form

$$G = \begin{bmatrix} E & 1 \end{bmatrix}$$

In this example the value of $E = 0.9$ is chosen to satisfy the condition of no-overshooting. The sliding mode control law defined in (3.15) using the fact that $GB = 1$ will become

$$\begin{aligned} u(t) &= -(GB)^{-1}GAx(t) - \rho(GB)^{-1}sgn(\sigma) \\ &= \begin{bmatrix} 2 & 2.1 \end{bmatrix} x(t) - \rho\, sgn(\sigma) \end{aligned} \tag{3.33}$$

Finally in order to verify that the control law $u(t)$ in (3.33) satisfies the reachability condition (3.18), by substituting (3.33) and (3.29) into the time derivative of (3.30) which yields

$$\begin{aligned} \dot{\sigma}(t) &= G_1\dot{x}_1(t) + G_2\dot{x}_2(t) \\ &= G_1x_2(t) - 2x_1(t) - 3x_2(t) + 2x_1(t) + 2.1x_2(t) - \rho sgn(\sigma) + 0.1sin(x_1(t)) \\ &= -\rho sgn(\sigma) + 0.1sin(x_1(t)) \end{aligned} \tag{3.34}$$

Multiplying (3.34) with $\sigma(t)$ and with the choice of $\rho \geq |0.1sin(x_1(t)| + \eta$, the reachability condition in (3.18) for the controller (3.33) has been established and is given by

$$\sigma\dot{\sigma} \leq -\eta|\sigma| \tag{3.35}$$

which ensures the existence of an ideal sliding mode.

3.4.3 Simulation Results

A sliding mode controller (3.33) based on the nominal system (3.29) is now being tested in simulations using Matlab/Simulink environment. In the simulations, the value of ρ is selected

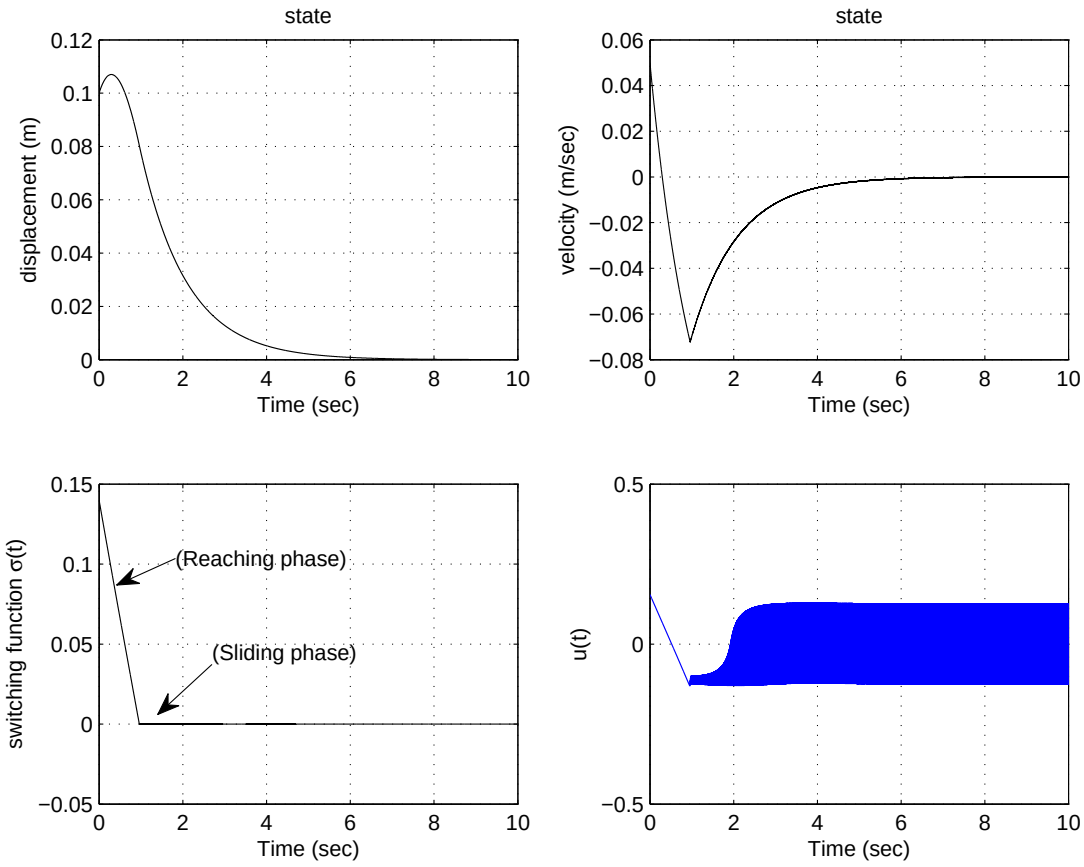

Figure 3.2: Simulation results for the SMDS with disturbance

as $\rho = 0.15$. From Figure 3.2 it is clear that the disturbance has no effect on the system per-

formance, which means that the design requirements of displacement reaching the equilibrium position with no overshoot and within 6 seconds is met. Switching function plot in Figure 3.2 shows that the sliding surface is attained in 1 sec i.e. sliding motion starts after $t \geq 1$ sec, however the discontinuous control signal exhibits high frequency switching which is undesired in some systems due to high wear of moving mechanical components [117]. Therefore smoothing the discontinuity in the control signal is required to avoid high frequency switching (chattering).

3.5 Practical Sliding Mode Control law

The discontinuity associated with the nonlinear discontinuous part of the control law (3.14) is the main hurdle in a practical implementation– especially in mechanical systems. Different methods have been used in the literature to smooth the transition near the sliding surface–see for example chapter 3 of [41] and [26]. By smoothing the control signal discontinuity, the state trajectories no longer slide on the sliding surface, instead they slide in the vicinity of the sliding surface, which is termed as pseudo sliding [41]. However this means total invariance against matched uncertainties is not guaranteed, however there is a possibility of obtaining close approximation of the discontinuous control term which ensures a certain level of robustness against matched uncertainties still remains.

One possibility to smooth the control signal in (3.14) is to use the boundary layer approach, where the discontinuous control signal $u_n(t)$ can be replaced with a continuous approximation:

$$u_n(t) := \begin{cases} -\rho(t,x)(GB)^{-1}\frac{\sigma(t)}{||\sigma(t)||} & \text{if } ||\sigma(t)|| \geq \delta \\ -\rho(t,x)(GB)^{-1}\frac{\sigma(t)}{\delta} & \text{otherwise} \end{cases} \tag{3.36}$$

where δ is a small positive design scalar, whose value determine the size of the boundary layer around the sliding surface. Another alternative approach is to use the fractional/sigmoidal approximation [41], where the unit vector term in (3.14) can be replaced by the following contin-

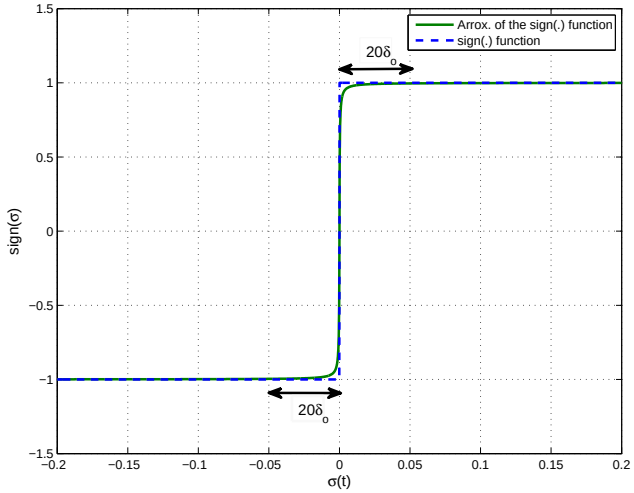

Figure 3.3: An approximation of the sign function [41]

uous approximation

$$u_n(t) = -\rho(t,x)(GB)^{-1}\frac{\sigma(t)}{(||\sigma(t)|| + \delta)} \tag{3.37}$$

where δ is a small positive design scalar.

An alternative approach to smooth the high frequency control switching which leads to chattering is to use the higher order sliding mode control approach [80], [14], and recently [52]. Now the sliding motion is on the constraint set $\sigma = \dot{\sigma} = ... = \sigma^{r-1} = 0$ and is called an r^{th} order sliding mode. Furthermore if it is possible to steer $\sigma(t,x)$ to zero using the discontinuous control $\dot{u}(t)$, then the associated actual control signal $u(t)$ will be continuous and the unwanted chattering effects can be alleviated [14].

In this Chapter the fractional approximation given in (3.37), as shown in Figure 3.3, is used, and is a tradeoff between the ideal sliding motion and chattering. Therefore by approximating the signum function in (3.15) with the fractional approximation $\frac{\sigma}{|\sigma|+\delta}$, where the value of δ is chosen as $\delta = 0.0001$, the control law in (3.33) becomes

$$u(t) = \begin{bmatrix} 2 & 2.1 \end{bmatrix} x(t) - 0.15\frac{\sigma}{(|\sigma| + 0.001)}$$

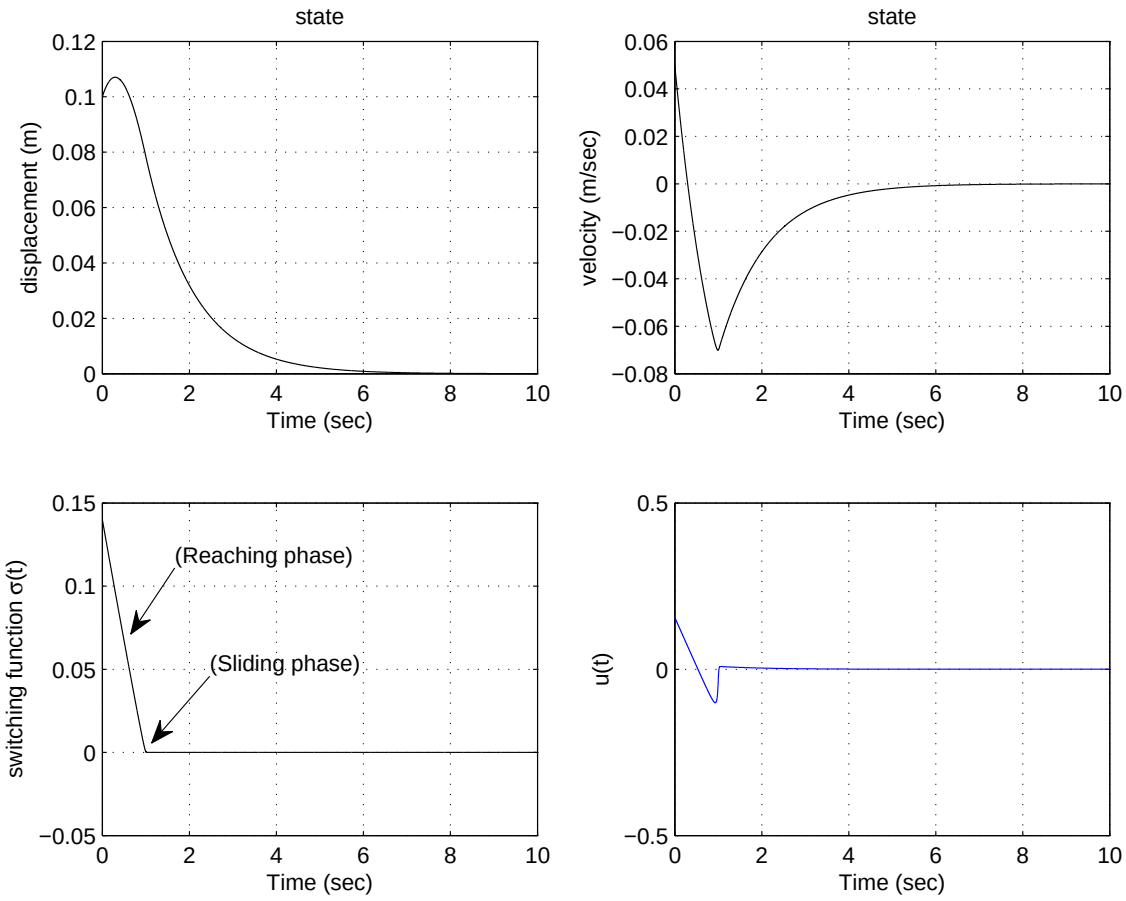

Figure 3.4: Simulation results for the SMDS with modified control law

From Figure 3.4, it is clear that the chattering or high frequency switching of the control signal has been removed. This is due to the approximation of the signum function with the fractional approximation as can be seen in the Figure 3.3. Due to this approximation, the sliding motion will be in the vicinity of the sliding surface and will be termed as pseudo sliding instead of an ideal sliding motion. The design requirements however are still met in the presence of external disturbance as can be seen in Figure 3.4.

3.6 Properties of the Sliding Mode

Some of the properties of siding modes are summarized as below:

1. during a sliding mode the order of the sliding motion is $n - m$ [118], [41], where n and m represent the number of states and the number of inputs respectively.

2. the stability of the closed-loop sliding motion depends only on these $n - m$ nonnegative eigenvalues.

3. the performance and stability of the closed loop sliding motion depends on the choice of the sliding surface.

4. during sliding mode the sliding motion is invariant to matched uncertainties [41], [118].

Remark 3.2: It is argued in [118], [119], [28] that the system is sensitive to model uncertainties and or external disturbances during the so called reaching phase.
In the coming sections, the ideas of Integral Sliding Mode Control (ISMC) are discussed which have the property to eliminate the reaching phase associated with the classical SMC approach discussed in the previous sections to improve the robustness against matched uncertainties by inducing the sliding mode in the entire closed-loop system response [27], [28].

3.7 Integral Sliding Mode Control (ISMC)

The basic idea of ISMC was initially proposed in [119], [118], [123] to enforce the sliding mode from the beginning of the system response, which means a controller based on ISMC ideas can provide compensation to matched uncertainties throughout the entire system response. In this section, a step by step design procedure for Integral Sliding Modes (ISM) controller is explained and the special features associated with ISMC design are discussed. In this section, it is assumed that the state information is available for the controller design.

3.7.1 Introduction

In ISMC, it is assumed that there exists an ideal nominal plant, for which a properly designed state feedback controller has already been designed to ensure the asymptotic stability of the

closed loop system [118], [119], and to satisfy predefined performance specifications. A discontinuous controller based on ISM ideas is added to the existing nominal state feedback controller to make sure the nominal performance is maintained, and the system is insensitive to external disturbances (faults/failures from a FTC perspective) and variations of system parameters in a more traditional setting i.e. the system motion while in the sliding mode behaves as the nominal system. This design philosophy provides the opportunity to retro-fit an ISM to the existing baseline controller to compensate the matched uncertainties and external disturbances from the very beginning. More specifically "*a sliding mode based auxiliary controller that compensates the perturbation from the very begging of the control action, while retaining the order of the uncompensated system is the ISM controller*" [103].

ISMC has been used to tackle different set of control problems. A practical implementation of ISMC was considered for example in [11], [13] for the speed control of synchronous and induction motors, where the boundary layer approach is used to avoid the chattering associated with the discontinuous part of the ISM controller. It is known from the early sections of this Chapter that using sliding mode based schemes the system state trajectories are insensitive to matched uncertainties while in the sliding mode. But the system state trajectories can be sensitive to unmatched uncertainties i.e. the uncertainties which do not match to the control or are not in the range space of input distribution matrix. Therefore while designing a controller such that the effect of matched uncertainty is rejected in the sliding mode, the unmatched uncertainty in the system should not deviate the system trajectories away from the sliding surface. In [27], [128] and [28], ISM ideas were used for an uncertain system considering both matched and unmatched uncertainties and have shown that the system dynamics while on the sliding surface meets the performance specifications of the nominal system (which is assumed to be known *a priori* in ISM framework) in the presence of matched uncertainties.

3.7.2 Problem Statement and ISM Controller design

To explain the design procedure, consider an uncertain LTI of the form

$$\dot{x}(t) = Ax(t) + Bu(t) + M\xi(t,x) + f_u(t,x) \tag{3.38}$$

where $\xi(t,x)$ is a bounded unknown disturbance and the matrix M satisfies the matching condition i.e $\mathscr{R}(M) \subset \mathscr{R}(B)$ and can be written as $M = BD$ [41], for some $D \in \mathbb{R}^{m\times l}$. The pair (A,B) is assumed to be controllable and B is of full rank i.e. $rank(B) = m$, where $1 \leq m < n$. The function $f_u(t,x)$ represents an unmatched uncertainty i.e. does not lie within the range space of matrix B [41], but is assumed to be bounded with known upper bound. The nominal linear system associated with equation (3.38) can be written as

$$\dot{x}(t) = Ax(t) + Bu_o(t) \tag{3.39}$$

where $u_o(t)$ is a nominal control law which can be designed by any suitable state feedback controller design method to achieve the desired nominal performance of the system. Since it is assumed that the pair (A,B) is controllable, then there exists a state feedback controller of the form

$$u_o(t) = -Fx(t) \tag{3.40}$$

where $F \in \mathbb{R}^{m\times n}$ is a state feedback gain to be designed so that the state trajectories of the nominal system (3.39), say $x_o(t)$, are stable and meet performance specifications. The matrix F can be designed by using any state feedback design approach. The objective is to design a control law $u(t)$, such that the state trajectories $x(t)$ of (3.38) while in the sliding mode satisfy the condition $x(t) \equiv x_o(t)$ for all time, starting from the initial time instant $i.e\, x(0) \equiv x_o(0)$ [118]. To achieve $x(0) \equiv x_o(0)$ the order of the sliding dynamics should be of the same order as the nominal system.

3.7.3 Design Principles

Define a control law $u(t)$ of the form

$$u(t) = u_o(t) + u_n(t) \tag{3.41}$$

then equation (3.38) using (3.41) can be written as

$$\dot{x}(t) = Ax(t) + Bu_o(t) + Bu_n(t) + BD\xi(x,t) + f_u(t,x) \tag{3.42}$$

where $u_o(t)$ is the state feedback controller as defined in (3.40), and $u_n(t)$ is defined to reject the disturbance term $\xi(x,t)$ while in the sliding mode. The choice of the switching function as in [118] incorporates the nominal performance into the design procedure and is defined as

$$\sigma(x,t) = Gx(t) + z(t) \tag{3.43}$$

where $G \in \mathbb{R}^{m\times n}$ is design freedom. Since matrix B is of full rank, with the design of the switching matrix G it can be ensured that the matrix GB is nonsingular i.e. $\det(GB) \neq 0$. The second part $z(t)$ introduces the integral term in the switching function [118]. Now in the sequel the properties while the system is in the sliding mode are explored.

During sliding $\sigma(t) = \dot{\sigma}(t) = 0$ [41], so in order to obtain the expression for the equivalent control, the time derivative of (3.43) is

$$\dot{\sigma} = G\dot{x}(t) + \dot{z}(t) = 0 \tag{3.44}$$

Substituting the value of (3.42) into (3.44) gives:

$$\dot{\sigma} = G\Big(Ax(t) + Bu_o(t) + Bu_n(t) + BD\xi(x,t) + f_u(t,x)\Big) + \dot{z}(t) = 0 \tag{3.45}$$

To satisfy the condition $x(t) \equiv x_o(t)$ at all times $t > 0$ (when $f_u = 0$) while sliding, the value of $\dot{z}(t)$ should be selected as

$$\dot{z}(t) = -G(Ax(t) + Bu_o(t)), \quad z(0) = -Gx(0) \tag{3.46}$$

Substituting the value of $\dot{z}(t)$ into (3.45) gives,

$$\dot{\sigma} = G\Big(Ax(t) + Bu_o(t) + Bu_n(t) + BD\xi(x,t) + f_u(t,x)\Big) - G(Ax(t) + Bu_o(t)) \tag{3.47}$$

and the equivalent control expression can be written as

$$\begin{aligned} GBu_{n_{eq}}(t) &= -GBD\xi(x,t) - Gf_u(t,x) \\ u_{n_{eq}}(t) &= -(GB)^{-1}GBD\xi(x,t) - (GB)^{-1}Gf_u(t,x) \\ &= -D\xi(x,t) - (GB)^{-1}Gf_u(t,x) \end{aligned} \tag{3.48}$$

where $u_{n_{eq}}(t)$ is the equivalent control associated with $u_n(t)$. Substituting the value of equivalent control $u_{n_{eq}}(t)$ into equation (3.42) and after simplifying, the expression for the integral sliding mode becomes

$$\dot{x}(t) = Ax(t) + Bu_o(t) + \underbrace{(I - B(GB)^{-1}G)}_{\Gamma} f_u(t,x) \tag{3.49}$$

and define $f_{u_{eq}} := \Gamma f_u(t,x)$ as an equivalent uncertainty. From equation (3.49), it is straightforward to see that the the effect of the matched uncertainty has been completely rejected while in the sliding mode.

Remark 3.3: In the case when $f_u = 0$, the equation (3.49) will simplify to become

$$\dot{x}(t) = Ax(t) + Bu_o(t) \tag{3.50}$$

and the condition $x(t) \equiv x_o(t)$ will be satisfied i.e. the system state trajectories coincide with the nominal trajectories in the integral sliding mode. But if $f_u \neq 0$, the matrix Γ in (3.49) can

amplify the effect of unmatched uncertainty $f_u(t,x)$ and the system trajectories can deviate from the sliding surface.

The objective is to understand how the integral sliding surface can be designed to avoid the amplification of the unmatched uncertainty.

3.7.4 Integral Switching Surface

One of the key ideas behind an ISMC approach is to eliminate the reaching phase associated with the classical SMC approach explained earlier. Using equations (3.43) and (3.46), an integral switching function which eliminates the reaching phase is defined as [27], [28]

$$\sigma(x,t) = Gx(t) - Gx(0) - G\int_0^t \big(Ax(\tau) + Bu_o(\tau)\big)d(\tau) \tag{3.51}$$

The term $-Gx(0)$ achieves the property that $\sigma(x(0),t(0)) = 0$, so the reaching phase is eliminated [28]. The sliding mode will exist from the very beginning and the system will be robust throughout the closed-loop system response against matched uncertainties [119], [27]. In [28], a choice of G was proposed as

$$G = B^{\ddagger} = (B^T B)^{-1} B^T \tag{3.52}$$

which is the Moore-Penrose left pseudo inverse of the input distribution matrix B (with the assumption that B is of full rank).

Remark 3.4: From the previous analysis, it is clear that in the case of only matched uncertainty, then any choice of G which ensures GB is invertible is sufficient for the ISM design, but for unmatched uncertainty a specific choice of G is needed.

The advantages this particular choice of G in (3.52) brings are: the gain of the discontinuous control ρ is minimal i.e the amplitude of the chattering can be reduced; it helps not to amplify the unmatched disturbance when the ISM is combined with other techniques to have robustness against unmatched disturbance [28], and is demonstrated in the sequel. This choice of G has the

simplifying property that

$$GB = \underbrace{(B^T B)^{-1} B^T}_{G} B = I_m$$

which ensures that the square matrix GB is nonsingular. With the choice of G in (3.52), the matrix Γ in (3.49) becomes

$$\Gamma = I_n - BB^{\ddagger} \tag{3.53}$$

where $rank(BB^{\ddagger}) < n$, which means that $rank(\Gamma) = rank(I_n - BB^{\ddagger})$ can not be zero, and there must be at least one nonzero eigenvalue [28]. It can be verified that Γ in (3.53) is a symmetric matrix i.e.

$$\begin{aligned} \Gamma^T \Gamma &= [I_n - BB^{\ddagger}][I_n - BB^{\ddagger}] \\ &= I_n - BB^{\ddagger} = \Gamma \end{aligned}$$

and a symmetric matrix always has real eigenvalues. In [28], it was argued that $\|\Gamma\| = 1$, and is explained as follows: for each eigenvalue λ of Γ, there exists an eigenvector v such that

$$\Gamma v = \lambda v \Rightarrow v^T \Gamma^T \Gamma v = \lambda^2 \|v\|^2 \tag{3.54}$$

However from the fact that $\Gamma^T \Gamma = \Gamma$,

$$v^T \Gamma^T \Gamma v = v^T \Gamma v = \lambda \|v\|^2 \tag{3.55}$$

Using equations (3.54)–(3.55), it can be seen that relation $\lambda(\lambda - 1) = 0$ must be satisfied by the eigenvalues of Γ [28]. Consequently the eigenvalues are $\lambda = 0$ or $\lambda = 1$. Clearly $\lambda = 1$ is the maximum eigenvalue. Hence the choice of G in (3.52) ensures that $\|\Gamma\| = 1$, which means that the effect of f_u is not amplified i.e $f_{u_{eq}}$ is equivalent to f_u, which is assumed to be bounded.

3.7.5 Integral Sliding Mode Control Laws

An integral sliding mode controller will be designed based on the nominal system (3.39). The control law has a structure given by

$$u(t) = u_o(t) + u_n(t) \tag{3.56}$$

where, $u_o(t)$ is the linear part of the controller, and $u_n(t)$ is the discontinuous part to enforce the sliding mode along the sliding surface (3.51). Hence the physical control law $u(t)$ can be written as

$$u(t) = -Fx(t) - \rho(GB)^{-1}\frac{\sigma}{\|\sigma\|} \qquad \text{for}\, \sigma \neq 0 \tag{3.57}$$

where F is the state feedback controller, which is responsible for the performance of nominal system and ρ is the controller gain to enforce the sliding mode and whose precise value is given in the next subsection.

Remark 3.5: For a single input system, the ISM control law in (3.57) can be written as

$$u(t) = -Fx(t) - \rho(GB)^{-1}sgn(\sigma) \qquad \text{for}\, \sigma \neq 0 \tag{3.58}$$

3.7.6 The Reachability Condition

To justify that the controller designed in (3.57) satisfy the η-reachability condition (3.24), which is a sufficient condition to ensure the existence of an ideal sliding motion, the time derivative of (3.51) is

$$\dot{\sigma} = G\dot{x}(t) - GAx(t) - GBu_o(t) \tag{3.59}$$

Substituting the value of (3.38) and (3.40), it follows that

$$\dot{\sigma} = G\Big(Ax(t) + Bu(t) + BD\xi(t,x) + f_u(t,x)\Big) - GAx(t) + GBFx(t)$$

Furthermore by substituting the value of (3.57) and after some simplification it becomes

$$\begin{aligned}\dot{\sigma} &= GAx(t) + GB\left(-Fx(t) - \rho(GB)^{-1}\frac{\sigma}{\|\sigma\|}\right) + GBD\xi(t,x) + Gf_u(t,x) - GAx(t) + GBFx(t) \\ &= -\rho\frac{\sigma}{\|\sigma\|} + GBD\xi(t,x) + Gf_u(t,x) \end{aligned} \tag{3.60}$$

Now by choosing a positive definite Lyapunov candidate function as

$$V(\sigma) = \frac{1}{2}\sigma^T\sigma \tag{3.61}$$

which characterizes the system state trajectories on the sliding surface. Taking the time derivative of (3.61) along the system state trajectories and substituting the value of (3.60) into it gives

$$\begin{aligned}\dot{V}(\sigma) &= \sigma^T\dot{\sigma} \\ &= -\rho\|\sigma\| + \sigma^T D\xi(t,x) + \sigma^T G f_u(t,x) \\ &\leq \|\sigma\|(-\rho + \|D\xi(t,x)\| + \|Gf_u(t,x)\|) \end{aligned} \tag{3.62}$$

where the fact $GB = I_m$, has been used. In order to enforce the sliding mode the value of the nonlinear controller gain ρ should be greater than any disturbance or uncertainty in the system, therefore with the choice of ρ which satisfies

$$\rho \geq \|D\|\|\xi(t,x)\| + \|G\|\|f_u(t,x)\| + \eta \tag{3.63}$$

where η is some positive scalar, then the inequality in (3.62) after substituting the value of ρ from (3.63) becomes

$$\dot{V}(\sigma) \leq -\eta||\sigma|| \tag{3.64}$$

The inequality in (3.64) is a standard η-reachability condition [41], which implies that the ideal sliding motion is maintained for all the time.

3.7.7 Properties of Integral Sliding Mode

The properties of integral sliding modes can be summarized as follows:

1. there is no reaching phase [118], *i.e* a sliding mode is enforced throughout the entire system response;
2. during the sliding mode, the order of the motion equation is the same as the original system [119];
3. By a suitable choice of sliding surface, the effect of unmatched uncertainty can be ameliorated;
4. during sliding mode, system motion is invariant to matched uncertainties [118], [41].
5. the ISM approach has the ability to be retro-fitted to an existing feedback controller.

3.7.8 Simulation Example

Here in this section, to make a direct comparison, the same simulation scenario of a spring-mass-damper system considered in early sections will be simulated and reproduced here as

$$\begin{bmatrix} \dot{x}_1(t) \\ \dot{x}_2(t) \end{bmatrix} = \underbrace{\begin{bmatrix} 0 & 1 \\ -2 & -3 \end{bmatrix}}_{A} \begin{bmatrix} x_1(t) \\ x_2(t) \end{bmatrix} + \underbrace{\begin{bmatrix} 0 \\ 1 \end{bmatrix}}_{B} (u(t) + 0.1sin(x_1(t)))$$

The objective here is to design an ISM controller to bring the system back to the equilibrium position from the initial conditions without overshooting in terms of displacement and with a settling time not more than 6 seconds. To begin with the ISM controller design, the integral switching function, from equation (3.51) is

$$\sigma(x,t) = Gx(t) - Gx(0) - G\int_0^t \big(A - BF\big)x(\tau)d(\tau)$$

where the value of G is chosen as in (3.52) and is equal to

$$G = (B^T B)^{-1} B^T = \begin{bmatrix} 0 & 1 \end{bmatrix}$$

The gain F in this example has been designed using the linear quadratic regulator (LQR) method, which aims to regulate the system states to the origin by minimizing the cost function

$$J = \int_0^\infty (x(t)^T Q x(t) + u_o(t)^T R u_o(t)) dt \tag{3.65}$$

where R and Q are symmetric positive definite $s.p.d.$ matrices which penalize the magnitude of the control signal $u_o(t)$ and the deviation of the system states from the origin respectively. Here the values of Q and R metrics as chosen as $Q = diag\{1, 0.5\}$ and $R = 1$, which results in the matrix F as

$$F = \begin{bmatrix} 0.2361 & 0.1579 \end{bmatrix}$$

Now as a second step, considering the ISM control law for a single input system (3.58) as

$$u(t) = -Fx(t) - \rho(GB)^{-1} sgn(\sigma) \qquad \text{for } \sigma \neq 0 \tag{3.66}$$

where the choice of G makes sure that $GB = 1$. By using similar arguments of reachability condition as mentioned before, it is easy to check that the control law $u(t)$ satisfies the reachability condition $\sigma\dot{\sigma} \leq -\rho|\sigma|$. In this section, the fractional approximation given in (3.37) as shown in Figure 3.3 is used, therefore the ISM control law in (3.66) will be modified to become

$$u(t) = -Fx(t) - \rho(GB)^{-1} \frac{\sigma}{|\sigma| + \delta} \tag{3.67}$$

where the value of a small positive scalar δ is chosen as $\delta = 0.0001$, to eliminate the chattering or high frequency switching, and the control law $u(t)$ after substituting the value of F can be

written as

$$u(t) = -0.2361x_1(t) - 0.2361x_2(t) - \rho\frac{\sigma}{|\sigma| + \delta}$$

The displacement plots in Figures 3.5–3.6 show that the design requirements (which are to

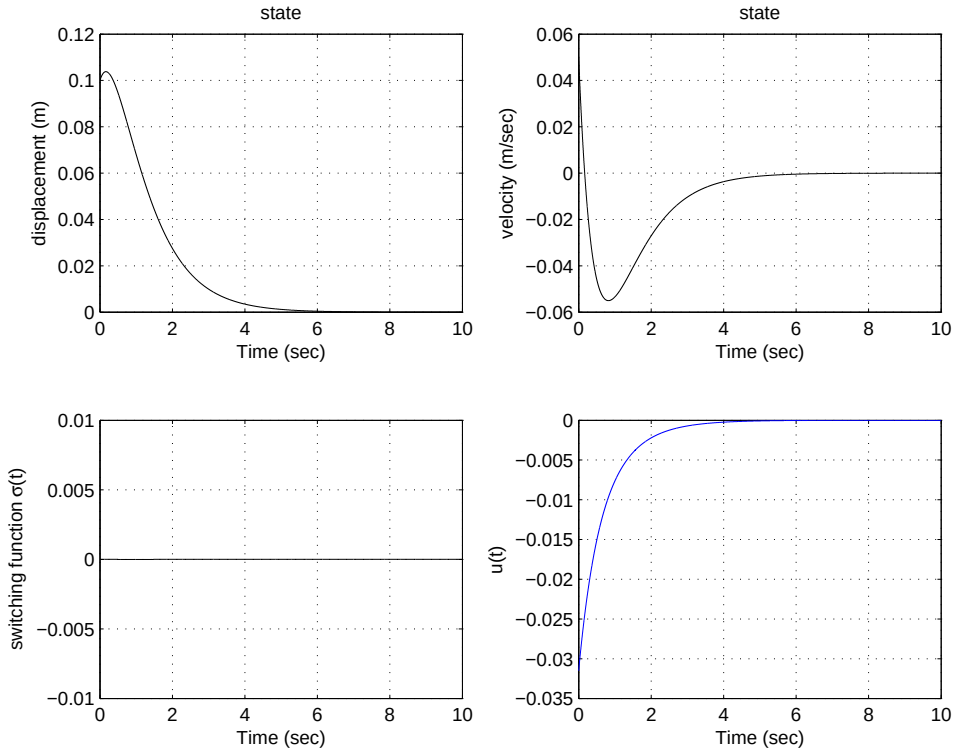

Figure 3.5: Simulation results for the SMDS nominally (with ISMC)

bring the system back to the equilibrium position without overshoot and have a settling time of not more than 6 seconds) are met both nominally (without disturbance) and in the presence of disturbance term. From Figure 3.6, it is clear that the effect of the disturbance $0.1sinx_1(t)$ is completely rejected, whilst achieving the same design requirements. In the switching function plots of Figures (3.5–3.6), it is demonstrated that there is no reaching phase i.e. the sliding mode starts from the beginning.

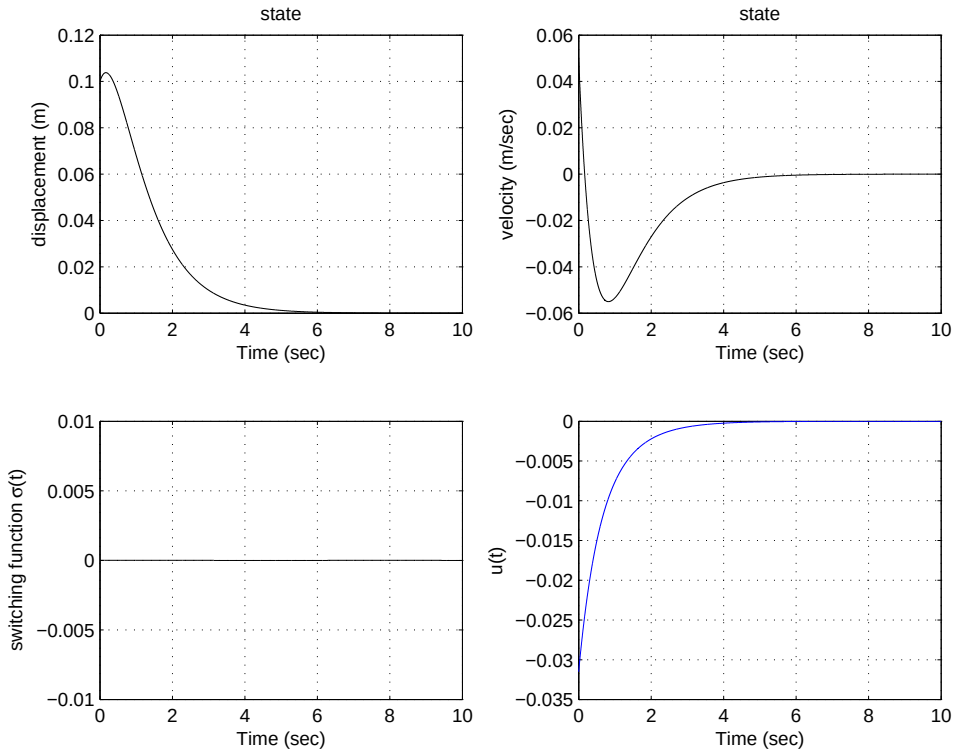

Figure 3.6: Simulation results for the SMDS with disturbance (with ISMC)

3.8 Output Integral Sliding Mode Control

In the early sections of this Chapter, it was assumed that the state information of the plant is available in order to design a state feedback control law. In this section such an assumption is relaxed and the ISM ideas discussed before are extended for the systems where only the measured system output is available i.e. the full state information is not known. To cope with such situation one possibility is to construct a state observer based on the plant model [41], [29], [15], [66] to be considered in order to estimate the system states, such that the estimated states converge to the true states in a finite time.

Considering an extension, the design steps for the ISM controller design are the same, but the sliding surface is based on the plant output information which is available in this case. Recently in [29], the state dependent ISM ideas reported in [27] were extended for the systems where only the system output information was available and a full-order linear unknown input observer was incorporated in the design to estimate the real plant states considering both matched and

unmatched uncertainty, where as in [15] an output dependent ISM scheme was considered for the systems with matched uncertainties, and argued that for the systems where $p \leq m$, the closed-loop dynamics lose observability. Recently in [47], the output ISM ideas of [15] were applied on the inverted stewart platform in the presence of permanent disturbance (wind), which is normally used for surveillance purposes.

In order to explain the design procedure, consider an uncertain LTI system as in (3.38),

$$\begin{aligned} \dot{x}(t) &= Ax(t) + Bu(t) + BD\xi(t,x) + f_u(t,x) \\ y(t) &= Cx(t) \end{aligned} \tag{3.68}$$

where $C \in \mathbb{R}^{p\times n}$ is the output distribution matrix with the assumption that $rank(C) = p$, with $1 \leq p < n$ and $p \geq m$. In this section, it is assumed that

A1 The pair (A, B) is controllable.

A2 $rank(CB) = rank(B) = m$.

A2 The pair (C,A) is observable.

Arguing as before it is assumed that a nominal controller $u_o(t)$ achieving the desired performance is already available. Having only the information of plant output, the ISM control law can be designed by defining first the ISM sliding function as [29],

$$\sigma(t) = Gy(t) - Gy(0) - \int_0^t u_o(\tau)d\tau \tag{3.69}$$

where $G \in \mathbb{R}^{m\times p}$ is a design freedom and must be designed such that $\det(GCB) \neq 0$. A choice of G proposed in [15] ensuring $GCB = I_m$ is given by

$$G = (CB)^{\ddagger} = ((CB)^T(CB))^{-1}(CB)^T \tag{3.70}$$

where $(CB)^{\ddagger}$ is the Moore-Penrose left pseudo inverse of CB. Since $\sigma(0) = 0$, suppose an ISM control law exists which can guarantee $\sigma(t) = \dot{\sigma}(t) = 0$ starting from the beginning. By taking the time derivative of (3.69) along the system trajectories and substituting (3.68) into it yields

$$\begin{aligned}\dot{\sigma}(t) &= G\dot{y}(t) - u_o(t) \\ &= GC(Ax(t) + Bu(t) + BD\xi(t,x) + f_u(t,x)) - u_o(t) \\ &= GCAx(t) + u(t) + D\xi(t,x) + GCf_u(t,x) - u_o(t) \end{aligned} \tag{3.71}$$

Equating $\dot{\sigma}(t) = 0$ and solving for the equivalent control $u_{eq}(t)$ yields

$$u_{eq}(t) = -GCAx(t) - D\xi(t,x) - GCf_u(t,x) + u_o(t) \tag{3.72}$$

The expression for the sliding motion can be obtained by substituting the equivalent control into (3.68) to get

$$\begin{aligned}\dot{x}(t) &= Ax(t) + B\big(-GCAx(t) - D\xi(t,x) - GCf_u(t,x) + u_o(t)\big) + BD\xi(t,x) + f_u(t,x) \\ &= Ax(t) - BGCAx(t) + Bu_o(t) - BGCf_u(t,x) + f_u(t,x) \\ &= (I_n - BGC)Ax(t) + Bu_o(t) + (I_n - BGC)f_u(t,x) \end{aligned} \tag{3.73}$$

By defining the matrix $A_c := (I_n - BGC)A$ and $E := (I_n - BGC)$, the sliding mode equation (3.73) can be written as

$$\dot{x}(t) = A_c x(t) + Bu_o(t) + Ef_u(t,x) \tag{3.74}$$

In [29], it is argued that the feedback control input $u_o(t)$ should be designed such that when the system is in the sliding mode, robust disturbance attenuation against $f_u(t,x)$ can be achieved. With the definition of the error signal $e(t) = x(t) - \hat{x}(t)$, the control input $u_o(t)$ is defined as

$$u_o(t) = -F\hat{x}(t) = -Fx(t) + Fe(t) \tag{3.75}$$

where $\hat{x}(t)$ is an estimated state vector. The details of how an estimated state vector can be obtained together with closed-loop stability analysis are given in Chapter 8. Substituting (3.75) into (3.74) gives

$$\dot{x}(t) = A_c x(t) - BFx(t) + BFe(t) + E f_u(t,x) \tag{3.76}$$

Furthermore to enforce the sliding mode (motion on the sliding surface $\sigma(t) = 0$) and thereafter to maintain it from the beginning, define an ISM control law as

$$u(t) = -F\hat{x}(t) - \rho\frac{\sigma}{||\sigma||} \tag{3.77}$$

To validate that the control law in (3.77), ensures that the reachability condition is satisfied, substitute $u(t)$ into (3.71), and exploiting the fact that $e(t) = x(t) - \hat{x}(t)$ yields

$$\begin{aligned}
\dot{\sigma}(t) &= GCAx(t) - F\hat{x}(t) - \rho\frac{\sigma}{||\sigma||} + D\xi(t,x) + GC f_u(t,x) + F\hat{x}(t) \\
&= -\rho\frac{\sigma}{\|\sigma\|} + GCAx(t) + D\xi(t,x) + GC f_u(t,x) \\
&= -\rho\frac{\sigma}{\|\sigma\|} + GCA\hat{x}(t) + GCAe(t) + D\xi(t,x) + GC f_u(t,x) \\
\sigma^T\dot{\sigma} &= -\rho\|\sigma\| + \sigma^T\left(GCA\hat{x}(t) + GCAe(t) + D\xi(t,x)) + GC f_u(t,x)\right) \\
\sigma^T\dot{\sigma} &\leq -\rho\|\sigma\| + \|\sigma\|(\|GCA\|(\|\hat{x}(t)\| + \|e(t)\|) + \|D\|\|\xi(t,x)\| + \|GC\|\|f_u(t,x)\|)
\end{aligned} \tag{3.78}$$

where the reachability condition $\sigma^T\dot{\sigma} \leq -\eta||\sigma||$, can be satisfied if the modulation gain $\rho(t)$ is selected as

$$\rho(t) \geq \|GCA\|(\|\hat{x}(t)\| + \|e(t)\|) + \|D\|\|\xi(t,x)\| + \|GC\|\|f_u(t,x)\| + \eta \tag{3.79}$$

But the gain in (3.79) cannot be realized because the bound of the signal $\|e(t)\|$ is not known. In [15], it is argued that if the error signal $e(t)$ is exponentially stable, then there exist the

constants ε, μ such that

$$\begin{aligned} \|e(t)\| &\leq \varepsilon e^{-\mu(t)}\|e(0)\| \\ &\leq \varepsilon e^{-\mu(t)}(\eta + \|\hat{x}(0)\|) \end{aligned} \tag{3.80}$$

where $\hat{x}(0)$ is the initial condition of the estimated state vector and η is some positive scalar. Therefore in the expression of $\rho(t)$ in (3.79) the bound on $\|e(t)\|$ can be replaced by the expression in (3.80). The reachability condition is sufficient to guarantee that the sliding motion is maintained for all the subsequent time.

Due to a very little work on ISM in terms of FTC, and by considering the ISMC properties mentioned in this Chapter, there is a scope to design controllers which provide robustness and tolerance against actuator faults or failures throughout the entire closed-loop system response.

3.9 Sliding Modes as a candidate for FTC

Sliding mode based control schemes, could be a strong candidate for FTC purpose, because of the inherent advantages against matched uncertainties and the special properties as explained in the early sections of this Chapter. It has already been explained in the Fault Tolerant Control Chapter that the actuator faults can be effectively modeled as matched uncertainties, therefore sliding mode based control schemes have the capability to directly deal with the actuator faults. The researchers for example in [126], [62], [122], [106], [105] have already documented SMC as a potential candidate for FTC. In [62], [126], it was argued that SMC could deal with large and sudden changes in the system dynamics due to actuator faults and has the capability to become an alternative to reconfigurable systems, where as in [122], the SMC technique was used to ensure the stability of a damaged aircraft (where effectiveness of the actuators were reduced by 50%). However actuator failures cannot be handled directly by the sliding modes schemes, because the complete loss of effectiveness of a channel destroys the regularity of the sliding mode, and a unique equivalent control signal can no longer be determined. Also in the case of a

failure the actuator is not able to respond to control signals, and a redundant actuator is required to accomplish the job. Redundancy is the key parameter in order to tolerate the actuator failure. In the subsequent Chapters, Control allocation (as discussed in Chapter 2) is considered as a potential candidate to be combined with ISM control to deal with actuator faults or failures due to its ability to effectively manage the actuator redundancy and to redistribute the control signals to the healthy actuators in the case of actuator failure without reconfiguring the underlying controller. An obvious difference between the FTC schemes proposed in this thesis as compared to [3] is the use of integral sliding mode control to design the underlying controller instead of 'classical' SMC based methods. The use of integral sliding modes ensures robustness against the matched uncertainties starting from the beginning by eliminating the reaching phase associated with 'classical' SMC based methods. Integral sliding modes have the capacity to be retrofitted to the existing controller design to introduce fault tolerance without changing or altering the existing control loops, which is advantageous in an industrial perspective. The closed-loop stability analysis in [3] requires a 'synthesis-followed-by-analysis' procedure, whereas the synthesis and analysis is totally integrated in this thesis. Multiple actuator faults/failures can also be handled using this idea. The potential features of this combination will be exploited in the coming Chapters to design various novel robust FTC schemes to deal with actuator faults/failure without the need to reconfigure the underlying controller.

3.10 Conclusion

This Chapter has focused on describing detailed design procedures for 'classical' SMC based controllers and subsequently integral sliding modes approaches for controller design. The inherent robustness properties while in the sliding mode against matched disturbances were examined, and necessary conditions for the existence of a sliding mode were discussed to check the validity of the control law. The integral sliding mode scheme has the capability to ensure the robustness against matched uncertainties throughout the entire closed-loop system response. To deal with bounded unmatched uncertainties a special choice of sliding surface was discussed,

which help not to amplify the effect of unmatched uncertainty, while rejecting the effect of matched ones. From the FTC viewpoint, the insensitivity property of sliding mode controllers against matched uncertainties is very attractive, and will be exploited in the coming Chapters.

Chapter 4

Design and Analysis of an Integral Sliding Mode Fault Tolerant Control Scheme

In this Chapter a new fault tolerant control scheme is proposed, where the ideas of integral sliding modes (ISM) presented in Chapter 3 are incorporated with a control allocation scheme documented in Chapter 2 (Section 2.4.2.2) to cope with actuator faults and the total failure of certain actuators, under the assumption that actuator redundancy is available in the system. The proposed scheme uses the estimated effectiveness level of the actuators to redistribute the control signals to healthy actuators without reconfiguring the ISM controller. A relative error in the estimation of actuator redundancy is taken into account in the closed-loop stability analysis. The effectiveness of the proposed scheme against faults or failures is tested in simulation based on a large transport aircraft model.

4.1 Introduction

As discussed in Chapter 2, one of the important elements necessary for achieving FTC, is the availability of redundant actuators. This provides increased freedom in terms of controller design to mitigate the effects of faults and failures. Although these 'redundant' actuators are often designed for different purposes, in the event of an emergency (such as faults or failures to the

primary actuators), they can be used to retain satisfactory performance.

This Chapter is concerned with the development of fault tolerant controllers for a class of linear systems having redundant actuators. This redundancy in the system will be exploited to achieve tolerance to a specified class of faults/failures, which includes the possibility of total failure to certain primary actuators. The precise class of total actuator failure which can be accommodated is identified. A novel control scheme is proposed in this Chapter, which involves a combination of control allocation as discussed in Chapter 2 (Section 2.4.2.2) and integral sliding mode techniques which are explained in Chapter 3. In aircraft systems for example, the idea is to design a controller based on a 'virtual' system which provides the desired moments about the centre of mass [60]. The virtual control signal is then translated into actual control surface deflections using CA. This distinctive design strategy is beneficial since only one controller is designed to cover a wide range of fault/failure cases, while the CA redistributes the signals to the available 'healthy' actuators.

The novel combination of integral sliding modes and CA considered in this Chapter, allows total *failures* of a certain subset of the actuators (as well as faults in all actuators) to be accounted for. (Sliding mode systems as explained in (Section 3.9), in common with other traditional feedback systems, are not capable of mitigating total actuator failures without some form of reconfiguration/accommodation). The proposed scheme uses the measured or estimated effectiveness level of the actuators to redistribute the control effort during faults/failures to maintain close to nominal closed-loop performance without reconfiguring the controller. In the proposed scheme a relative error in the estimation of actuator effectiveness gains is also taken into consideration. Furthermore the stability test proposed in this Chapter allows a more effective *synthesis procedure* to be employed using Linear Matrix Inequalities (LMI) optimization to compute the parameters involved in the control law.

4.2 System description and problem formulation

In Chapter 3 (Sections 3.2 and 3.7.3) it has been shown that the sliding mode based schemes are inherently robust against matched uncertainties. In this section these ideas are used to deal with actuator faults which can be effectively medelled as matched uncertainties. In Section 2.1.1 different models representing actuator faults or failures are discussed. A multiplicative fault model given in equation (2.1) is considered here because a multiplicative fault model is a natural way to represent the actuator faults or failures and in addition it makes the closed-loop stability analysis simple (which is demonstrated in the sequel). In case of an actuator failure, using the model in equation (2.1), the relevant column of the input matrix B is nullified, and the control component $u_i(t)$ has no effect on the system dynamics. The fault model given in equation (2.2) replaces the control component u_i with the uncontrollable offset vector $\bar{u_i}(t)$ in the failure of an ith actuator, which can be treated as a disturbance.

An LTI system with actuator faults or failures discussed in equation (2.1) is

$$\dot{x}(t) = Ax(t) + BW(t)u(t) \tag{4.1}$$

where $A \in \mathbb{R}^{n\times n}$, $B \in \mathbb{R}^{n\times m}$, and $W(t) = diag\{w_1(t), .., w_m(t)\}$ is a diagonal matrix. The pair (A, B) is assumed to be controllable. The time varying scalars $w_1(t), .., w_m(t)$ model the effectiveness level of the actuators. As mentioned in Section 2.1.1, if $w_i(t) = 1$, it means that the ith actuator has no fault (100% healthy actuator) and is working perfectly, whereas if $1 > w_i(t) > 0$, an actuator fault is present $i.e.$ the actuator functions with reduced capability. If $w_i(t) = 0$, actuator i has completely failed and the control input component u_i has no effect on the system dynamics. The matrix W will be termed the efficiency matrix indicating the health level of each actuator. Associate with (4.1) a set of controlled outputs

$$y_c(t) = Cx(t) \tag{4.2}$$

where $C \in \mathbb{R}^{l\times n}$ and $l < m$. The variables $y_c(t)$ are required to respond to desired (external)

commands. In terms of 'controlling' these outputs only l independent actuators are sufficient to induce the required closed-loop performance (for example see the aircraft example). The remaining $m-l$ actuators constitute redundancy and can be exploited to achieve fault tolerance. In this Chapter an estimate of the actuator efficiency, $\widehat{W}(t) = diag\{\hat{w}_1(t),..,\hat{w}_m(t)\}$, where the scalars $0 \leq \hat{w}_i(t) \leq 1$, will be used explicitly in the control law. One way to obtain an estimate of the actuator efficiency is by using a measurement of the actual actuator deflection compared to the demand. Such information is typically available in many safety critical systems e.g. passenger aircraft [22]. In other situations $\widehat{W}(t)$ would need to be provided by an FDI scheme, see for example [131], [127], [5]. It is important to note that whatever method is employed the estimate $\widehat{W}(t)$ will not be perfect and in this Chapter the difference between the actual efficiency matrix $W(t)$, and its estimate $\widehat{W}(t)$ is assumed to satisfy

$$W(t) = (I - \triangle(t))\widehat{W}(t) \tag{4.3}$$

where the 'uncertainty' $\triangle(t) = diag\{\delta_1(t),...\delta_m(t)\}$ represents the estimation error. The unknown scalars $\delta_1(t),..,\delta_m(t)$ model the level of imperfection in the fault estimation. The effect of this imperfection will be analyzed later in the Chapter. In this Chapter a virtual control concept [60] for resolving actuator redundancy will be employed. In Chapter 2 (equation 2.10) it is shown that the input distribution matrix B can be factorized into two matrices (i.e. $B = B_v B_u$, where $B_v \in \mathbb{R}^{n\times k}$ and $B_u \in \mathbb{R}^{k\times m}$ and both have $rank\ k < m$). This factorization is only possible if $rank(B) = k < m$ [60]. In many actuator redundant systems (as mentioned in the simulation part), this condition is not satisfied[1]. However reordering of the states is possible, and the input distribution matrix B can be partitioned as:

$$B = \begin{bmatrix} B_1 \\ B_2 \end{bmatrix} \tag{4.4}$$

where $B_1 \in \mathbb{R}^{(n-l)\times m}$, $B_2 \in \mathbb{R}^{l\times m}$ *of rank* $l < m$. *Suppose that by design of the partition in (4.4),*

[1] In equation (4.55), $rank(B) = 3$ and l which is associated with B_2 in (4.4) is $rank(B_2) = l = 2$.

the pair (A, B_v) *where* $B_v = BB_2^T$ *is controllable*. The partition in equation (4.4) is following the notion of splitting the control law from the control allocation [59] as can be seen in Figure 4.1. In aircraft systems, for example the partition B_2 can be associated with the equation of angular accelerations in pitch, roll and yaw [60], because *the control objectives in (most) aircraft systems can be obtained by commanding the desired moment which to are be obtained by the control surfaces [59]*. The partition of matrix B is such that the elements of B_2 have large magnitude compared to $||B_1||$, so that B_2 represents the dominant contribution of the control action on the system compared to B_1 [6]. Although this is a restriction, aircraft systems often satisfy such a constraint. By hypothesis $\|B_1\|$ is assumed to be small, because it has a direct impact on the closed-loop stability analysis (Section 4.3.2). To create this separation, a permutation of the states must usually be undertaken. The virtual control input is defined as

$$\nu(t) := B_2 u(t) \tag{4.5}$$

where $\nu(t) \in \mathbb{R}^l$ can be interpreted as the total control effort produced by the actuators [60]. Once the partition of B in (4.4) has been achieved, scale the states so that $B_2 B_2^T = I_l$ i.e $\|B_2\| = 1$. This can be achieved without loss of generality, because $rank(B_2) = l$. The physical control signal $u(t)$ sent to the actuators can be determined from equation (4.5) as

$$u(t) = B_2^{\dagger,\widehat{W}(t)} \nu(t) \tag{4.6}$$

where $B_2^{\dagger,\widehat{W}(t)} \in \mathbb{R}^{m\times l}$ is a weighted right pseudo-inverse of the matrix B_2. Thus the matrix $B_2^{\dagger,\widehat{W}(t)}$ provides some design freedom and 'distributes' the virtual control signal to the physical actuators via (4.6). As mentioned before in Chapter 2, different researchers utilize the design freedom in the pseudo inverse matrix in different ways [60], [6]. A generic choice of $B_2^{\dagger,\widehat{W}(t)}$ such that $B_2 B_2^{\dagger,\widehat{W}(t)} = I_l$ is

$$B_2^{\dagger,\widehat{W}(t)} = \widehat{W}(t) B_2^T (B_2 \widehat{W}(t) B_2^T)^{-1} \tag{4.7}$$

assuming $\det(B_2 \widehat{W}(t) B_2^T) \neq 0$.

Remark 4.1: In the special case when there are no faults present in the system i.e. $\widehat{W}(t) = I_m$, then the weighted right pseudo inverse matrix $B^{\dagger,\widehat{W}(t)}$ in (4.7) using the fact that $B_2 B_2^T = I_l$, simplifies to $B_2^{\dagger,\widehat{W}(t)} = B_2^T$. This means the physical control law in (4.6) will become

$$u(t) = B_2^T v(t) \tag{4.8}$$

The overall control structure of the proposed scheme to better explain how the integral sliding modes and control allocation techniques relate, a block diagram is presented in Figure 4.1, where the virtual control signal $v(t)$ is designed by using the integral sliding mode control which is translated into actual control signal $u(t)$ by using the control allocation with the knowledge of estimated $\widehat{W}$ matrix.

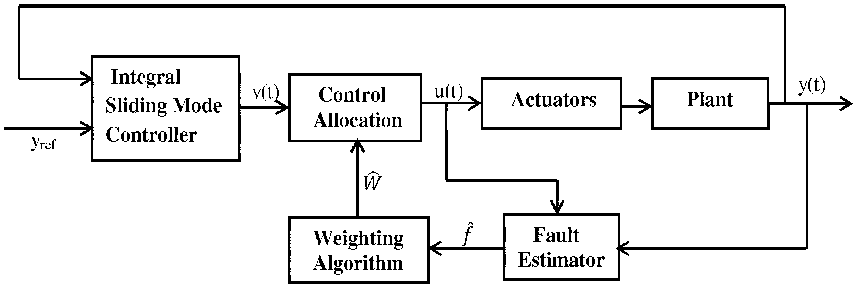

Figure 4.1: Schematic of the Overall Control Strategy

In Figure 4.1, it is assumed that the *Fault Estimator* is able to identify the *actuator* faults/failures from all other possible faults/failures in the system. Now in order to clarify the set of faults or failures the scheme proposed in this Chapter can tolerate, define the set

$$\mathscr{W} = \{(\hat{w}_1, .., \hat{w}_m) \in \underbrace{[0 \quad 1] \times ... \times [0 \quad 1]}_{m \text{ times}} : \det(B_2 \widehat{W} B_2^T) \neq 0\} \tag{4.9}$$

Because $l < m$, it is possible that $\det(B_2 \widehat{W} B_2^T) \neq 0$ even if up to $m-l$ of the entries $\hat{w}_i(t) = 0$ in the matrix $\widehat{W}(t)$: in other words, potentially up to $m-l$ can totally fail and yet $\det(B_2 \widehat{W} B_2^T) \neq 0$. However if more than $m-l$ entries are zero, then $\text{rank}(\widehat{W}(t)) < l$ and $\det(B_2 \widehat{W} B_2^T) = 0$. The set $\mathscr{W}$ will be shown to constitute the faults/failures for which closed-loop stability can be

maintained.

Substituting (4.6) into (4.1) and using (4.7) results in

$$\dot{x}(t) = Ax(t) + \begin{bmatrix} B_1(I-\triangle(t))\widehat{W}^2(t)B_2^T(B_2\widehat{W}(t)B_2^T)^{-1} \\ B_2(I-\triangle(t))\widehat{W}^2(t)B_2^T(B_2\widehat{W}(t)B_2^T)^{-1} \end{bmatrix} \nu(t) \tag{4.10}$$

with

$$\hat{\nu}(t) := (B_2\widehat{W}^2(t)B_2^T)(B_2\widehat{W}(t)B_2^T)^{-1}\nu(t) \tag{4.11}$$

then (4.10) can be written as

$$\dot{x}(t) = Ax(t) + \underbrace{\begin{bmatrix} B_1(I-\triangle(t))B_2^{\dagger,\widehat{W}^2(t)} \\ B_2(I-\triangle(t))B_2^{\dagger,\widehat{W}^2(t)} \end{bmatrix}}_{\widehat{B}(t)} \hat{\nu}(t) \tag{4.12}$$

where

$$B_2^{\dagger,\widehat{W}^2(t)} := \widehat{W}^2(t)B_2^T(B_2\widehat{W}^2(t)B_2^T)^{-1} \tag{4.13}$$

Notice that $B_2^{\dagger,\widehat{W}^2(t)}$ is a weighted right pseudo inverse of B_2 since $B_2B_2^{\dagger,\widehat{W}^2(t)} = I_l$, for all $\widehat{W}(t) \in \mathscr{W}$. Furthermore in the special case when $\widehat{W}(t) = I$, then $B_2^{\dagger,\widehat{W}^2(t)} = B_2^T(B_2B_2^T)^{-1} = B_2^T$. Note that whilst the pseudo inverse $B_2^{\dagger,\widehat{W}(t)}$ defined in (4.7) is used for control allocation, the pseudo inverse $B_2^{\dagger,\widehat{W}^2(t)}$ defined in (4.13) plays a significant role in the closed-loop analysis which will be demonstrated in the sequel.

For the closed-loop stability analysis, the upper bound on the norm of the weighted pseudo inverse $B_2^{\dagger,\widehat{W}^2(t)}$ is required. In [111], the properties of pseudo inverses are detailed, and showed that for a full column rank matrix X, and a diagonal matrix W with positive scalars, the weighted left pseudo inverse of X, defined by $X^{\dagger,W} = (X^TWX)^{-1}X^TW$ is norm bounded by some number that is independent of W. In this Chapter, the ideas of [111] are used which follows: there exists

a scalar γ_o such that

$$\|B_2^{\dagger,\widehat{W}^2(t)}\| = \|\widehat{W}^2(t)B_2^T(B_2\widehat{W}^2(t)B_2^T)^{-1}\| < \gamma_o \tag{4.14}$$

for all $(\hat{w}_1(t),..,\hat{w}_m(t)) \in \mathscr{W}$. The upper bound on the norm of $B_2^{\dagger,\widehat{W}^2(t)}$ in (4.14) follows from the result in [111], where the weighted left pseudo inverse was used. But due to the fact that $(B_2^{\dagger,\widehat{W}^2(t)})^T = (B_2^T)^{\dagger,\widehat{W}^2(t)}$, therefore the result in (4.14) agrees with [111].

In the case when the estimates of the efficiency matrix are perfect (i.e. $\triangle(t) = 0$), and when there are no faults present (i.e. $\widehat{W}(t) = I$), equation (4.12) simplifies to

$$\dot{x}(t) = Ax(t) + \underbrace{\begin{bmatrix} B_1B_2^T \\ I_l \end{bmatrix}}_{B_v} \nu(t) \tag{4.15}$$

since $B_2^{\dagger,\widehat{W}^2(t)}|_{\widehat{W}(t)=I} = B_2^T$. The nominal fault free equation (4.15) will be used to *design* the control scheme. During faults or failures the inherent properties of integral sliding modes will be replied upon. *Since the pair (A,B_v) associated with (4.15) is assumed to be controllable*, then there exists a state feedback controller $\nu(t) = -Fx(t)$, so that the nominal system

$$\dot{x}(t) = (A - B_vF)x(t) \tag{4.16}$$

is stable. The state feedback controller can be designed to achieve optimality against some appropriate criteria. The choice of the matrix F will be discussed in the sequel.

4.3 Integral Sliding Mode Controller Design

This section, develops a systematic design procedure for the synthesis of an ISM controller. As mentioned before in Chapter 3, there are two steps to design an ISM controller, first a sliding surface is designed, and then in the second step, a control law to induce and maintain a sliding

motion is created.

4.3.1 Integral-type switching surface design

The ideas of integral sliding surface suggested by [28] as discussed in Chapter 3 will be used here for the system in (4.15) associated with the virtual control of input $v(t)$. The sliding surface is defined by the set:

$$\mathscr{S} = \{x \in \mathbb{R}^n : \quad \sigma(x,t) = 0\} \tag{4.17}$$

where the switching function $\sigma(x,t) \in \mathbb{R}^l$ is defined as

$$\sigma(x,t) := Gx(t) - Gx(0) - G\int_0^t \big(A - B_v F\big)x(\tau)d\tau \tag{4.18}$$

and $G \in \mathbb{R}^{l\times n}$ is design freedom. Arguing as before in Chapter 3, at $t = 0$, the switching function $\sigma(x(0),0) = 0$, and hence the reaching phase is eliminated. In Chapter 3, it has been shown that, in case of matched uncertainty (see for example) [119], that the sliding motion associated with (4.18) is always nominally governed by $(A - B_v F)$ independent of the choice of G, but the effects of unmatched uncertainty cannot be rejected while in the sliding motion. Recently an approach was suggested for the selection of G which attempts to ameliorate the effects of unmatched uncertainty [28] while in the sliding mode and is discussed in Chapter 3. In this Chapter

$$G := B_2(B^TB)^{-1}B^T \tag{4.19}$$

is suggested. Notice that since by definition $B_v = BB_2^T$, this choice of G in (4.19) has the property that

$$GB_v \quad = \quad B_2(B^TB)^{-1}B^TBB_2^T \;=\; B_2B_2^T = I_l$$

and so is a specific choice of a left-pseudo inverse of B_v which parallels the suggestion in [28] given in equation 3.52

Remark 4.2: The choice of G in equation 3.52, is the left-pseudo inverse of input matrix B, and ensures that while in the sliding mode the impact of unmatched uncertainty will not amplify. With the choice of G in (4.19) generically $G\widehat{B}(t) = I_l - B_2 \triangle(t) B_2^T$ creates a symmetric matrix. The symmetry is important and simplifies much of the subsequent analysis and avoids the introduction of conservatism. Also nominally, when there are no faults and $W(t) = I$, from the special properties of the matrix B_2, it follows that $G\widehat{B}(t)|_{W=I} = B_2 B_2^T = I$. This means, nominally, G has the pseudo inverse properties which [28] argues as explained in Chapter 3 (Section 3.7.4) are optimal from the point of view of minimizing the impact of unmatched uncertainties on the closed loop dynamics.

Remark 4.3: The following analysis is novel compared to the ISM schemes in [119], [27], [28], since the effects of faults and the actuator redundancy must be taken into account. As a consequence, the analysis in this section is quite distinct compared to the papers cited above because of the incorporation of the ideas from control allocation to exploit the redundancy to ensure sliding can be maintained even in the face of certain total actuator failures.

Now in order to analyze the sliding motion associated with the surface in (4.18) and G in (4.19) in the presence of faults, compute the time derivative of equation (4.18). It is easy to see

$$\dot{\sigma}(t) = G\dot{x}(t) - GAx(t) + GB_v Fx(t) \tag{4.20}$$

Substituting (4.12) in (4.20), and using the fact that $GB_v = I$, yields

$$\dot{\sigma}(t) = G\widehat{B}\hat{v}(t) + Fx(t) \tag{4.21}$$

The equivalent control [118], can be obtained by solving for $\hat{v}(t)$ in $\dot{\sigma}(t) = 0$ which yields

$$\hat{v}_{eq}(t) = -(G\widehat{B})^{-1} Fx(t) \tag{4.22}$$

Adding and subtracting $Fx(t)$ in equation (4.22) and substituting into (4.12) and simplifying

yields

$$\dot{x}(t) = (A - B_v F)x(t) + \left(B_v - \widehat{B}(G\widehat{B})^{-1}\right)Fx(t) \tag{4.23}$$

where B_v is defined in (4.15) and $\widehat{B}$ in (4.12). Using G as defined in (4.19), further simplifying equation (4.23) gives:

$$\dot{x}(t) = (A - B_v F)x(t) + \tilde{B}\tilde{\Phi}(t)Fx(t) \tag{4.24}$$

where the time varying uncertain term is

$$\tilde{\Phi}(t) := B_1 B_2^T - B_1(I - \triangle(t))B_2^{\dagger,\widehat{W}^2(t)}(B_2(I - \triangle(t))B_2^{\dagger,\widehat{W}^2(t)})^{-1} \tag{4.25}$$

and

$$\tilde{B} := \begin{bmatrix} I_{n-l} \\ 0 \end{bmatrix} \tag{4.26}$$

Remark 4.4: Notice in the case of perfect knowledge of the actuator efficiency (i.e. $\triangle(t) = 0$), and when there are no faults in the system (i.e. $\widehat{W}(t) = I$), the matrices $\widehat{B}|_{\widehat{W}(t)=I} = B_v$ and $B_2^{\dagger,\widehat{W}^2(t)}|_{\widehat{W}(t)=I} = B_2^T$. Then using the fact that $GB_v = I$, equation (4.24) simplifies to become

$$\dot{x}(t) = (A - B_v F)x(t) \tag{4.27}$$

which is stable by design of the state feedback gain F. The nominal equation (4.27) constitutes ideal fault free behavior. It is important to note that the uncertain term $\tilde{\Phi}(t) = 0$ when $\triangle(t) = 0$, and $\widehat{W}(t) = I_m$ while in the sliding mode. In the case, when there is some uncertainty in fault estimation i.e. $\triangle(t) \neq 0$, and during actuators fault or failure i.e. $\widehat{W}(t) \neq I_m$, the uncertain term $\widetilde{\Phi}(t) \neq 0$ and will be treated as unmatched uncertainty in the closed-loop stability analysis. Therefore for the generic fault/failure case, the *closed-loop stability needs to be proven* since the closed-loop system equation (4.24) depends on matrices $\widehat{W}(t)$ and $\triangle(t)$.

4.3.2 Closed-loop Stability Analysis

In the presence of faults/failures, the closed-loop system (assuming a sliding motion is maintained) is governed by

$$\dot{x}(t) = (A - B_v F + \tilde{B}\tilde{\Phi}(t)F)x(t) \tag{4.28}$$

where to ensure the closed-loop stability in the presence of unmatched term $\tilde{\Phi}(t)$, the small gain theorem [75] is used, which is a systematical approach to check the input-output stability of the interconnected systems. For the subsequent analysis, define a transfer function matrix

$$\tilde{G}(s) = F(sI - \tilde{A})^{-1}\tilde{B} \tag{4.29}$$

where $\tilde{A} := A - B_v F$. By construction, $\tilde{G}(s)$ is stable, and define a scalar

$$\gamma_2 = \|\tilde{G}(s)\|_\infty \tag{4.30}$$

Proposition 4.1: Assume the effectiveness gain estimate $\widehat{W}(t)$ is sufficiently accurate so that the condition $\triangle_{max}\gamma_o < 1$ holds, where γ_o is defined in (4.14) and $\|\triangle(t)\| < \triangle_{max}$ bounds the relative error in the estimation of the effectiveness gains. Then during a fault or failure condition, for any $(\hat{w}_1(t), .., \hat{w}_m(t)) \in \mathscr{W}$, the sliding motion in (4.28) will be stable if:

$$\frac{\gamma_2\ \gamma_1(1+\gamma_o)}{1-\triangle_{max}\gamma_o} < 1 \tag{4.31}$$

where $\gamma_o > \|B_2^{\dagger,\widehat{W}^2(t)}\|$, $\gamma_1 = \|B_1\|$ and γ_2 is as defined in (4.30).

Proof. The system in (4.28), which represents the sliding motion can be written as:

$$\dot{x}(t) = \tilde{A}x(t) + \tilde{B}\tilde{u}(t) \tag{4.32}$$

$$\tilde{y}(t) = Fx(t) \tag{4.33}$$

where

$$\tilde{u}(t) = \tilde{\Phi}(t)\tilde{y} \tag{4.34}$$

In this form, the differential equation in (4.28) may be considered to be the closed loop dynamics of the negative feedback interconnection of $\tilde{G}(s)$ and the 'feedback gain' in (4.34). According to the small gain theorem [75], as discussed in the Appendix B.1.2 if

$$\|\tilde{G}(s)\|_\infty \|\tilde{\Phi}(t)\| < 1 \tag{4.35}$$

then (4.28) will be stable. In (4.35), $\|\tilde{G}(s)\|_\infty$ is the H_∞ norm of the system $\tilde{G}(s)$ which is equal to the $\mathscr{L}_2$ gain of the system in the time domain and $\|.\|$ is the induced spectral norm. From (4.25) it is clear that

$$\|\tilde{\Phi}(t)\| \leq \|B_1 B_2\| + \|B_1(I - \triangle(t))B_2^{\dagger,\widehat{W}^2(t)}\| \|(B_2(I - \triangle(t))B_2^{\dagger,\widehat{W}^2(t)})^{-1}\|$$

Using the fact that $\|B_2\| = 1$, $B_2 B_2^{\dagger,\widehat{W}^2(t)} = I_l$ and also that in general $\|(I-X)^{-1}\| \leq (1 - \|X\|)^{-1}$ if $\|X\| < 1$ [63], then

$$\|\tilde{\Phi}(t)\| \leq \|B_1\| + \|B_1\|(1 + \triangle_{max})\|B_2^{\dagger,\widehat{W}^2(t)}\|(I - \|B_2\triangle(t)B_2^{\dagger,\widehat{W}^2(t)}\|)^{-1} \tag{4.36}$$

This is well defined since $\|B_2\triangle(t)B_2^{\dagger,\widehat{W}^2(t)}\| < \triangle_{max}\gamma_o < 1$. Since $\gamma_o > \|B_2^{\dagger,\widehat{W}^2(t)}\|$ and $\gamma_1 = \|B_1\|$, inequality (4.36) becomes

$$\|\tilde{\Phi}(t)\| \leq \frac{\gamma_1(1+\gamma_o)}{1 - \triangle_{max}\gamma_o} \tag{4.37}$$

Since $\gamma_2 = \|\tilde{G}(s)\|_\infty$, in conjunction with (4.37), it is clear that if inequality (4.31) holds, the small gain condition (4.35) holds, and consequently the system in (4.28) is stable. ■

Remark 4.5:By hypothesis, $\gamma_1 = \|B_1\|$ is assumed to be small. Basically the size $\|B_1\|$ has a significant impact on the norm of the nonlinearity in the small gain feedback loop, and so if $\|B_1\|$ is small, the gain of the nonlinearity is small, and there is a less stringent requirement on

the magnitude of the H_∞ norm of the linear part. Furthermore, $\|\Phi\| \longrightarrow 0$ as $\|B_1\| \longrightarrow 0$ and *Proposition* 4.1 is trivially satisfied.

Remark 4.6: In the case of exact estimation of effectiveness matrix $W(t)$, then $\widehat{W}(t) = W(t)$ and $\triangle(t) = 0$, and the stability condition (4.31) reduces to

$$\gamma_2\gamma_1(1+\gamma_o) < 1 \tag{4.38}$$

4.3.3 Integral Sliding Mode control laws

Now a sliding mode control law must be designed based on the virtual system (4.12) with respect to $\hat{v}(t)$. The proposed control structure has a form given by:

$$\hat{v}(t) = \hat{v}_l(t) + \hat{v}_n(t) \tag{4.39}$$

where

$$\hat{v}_l(t) := -Fx(t) \tag{4.40}$$

The scaled unit vector

$$\hat{v}_n(t) := \begin{cases} -\rho(t,x)\frac{\sigma(x,t)}{\|\sigma(x,t)\|} & \text{if } \sigma \neq 0 \\ 0 & \text{otherwise} \end{cases} \tag{4.41}$$

where $\rho(t,x)$ is a scalar modulation function to enforce the sliding motion. A suitable choice of $\rho(t,x)$ will be described explicitly in the sequel.

Proposition 4.2: Suppose that

$$\|\triangle(t)\| \leq \triangle_{max} < \frac{1}{\gamma_o} \tag{4.42}$$

where γ_o is defined in (4.14). If $\rho(t,x)$ is chosen as

$$\rho(t,x) = \frac{\triangle_{max}\gamma_o\|\hat{v}_l\| + \eta}{1 - \triangle_{max}\gamma_o} \tag{4.43}$$

where η is a positive scalar, then, the control law proposed in (4.39) satisfies the so-called

reachability condition and sliding on $\mathscr{S}$ in (4.17) is maintained.

Proof. Substituting (4.12) in (4.20) gives

$$\dot{\sigma} = (G\widehat{B})\hat{v}(t) + Fx(t) \tag{4.44}$$

Substituting for $\hat{v}(t)$ from (4.39)-(4.41) and using the fact that $G\widehat{B} = (I - B_2\triangle(t)B_2^{\dagger,\widehat{W}^2(t)})$, gives

$$\dot{\sigma} = -\rho\frac{\sigma}{||\sigma||} - B_2\triangle(t)B_2^{\dagger,\widehat{W}^2(t)}\big(-Fx(t) - \rho\frac{\sigma}{||\sigma||}\big) \qquad \text{for } \sigma \neq 0 \tag{4.45}$$

Consider the candidate Lyapunov function

$$V = \frac{1}{2}\sigma^T\sigma \tag{4.46}$$

The time derivative of the Lyapunov function along the trajectories satisfies

$$\dot{V} = -\rho\|\sigma\| + \sigma^T B_2\triangle(t)B_2^{\dagger,\widehat{W}^2(t)}Fx(t) + \rho\sigma^T(B_2\triangle(t)B_2^{\dagger,\widehat{W}^2(t)})\frac{\sigma}{\|\sigma\|} \qquad \text{for } \sigma \neq 0$$

and therefore

$$\begin{aligned}
\dot{V} &\leq -\rho\|\sigma\| + \|\sigma\|\|B_2\triangle(t)B_2^{\dagger,\widehat{W}^2(t)}\|\|\underbrace{Fx(t)}_{-\hat{v}_l}\| + \rho\|\sigma\|\|B_2\triangle(t)B_2^{\dagger,\widehat{W}^2(t)}\| \\
&\leq -\rho\|\sigma\| + (\rho + \|\hat{v}_l\|)\|\sigma\|\triangle_{max}\gamma_o \\
&\leq -\rho(1 - \triangle_{max}\gamma_o)\|\sigma\| + \|\hat{v}_l\|\|\sigma\|\triangle_{max}\gamma_o
\end{aligned} \tag{4.47}$$

Substituting for ρ from (4.43) into (4.47) gives $\dot{V} \leq -\eta\|\sigma\|$, which is the standard η-reachability condition [41], and implies that the sliding motion is maintained for all time. ■

Finally using equations (4.6), (4.7) and (4.11) it follows that the physical control law is given by

$$u(t) = \widehat{W}(t)B_2^T(B_2\widehat{W}^2(t)B_2^T)^{-1}(-Fx(t) - \rho\frac{\sigma}{||\sigma||}) \quad \text{if } \sigma \neq 0 \tag{4.48}$$

This is the actual control signal which will be sent to the actuators, and depends on the effectiveness levels. The proposed ISM controller (4.48) can deal with actuator faults and total actuator failures, provided that $(\hat{w}_1(t),..,\hat{w}_m(t)) \in \mathscr{W}$ and the conditions of *Proposition 4.1* are satisfied.

Remark 4.7: In this Chapter, actuator position limits are not considered formally in the control design, However the fault estimation scheme would declare it as a fault if an actuator exceeds its position limits. This would be due to the reason that the actual position of the actuator will be different from the expected position based on commanded control signal. The proposed scheme attempts to reduce the burden on the faulty actuator channel ($\hat{w}_i(t) < 1$) and to mitigate the effects of actuator saturation, redistributes the control effort among the redundant actuators.

The results developed in this section can be summarized in the form of the following theorem:

Theorem 4.1: The system in (4.1) is closed-loop stable for any fault/failure combination belonging to $\mathscr{W}$ in (4.9) under the control law (4.48), if a feedback gain F can be found such that

$$\frac{\gamma_2\ \gamma_1(1+\gamma_o)}{1-\triangle_{max}\gamma_o} < 1$$

where γ_2 is defined in (4.30), $\gamma_1 = \|B_1\|$, γ_o satisfies $\gamma_o \geq \|B_2^{\dagger,\widehat{W}^2(t)}\|$ where $B_2^{\dagger,\widehat{W}^2(t)}$ is defined in (4.13), and $\triangle_{max}$ bounds the relative error in the estimation of the effectiveness gains in (4.3).

4.3.4 Design of the Controller Gains

This section demonstrates one of the key advantages of this approach compared to [6]. It will be demonstrated that the stability test in *Proposition 4.1* is amenable to incorporation within a synthesis framework for determining the feedback gain F in (4.16). For the nominal system (4.16), the matrix F must be chosen to stabilize $(A-B_vF)$. Since (A,B_v) is assumed to be controllable, the LQR formulation [21] adopted here is to seek the control signal $v(t)$ to minimize the energy cost function

$$J = \int_0^\infty z^T z dt \tag{4.49}$$

where

$$z = \begin{bmatrix} Q_1 & 0 \\ 0 & R_1 \end{bmatrix} \begin{bmatrix} x \\ v \end{bmatrix} \tag{4.50}$$

where the matrices Q_1 and R_1 are symmetric positive definite matrices. The optimal solution of the LQR problem is $v(t) = Fx(t)$. The details of the LMI formulation are given in Appendix (B.3.1). The LQR problem can be posed as an LMI optimization [21]: Minimize $trace(X^{-1})$ subject to

$$\begin{bmatrix} AX + XA^T - B_v Y - Y^T B_v^T & (Q_1 X - R_1 Y)^T \\ Q_1 X - R_1 Y & -I \end{bmatrix} < 0 \tag{4.51}$$

$$X > 0 \tag{4.52}$$

where $Q_1 = [(Q^{\frac{1}{2}})^T \quad 0_{l\times n}^T]^T$ and $R_1 = [0_{n\times l}^T \quad (R^{\frac{1}{2}})^T]^T$. The variable $Y := FX$ with $Y \in \mathbb{R}^{l\times n}$ and $X^{-1} \in \mathbb{R}^{n\times n}$ is the Lyapunov matrix. In this LMI formulation, the decision variables are X and Y.

Since, in addition, the small gain stability condition (4.31) needs to be satisfied, from the Bounded Real Lemma [21], the $\mathscr{L}_2$ gain from $\tilde{u}$ to $\tilde{y}$, which in this situation is equal to the $\mathscr{H}_\infty$ norm of its transfer matrix $\tilde{G}$, satisfies $||\tilde{G}||_\infty < \gamma$ iff there exist $X > 0$ and $\gamma \geq 0$ such that

$$\begin{bmatrix} AX + XA^T - B_v Y - Y^T B_v^T & \tilde{B} & Y^T \\ \tilde{B}^T & -\gamma^2 I & 0 \\ Y & 0 & -I \end{bmatrix} < 0 \tag{4.53}$$

where $\tilde{B}$ is defined in (4.26). The details of the LMI formulation are given in Appendix (B.3.2). Here γ is an a-priori fixed scalar gain which may be viewed as a tuning parameter. The decision variables in this LMI formulation are again X and Y. If

$$\gamma < \frac{(1 - \Delta_{max}\gamma_o)}{\gamma_1(1 + \gamma_o)}$$

then the conditions of Theorem 1 are satisfied and closed loop stability for a fault/failure combination belonging to $\mathscr{W}$ is guaranteed.

Since the common Lyapunov matrix is sought in the LMI formulations, the overall optimization process is: Minimize $trace(Z)$ subject to

$$\begin{bmatrix} -Z & I_n \\ I_n & -X \end{bmatrix} < 0 \tag{4.54}$$

together with (4.51), (4.52) and (4.53). The matrix Z is a slack variable which using the Schur complements satisfies $Z > X^{-1}$ and therefore $trace(Z) \geq trace(X^{-1})$. Finally the feedback gain F can be recovered as $F = YX^{-1}$.

4.4 Simulations

In this section control of the lateral axis of a large transport aircraft discussed in Appendix A.1 will be considered to demonstrate the effectiveness and feasibility of the proposed scheme. To design the state feedback gain F in (4.40), a linear model has been obtained using FTLAB747 around an operating condition of straight and level flight at 263,000 Kg, 92.6 m/s true airspeed, and at an altitude of 600m based on 25.6% of maximum thrust and at a 20 deg flap position. The lateral axis states (in Appendix A.1) which are considered for the controller design are $[\phi, \beta, r, p]^T$, where ϕ is roll angle (rad), β is sideslip angle (rad), r is yaw rate (rad/sec), and p is roll rate (rad/sec). The controlled outputs $y_c(t) = Cx(t)$ are $[\beta, \phi]$ where

$$C = \begin{bmatrix} 0 & 1 & 0 & 0 \\ 1 & 0 & 0 & 0 \end{bmatrix}$$

which means $l = 2$. For the lateral control, the inner and outer ailerons $(\delta_{air}, \delta_{aor})$ on the right wing (in Appendix A.1) are aggregated to produce one control input. The available control surfaces are $\delta = [\delta_a, \delta_r, \delta_{epr}]^T$, which represent anti-symmetric aileron deflection (rad), rudder deflection (rad) and differential aggregated engine pressure ratios (EPR). Note in this example

the number of control inputs $m = 3$, while the number of controlled outputs $l = 2$, and so in theory only two control inputs would be required to force the controlled outputs to follow a commanded trajectory. Here the fact that three control inputs can be manipulated, indicates the existence of redundancy in the system which can be exploited to achieve fault tolerance. The ordering of the states ensures $\|B_1\| << \|B_2\|$, so that B_2 represent dominant contribution to the control action as compared to B_1. After scaling the states to ensure $B_2 B_2^T = I_l$ the state-space representation is

$$A = \begin{bmatrix} 0 & 0 & 0.0084 & 0.3334 \\ 0.1055 & -0.0999 & -0.3170 & 0.0538 \\ -0.0059 & 0.5617 & -0.1856 & -0.1796 \\ 0.0008 & -4.8828 & 0.2154 & -1.0789 \end{bmatrix} \quad B = \left[\begin{array}{ccc} 0 & 0 & 0 \\ 0 & 0.0174 & -0.0010 \\ \hline -0.1459 & -0.7584 & -0.6352 \\ -0.9387 & 0.3089 & -0.1531 \end{array}\right] \begin{matrix} \} B_1 \\ \\ \} B_2 \end{matrix} \tag{4.55}$$

For tracking the $[\beta, \phi]$ commands, the integral action method [97] is used. To accomplish it, the integral action states $x_r(t)$ satisfying the relation

$$\dot{x}_r(t) = r(t) - Cx(t) \tag{4.56}$$

are introduced, where $r(t)$ is the reference signal to be tracked. By defining $x_a(t) = col[x_r(t), x(t)]$, the system in (4.15) will be augmented with the integral action states to become

$$\dot{x}_a(t) = A_a x_a(t) + B v_a v(t) + B_r r(t) \tag{4.57}$$

where

$$A_a = \begin{bmatrix} 0 & -C \\ 0 & A \end{bmatrix} \quad B_{v_a} = \begin{bmatrix} 0 \\ B_v \end{bmatrix} \quad B_v = \begin{bmatrix} B_1 B_2^T \\ I_l \end{bmatrix} \quad B_r = \begin{bmatrix} I_l \\ 0 \end{bmatrix} \tag{4.58}$$

By design the pair (A_a, B_{v_a}) is controllable and a state feedback gain $v(t) = -F x_a(t)$ is to be designed to stabilize the nominal system in (4.57). The integral switching function in (4.18) for

the augmented system will become

$$\sigma(x_a,t) = G_a x_a(t) - G_a x_a(0) - G_a \int_0^t \big((A_a - B_{v_a}F)x_a(\tau) + B_r r(\tau)\big)d\tau \tag{4.59}$$

where $G_a := B_2(B_a^T B_a)^{-1}B_a^T$, where the augmented input distribution matrix B_a is

$$B_a = \begin{bmatrix} B_{1_a} \\ B_2 \end{bmatrix} \quad B_{1_a} = \begin{bmatrix} 0_{l\times m} \\ B_1 \end{bmatrix}$$

In a fault free scenario, i.e in normal flight, the primary control surfaces for ϕ and β tracking are the ailerons and rudder respectively; however the engine thrust can be used as redundancy for both surfaces. Based on these assumptions, using a numerical search, it was found that a suitable bound for the scalar in (4.14) is $\gamma_o = 3.2020$. It can be easily verified that $\gamma_1 = \|B_{1_a}\| = 0.0174$. The nominal state feedback controller gain F associated with equation (4.16) for the augmented system has been designed using the LMI approach proposed in Section 4.3.4 and is given by

$$F = \begin{bmatrix} 0.4165 & -0.0839 & 0.2936 & -1.9273 & 0.7983 & -0.1356 \\ -0.5265 & -0.1241 & 1.1878 & -0.6954 & -0.1000 & 0.3879 \end{bmatrix} \tag{4.60}$$

The nominal performance design matrices Q and R in LMI (4.51) have been chosen as $Q = diag\{0.95, 0.08, 2, 1, 15, 5\}$ and $R = diag\{10, 2\}$ respectively, where the first two states in Q are the integral action states. Here $\triangle_{max} = 0.17$ is chosen which implies an upper bound on the relative error in $\widehat{W}$ of 17%. The choice of $\gamma = 8.8$ in LMI (4.53) results in $\gamma_2 = 5.8832$ and it can be verified that

$$\frac{\gamma_2\ \gamma_1(1+\gamma_o)}{1-\triangle_{max}\gamma_o} = 0.9440 < 1$$

and therefore the condition of Theorem 1 is satisfied. Consequently the closed-loop stability of the system for any combination of faults $(\hat{w}_1, .., \hat{w}_3) \in \mathscr{W}$ is ensured.

4.4.1 Sliding mode fault reconstruction scheme

The control law $u(t)$ in (4.48) depends on the estimate of $W(t)$ matrix to distribute the control effort among the actuators. A sliding mode fault reconstruction scheme, proposed in [5] can be used to estimate the actuator effectiveness levels. To explain this without loss of generality the actuator fault model in (4.1) can be written as

$$\dot{x}(t) = Ax(t) + B\underbrace{(I_m - K)}_{W}u(t) \tag{4.61}$$

where it is assumed that input matrix B is of full column rank. The matrix $K = \text{diag}\{k_i, ..., k_m\}$ where the scalars $k_i = 1 - w_i$. By writing this way the term $Ku(t)$ in (4.61) can be considered as the fault term. To estimate the fault term $Ku(t)$ a fault estimator [5] is given by

$$\dot{z}(t) = Az(t) + Bu(t) + G_n\vartheta(t) \tag{4.62}$$

where, G_n is an appropriate gain matrix, $z(t)$ is the estimator state and $\vartheta(t)$ is termed as discontinuous injection term [40], [5] and is defined as

$$\vartheta(t) := -\rho_e \frac{e(t)}{\|e(t)\|} \qquad \text{for } e(t) \neq 0 \tag{4.63}$$

where the value of ρ_e must be chosen such that $\rho_e \geq \|Ku(t)\|$. From (4.62) and (4.61) it is clear that the error dynamics using the relation $e(t) = x(t) - z(t)$ can be written as

$$\begin{aligned} \dot{e}(t) &= \dot{x}(t) - \dot{z}(t) \\ &= Ae(t) - \vartheta(t) - BKu(t) \end{aligned} \tag{4.64}$$

When the motion on $e(t) = 0$ will be enforced by the discontinuous injection term $\vartheta(t)$ i.e. while sliding $e(t) = \dot{e}(t) = 0$ [5], then the fault signal $Ku(t)$ can be reconstructed using equation (4.64)

as

$$-Ku(t) \approx (B^T B)^{-1} B^T \vartheta_{eq}(t) \tag{4.65}$$

where $\vartheta_{eq}(t)$ is the equivalent injection term and is necessary to maintain sliding. The injection term is discontinuous and can be approximated to any level of accuracy using the relation

$$\vartheta_{\delta}(t) := -\rho_e \frac{e(t)}{\|e(t)\| + \delta} \tag{4.66}$$

where δ is the small positive scalar. The scalars k_i can be obtained from (4.65) by introducing a small threshold ε [5] such that for the time t_ε if $|u_i(t)| \leq \varepsilon$ then

$$k_i(t) = \begin{cases} \frac{((B^T B)^{-1} B^T \vartheta_{\delta}(t))_i}{u_i(t)} & \text{if } |u_i(t)| > \varepsilon \\ k_i(t_\varepsilon) & \text{otherwise} \end{cases} \tag{4.67}$$

The idea is to provide a constant value when $|u_i(t)| < \varepsilon$. A saturation block with the limits $[0 \quad 1]$ is used before the information is provided to the control allocation unit to keep the theoretical limits.

4.4.2 Manoeuvre and fault scenarios

In the simulations which follow the linear aircraft model undertakes a turning manoeuvre, where the reference command requests a change in ϕ to 25 deg during the period of time $60-90$ sec, whilst a 0 deg reference command is applied to β throughout. In the simulations, the discontinuity associated with the nonlinear control term in (4.41) is smoothed by using the fractional approximation (3.37), discussed in Section 3.5, and is given by $\frac{\sigma}{||\sigma||+\delta_o}$ where the value of the positive scalar δ_o is chosen to be 0.001. An ideal sliding motion will not be obtained in this situation, and instead a pseudo sliding will be achieved, where the sliding motion is in the vicinity of the sliding surface $\mathscr{S}$. This can be made arbitrarily small by selecting δ_o sufficiently small.

4.4.2.1 Aileron faults and Lock in place failure

In this subsection to test the efficacy of the proposed scheme, aileron (which is the primary actuator for ϕ tracking) faults and failure are considered. Various levels of aileron faults (from $0\% - 100\%$) are tested each occurring at 80-sec in 15% increments. In Figure 4.2 and Figure 4.3, the plant states and actuator deflections are shown during the aileron fault scenario (when the estimation of W is perfect), where it can be seen that the CA scheme systematically redistributes the control signals to the rudder and the engines, while maintaining the same level of tracking performance as in the fault free condition.

In Figures 4.4-4.5, the aileron undergoes lock in place failure (where the actuator jams at some offset position) and is unable to create any moment, which means the effectiveness of the aileron after the failure time ($80sec$) is 0%. If the estimate of the actuator effectiveness is perfect then the information provided to the CA unit regarding the actuator effectiveness ($\hat{w}_i(t)$) should be 0%. But since the estimate $\widehat{W}(t)$ can not be perfect, which is the case considered in this Chapter, the effect of 17% error in the estimation of $W(t)$ can be seen in Figure 4.5, which is the maximum theoretical percentage error $\triangle_{max}$ which can be tolerated by the proposed scheme without violating the stability condition of *Theorem* 1. Due to the availability of redundancy in the system, the CA scheme involves the engines more actively to achieve the performance close to the nominal (Figure 4.4).

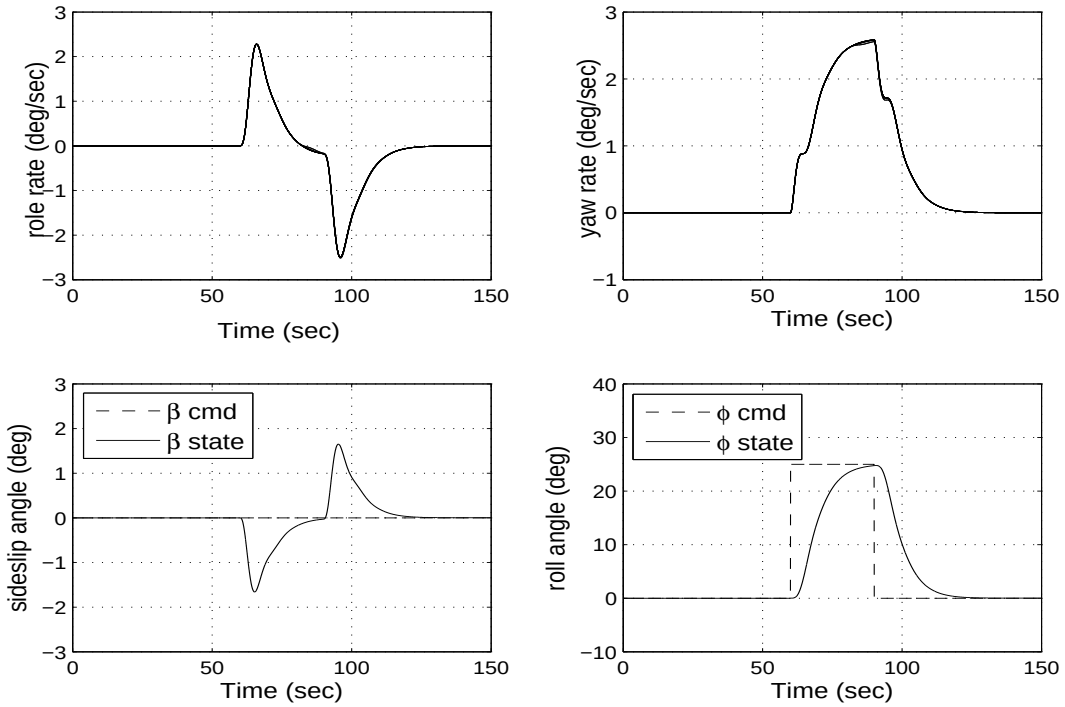

Figure 4.2: Aileron-fault, Loss in effectiveness: plant states

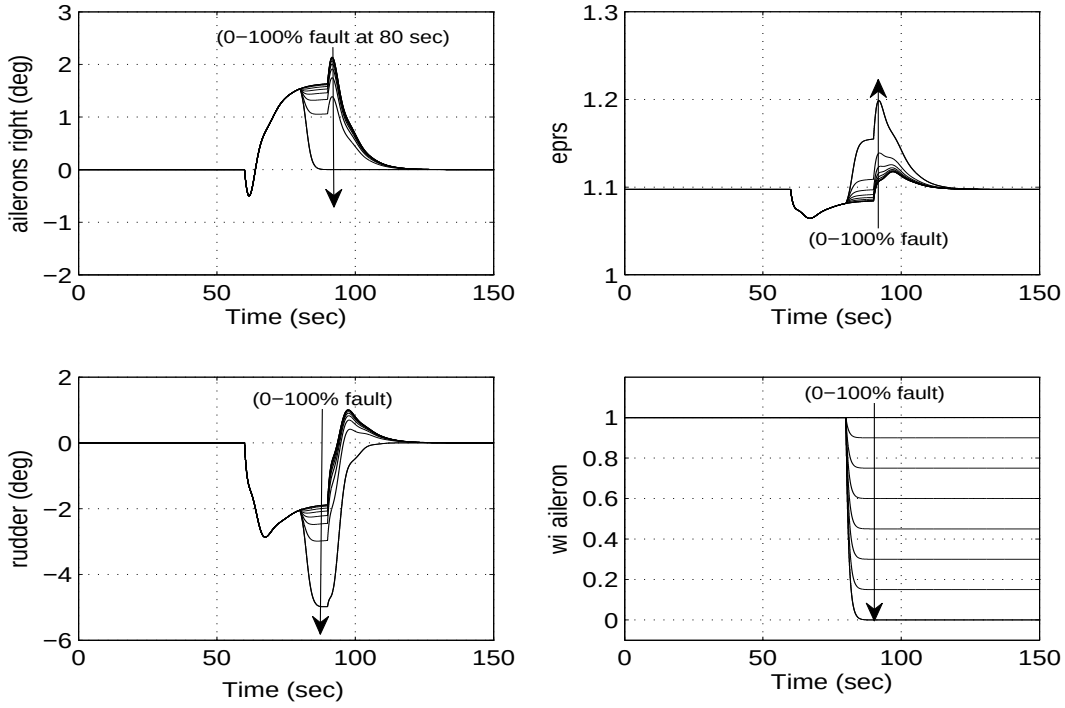

Figure 4.3: Aileron-fault, Loss in effectiveness: actuator deflections

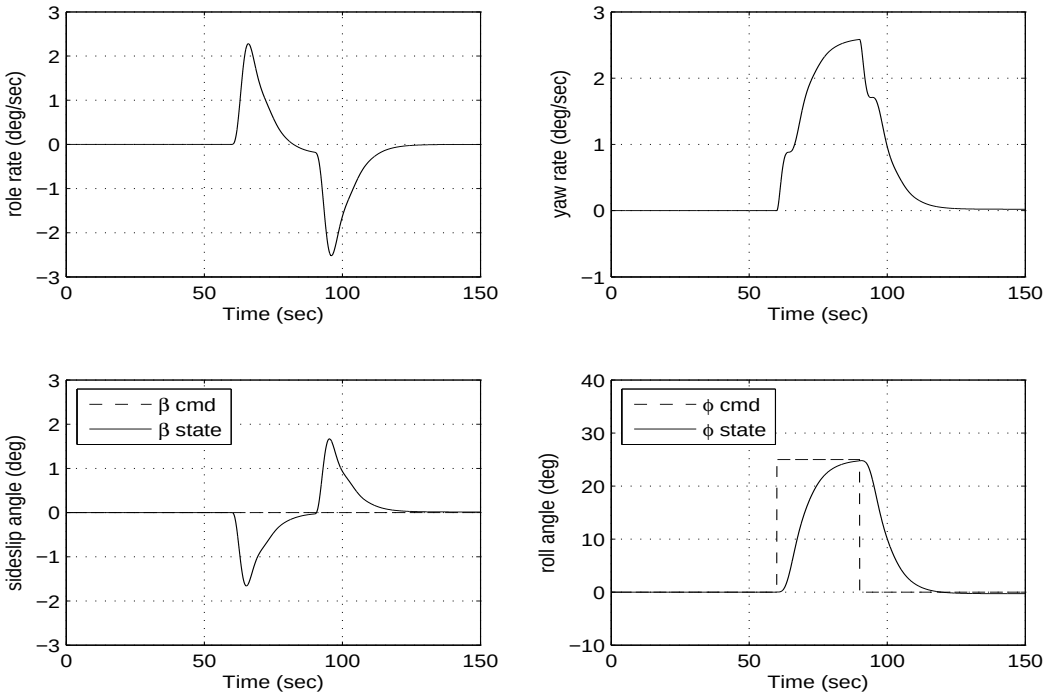

Figure 4.4: Aileron Jam/Lock in place failure: plant states

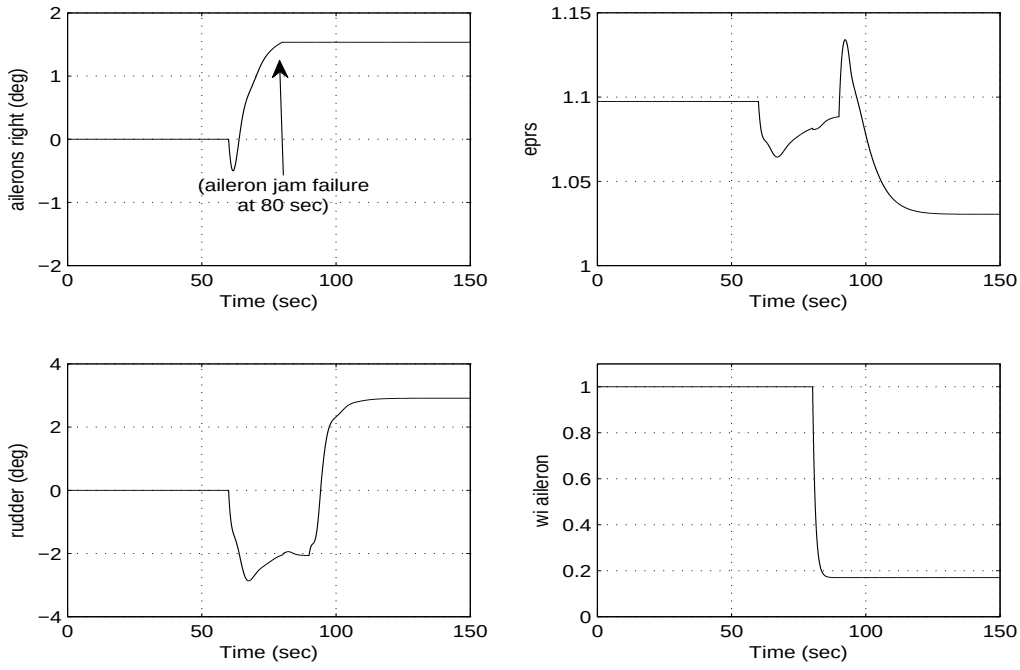

Figure 4.5: Aileron Jam/Lock in place failure: actuator deflections

4.4.2.2 Rudder Lock in place failure

This subsection validates the scheme, by considering the rudder (which is the primary actuator for β tracking) failure scenario. Figure 4.6 and Figure 4.7 show the tracking performance of the states and the control surface deflections, when a rudder jam/lock in place occurs at 80-sec -2 deg and the estimate of the rudder effectiveness is not perfect i.e effect of 17% error in the estimation of rudder effectiveness can be seen in Figure 4.7. The proposed FTC scheme redistributes the control effort among the aileron and the engines to cope with the rudder failure, and to maintain the nominal tracking performance (Figure 4.6). Figure 4.8 shows that the sliding is maintained throughout the simulations, even in the presence of actuator faults or failures.

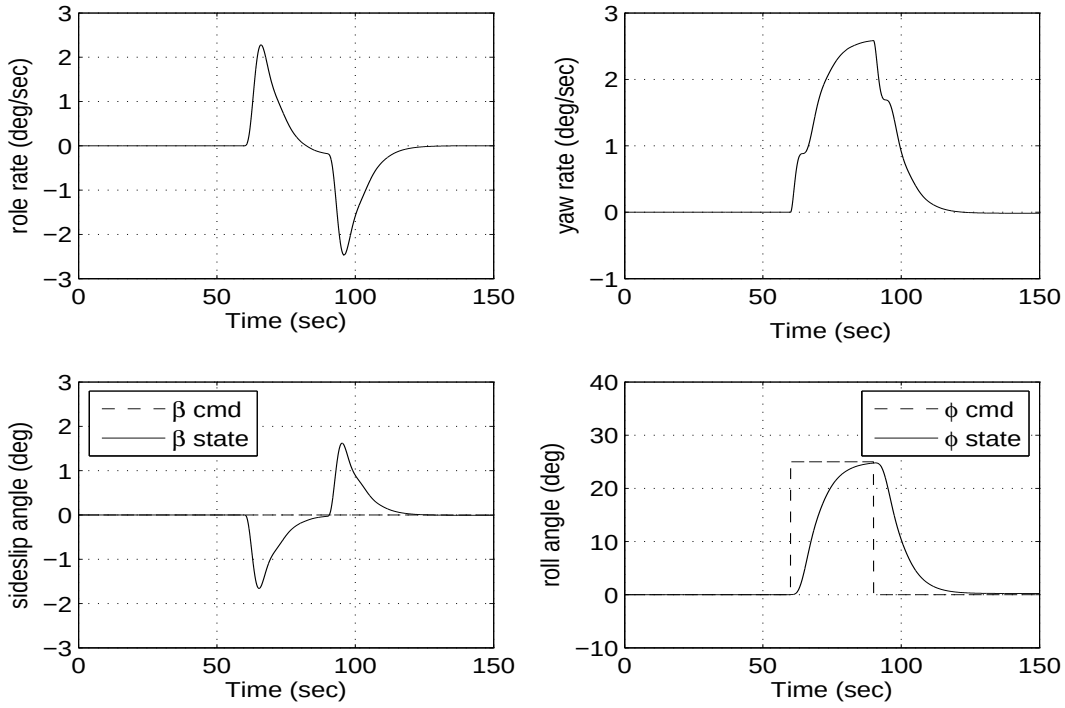

Figure 4.6: Rudder Jam/Lock in place failure: plant states

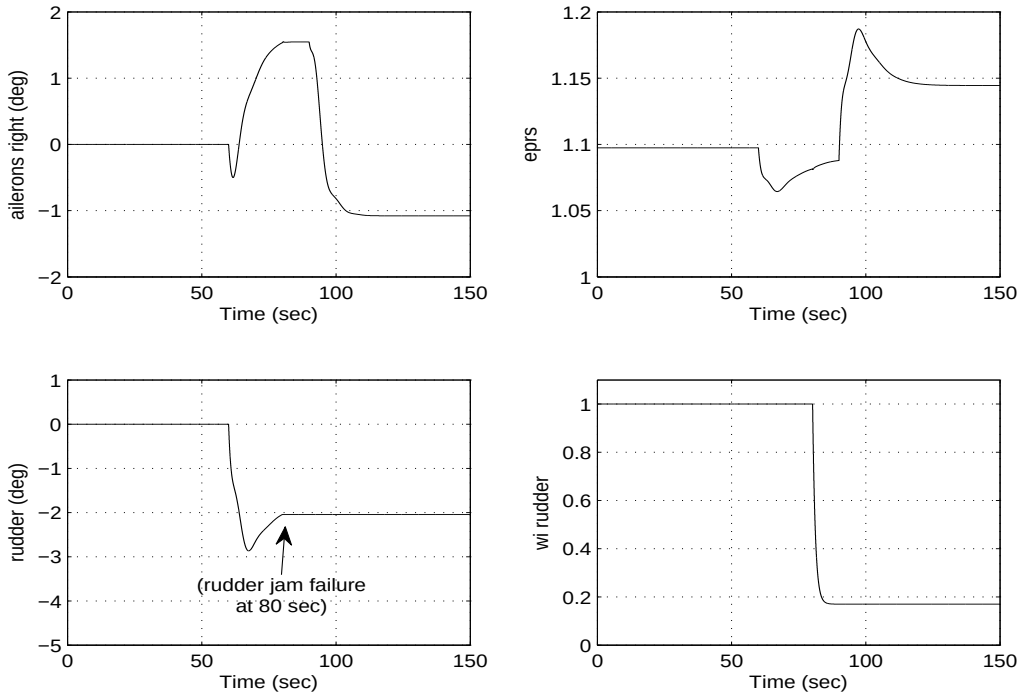

Figure 4.7: Rudder Jam/Lock in place failure: actuator deflections

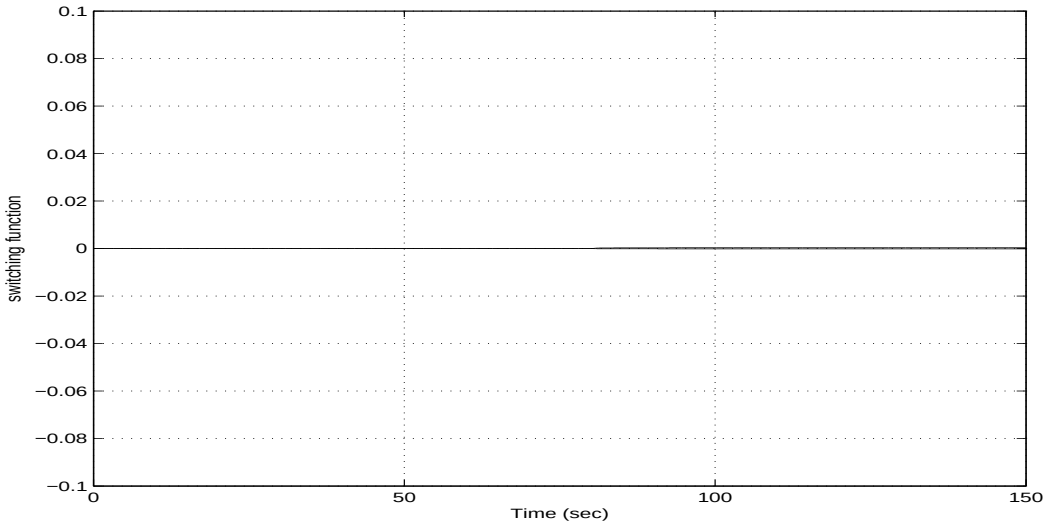

Figure 4.8: Switching function

4.5 Conclusion

A novel Integral Sliding Mode fault tolerant control scheme has been proposed in this Chapter. To handle total actuator failures, integral sliding mode ideas were incorporated into a control allocation framework, which has the capability to redistribute the control effort among the healthy redundant actuators automatically in the case of faults or failures without reconfiguring the controller. The estimation of the actuator effectiveness levels was a key source of information for the control allocation scheme. The stability analysis ensured closed-loop stability of the system for a certain level of mismatch between the actual and the estimated fault and in fact the synthesis procedure was carried out in the LMI framework to obtain the parameters of the controller. The efficacy of the proposed fault tolerant scheme was demonstrated through simulation based on different fault or failure scenarios in a large civil aircraft.

In the coming Chapter, the ideas of integral sliding modes control allocation discussed here will be applied on the benchmark high fidelity nonlinear model of a civil aircraft using the FTLAB747 software.

Chapter 5

Application of an Integral Sliding Mode FTC for a Large Transport Aircraft

Integral sliding mode control ideas incorporated with control allocation, discussed in Chapter 4 are used here to design fault tolerant controllers for the longitudinal and lateral axis control of a high fidelity nonlinear model of a large transport aircraft. The proposed scheme has the capability to retain nominal performance even in the face of total failure of certain actuators, provided there is enough redundancy in the system. During faults or failures, the control signals are redistributed by the control allocation unit to the healthy actuators based on their effectiveness level, without reconfiguring the controller. Nonlinear simulations using the Flight lab 747 FTLAB747 software are carried out in order to demonstrate the effectiveness of the novel combination of ISMC and CA for FTC purpose.

5.1 INTRODUCTION

In safety critical systems, to ensure reliable operation, redundant actuators are used, which can be exploited to achieve fault tolerance. Actuator redundancy is the key component of FTC design, and can be resolved by the virtual control concept [60]. It is discussed in Appendix A.1 as shown in Figure A.4, the benchmark model has abundant actuator redundancy which can be

used to tolerate the actuator faults or failures at the primary or secondary level. For example in case of faults or failures in the elevator channel (the primary actuator for pitch moment) the horizontal stabilizer can be used.

In aircraft systems, the idea is often to design a virtual controller to provide the desired moments [60]; then the CA translates the virtual control signals to the actual control surface deflections. In this way as explained in Chapter 4, one controller can be used to deal with a wide range of faults or failures without reconfiguration, whereby the CA redistributes the control signals to healthy actuators.

5.2 Integral sliding mode FTC Design

By considering the generic system representing the actuator faults or failures given in (4.1), for which the nominal fault free system (4.15) when $W(t) = I_m$ will be used to design the fault tolerant controller. The complete design phase for the ISM FTC design is explained in the next subsection.

5.2.1 Design procedure

The control law proposed in this Chapter is based on the ideas presented in Chapter 4. To track the commanded reference inputs, integral action in the nominal controller will be used. Some details which have already been explained in Chapter 4, are reproduced here for completeness. The design procedure employed in designing the ISM controller is outlined in the following steps:

1. As argued in section (4.2), rearrange and partition the input distribution matrix B such that $\|B_2\| \gg \|B_1\|$, so that B_2 dominantly represent the contribution of the control action as compared to B_1. Furthermore scale the states to ensure that $B_2 B_2^T = I_l$.

2. Define the virtual control input as

$$\nu(t) = B_2 u(t) \tag{5.1}$$

where $\nu(t) \in \mathbb{R}^l$, $l < m$. Using equation (5.1) the actual control signal $u(t)$ can be written as

$$u(t) = B_2^{\dagger,W(t)} \nu(t) \tag{5.2}$$

where $B_2^{\dagger,W(t)} \in \mathbb{R}^{m \times l}$ is a weighted right pseudo-inverse of matrix B_2 and a specific choice of $B_2^{\dagger,W(t)}$ is given by

$$B_2^{\dagger,W(t)} = W(t) B_2^T (B_2 W(t) B_2^T)^{-1} \tag{5.3}$$

provided that $\det(B_2 W(t) B_2^T) \neq 0$. Substituting (5.3) into (5.2) gives a parameterized expression for the control law

$$u(t) = W B_2^T (B_2 W B_2^T)^{-1} \nu(t) \tag{5.4}$$

3. Furthermore, if

$$\hat{\nu}(t) := (B_2 W^2 B_2^T)(B_2 W B_2^T)^{-1} \nu(t) \tag{5.5}$$

then $u(t)$ in (5.4) can be written as

$$u(t) = W B_2^T (B_2 W^2 B_2^T)^{-1} \hat{\nu}(t) \tag{5.6}$$

4. In order to include a tracking facility, consider the introduction of integral action states $x_r(t)$ [97], satisfying

$$\dot{x}_r(t) = r(t) - C x(t) \tag{5.7}$$

where $C \in \mathbb{R}^{l \times n}$ is the controlled output distribution matrix. Then the system dynamics can be described by augmenting the integral action states with the system states in (4.15)

by defining $x_a(t) = col[x_r(t), x(t)]$, which results in a system of the form

$$\dot{x_a}(t) = A_a x_a(t) + B_{v_a}\hat{v}(t) + B_r r(t) \tag{5.8}$$

where $r(t)$ is the reference signal to be tracked and the augmented matrices are:

$$A_a = \begin{bmatrix} 0 & -C \\ 0 & A \end{bmatrix} \quad B_{v_a} = \begin{bmatrix} 0 \\ B_v \end{bmatrix} \quad B_v = \begin{bmatrix} B_1 B_2^T \\ I_l \end{bmatrix} \quad B_r = \begin{bmatrix} I_l \\ 0 \end{bmatrix} \tag{5.9}$$

5. Suppose that by design the pair (A_a, B_{v_a}) is controllable, then a state feedback controller

$$\hat{v}(t) = \underbrace{\left[\begin{array}{c|c} K_I & -K \end{array}\right]}_{F} \underbrace{\begin{bmatrix} x_r(t) \\ x(t) \end{bmatrix}}_{x_a(t)} \tag{5.10}$$

where, $K_I \in \mathbb{R}^{l\times l}$, $K \in \mathbb{R}^{l\times n}$, so that the nominal system

$$\dot{x_a}(t) = (A_a - B_{v_a}F)x_a(t) + B_r r(t) \tag{5.11}$$

is stable, with steady state tracking properties with respect to $r(t)$.

6. Define the integral switching function based on the augmented nominal system (5.11), which aims to retain the nominal closed-loop performance as:

$$\sigma(x_a,t) = G_a x_a(t) - G_a x_a(0) - G_a \int_0^t \big((A_a - B_{v_a}F)x_a(\tau) + B_r r(\tau)\big)d\tau \tag{5.12}$$

where $G_a \in \mathbb{R}^{l\times(n+l)}$ is design freedom. The associated sliding surface is $\mathscr{S} = \{x_a \in \mathbb{R}^{n+l} : \quad \sigma(x_a,t) = 0\}$. Similarly as in (4.19), the choice of G_a is chosen as

$$G_a := B_2(B_a^T B_a)^{-1}B_a^T \tag{5.13}$$

where,

$$B_a = \begin{bmatrix} B_{1_a} \\ B_2 \end{bmatrix} \quad B_{1_a} = \begin{bmatrix} 0_{l\times m} \\ B_1 \end{bmatrix} \tag{5.14}$$

The choice of G_a has the property that

$$\begin{aligned} G_a B_{v_a} &= B_2(B_a^T B_a)^{-1} B_a^T B_a B_2^T \\ &= B_2 B_2^T = I_l \end{aligned}$$

7. Define the ISM control laws as

$$\hat{v}(t) = \hat{v}_l(t) + \hat{v}_n(t) \tag{5.15}$$

where

$$\hat{v}_l(t) := -F x_a(t) \tag{5.16}$$

and

$$\hat{v}_n(t) := \begin{cases} -\rho \frac{\sigma_a(x,t)}{||\sigma_a(x,t)||} & \text{if } \sigma_a(t) \neq 0 \\ 0 & \text{if } \sigma_a(t) = 0 \end{cases} \tag{5.17}$$

where ρ is a modulation gain to enforce sliding.

8. Design the state feedback matrix F for the linear part of the controller (5.16), by solving the LMIs (4.51)–(4.54) simultaneously given in section (4.3.4) for the augmented system (5.8).

9. Finally, the actual control signal sent to the actuators online, depending on their effectiveness level is obtained by substituting (5.15) into (5.6) which yields

$$u(t) = W B_2^T (B_2 W^2 B_2^T)^{-1} (-F x_a(t) - \rho \frac{\sigma_a}{||\sigma_a||}) \tag{5.18}$$

The integral sliding mode controller (5.18) can deal with actuator faults and certain total

actuator failures, provided that $\det(B_2 W^2 B_2^T) \neq 0$.

5.2.2 FTLAB747 v6.5/v7.1 Software and Design Objectives

In this Chapter, all the simulations are based on a high-fidelity non-linear aircraft model, using the FTLAB747 v6.5/v7.1 software which represents a 'real world' model of B747-100/200 aircraft. The details of the model are given in (Appendix A.1).

The scenario which is considered here is that the aircraft is at a straight and level flight at 600m and undergoes so-called up and away maneuver followed by a turning manoeuvre. The controllers design objective here is to increase the altitude and the speed of the aircraft from the current level of flight and after reaching the required altitude the aircraft takes the turn. This can be achieved by tracking the appropriate FPA and airspeed (V_{tas}) commands using longitudinal controller and tracking appropriate roll angle ϕ and sideslip β using lateral controller.

To proceed with the controller design, a linearization has been obtained around an operating condition of straight and level flight at $263,000$ Kg, 92.6 m/s true airspeed, and at an altitude of 600 m based on 25.6% of maximum thrust and at a 20 deg flap position using the FTLAB747 v6.5/v7.1 software. In this Chapter the objective is to design FTC for both the longitudinal and lateral axis such that the coupling between the two axis can be minimal.

5.2.3 Longitudinal Controller Design

In order to design the feedback gain F, the linear state space model representing the longitudinal system is obtained from AppendixA.1 and is given by

$$A_g = \begin{bmatrix} 0 & 0 & 0 & 1.0000 \\ 0 & -0.6284 & -0.0021 & 1.0064 \\ -9.8046 & 1.7171 & -0.0166 & 0 \\ 0 & -0.5831 & 0.0004 & -0.5137 \end{bmatrix} \quad B_g = \left[\begin{array}{ccc} 0 & 0 & 0 \\ -0.0352 & -0.0819 & -0.0084 \\ \hline 0 & -0.1756 & 5.7072 \\ -0.6228 & -1.3578 & 0.06 \end{array}\right] \begin{matrix} \} B_1 \\ \} B_2 \end{matrix} \tag{5.19}$$

where the input distribution matrix is rearranged and partitioned according to step 1 to have the structure as in (4.4). Further scaling of the input distribution matrix make sure $B_2B_2^T = I_l$. For the design of longitudinal control, the available system states are $x_{long} = [\theta, \alpha, V_{tas}, q]^T$ where θ is the pitch angle (rad), α is the angle of attack (rad), V_{tas} is the true airspeed (m/sec), and q is the pitch rate (rad/sec). For longitudinal control, the 4 engine pressure ratios (EPRs) (two engines on each wing) are aggregated to produce one control input. The available control surfaces for longitudinal control are $\delta_{long} = [\delta_e, \delta_s, \delta_{epr}]^T$ which represent elevator deflection (rad), horizontal stabilizer deflection (rad) and aggregated longitudinal EPRs. The controlled outputs for longitudinal control are $[\gamma, V_{tas}]^T$, where $\gamma = \theta - \alpha$ is the flight path angle (FPA). Therefore the output distribution matrices for the longitudinal system is

$$C_g = \begin{bmatrix} 1 & -1 & 0 & 0 \\ 0 & 0 & 1 & 0 \end{bmatrix}$$

The state feedback gain F for the longitudinal control is designed using the augmented system in (5.9) and the LMI approach proposed in section (4.3.4), where the Q and R matrices in (4.51) are chosen as $Q_{long} = diag\{0.95, 0.004, 0.01, 2, 0.1, 5\}$ and $R_{long} = diag\{4, 8\}$. The first two states in Q_{long} are the integral action states. For normal flight in a fault-fee scenario, elevator is the primary control surface for the FPA tracking, and the horizontal stabilizer is the redundancy. For V_{tas} tracking, collective engine thrust is the only actuator (i.e. without redundancy), so it is assumed that the engines are fault free. The choice of $\gamma = 7$ in (4.53) gives $\gamma_2 = 3.0012$ and ensures that

$$\gamma_2\gamma_1(1+\gamma_o) < 1$$

which means the closed-loop stability condition in (4.38) is satisfied for the current design of F for the longitudinal system and is given by

$$F = \begin{bmatrix} -0.5775 & -0.0219 & 0.7854 & 0.0115 & 0.9792 & 0.3714 \\ -1.9019 & 0.0377 & 8.0499 & 4.4238 & -0.1590 & 4.4302 \end{bmatrix} \tag{5.20}$$

The discontinuity in the nonlinear controller term (5.17) has been smoothed by using the fractional approximation $\frac{\sigma}{\|\sigma\|+\delta_{long}}$ given in section (3.5), where the value of the positive scalar is chosen as $\delta_{long} = 0.01$

and the value of the modulation gain ρ is chosen as $\rho = 1$.

5.2.4 Lateral Controller Design

The same approach discussed in the previous subsection is adopted, for the design of state feedback gain F for the lateral system. The state space model for the lateral system is taken from AppendixA.1 and is given by

$$A_l = \begin{bmatrix} 0 & 0 & 0.0893 & 1.0000 \\ 0.1055 & -0.0999 & -0.9887 & 0.1014 \\ -0.0019 & 0.2767 & -0.2066 & -0.1186 \\ 0.0004 & -1.6478 & 0.1718 & -1.0579 \end{bmatrix} \quad B_l = \left[\begin{array}{ccc} 0 & 0 & 0 \\ 0 & 0.0174 & 0.0010 \\ \hline -0.0277 & -0.2478 & -0.1993 \\ -0.3117 & 0.1187 & -0.0386 \end{array}\right] \begin{matrix} \\ \\ \} B_1 \\ \} B_2 \end{matrix} \tag{5.21}$$

where the input distribution matrix is the same as in longitudinal system is rearranged and partitioned according to step 1 to have the structure as in (4.4). Further scaling of the input distribution matrix make sure $B_2 B_2^T = I_l$. The available states are $x_{lat} = [\phi, \beta, r, p]^T$ where ϕ is the roll angle (rad), β is the sideslip angle (rad), r is the yaw rate (rad/sec) and p is the roll rate (rad/sec). For the lateral control, two ailerons (inner and outer on the right wing) are aggregated to produce one control input. For the lateral control $\delta_{lat} = [\delta_a, \delta_r, \delta_{epr}]$ are the available control surfaces, which represent anti-symmetric aileron deflection (rad), rudder deflection and differential aggregated EPRs. The controlled outputs for lateral control are $[\phi, \beta]^T$, so the output distribution matrix for the lateral system is

$$C_l = \begin{bmatrix} 1 & 0 & 0 & 0 \\ 0 & 1 & 0 & 0 \end{bmatrix}$$

Using the LMI approach in section (4.3.4) where the symmetric positive definite matrices Q and R are chosen as $Q_{lat} = diag\{0.95, 0.08, 2, 1, 15, 5\}$ and $R_{lat} = diag(\{10, 2\}$. During normal flight, the primary control surfaces for ϕ and β tracking are ailerons and the rudder respectively, while the differential engine thrust is the redundancy for both. Based on these assumptions, using a numerical search it can be verified that $\gamma_1(1+\gamma_o) = 0.0731$, where $\gamma_1 = \|B_{1_a}\|$ and γ_0 is defined in (4.14). The choice of $\gamma = 8.8$ in (4.53)

ensures that $\gamma_2 = 5.8832$ and therefore the closed-loop stability in (4.38) is satisfied.

$$\gamma_2\gamma_1(1+\gamma_o) < 1$$

The obtained state feedback gain F for the lateral control is

$$F = \begin{bmatrix} 0.4165 & -0.0839 & 0.2936 & -1.9273 & 0.7983 & -0.1356 \\ -0.5265 & -0.1241 & 1.1878 & -0.6954 & -0.1000 & 0.3879 \end{bmatrix} \tag{5.22}$$

The discontinuity of the nonlinear controller (4.41) has been smoothed by using the fractional approximation, where the value of the positive scalar is chosen as $\delta_{lat} = 0.01$, and the selected value of ρ for the lateral control is $\rho = 1$.

5.3 Non-linear FTC Simulations Results

The simulations are initially conducted at the trim conditions. For the up-and-away manoeuvre, a 3 deg reference command for FPA $(during\ 10-60sec)$, and a change in V_{tas} of $10m/sec$ at 100 sec are issued to increase the altitude and speed of the aircraft. For the turning manoeuvre, a reference command requests a change in ϕ of 25 deg during $(200-250sec)$. A 0 deg reference command to β is issued throughout.

5.3.1 Fault Free Scenario

In Figures 5.1-5.2, the tracking performance of the nominal fault free system is shown. It can be seen in Figure 5.1 that there is a small coupling between roll angle and sideslip when the roll angle command is issued at 200 sec. A small coupling with FPA is also visible due to roll command. In Figure 5.2, the corresponding actuator positions are shown, where the actuators effectiveness plot W shows that all the actuators are fault free.

5.3.2 Elevator Lock in place failure

Figures 5.3-5.4 demonstrate the system states and actuator positions and the actuator effectiveness level in the case when an elevator (the primary control surface for FPA tracking) lock in place/offset-jam failure

occurs at 50 *sec* during the climb. It can be seen in Figure 5.4 that the control signal sent to the elevator by the control allocation scheme is shutoff as the effectiveness level of the elevator is zero (Figure 5.4) and redistributed to the horizontal stabilizer, to maintain the nominal tracking performance (Figure 5.3).

5.3.3 Horizontal stabilizer Hardover/runaway failure

Figures 5.5-5.6 show no degradation in tracking performance as compared to (Figure 5.1) when the horizontal stabilizer (the redundant control surface for FPA tracking) runaway to the maximum positive deflection limit of 3 deg during the climb maneuver. It can be seen in Figure 5.6 that the elevator is deflecting in the negative side to counteract the horizontal stabilizer failure. The effectiveness level of the horizontal stabilizer can be seen in Figure 5.6 after the runaway failure.

5.3.4 Aileron Lock in place failure

In Figures 5.10-5.11, a scenario is demonstrated when aileron (the primary control surface for roll angle tracking) lock in place/offset-jam failure occurs at 250 *sec* during the turning manoeuvre, where it can be seen (Figure 5.11) that the engine thrust level and the rudder react more actively to compensate the aileron failure and it is clear from (Figure 5.10) that there is no degradation in system performance as compared to the nominal performance (Figure 5.1).

5.3.5 Rudder Hardover/runaway failure

Finally, in Figures 5.12-5.13, during the turning manoeuvre at 215 *sec*, a rudder (primary control surface for sideslip tracking) runaway to 7 *deg* occurs. During the runaway failure, the rudder moves with its maximum rate. This is a very severe failure and is very difficult to handle, but it can be seen (Figure 5.13) that the engine thrust level and the ailerons are actively involved by the control allocation scheme to handle this situation and the performance close to the nominal is still achieved (Figure 5.12). The effectiveness level of the rudder after the failure vanishes to zero.

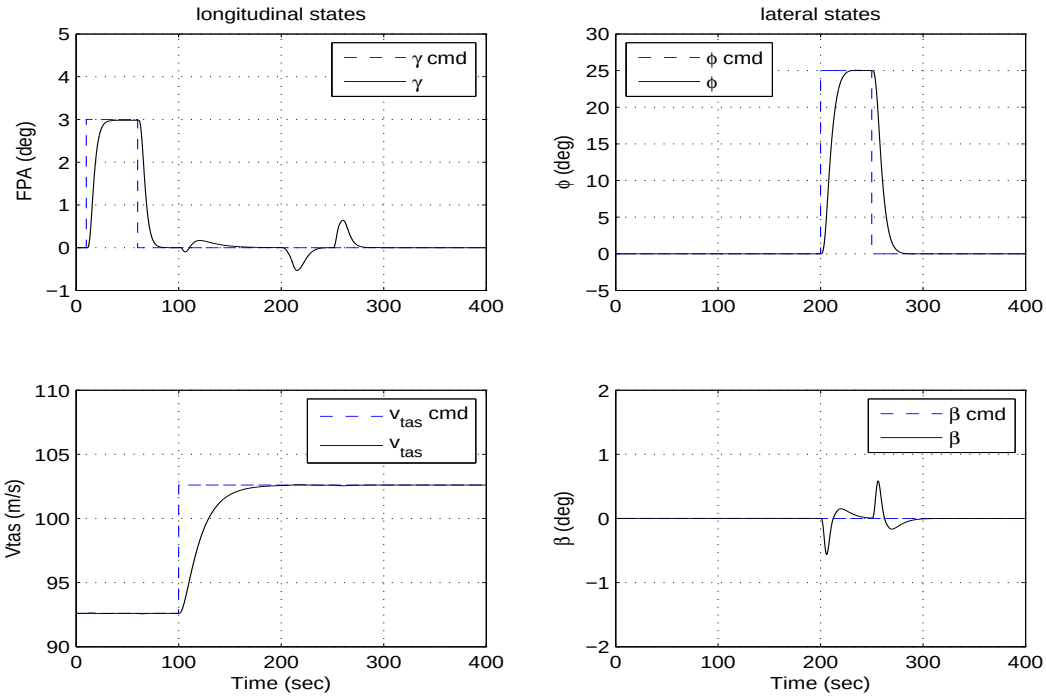

Figure 5.1: nominal scenario: System States

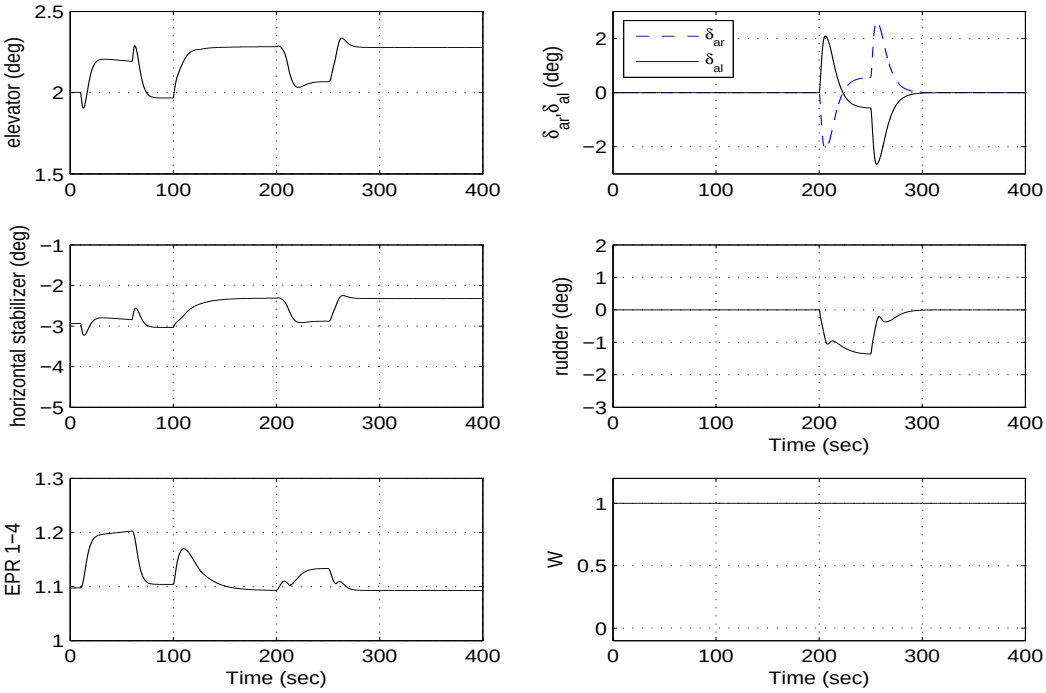

Figure 5.2: nominal scenario: actuators positions and effectiveness

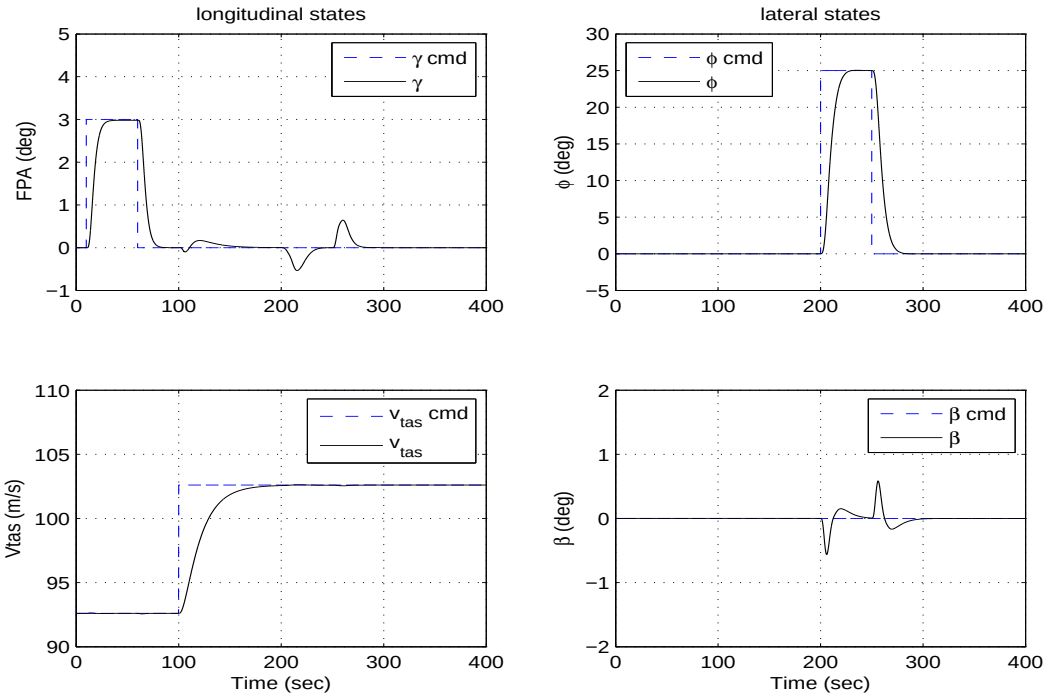

Figure 5.3: elevator offset-jam failure: System States

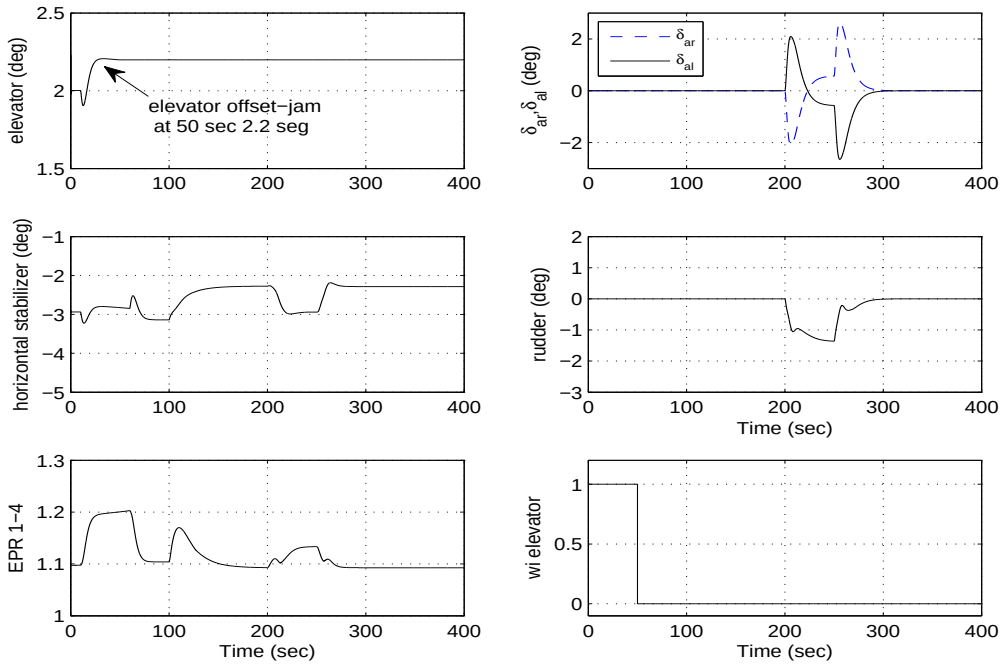

Figure 5.4: elevator offset-jam failure: actuators positions and effectiveness

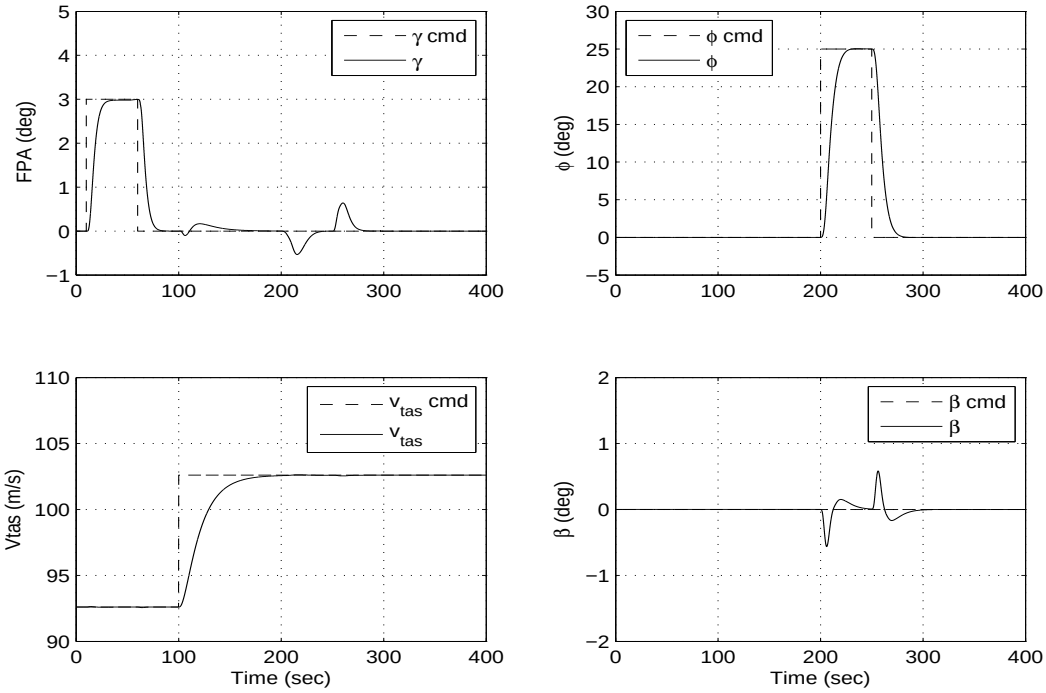

Figure 5.5: horizontal stabilizer runaway failure: System States

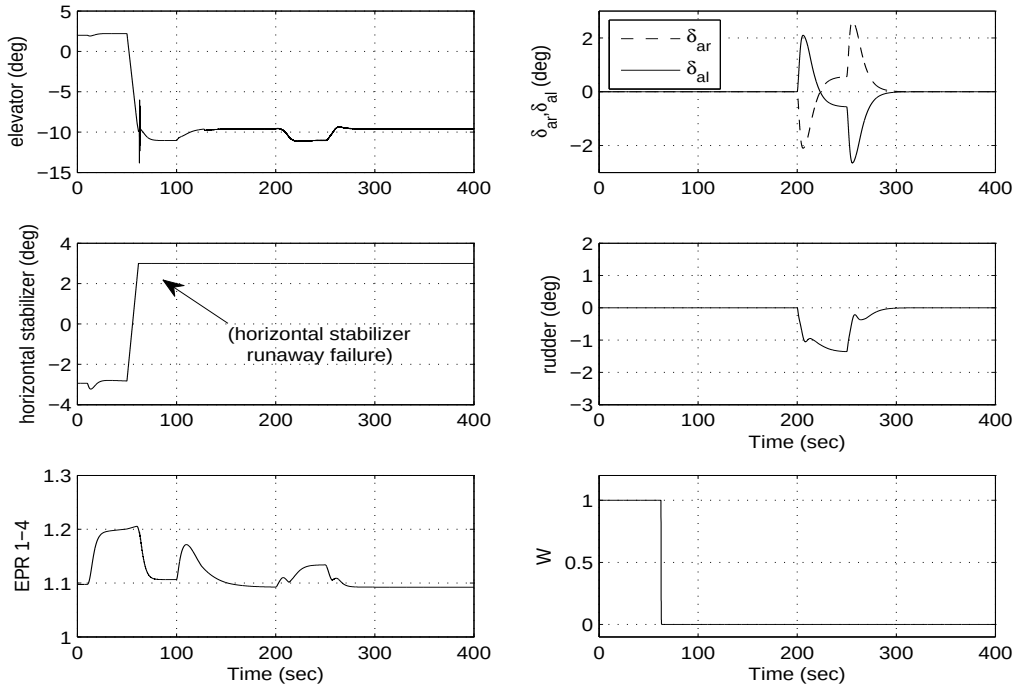

Figure 5.6: horizontal stabilizer runaway failure: actuators positions and effectiveness

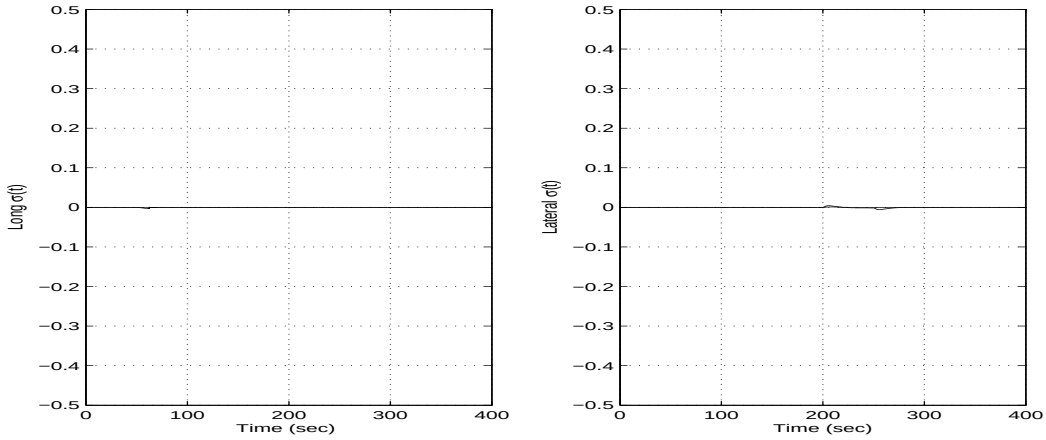

Figure 5.7: Switching function elevator lock in place failure

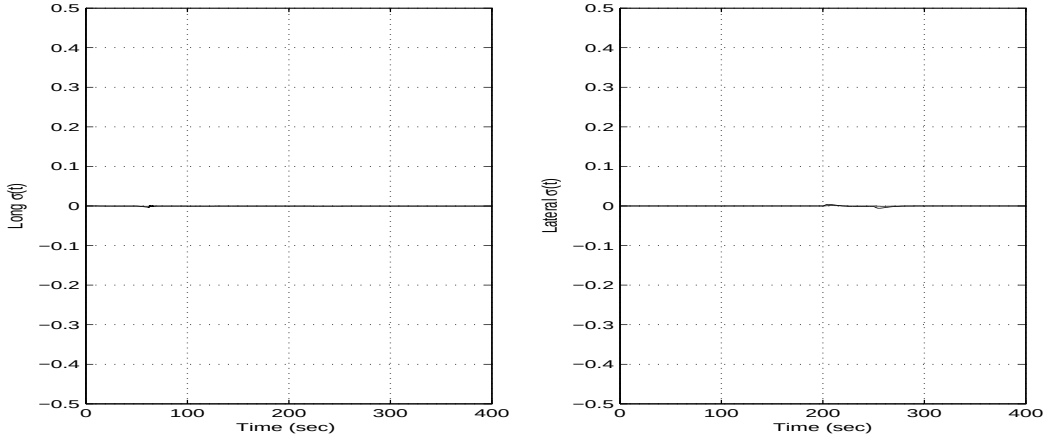

Figure 5.8: Switching function horizontal stabilizer runaway failure

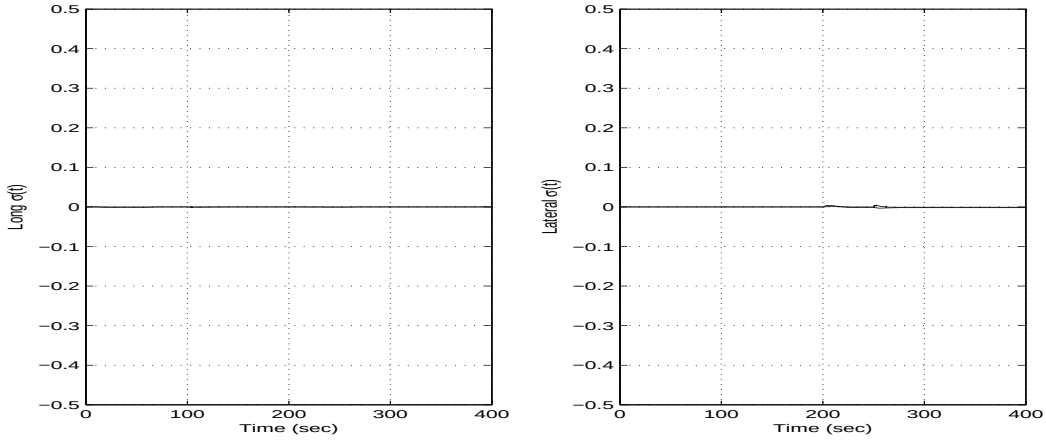

Figure 5.9: Switching function aileron lock in place failure

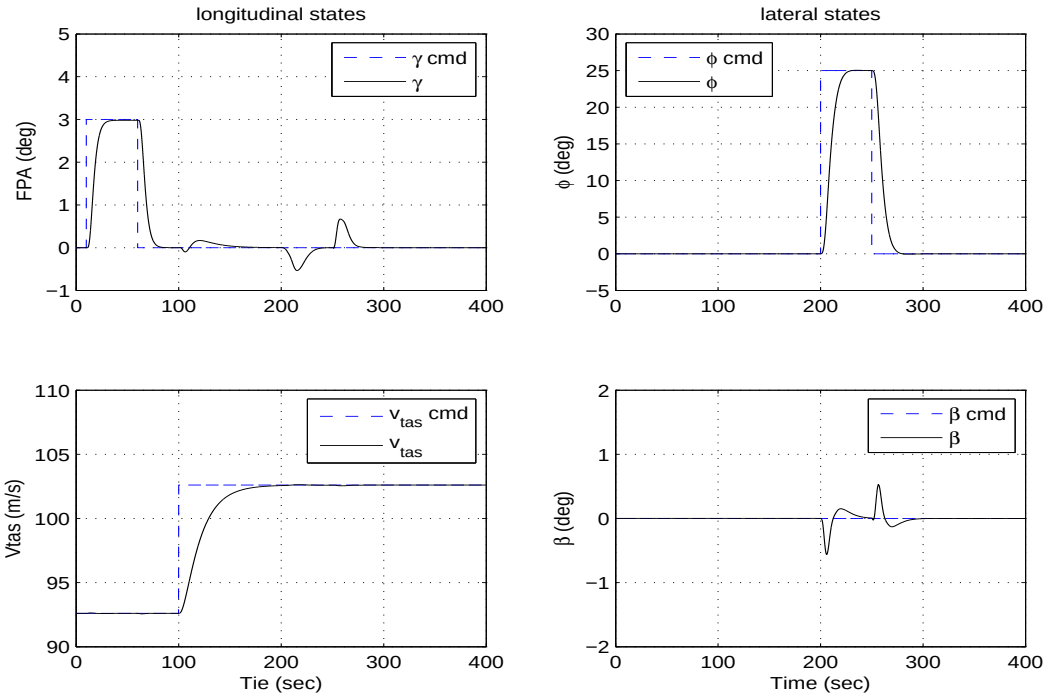

Figure 5.10: aileron offset-jam failure: System States

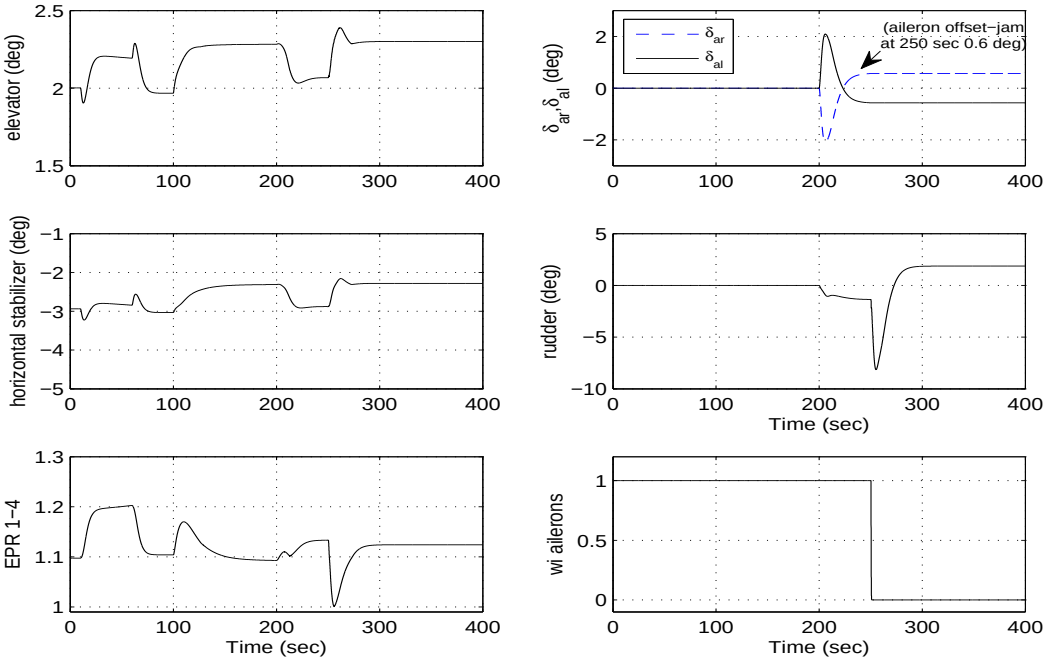

Figure 5.11: aileron offset-jam failure: actuators positions and effectiveness

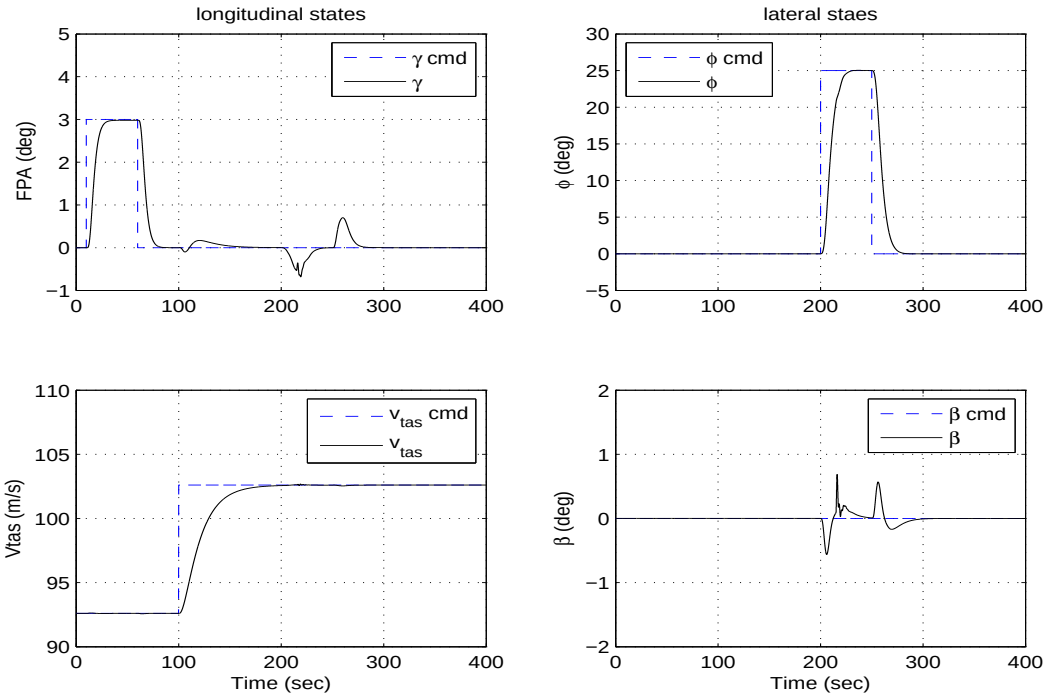

Figure 5.12: rudder runaway failure: System States

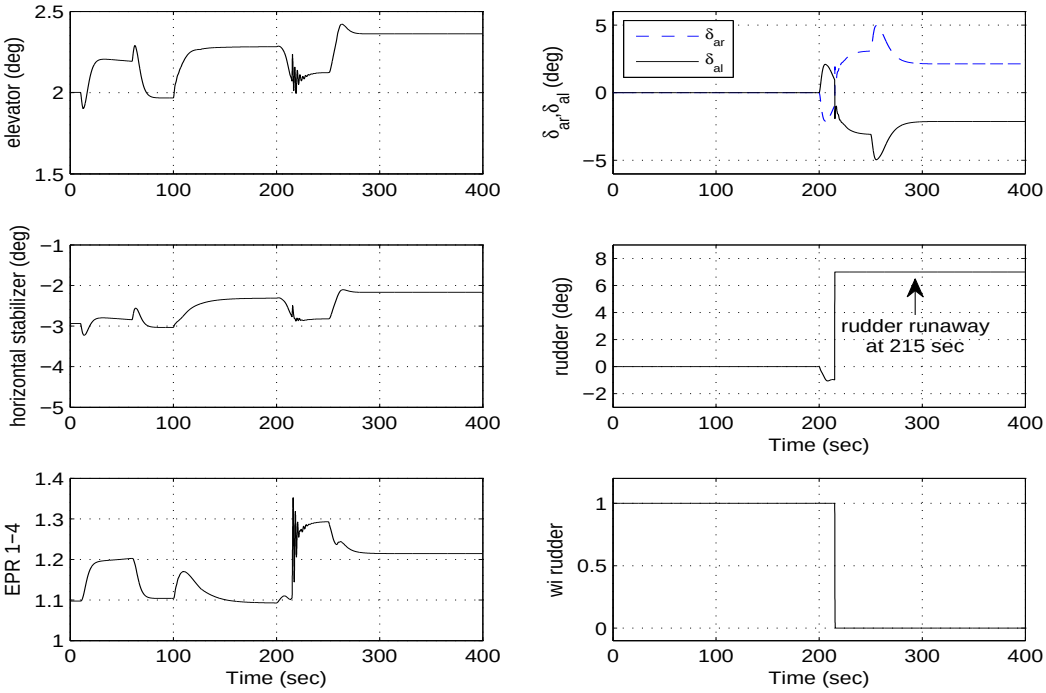

Figure 5.13: rudder runaway failure: actuators positions and effectiveness

5.4 Conclusion

This Chapter, considered the application of integral sliding mode FTC scheme on the high fidelity non-linear model of a large transport aircraft using the FTLAB747 v6.5/v7.1 software. FTLAB747 v6.5/v7.1 represents a 'real world' non-linear aircraft model in the software environment and was used to test the effectiveness of the proposed scheme. The proposed integral sliding mode FTC scheme used the effectiveness level of the actuators and has the capability to cope with total failures without reconfiguring the controller.

The FTC scheme proposed in Chapter 4 is designed for the open-loop plant with no cognizance of any existing controller. All the parameters for the FTC scheme are synthesized simultaneously and the closed loop performance in both fault free conditions and in the presence of the fault is completely determined by this design process. The coming Chapter builds on the ideas to retrofit integral sliding modes around the existing control scheme to induce fault tolerance. This is beneficial in an industrial perspective as the new controller does not affect the certification of the original underlying baseline controller.

Chapter 6

An Augmentation Scheme for Fault Tolerant Control using Integral Sliding Modes

In this Chapter the potential of integral sliding mode approach to be retro-fitted to an existing feedback controller, (as mentioned earlier in the properties of integral sliding mode control (Chapter 3)) is analysed. A novel fault tolerant control allocation scheme which is proposed in this Chapter, relies on an *a posteri* approach, building on an existing state feedback controller designed using only the primary actuators. An integral sliding mode scheme is integrated with the existing controller to introduce fault tolerance. The proposed scheme uses the measured or estimated actuator effectiveness levels in order to redistribute the control signals to the healthy ones which allows a certain class of total actuator failures to be mitigated. The effectiveness of the proposed scheme is tested in simulation using a high fidelity nonlinear model of a large transport aircraft model discussed in Appendix A.1.

6.1 Introduction

To achieve FTC, one paradigm is to subdivide and classify the different actuators into ones of primary and secondary status. Then, in the case of faults or failures in the primary actuators, secondary actuators can be exploited to retain acceptable performance [39]. One way to manage the redundancy which is created

by the use of primary and secondary actuators is to deploy control allocation (CA) schemes discussed in Section 2.4.2.2 to distribute the control effort over the effector suite.

The FTC technique proposed in this Chapter is quite different to the technique proposed in Chapter 4. The technique in Chapter 4 is designed based on the open loop plant with no cognizance of any existing controller and all the parameters associated with the integral sliding mode scheme are synthesized simultaneously based on a model of the open loop plant and the closed loop performance (in both fault free conditions and in the presence of faults) is completely determined by this design process. In this Chapter for controller design purposes the actuators are classified as primary and secondary. It is assumed a controller based only on primary actuators has already been designed to provide appropriate closed loop performance in a fault free scenario. The technique proposed in this Chapter involves creating an *a posteri* integral sliding mode design, building on the existing state feedback controller. The idea is to use only the primary actuators in the nominal fault free scenario, and to engage the secondary actuators only if faults or failures occur. Crucially, in the fault free case, the closed-loop system behaviour is entirely dependent on the original controller, and the overall scheme behaves exactly as though the ISM scheme were not present. Only in the fault/failure case does the FTC scheme become active. In this way the proposed integral sliding mode FTC scheme can be retrofitted to almost any existing control scheme to induce fault tolerance. This requires a totally different design philosophy as compared to the scheme discussed in Chapter 4. The scheme proposed here has an advantage from an industrial perspective, since the proposed scheme can be retrofitted to an existing control scheme to induce fault tolerance without the need to remove or alter existing control loops. Furthermore the nominal fault free performance can be specified according to any design paradigm. The scheme proposed in this Chapter uses measured or estimated actuator effectiveness levels in order to distribute the control signals among the actuators. In the case of faults/failures, the controller structure does not need to be changed and the control signals are automatically redistributed to healthy actuators to maintain the closed-loop performance close to nominal. A rigorous closed-loop stability analysis, under the assumption of imperfect estimates of actuator effectiveness levels, will be considered.

6.2 System description and problem formulation

An LTI system subject to actuator faults or failures can be modelled as

$$\dot{x}_p(t) = A_p x_p(t) + B_p W(t) u(t) \tag{6.1}$$

where $A_p \in \mathbb{R}^{n\times n}$, $B_p \in \mathbb{R}^{n\times m}$ and $W(t) \in \mathbb{R}^{m\times m}$ is a diagonal weighting matrix representing the effectiveness of each actuator where the elements $0 \leq w_i(t) \leq 1$ for $i = 1,...,m$. If $w_i(t) = 1$, the corresponding ith actuator has no fault, whereas if $1 > w_i(t) > 0$, an actuator fault is present. In a situation where $w_i(t) = 0$, the actuator has completely failed. To create the design philosophy, suppose the input distribution matrix can be partitioned as

$$B_p = \begin{bmatrix} B_1 & B_2 \end{bmatrix} \tag{6.2}$$

where $B_1 \in \mathbb{R}^{n\times l}$ and $B_2 \in \mathbb{R}^{n\times(m-l)}$ and $l < m$ and $l < n$. Here B_1 is the input distribution matrix associated with the primary actuators and is assumed to be of rank equal to l, whilst B_2 is associated with the secondary actuators which provide redundancy in the system. It is assumed that the pair (A_p, B_1) is controllable. For the primary and secondary actuators, the weighting matrix $W(t)$ is also partitioned as $W(t) = diag[W_1(t), W_2(t)]$ where $W_1(t) = diag[w_1(t),...,w_l(t)]$ and $W_2(t) = diag[w_{l+1}(t),...,w_m(t)]$ are weighting matrices for primary and secondary actuators respectively. In this Chapter, it is assumed that the matrix $W(t)$ is estimated by some FDI scheme, given in the Section 4.4.1 or by using a measurement of the actual actuator deflection compared to the demand [22]. The estimated value $\widehat{W}(t)$ will not be a perfect estimate of the real effectiveness matrix $W(t)$, and in this Chapter it is assumed the estimated matrix $\widehat{W}(t) = diag[\widehat{W}_1(t), \widehat{W}_2(t)]$ satisfies the relationship

$$W(t) = (I - \triangle(t))\widehat{W}(t) \tag{6.3}$$

where $\triangle(t) = diag[\triangle_1(t), \triangle_2(t)]$. Both $\triangle_1(t)$ and $\triangle_2(t)$ are assumed to be diagonal matrices such that the diagonal elements $\delta_i(t) \in \mathbb{R}$ satisfy $\delta_i(t) < \triangle_{max}$ for some $\triangle_{max} > 0$ where

$$\triangle_{max} = max(\|\triangle_1(t)\|, \|\triangle_2(t)\|) \tag{6.4}$$

The matrices $\triangle_1(t)$ and $\triangle_2(t)$ model the level of imperfection in the fault estimation, and satisfy

$$\begin{aligned} W_1(t) &= (I_l - \triangle_1(t))\widehat{W}_1(t) \\ W_2(t) &= (I_{m-l} - \triangle_2(t))\widehat{W}_2(t) \end{aligned}$$

Since B_1 is assumed to has full column rank equal to l and therefore there exists an orthogonal matrix $T_p \in \mathbb{R}^{n\times n}$ such that

$$T_p B_1 = \begin{bmatrix} 0 \\ B_{21} \end{bmatrix} \tag{6.5}$$

where $B_{21} \in \mathbb{R}^{l\times l}$ (and B_{21} is nonsingular). By a suitable change of coordinates $x \mapsto T_p x_p$ it can be ensured, the input plant distribution matrix has the form

$$T_p B_p = \begin{bmatrix} 0 & B_{12} \\ B_{21} & B_{22} \end{bmatrix} \tag{6.6}$$

where $B_{22} \in \mathbb{R}^{l\times(m-l)}$. Next scale the last l states to ensure that $B_{21}^T B_{21} = B_{21} B_{21}^T = I_l$ (i.e. B_{21} is orthogonal). Consequently it can be assumed without loss of generality the system (6.1) can be written as

$$\dot{x}(t) = Ax(t) + BW(t)u(t) \tag{6.7}$$

where

$$B = \left[\begin{array}{c|c} 0 & B_{12} \\ B_{21} & B_{22} \end{array}\right] := \left[\begin{array}{c|c} B_o & B_s \end{array}\right] \tag{6.8}$$

Controllability of (A_p, B_1) implies that the pair (A, B_o) is controllable. A state feedback control law

$$v_o(t) = Fx(t) \tag{6.9}$$

has been designed *a priori* to make the system

$$\dot{x}(t) = (A + B_o F)x(t) \tag{6.10}$$

stable. Note that the gain F is the baseline controller (discussed in Section 6.5) designed for the primary actuators. Now a control allocation scheme will be *retrofitted* to the control law $v_o(t)$. The physical control law $u(t)$ applied to *all the actuators* is defined as

$$u(t) = N(t)v(t) \tag{6.11}$$

where $v(t) \in \mathbb{R}^l$ is the virtual control effort produced by the actuators, and will be discussed in the next section. The overall control structure is given in Figure 6.1, where it is clear that the integral sliding mode FTC scheme is retrofitted to the existing baseline controller $v_o(t)$ (which is designed using only the primary actuators) and will be only active in case of faults or failures. In Figure 6.1, it is assumed that the

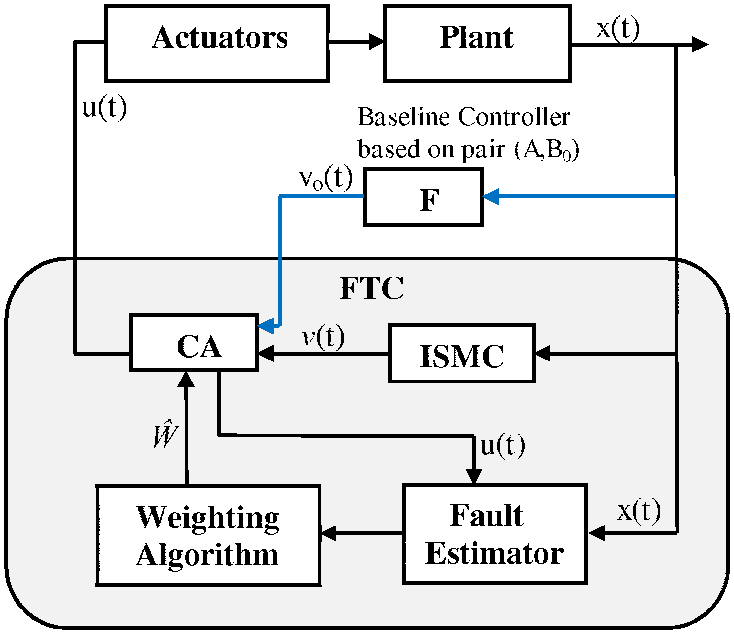

Figure 6.1: Schematic of the Overall Control Strategy

Fault Estimator is able to identify the *actuator* faults/failures from all other possible faults/failures in the system. The proposed control allocation matrix is given by

$$N(t) = \begin{bmatrix} I_l \\ N_2(t)(I_l - \widehat{W}_1(t)) \end{bmatrix} \tag{6.12}$$

where

$$N_2(t) := B_{22}^T B_{21}(B_{21}^T B_{22}\widehat{W}_2(t)B_{22}^T B_{21})^{-1} \tag{6.13}$$

and $\widehat{W}_1(t)$ and $\widehat{W}_2(t)$ are the estimates of the effectiveness levels. Now define

$$\mathscr{W} = \{(\hat{w}_{l+1},...,\hat{w}_m) \in \underbrace{[0 \quad 1] \times ... \times [0 \quad 1]}_{m-l \text{ times}} : \det(B_{22}\widehat{W}_2(t)B_{22}^T) \neq 0\} \tag{6.14}$$

Throughout this Chapter, it is assumed that $m \geq 2l$. This allows up to $m-2l$ of the entries $\hat{w}_i(t)$ in the matrix $\widehat{W}_2(t)$ to be zero, and yet guarantee $\det(B_{22}\widehat{W}_2(t)B_{22}^T) \neq 0$. The set $\mathscr{W}$ will be shown to constitute the class of faults/failures for which closed-loop stability can be maintained.

Substituting (6.3) and (6.11) into (6.7) yields

$$\dot{x}(t) = Ax(t) + \begin{bmatrix} B_{12}(I_{m-l} - \triangle_2(t))\widehat{W}_2(t)N_2(I_l - \widehat{W}_1(t)) \\ B_{21}(I_l - \triangle_1(t))\widehat{W}_1(t) + B_{22}(I_{m-l} - \triangle_2(t))\widehat{W}_2(t)N_2(I_l - \widehat{W}_1(t)) \end{bmatrix} v(t) \tag{6.15}$$

Since B_{21} is orthogonal by construction, $B_{21}B_{21}^T = I_l$, and using the definition of $N_2(t)$ in (6.13) it follows that

$$B_{22}\widehat{W}_2(t)N_2(t) = B_{21}B_{21}^T B_{22}\widehat{W}_2(t)N_2(t) \;=\; B_{21} \tag{6.16}$$

Consequently using (6.16), equation (6.15) simplifies to

$$\dot{x}(t) = Ax(t) + \begin{bmatrix} B_{12}(I - \triangle_2(t))\widehat{W}_2(t)N_2(I_l - \widehat{W}_1(t)) \\ B_{21}(I_l - \triangle_1(t))\widehat{W}_1(t) + B_{21}(I_l - \widehat{W}_1(t)) - B_{22}\triangle_2(t)\widehat{W}_2(t)N_2(I - \widehat{W}_1(t)) \end{bmatrix} v(t) \tag{6.17}$$

which can be further simplified to

$$\dot{x}(t) = Ax(t) + \underbrace{\begin{bmatrix} B_{12}(I_{m-l} - \triangle_2(t))\widehat{W}_2(t)N_2(I_l - \widehat{W}_1(t)) \\ B_{21} - B_{21}\triangle_1(t)\widehat{W}_1(t) - B_{22}\triangle_2(t)\widehat{W}_2(t)N_2(I_l - \widehat{W}_1(t)) \end{bmatrix}}_{\widehat{B}} v(t) \tag{6.18}$$

Remark 6.1: In the case of perfect estimation of $\widehat{W}(t)$ (i.e. $\triangle(t) = 0$) and when there is no fault in the primary and secondary actuators (i.e. $W_1(t) = I_l$ and $W_2(t) = I_{m-l}$), the system in (6.18) becomes

$$\dot{x}(t) = Ax(t) + B_o v(t) \tag{6.19}$$

and so only the primary control channels will be used.

In a fault/failure scenario, to maintain the closed-loop performance near to nominal, the concept of integral sliding mode control is combined with the control law from (6.11) and (6.12). The nominal fault free system in (6.19) will be used for the design of the augmentation scheme which will be demonstrated in the sequel.

6.3 Integral Sliding Mode Controller Design

As mentioned earlier in Chapter 3 and Chapter 4, first a sliding surface is designed and in the second step a control law is developed which can enforce and maintain a sliding motion on the sliding surface.

First choose the sliding surface as $\mathscr{S} = \{x \in \mathbb{R}^n : \quad \sigma(x,t) = 0\}$ where the switching function $\sigma(x,t)$, based on the nominal system (6.10), is defined as

$$\sigma(x,t) := Gx(t) - Gx(0) - G\int_0^t \big(A + B_o F\big)x(\tau)d\tau \tag{6.20}$$

where $G \in \mathbb{R}^{l\times n}$ is the design freedom to be selected. The elimination of the reaching phase, ensures the occurrence of the closed-loop sliding motion throughout the entire response of the system. In this Chapter, the choice of G is suggested as

$$G := B_o^T \tag{6.21}$$

where B_o is defined in (6.8). With this choice of G it follows

$$GB_o = B_{21}^T B_{21} = I_l$$

and this choice of G serves as the pseudo inverse of the matrix B_o. Also from (6.18)

$$(G\widehat{B})^{-1} \quad = \quad \left(B_{21}^T\Big(B_{21} - B_{21}\triangle_1(t)\widehat{W}_1(t) - B_{22}\triangle_2(t)\widehat{W}_2(t)N_2(I_l - \widehat{W}_1(t))\Big)\right)^{-1} \tag{6.22}$$

which will be used while obtaining the expression for the equivalent control. To analyze the closed-loop sliding motion associated with the integral switching function in (6.20) and the choice of G in (6.21),

taking the time derivative of $\sigma(x,t)$ defined in (6.20) yields

$$\dot{\sigma} = G\dot{x}(t) - GAx(t) - GB_oFx(t) \tag{6.23}$$

Substituting (6.18) into (6.23), the resulting expression simplifies to

$$\dot{\sigma} = G\widehat{B}v(t) - GB_oFx(t) \tag{6.24}$$

Equating $\dot{\sigma}(t) = 0$, and by using the fact that $GB_o = I_l$, the expression for the equivalent control is given by

$$v_{eq}(t) = (G\widehat{B})^{-1}Fx(t) \tag{6.25}$$

The equation of motion governing sliding can be obtained by substituting (6.25) into (6.18) which yields

$$\dot{x}(t) = Ax(t) + \widehat{B}(G\widehat{B})^{-1}Fx(t) \tag{6.26}$$

Adding and subtracting the term $B_oFx(t)$, equation (6.26) can be written as

$$\dot{x}(t) = (A + B_oF)x(t) + (\widehat{B}(G\widehat{B})^{-1} - B_o)Fx(t) \tag{6.27}$$

which can be further simplified to

$$\dot{x}(t) = (A + B_oF)x(t) + \begin{bmatrix} B_{12}(I_{m-l} - \triangle_2(t))\widehat{W}_2(t)N_2(I_l - \widehat{W}_1(t))(G\widehat{B})^{-1} \\ 0_l \end{bmatrix} Fx(t) \tag{6.28}$$

Remark 6.2: Note that in the nominal fault free case when $W(t) = I$, and in the case of perfect estimation of $\widehat{W}(t)$ matrix, the top row in the second term is zero, and the closed-loop sliding motion is stable. In the case of faults or failures when $\widehat{W}(t) \neq I$, then the second term is not zero and will be treated as unmatched uncertainty.

For the stability analysis which follows, write (6.28) as

$$\dot{x}(t) = (A + B_oF)x(t) + \tilde{B}\Phi(t)Fx(t) \tag{6.29}$$

where

$$\tilde{B} := \begin{bmatrix} B_{12} \\ 0 \end{bmatrix} \tag{6.30}$$

and the time varying uncertain term

$$\Phi(t) := (I_{m-l} - \triangle_2(t))\Psi(t)\Big(I_l - \triangle_1(t)\widehat{W}_1(t) - B_{21}^T B_{22}\triangle_2(t)\Psi(t)\Big)^{-1} \tag{6.31}$$

where

$$\Psi(t) := \widehat{W}_2(t)N_2(I_l - \widehat{W}_1(t)) \tag{6.32}$$

From (6.16) it is clear that $\widehat{W}_2(t)N_2(t)$ is a right pseudo inverse for $B_{21}^T B_{22}$. Then by using arguments similar to those as given in Chapter 4 as proved in [111], it follows $\|\widehat{W}_2(t)N_2(t)\| < \gamma_1$ for some positive scalar γ_1, provided that $\det(B_{22}\widehat{W}_2(t)B_{22}^T) \neq 0$. Since

$$\|\Psi(t)\| \leq \|(I_l - \widehat{W}_1(t))\|\|\widehat{W}_2(t)N_2(t)\| < \|\widehat{W}_2(t)N_2(t)\| < \gamma_1$$

$\|\Psi(t)\|$ remains bounded. Define γ_1^* as the smallest number (which will be used in the *Proposition 6.1*) satisfying

$$\|\Psi(t)\| < \gamma_1^* \tag{6.33}$$

In the following subsections the main results of the Chapter are presented.

6.3.1 Stability Analysis of the Closed-loop Sliding motion

In the case of perfect estimation of the $\widehat{W}(t)$ matrix, (i.e. $\triangle(t) = 0$) and when there are no faults in the system (i.e. $W(t) = I$) the uncertain term $\Phi(t)$ in (6.29) vanishes (i.e. $\Phi(t) = 0$) and the closed-loop sliding motion in (6.29) simplifies to

$$\dot{x}(t) = (A + B_o F)x(t) \tag{6.34}$$

which is stable by the choice of the baseline controller F.

In the case of non-perfect estimation of $\widehat{W}(t)$ and in the presence of faults, the stability of (6.29) needs to be proven. To this end, in this most general situation the equation governing the sliding motion in (6.29)

can be written as

$$\dot{x}(t) = \underbrace{(A+B_oF)}_{\tilde{A}}x(t) + \tilde{B}\overbrace{\Phi(t)\underbrace{Fx(t)}_{\tilde{y}}}^{\tilde{u}} \tag{6.35}$$

For the subsequent stability analysis, define the $\mathscr{L}_2$ gain between $\tilde{u}$ to $\tilde{y}$ as

$$\gamma_2 = \|\tilde{G}(s)\|_\infty \tag{6.36}$$

where the transfer function matrix

$$\tilde{G}(s) := F(sI-\tilde{A})^{-1}\tilde{B} \tag{6.37}$$

and is stable by design.

Proposition 6.1: Suppose that the condition

$$(1+\gamma_3\gamma_1^*)\triangle_{max} < 1 \tag{6.38}$$

holds, where γ_1^* and $\triangle_{max}$ are defined in (6.33) and (6.4) and $\gamma_3 = \|B_{22}\|$, then during fault or failure conditions including failure of all primary actuators and for any $\hat{w}_{l+1}(t),...,\hat{w}_m(t) \in \mathscr{W}$ where $\mathscr{W}$ is defined in (6.14), the closed loop system in (6.35) will be stable if:

$$\frac{\gamma_2\gamma_1^*(1+\triangle_{max})}{1-(1+\gamma_3\gamma_1^*)\triangle_{max}} < 1 \tag{6.39}$$

where γ_2 is defined in (6.36).

Proof. The closed-loop sliding motion in (6.35) can be written as

$$\dot{x}(t) = \tilde{A}x(t) + \tilde{B}\tilde{u}(t) \tag{6.40}$$

$$\tilde{y}(t) = Fx(t) \tag{6.41}$$

where

$$\tilde{u}(t) = \Phi(t)\tilde{y}(t) \tag{6.42}$$

By using the small gain theorem as discussed in the Appendix B.1.2, the feedback interconnection of the known stable matrix $\tilde{G}(s)$ with the bounded uncertain term $\Phi(t)$ and hence equation (6.35) will be stable

if

$$\|\tilde{G}(s)\|_\infty \|\Phi(t)\| < 1 \tag{6.43}$$

From equation (6.31), it is clear that

$$\|\Phi(t)\| \leq \|\big(I_l - \underbrace{\triangle_1(t)\widehat{W}_1(t) - B_{21}^T B_{22}\triangle_2(t)\Psi(t)}_{X(t)}\big)^{-1}\| \|(I_{m-l} - \triangle_2(t))\Psi(t)\| \tag{6.44}$$

Using the fact that $\|\widehat{W}_1(t)\| \leq 1$, and $\|B_{21}^T\| = 1$ (since $B_{21}^T B_{21} = I_l$), from (6.44)

$$\begin{aligned} \|X(t)\| &\leq \|\triangle_1(t)\widehat{W}_1(t)\| + \|B_{21}^T B_{22}\triangle_2(t)\Psi(t)\| \\ &\leq \|\triangle_1(t)\| + \|B_{22}\|\|\triangle_2(t)\|\|\Psi(t)\| \\ &\leq (1+\gamma_3\gamma_1^*)\triangle_{max} < 1 \end{aligned}$$

if the conditions of *Proposition 6.1* hold. Hence from (6.44), and using the fact [63] that in general

$$\|(I-X)^{-1}\| \leq (1-\|X\|)^{-1} \quad \text{if} \quad \|X\| < 1$$

therefore

$$\|\Phi(t)\| \leq \frac{\gamma_1^*(1+\triangle_{max})}{1-(1+\gamma_3\gamma_1^*)\triangle_{max}} \tag{6.45}$$

From the expression in (6.45) and the fact that $\|\tilde{G}(s)\|_\infty = \gamma_2$, a sufficient condition to ensure the conditions of the small gain theorem in (6.43) hold is that

$$\frac{\gamma_2\gamma_1^*(1+\triangle_{max})}{1-(1+\gamma_3\gamma_1^*)\triangle_{max}} < 1$$

This is the condition in (6.39), and the proof of *Proposition 6.1* is complete. ■

***Remark 6.3*:** If B_{12} is zero in (6.30) (which is the assumption in many CA schemes, see for example [60], [105]) then $\widetilde{B} = 0$, and the condition of *Proposition 6.1* is trivially satisfied. The scheme in this Chapter considers $B_{12} \neq 0$, and consequently proposes a more general solution which helps target a wider range of potential applications.

6.3.2 Integral Sliding Mode control laws

Now a control law will be designed such that the sliding motion on the sliding surface in (6.20) can be ensured. Define the integral sliding mode control law as

$$v(t) = v_l(t) + v_n(t) \tag{6.46}$$

where the linear part of the control law same as in (6.9) which is known *a priori* is

$$v_l(t) := Fx(t) \tag{6.47}$$

and the nonlinear part, which induces the sliding motion, is

$$v_n(t) := -\rho(t,x)\frac{\sigma(t,x)}{\|\sigma(t,x)\|} \qquad \text{for } \sigma(t,x) \neq 0 \tag{6.48}$$

where $\rho(t,x)$ is the modulation gain whose precise value is proposed in the statement of *Proposition 6.2*. Now in the sequel it is demonstrated that the integral sliding mode control law in (6.46)-(6.48) satisfies the reachability condition.

Proposition 6.2: Assume the conditions of *Proposition 6.1* hold. Then if $\rho(t,x)$ is chosen as

$$\rho(t,x) \geq \frac{(1+\gamma_3\gamma_1^*)\triangle_{max}\|v_l(t)\| + \eta}{1-(1+\gamma_3\gamma_1^*)\triangle_{max}} \tag{6.49}$$

where $\eta > 0$ is a small positive scalar, the integral sliding mode control law in (6.46)-(6.48) satisfies the reachability condition and sliding on $\mathscr{S}$ in (6.20) is maintained.

Proof. By substituting the control law proposed in (6.46)-(6.48) into (6.24) and by using the fact that $GB_o = I$, it gives

$$\dot{\sigma}(x,t) = (G\widehat{B})(Fx(t) - \rho\frac{\sigma(t)}{\|\sigma(t)\|}) - Fx(t) \tag{6.50}$$

Since by construction $B_{21}^T B_{21} = I_l$, using (6.22) and (6.32) equation (6.50) can be written as

$$\begin{aligned}\dot{\sigma}(t) &= \Big(I_l - \triangle_1(t)\widehat{W}_1(t) - B_{21}^T B_{22}\triangle_2(t)\Psi(t)\Big)(Fx(t) - \rho\frac{\sigma(t)}{\|\sigma(t)\|}) - Fx(t) \\ &= -\rho\frac{\sigma(t)}{\|\sigma(t)\|} - \Big(\triangle_1(t)\widehat{W}_1(t) + B_{21}^T B_{22}\triangle_2(t)\Psi(t)\Big)(Fx(t) - \rho\frac{\sigma(t)}{\|\sigma(t)\|}) \end{aligned} \tag{6.51}$$

Now consider the candidate Lyapunov function

$$V(t) = \frac{1}{2}\sigma^T\sigma \tag{6.52}$$

Taking the time derivative of (6.52) and substituting for $\dot{\sigma}(t)$ from (6.51) yields

$$\begin{aligned}\dot{V} &= -\rho\|\sigma\| - \sigma^T\Big(\triangle_1(t)\widehat{W}_1(t) + B_{21}^T B_{22}\triangle_2(t)\Psi(t)\Big)Fx(t) \\ &\quad +\rho\sigma^T\Big(\triangle_1(t)\widehat{W}_1(t) + B_{21}^T B_{22}\triangle_2(t)\Psi(t)\Big)\frac{\sigma}{\|\sigma\|} \\ &\leq -\rho\|\sigma\| + \|\sigma\|(\triangle_{max} + \gamma_3\triangle_{max}\gamma_1^*)\|\nu_l\| + \rho\|\sigma\|(\triangle_{max} + \gamma_3\triangle_{max}\gamma_1^*) \\ &\leq -\rho(1 - (\triangle_{max} + \gamma_3\triangle_{max}\gamma_1^*))\|\sigma\| + \|\sigma\|(\triangle_{max} + \gamma_3\triangle_{max}\gamma_1^*)\|\nu_l\| \end{aligned} \tag{6.53}$$

where $\triangle_{max}$ is defined in (6.4). By choosing the value of $\rho(t,x)$ as proposed in (6.49), the expression in (6.53) becomes $\dot{V} \leq -\eta\|\sigma\|$ which is the standard reachability condition, and is sufficient to guarantee that sliding on the surface $\mathscr{S}$ is maintained. ■

Finally in order to obtain the overall physical control law which is used to create the actual control signals sent to all the available control surfaces, substituting (6.46)-(6.48) into (6.11) yields

$$u(t) = \begin{bmatrix} I_l \\ N_2(t)(I_l - \widehat{W}_1(t)) \end{bmatrix}\Big(Fx(t) - \rho(t,x)\frac{\sigma(t,x)}{\|\sigma(t,x)\|}\Big) \tag{6.54}$$

where $N_2(t)$ is defined in (6.13). The efficacy of the proposed scheme is tested in the following section using the high fidelity nonlinear model of the large transport aircraft.

6.4 Simulations: yaw damping of a large transport aircraft

The proposed integral sliding mode FTC scheme employs an a-posteri approach building on an existing state feedback controller designed using only the primary actuators. In the physical control law proposed in (6.54), the baseline control law F is assumed to exist *a-priori*. The technique implemented in the proposed FTC scheme is to use the baseline controller in the nominal fault free scenario, and activates the fault tolerant features only in the case when faults or failures occur in the actuators. All the simulations which follow have been based on the high fidelity nonlinear model of the large transport aircraft using the FTLAB 747 $V6.5/7.1$ software environment which was used as the basis for the GARTEUR AG16 benchmark [39].

The objective of the simulations is to damp the lateral dynamics of the aircraft when the initial sideslip $\beta(0)$ is perturbed by 1^o while the aircraft is flying at a high altitude say $40,000$ ft with a high speed say 774 ft/sec. The lateral dynamics of a large transport aircraft discussed in Appendix A.1 are used to evaluate the proposed scheme. For yaw damping the washout filter state which is obtained using the relation [48]:

$$\dot{x}_{wo} = r - 0.333x_{wo} \tag{6.55}$$

is augmented with the lateral dynamics, where r is the yaw rate and x_{wo} is the washout filter state. The nominal state feedback controller F associated with the primary actuators for yaw damping (which is a stability augmentation system for the lateral dynamics of an aircraft) has been taken from the literature, which is based on the ideal closed-loop eigenvalues in (6.59) and eigenvectors in (6.60) (Section 6.5) and is not part of the design process. For design purpose, a linearization of the benchmark model is obtained about an operating condition of $40,000$ ft altitude and 774 ft/sec forward speed (Mach 0.8) as defined in [48], [61]. By augmenting a washout filter state given in equation (6.55), the state space representation of the model is given as

$$A_p = \begin{bmatrix} -0.3330 & 0 & 0 & 1 & 0 \\ 0 & 0 & 0 & 0.0816 & 1 \\ 0 & 0.0413 & -0.0537 & -0.9944 & 0.0823 \\ 0 & -0.0012 & 0.6090 & -0.0869 & -0.0335 \\ 0 & 0.0002 & -2.9236 & 0.3681 & -0.4514 \end{bmatrix}$$

$$B_p = \left[\begin{array}{cc|cccc} 0 & 0 & 0 & 0 & 0 & 0 \\ 0 & 0 & 0 & 0 & 0 & 0 \\ 0.0070 & 0 & 0.0003 & -0.0003 & 0.0002 & -0.0002 \\ -0.4438 & -0.0082 & -0.0046 & 0.0046 & 0.0493 & -0.0493 \\ 0.1451 & -0.1329 & -0.0625 & 0.0625 & 0.0085 & -0.0085 \end{array}\right] \tag{6.56}$$

The states are $(x_{wo}, \phi, \beta, r, p)^T$, where x_{wo} is the washout filter state (rad) in equation (6.55) and is only augmented in this Chapter in the lateral dynamics for yaw damping, ϕ is the roll angle (rad), β is the side slip (rad), r is the yaw rate (rad/sec) and p is the roll rate (rad/sec). The control surfaces which are considered for the design are $\delta_{lat} = \{\delta_r, \delta_a, \delta_{sp5}, \delta_{sp8}, Tn_l, Tn_r\}^T$ where δ_r is the rudder deflection (rad), δ_a is the aileron deflection (rad), δ_{sp5} is the left inner spoiler (rad), δ_{sp8} is the right inner spoiler (rad) and Tn_l and Tn_r are aggregated engine thrusts (N) (scaled by 10^5) on the left and right wing. It is assumed that the left aileron moves in an antisymmetrical fashion to the right aileron[1]. In (6.56) the input distribution matrix B_p is divided into primary $(\delta_r, \delta_a)^T$ and secondary $(\delta_{sp5}, \delta_{sp8}, Tn_l, Tn_r)^T$ actuators. A further transformation is required in order to have the structure in (6.8) and to ensure that $B_{21}B_{21}^T = I_2$. Using the set of eigenvalues and eigenvectors as mentioned in the Section 6.5, the ideal baseline control law F for yaw damping (considering only the primary actuators $(\delta_r, \delta_a)^T$), based on eigenstructure assignment [81] is

$$F = \begin{bmatrix} -0.5342 & -0.4817 & 0.0665 & 1.1836 & -0.0133 \\ -21.9319 & -0.5188 & 0.1313 & 1.9001 & 0.6705 \end{bmatrix} \tag{6.57}$$

The state feedback control gain matrix in (6.57) will be taken as the *a priori* given controller around which the novel integral sliding mode scheme from Section III is created.

6.4.1 Fault Tolerant Control Law for Yaw Damping

In the case of faults or failures the baseline control law in (6.57) can not be used alone; instead the fault tolerant control law proposed in (6.54) will be employed to retain performance close to the nominal. In the nominal case, the aileron is the primary control surface for ϕ tracking, and the spoilers are the redundancy; whereas the rudder is the primary control surface for β tracking (i.e. yaw damping), and differential

[1]The outer ailerons and spoilers ($sp1-4, sp9-12$) are not active at high speed cruise condition due to structural limit. The spoilers ($sp6, sp7$) are ground spoilers and not used in flight

engine thrust is the redundancy. The closed-loop stability condition in (6.39) should be guaranteed in nominal and in faults/failures scenarios. The value of γ_2 for the *a priori* F using equation (6.36) is $\gamma_2 = 0.0424$. Using (6.33) it can be verified using a numerical search that $\gamma_1^* = 7.5920$. Hence to satisfy the stability conditions of *Proposition 6.1* in (6.38) and (6.39) where $\gamma_3 = 0.7176$, the maximum value of the error in estimation of the actuator effectiveness levels which can be handled by the physical control law in (6.54) is $\triangle_{max} = 10\%$.

6.5 Baseline control law for yaw damping

Eigenstructure assignment is a method which provides the freedom to allow the appropriate set of eigenvalues and associated eigenvectors to be considered in the design procedure to achieve the desired performance or shape of the closed-loop system response. The feedback gain F, based only on the primary actuator, is assumed to be available *a priori* and should stabilize the nominal closed-loop system in (6.10). The design of F is based on the set of eigenvalues given in (6.59) and the best possible eigenvectors suggested in [45]. Based on this available eigenstructure, the feedback gain F can be obtained using the relation

$$(A + B_o F)v_i = \lambda_i v_i \quad i = 1, ..., n \tag{6.58}$$

where λ_i is an eigenvalue and v_i is the associated eigenvector. It is argued in [93] that if B_o is of full rank then, *"a maximum of n eigenvectors can be partially assigned with a minimum of l entries in each eigenvector arbitrarily chosen"*.

The ideal closed-loop eigenvalues for the nominal state feedback controller F associated with the primary actuators for yaw damping (which is a stability augmentation system for the lateral dynamics of an aircraft) are

$$\{-0.0051, -0.468, -0.6 \pm 0.628\,j, -1.106\} \tag{6.59}$$

The motions corresponding to the stable real poles are referred to as the spiral mode (-0.0051), the washout filter (-0.468) and the roll mode (-1.106). The motion corresponding to the complex poles is referred to as the Dutch roll mode. The best possible eigenvectors to ensure decoupling between these

modes as described in [45] are represented as

$$\underbrace{\begin{bmatrix}*\\0\\1\\*\\*\end{bmatrix}\begin{bmatrix}*\\0\\1\\*\\*\end{bmatrix}}_{\text{Dutch roll mode}} \quad \underbrace{\begin{bmatrix}*\\1\\0\\*\\*\end{bmatrix}}_{\text{roll mode}} \quad \underbrace{\begin{bmatrix}*\\1\\0\\*\\*\end{bmatrix}}_{\text{spiral mode}} \quad \underbrace{\begin{bmatrix}0\\0\\0\\1\\0\end{bmatrix}}_{\text{washout filter}} \quad \underbrace{\begin{bmatrix}x_{wo}\\\phi\\\beta\\r\\p\end{bmatrix}}_{x(t)} \tag{6.60}$$

where $*$ denotes that the magnitude of the element is unimportant. The above selection of eigenvectors ensures no coupling of dutch roll with the roll angle and or roll rate. Furthermore the spiral mode and roll mode are associated with the roll angle only, and should ensure decoupling from the sideslip angle to avoid sideslip in the course of a steady turn [93]. The washout filter which is used for the yaw damping is only associated with the yaw rate.

6.6 Nonlinear Simulation Results for Yaw Damper

Practically the integral sliding mode control law proposed in (6.48) cannot be directly used in this case, and the discontinuities in the unit vector have been smoothed using fractional approximation $\frac{\sigma}{\|\sigma\|+\delta}$ [41] given in section 3.5, where value of the positive scalar is chosen as $\delta = 0.01$. In the sequel three simulation scenarios are investigated: one a fault free case and considering the estimation of the $W(t)$ matrix is perfect; the second considering the same scenario as in case 1, but when the estimation of the $W(t)$ matrix is imperfect; and the third a scenario involving a primary actuator failure and with imperfect estimation of $W(t)$.

6.6.1 Case 1: Fault Free Case With Perfect Estimation of W(t)

In the case when the estimation of the effectiveness level matrix $W(t)$ is perfect, $\triangle(t) = 0$ and $\triangle_{max} = 0$. Consequently the stability condition in (6.39) reduces to $\gamma_2\gamma_1^* = 0.3217 < 1$.

Figures 6.2-6.3 demonstrate the nominal fault free performance. In Figure 6.2 it can be seen that the roll and yaw modes are decoupled. During the nominal fault free scenario the secondary actuators are not

active (Figure 6.3) because the integral sliding mode FTC scheme is not active in this case and only the baseline controller F is employed to achieve the nominal performance.

6.6.2 Case 2: Fault Free Case With Imperfect Estimation of W(t)

A second scenario is considered here to demonstrate the efficacy of the scheme when the system is fault free and estimation of the $W(t)$ matrix is not perfect. Figure 6.4 shows that due to imprecise information provided by the FDI, the estimate $\widehat{W}(t) \neq I$, (indicating the presence of faults) although in reality there is no fault in the system. In response to this the control allocation scheme engages the secondary actuators (spoilers for ϕ performance and differential engine thrust for β performance) as shown in Figure 6.5 to maintain the closed-loop stability of the system and to retain nominal performance same as in Figure 6.2.

6.6.3 Case 3: Primary Failure With Imperfect Estimation of W(t)

The third scenario demonstrates the scheme with imperfect estimates $\widehat{W}(t)$ in the case of failure in the primary actuators. Theoretically the maximum percentage error $\triangle_{max}$ the proposed scheme can handle and yet ensure the stability conditions of *Proposition 6.1*, is 10%. Figure 6.7, shows the scenario when both the primary actuators (rudder and ailerons) have jammed at offset positions at 6 sec, and due to imprecise information provided by the FDI scheme, the effectiveness of the primary actuators is estimated at 10%, instead of 0% (Figure 6.6). Due to this failure, the right wing spoiler $sp8$ is actively engaged by the control allocation scheme together with left and right wing engines thrust to cope with this situation, and to maintain the performance close to the nominal Figure 6.7. The switching function plot in Figure 6.7 shows that the sliding is maintained in the entire system response.

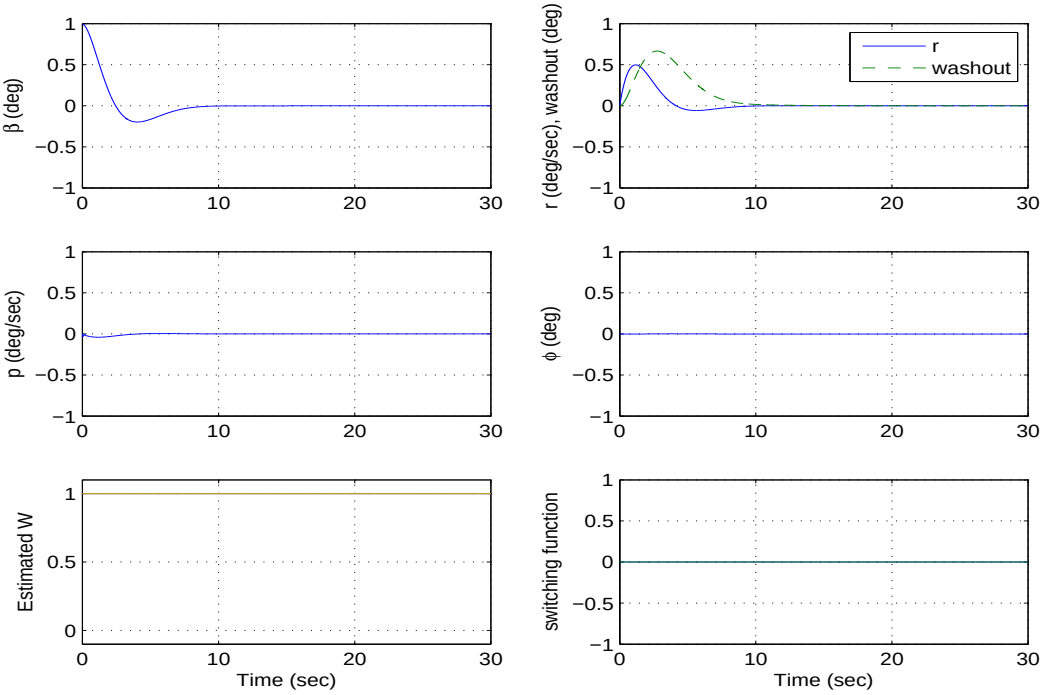

Figure 6.2: No fault (perfect estimation of W): plant states

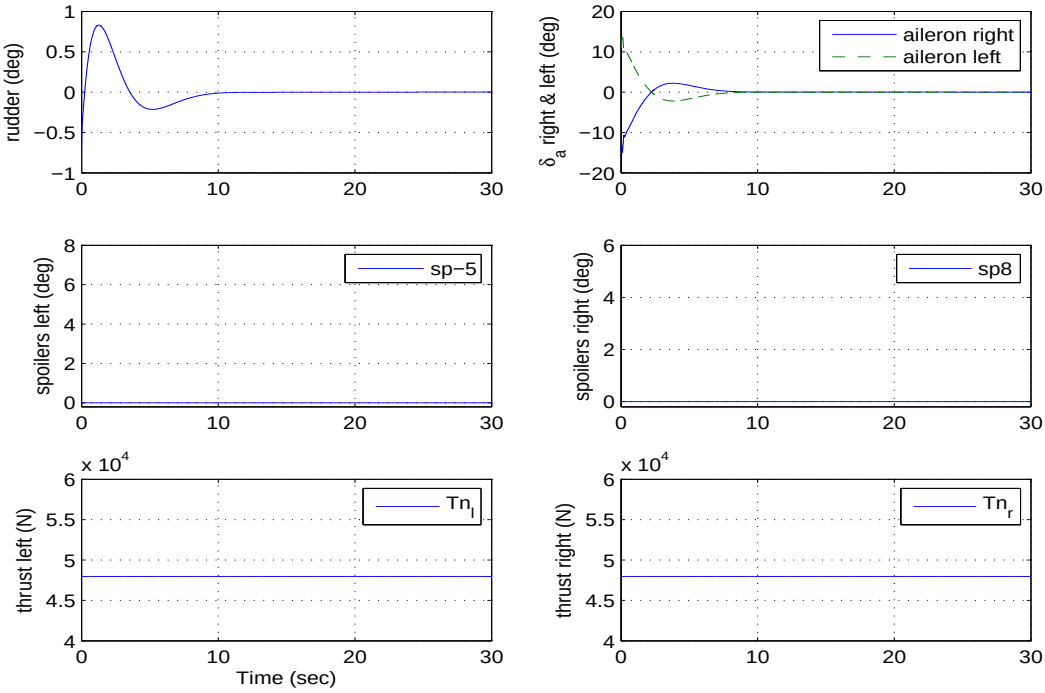

Figure 6.3: No fault (perfect estimation of W): actuators

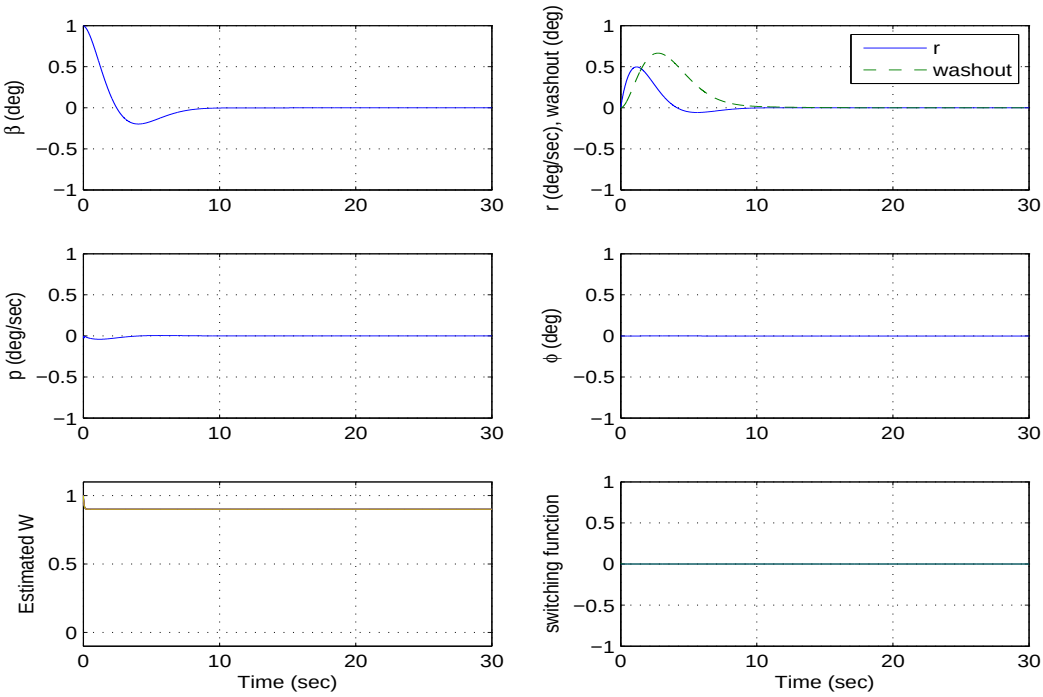

Figure 6.4: No fault (imperfect estimation of W): plant states

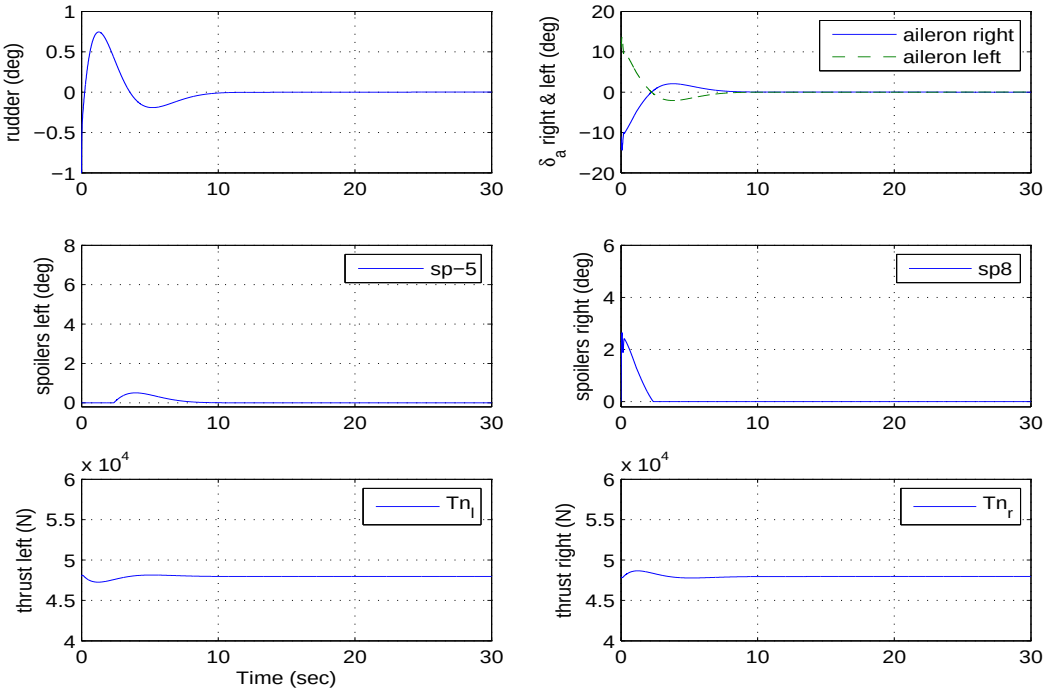

Figure 6.5: No fault (imperfect estimation of W): actuators

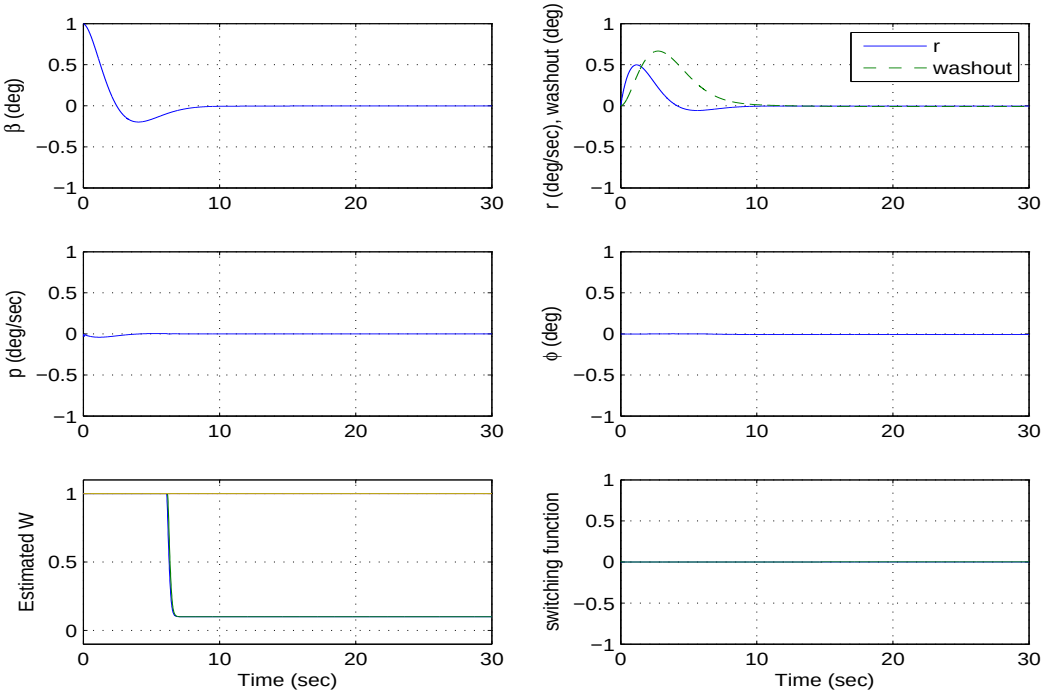

Figure 6.6: Primary failure (imperfect estimation of W): plant states

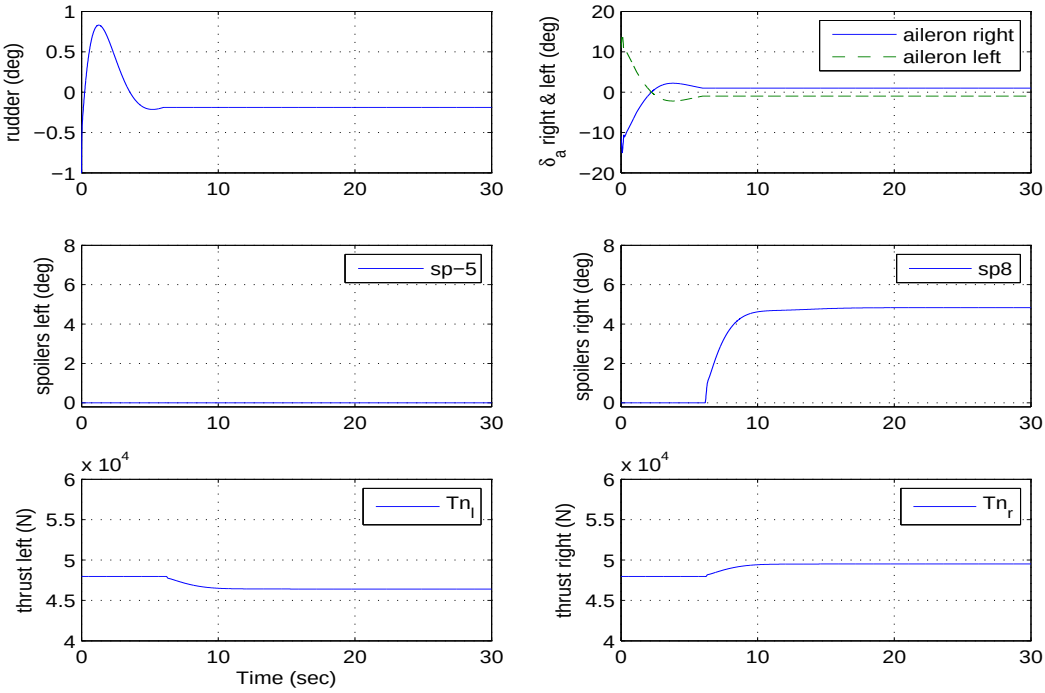

Figure 6.7: Primary failure (imperfect estimation of W): actuators

6.7 Conclusion

In this Chapter a novel fault tolerant control allocation scheme was proposed by incorporating integral sliding modes. The controller structure does not need to be changed and the same controller is used in both nominal as well as in fault/failure scenarios. The proposed scheme employed an *a posteri* approach building on an existing state feedback controller designed using only the primary actuators. To distribute the control signals to the functional actuators, the scheme used the estimated effectiveness levels of the actuators provided by an FDI scheme. Furthermore the proposed FTC scheme can handle a level of error in terms of estimation of the actuator effectiveness. A rigorous stability analysis for imperfect actuator effectiveness estimate has been developed. The efficacy of the proposed scheme was tested in simulation using a nonlinear benchmark model of a large transport aircraft.

The FTC scheme in the coming Chapter considers an extension of the ideas proposed in Chapter 4 for the Linear Parameter Varying systems. Due to the fact that the operating conditions frequently change in safety critical systems, the extended ideas of FTC in the coming Chapter will allow to investigate the closed-loop performance of the FTC scheme in the wider range of operating conditions.

Chapter 7

Linear Parameter Varying FTC Scheme using Integral Sliding Modes

This Chapter introduces a new fault tolerant control scheme for linear parameter varying (LPV) plants by incorporating ideas of integral sliding modes and control allocation. This Chapter considers *an extension* of FTC scheme proposed in Chapter 4 by exploiting the global properties (in a sense of concern of the system behaviour along all possible parameter variations) of linear parameter varying systems. An LPV control design methodology seeks for a single control law which explicitly depends on these varying parameters [50]. The effectiveness of the scheme is tested in simulation by applying it to a benchmark LPV model of a transport aircraft. The closed-loop stability of the overall system is guaranteed throughout the entire operating conditions envelope even in the presence of total failure of certain actuators.

7.1 Introduction

Many different control paradigms see for example Chapter 2 which have been explored in the literature to tackle the fault tolerant control problem. However, it is probably fair to say that most of the FTC methods have been proposed for linear time invariant (LTI) systems. However there are notable exceptions. FTC methods based on LTI system descriptions are somewhat restricted to near trim conditions. Linear parameter varying systems can be considered as an extension of LTI systems and are a certain class of finite dimensional linear systems, in which the entries of the state space matrices continuously

depend on a time varying parameter vector which belongs to a bounded compact set [85]. LPV methods have attracted much attention in recent years– especially for aircraft systems [50] and are appealing for nonlinear plants which can be modelled as time varying systems with state dependent parameters which are measurable online [101].

In this Chapter an LPV system representation is considered, as a natural extension of LTI systems. The objective is to synthesize an FTC scheme which will work over a wider range of operating conditions. There is almost no literature on the use of sliding model controllers for LPV systems with the exception of [107] and [95]. The work in [107] and [95] has proposed SMC schemes for LPV systems although not in the context of fault tolerant control. The *main contribution* of this Chapter is to *extend* the integral sliding modes control allocation ideas proposed in Chapter 4 to a class of LPV systems. Same as in Chapters 4 and 6 the inclusion of CA with integral sliding modes has enabled a baseline controller to be design for both fault free and faulty condition, by avoiding the need to reconfigure the controller. In the proposed scheme, it is assumed that (fault free) state information is available for controller design together with estimates of the actuator health levels. To design the virtual control law, the varying input distribution matrix is factorized into a fixed and a varying matrix. The virtual control law designed by the ISM technique is translated into the actual actuator commands using the CA scheme. In the proposed scheme the controller is automatically 'scheduled' and closed-loop stability is established throughout the entire operating envelope. The proposed FTC scheme can maintain closed-loop stability even in the presence of total failures of certain actuators, provided that redundancy is available in the system. The efficacy of the proposed FTC scheme is tested in simulation by applying it to an LPV model of a benchmark transport aircraft previously used in the literature [50].

7.2 Problem Formulation

An LTI plant subject to actuator faults or failures considered in Chapter 4 (equation 4.1) can be extended for linear parameter varying plant which can be represented as

$$\dot{x}(t) = A(\rho)x(t) + B(\rho)W(t)u(t) \tag{7.1}$$

where $A(\rho) \in \mathbb{R}^{n\times n}$, $B(\rho) \in \mathbb{R}^{n\times m}$ and $W(t) \in \mathbb{R}^{m\times m}$ is a diagonal semi-positive definite weighting matrix whose diagonal entries $w_1(t),..,w_m(t)$ model the efficiency level of the actuators. If $w_i(t) = 1$ it means that the i_{th} actuator is working perfectly and is fault free, whereas if $1 > w_i(t) > 0$ some level of fault is present (and that particular actuator works at reduced efficiency). If $w_i(t) = 0$ it means the i_{th} actuator has completely failed and the actuator does not respond to the control signal $u_i(t)$. The time varying parameter vector $\rho(t)$ is assumed to lie in a specified bounded compact set $\Omega \subset \mathbb{R}^r$ and is assumed to be available for the controller design. Further assume that the varying plant matrices $A(\rho)$ and $B(\rho)$ depend affinely on the parameter $\rho(t)$ that is

$$A(\rho) = A_0 + \sum_{i=1}^{r} \rho_i A_i \qquad B(\rho) = B_0 + \sum_{i=1}^{r} \rho_i B_i$$

To design the virtual control law, which is designed in the sequel, assume that the parameter varying matrix $B(\rho)$ can be factorized as

$$B(\rho) = B_f E(\rho) \tag{7.2}$$

where $B_f \in \mathbb{R}^{n\times m}$ is a fixed matrix and $E(\rho) \in \mathbb{R}^{m\times m}$ is a matrix with varying components and is assumed to be invertible for all $\rho(t) \in \Omega$. This of course is a restriction on the class of systems for which the results in this Chapter are applicable, but for example many aircraft systems fall into this category.

As discussed in Chapter 4, to resolve actuator redundancy, assume that by permuting the states the matrix B_f can be partitioned as

$$B_f = \begin{bmatrix} B_1 \\ B_2 \end{bmatrix} \tag{7.3}$$

where $B_1 \in \mathbb{R}^{(n-l)\times m}$, and $B_2 \in \mathbb{R}^{l\times m}$ is of rank $l < m$. Here it is assumed as in Chapter 4 that $\|B_2\| \gg \|B_1\|$ so that B_2 provides the dominant contribution to the control action as compared to B_1. Again, although this is a restriction, the aircraft example satisfies such a constraint. Furthermore scale the last l states to ensure that $B_2 B_2^T = I_l$. This can be done without loss of generality.

Using (7.2) and (7.3), the system in (7.1) can be written as

$$\dot{x}(t) = A(\rho)x(t) + \begin{bmatrix} B_1 E(\rho)W(t) \\ B_2 E(\rho)W(t) \end{bmatrix} u(t) \tag{7.4}$$

The design of the virtual control, will be based on the fault free system i.e. when $W(t) = I$. Define the virtual control input signal as:

$$v(t) := B_2 E(\rho) u(t) \tag{7.5}$$

where $v(t) \in \mathbb{R}^l$ is the total control effort produced by the actuators [60]. Using the fact $B_2 B_2^T = I_l$, one particular choice for the physical control law $u(t) \in \mathbb{R}^m$ which is used to distribute the control effort among the actuators is

$$u(t) := (E(\rho))^{-1} B_2^T v(t) \tag{7.6}$$

Substituting (7.6) into (7.4) yields

$$\dot{x}(t) = A(\rho)x(t) + \underbrace{\begin{bmatrix} B_1 E(\rho) W(t) (E(\rho))^{-1} B_2^T \\ B_2 E(\rho) W(t) (E(\rho))^{-1} B_2^T \end{bmatrix}}_{B_w(\rho)} v(t) \tag{7.7}$$

In the nominal case, when there is no fault in the system, i.e. when $W(t) = I$, equation (7.7) simplifies to

$$\dot{x}(t) = A(\rho)x(t) + \underbrace{\begin{bmatrix} B_1 B_2^T \\ I_l \end{bmatrix}}_{B_v} v(t) \tag{7.8}$$

A1: The pair $(A(\rho), B_v)$ is controllable for all the values of $\rho(t) \in \Omega$.

In this Chapter all the states are assumed to be available for the controller design, therefore a state feedback gain $v(t) = -F(\rho)x(t)$ can be appropriately designed in order to stabilize the nominal system

$$\dot{x}(t) = (A(\rho) - B_v F(\rho))x(t)$$

for all values of $\rho(t) \in \Omega$, as well as to achieve the desired closed-loop performance. The nominal fault free system in (7.8) is used in the next section to design the virtual control law.

7.3 Integral sliding mode controller design

This section focuses first on the design of the sliding surface and then subsequently the control law so that the sliding motion on the sliding surface can be ensured for all the time.

7.3.1 Design of Integral switching function:

The integral switching function suggested in Chapter 4 (equation 4.18) ensures that the sliding mode will exist from the time instant the controller is switched online. Consequently invariance to matched uncertainty is guaranteed throughout the entire response of the system. Here the switching function suggested in equation (4.18) is extended to the use for LPV plants. Choose the sliding surface as $\mathscr{S} = \{x \in \mathbb{R}^n : \quad \sigma(x,\rho,t) = 0\}$, where the choice

$$\sigma(x,\rho,t) := Gx(t) - Gx(0) - G\int_0^t \big(A(\rho) - B_v F(\rho)\big)x(\tau)d\tau \tag{7.9}$$

is advocated where $G \in \mathbb{R}^{l\times n}$ represents design freedom. The choice of G is based on the fixed matrix B_f and is suggested as

$$G := B_2(B_f^T B_f)^{-1}B_f^T \tag{7.10}$$

The choice of G in (7.10) is of similar structure as in (4.19). With this choice of G, and using the special properties of matrix B_2 such that $B_2B_2^T = I_l$, it is easy to verify that

$$GB_v = B_2(B_f^T B_f)^{-1}B_f^T B_f B_2^T = I_l \tag{7.11}$$

which means that nominally when there are no faults in the system $W = I_m$, the special choice of G in (7.10) serves as the left pseudo inverse of matrix B_v. Also from equation (7.7)

$$\begin{aligned} GB_w(\rho) &= B_2(B_f^T B_f)^{-1}B_f^T B_f E(\rho)W(t)(E(\rho))^{-1}B_2^T \\ &= B_2E(\rho)W(t)(E(\rho))^{-1}B_2^T \end{aligned} \tag{7.12}$$

and will be used in the sequel while defining the control law. From the result in (7.12), it is clear that it agrees with that of the result in (7.11) nominally.

To maintain the sliding on the sliding surface, equivalent control (which is the average value of the virtual control $v(t)$) is required and can be obtained by using the relation $\sigma = \dot{\sigma} = 0$. By taking the time derivative of the switching function σ along the trajectories yields

$$\dot{\sigma}(x,\rho,t) = G\dot{x}(t) - GA(\rho)x(t) + GB_vF(\rho)x(t) \tag{7.13}$$

and after substituting from (7.7),

$$\dot{\sigma}(x,\rho,t) = GB_w(\rho)v(t) + GB_vF(\rho)x(t) \tag{7.14}$$

and therefore the expression for the equivalent control can be written as

$$v_{eq}(t) = -(B_2E(\rho)W(t)(E(\rho))^{-1}B_2^T)^{-1}F(\rho)x(t) \tag{7.15}$$

provided the actuator effectiveness matrix $W(t)$ is such that $\det(B_2E(\rho)W(t)(E(\rho))^{-1}B_2^T) \neq 0$. The expression in (7.15) is obtained from solving for $\dot{\sigma} = 0$ in (7.14) using the expression for $GB_w(\rho)$ in (7.12) and the fact that $GB_v = I_l$. Substituting (7.15) into (7.7) yields the expression for the sliding motion as

$$\dot{x}(t) = A(\rho)x(t) - B_w(\rho)(B_2E(\rho)W(t)(E(\rho))^{-1}B_2^T)^{-1}F(\rho)x(t) \tag{7.16}$$

Furthermore by adding and subtracting the term $B_vF(\rho)x(t)$ to the right hand side of equation (7.16) yields

$$\dot{x}(t) = \big(A(\rho) - B_vF(\rho)\big)x(t) + \begin{bmatrix} \Delta(t,\rho) \\ 0_l \end{bmatrix} F(\rho)x(t) \tag{7.17}$$

where the term which models the uncertainty part is

$$\Delta(t,\rho) := B_1B_2^T - B_1E(\rho)W(t)(E(\rho))^{-1}B_2^T(B_2E(\rho)W(t)(E(\rho))^{-1}B_2^T)^{-1}$$

Remark 7.1: From equation (7.17) it is clear that when there are no actuator faults in the system (i.e. $W(t) = I_m$) the second term disappears and ends up with a stable system. However in the case of faults or failures (i.e. when $W(t) \neq I_m$) the second term does not vanish and will be treated as unmatched

uncertainty while sliding.

The closed-loop stability of the motion while sliding must be ensured in the presence of uncertainty $\Delta(t,\rho)$. To facilitate the closed-loop stability analysis the equation (7.17) can be written in the special structure as

$$\dot{x}(t) = \big(A(\rho) - B_v F(\rho)\big)(t) + \widetilde{B}\Delta(t,\rho)F(\rho)x(t) \tag{7.18}$$

where

$$\widetilde{B} := \begin{bmatrix} I_{n-l} \\ 0 \end{bmatrix} \tag{7.19}$$

Now in order to define the class of faults or failures for which the FTC scheme proposed in this Chapter can cope, let the diagonal entries of $W(t)$ belong to the set

$$\mathscr{W}_\varepsilon = \{(w_1,...,w_m) \in \underbrace{\begin{bmatrix} 0 & 1 \end{bmatrix} \times ... \times \begin{bmatrix} 0 & 1 \end{bmatrix}}_{m \text{ times}} : (GB_w(\rho))^T (GB_w(\rho)) > \varepsilon I\} \tag{7.20}$$

where ε is a small positive scalar satisfying $0 < \varepsilon \ll 1$. Note that when $W(t) = I_m$, $(GB_w(\rho))^T (GB_w(\rho)) = I > \varepsilon I$ and therefore $\mathscr{W} \neq \emptyset$. If the actuator effectiveness matrix $W(t) = diag(w_1,...,w_m) \in \mathscr{W}_\varepsilon$ then by construction

$$\|(GB_w(\rho))^{-1}\| = \|(B_2 E(\rho) W (E(\rho))^{-1} B_2^T)^{-1}\| < \frac{1}{\sqrt{\varepsilon}}$$

The set $\mathscr{W}_\varepsilon$ will be shown to constitute the class of faults/failures for which closed-loop stability can be maintained. From (7.18) note that for any $W \in \mathscr{W}_\varepsilon$

$$\|\Delta(t,\rho)\| \leq \gamma_1 (1 + \frac{c}{\varepsilon}) \tag{7.21}$$

where $c = \max_{\rho\in\Omega} \|E(\rho)\| \|(E(\rho))^{-1}\|$ i.e. the worst case condition number associated with $E(\rho)$ and $\gamma_1 = \|B_1\|$, which is very small by hypothesis. Proving the stability of the closed-loop sliding motion in (7.18) (in the nominal as well as in the fault/failure scenarios) is one of the important parts of the design process which is demonstrated in the following subsection.

Remark 7.2: The conditions in this Chapter are subtly different to those in Chapter 4. In (7.20) the norm of $(GB_w(\rho))^{-1}$ must be guaranteed to be bounded by limiting $W \in \mathscr{W}_\varepsilon$ thus introducing an explicit ε

to bound $\|GB_w(\rho)\|$ away from zero. This is not necessary in Chapter 4 and so the 'price' for a wider operating envelope is a more restricted set of possible failures.

7.3.2 Closed-loop stability analysis:

In the nominal fault free scenario when $W(t) = I_m$, it is easy to verify $\Delta(t,\rho) = 0$ in equation (7.18) and simplifies to

$$\dot{x}(t) = \big(A(\rho) - B_v F(\rho)\big)x(t) \tag{7.22}$$

which is stable by design of $F(\rho)\big)$. However in fault/failure scenarios, closed-loop stability needs to be proven. To this end, equation (7.18) can also be represented by

$$\dot{x}(t) = \underbrace{(A(\rho) - B_v F(\rho))}_{\widetilde{A}(\rho)} x(t) + \widetilde{B}\overbrace{\Delta(t,\rho)\underbrace{F(\rho)x(t)}_{\widetilde{y}(t)}}^{\widetilde{u}(t)} \tag{7.23}$$

Define γ_0 to be the $\mathscr{L}_2$ gain associated with the operator

$$\widetilde{G}(s) := F(\rho)(sI - \widetilde{A}(\rho))^{-1}\widetilde{B} \tag{7.24}$$

Proposition 7.1: For any possible combination of faults or failures belonging to the set $\mathscr{W}_\varepsilon$, the closed-loop sliding motion in (7.23) will be stable if

$$\gamma_0\gamma_1(1 + \frac{c}{\sqrt{\varepsilon}}) < 1 \tag{7.25}$$

Proof. The specially written structure in (7.23) can be thought of as a feedback interconnection of an LPV plant and a time varying feedback gain associated with

$$\dot{x}(t) = \widetilde{A}(\rho)x(t) + \widetilde{B}\widetilde{u}(t) \tag{7.26}$$

$$\widetilde{y}(t) = F(\rho)x(t) \tag{7.27}$$

where

$$\widetilde{u}(t) = \Delta(t,\rho)\widetilde{y}(t) \tag{7.28}$$

If (7.25) is satisfied then according to the small gain theorem [75] as discussed in the Appendix B.1.2

$$\|\widetilde{G}(s)\|\|\Delta(t,\rho)\| < 1 \tag{7.29}$$

the closed-loop system in (7.23) will be stable. ■

In the next subsection the ideas of integral sliding modes are used to design the virtual control law $v(t)$ in order to produce the virtual control effort.

7.3.3 ISM Control Laws:

The integral sliding mode control law is based on the nominal fault free system in (7.8) and comprises two components:

$$v(t) = v_l(t) + v_n(t) \tag{7.30}$$

The linear part which ensures nominal performance is defined as

$$v_l(t) := -(GB_w(\rho))^{-1}F(\rho)x(t) \tag{7.31}$$

and the nonlinear discontinuous part which induces sliding and provides robustness against fault/failure scenarios is defined as

$$v_n(t) := -\mathscr{K}(t,x,\rho)(GB_w(\rho))^{-1}\frac{\sigma(x,\rho,t)}{\|\sigma(x,\rho,t)\|} \quad \text{for } \sigma \neq 0 \tag{7.32}$$

where $\mathscr{K}(t,x,\rho)$ is the scalar modulation function, whose value is proposed in *Proposition 7.2*.

Proposition 7.2: Assume that the *Proposition 7.1* holds, then if $\mathscr{K}(t,x,\rho)$ is chosen as

$$\mathscr{K}(t,x,\rho) > \eta_o \tag{7.33}$$

where $\eta_o > 0$ is a positive scalar, the integral sliding mode control laws defined in (7.30-7.32) satisfy the reachability condition and sliding on $\mathscr{S}$ is maintained.

Proof. To demonstrate this, substitute the integral sliding mode control law in (7.31)-(7.32) into (7.14)

which yields

$$\dot{\sigma}(x,\rho,t) = -\mathscr{K}(t,x,\rho)\frac{\sigma(x,\rho,t)}{\|\sigma(x,\rho,t)\|} \quad \text{for } \sigma(x,\rho,t) \neq 0 \tag{7.34}$$

Consider the positive definite candidate Lyapunov function

$$V(t) = \frac{1}{2}\sigma^T(x,\rho,t)\sigma(x,\rho,t) \tag{7.35}$$

Taking the time derivative of (7.35) and substituting the value of (7.34), yields

$$\begin{aligned} \dot{V} &= -\mathscr{K}(t,x,\rho)\|\sigma(x,\rho,t)\| \\ &\leq -\eta_o\sqrt{2V(t)} \end{aligned} \tag{7.36}$$

Equation (7.36) is a standard reachability condition [41] and is sufficient to ensure that the system trajectories always remain on the sliding surface. ■

Finally the physical control law which is used to distribute the control effort among the available actuators is obtained by substituting (7.30)-(7.32) into (7.6) which yields

$$u(t) = -(E(\rho))^{-1}B_2^T(B_2E(\rho)W(t)(E(\rho))^{-1}B_2^T)^{-1}(F(\rho)x(t)+\mathscr{K}(t,x,\rho)\frac{\sigma(x,\rho,t)}{\|\sigma(x,\rho,t)\|}) \text{ for } \sigma \neq 0 \tag{7.37}$$

The physical control law (7.37), requires the information about the effectiveness level of the actuators contained in $W(t)$, which can be obtained through some FDI scheme– see for example Subsection (4.4.1) or [113]. This information can also be obtained by directly comparing the controller signals with the actual actuator deflection, as measured by control surface sensors, which are available in many aircraft systems [22].

7.3.4 Design of the state feedback gain

In this section, the state feedback gain $F(\rho)$ using the nominal system (7.8) will be designed. In designing $F(\rho)$ two objectives must be met: the first is equivalent to achieving pre-specified nominal performance for all the admissible values of $\rho(t)$, and the second one is to satisfy the closed-loop stability condition in (7.25) via the small gain theorem. Nominal performance will be incorporated by the use of a LQR type

cost function $J = \int_0^\infty (x^T Qx + u^T Ru)dt$, where Q and R are s.p.d matrices. By using the arguments outlined in [8], which say the LPV system matrices $(\widetilde{A}(\rho), \widetilde{B}, F(\rho))$ which depend affinely on the parameter vector $\rho(t)$ in (7.26) and (7.27) can be represented by the polytopic system $(\widetilde{A}(\omega_i), \widetilde{B}, F(\omega_i))$ where the allowable range of $\rho \in \Omega$ corresponds to a polytope with vertices $\omega_1, \omega_2, ..., \omega_{n_\omega}$ where $\omega_{n_w} = 2^r$. This approach can be posed as an optimization problem: Minimize $trace(X^{-1})$ subject to

$$\begin{bmatrix} A(\omega_i)X + XA^T(\omega_i) - B_v Y(\omega_i) - Y(\omega_i)^T B_v^T & (Q_1 X - R_1 Y(\omega_i))^T \\ Q_1 X - R_1 Y(\omega_i) & -I \end{bmatrix} < 0 \tag{7.38}$$

$$X > 0 \tag{7.39}$$

where $Q_1 = [(Q^{\frac{1}{2}})^T \quad 0_{l\times n}^T]^T$ and $R_1 = [0_{n\times l}^T \quad (R^{\frac{1}{2}})^T]^T$ and $Y(\omega_i) := F(\omega_i)X$ and $X^{-1} \in \mathbb{R}^{n\times n}$ is the Lyapunov matrix. To satisfy the closed-loop stability condition in (7.25), it is sufficient to apply Bounded Real Lemma (BRL) at each vertex of the polytope such that

$$\begin{bmatrix} A(\omega_i)X + XA^T(\omega_i) - B_v Y(\omega_i) - Y(\omega_i)^T B_v^T & \tilde{B} & Y(\omega_i)^T \\ \tilde{B}^T & -\gamma^2 I & 0 \\ Y(\omega_i) & 0 & -I \end{bmatrix} < 0 \tag{7.40}$$

Since the objective is to seek the common Lyapunov matrix for the LMI formulations at each vertex, this can be achieved by introducing the slack variable $Z \in \mathbb{R}^{n\times n}$ and posing the problem as:
Minimize $trace(Z)$ subject to

$$\begin{bmatrix} -Z & I_n \\ I_n & -X \end{bmatrix} < 0 \tag{7.41}$$

together with (7.38), (7.39) and (7.40). The decision variables are X and $Y(\omega_i)$. The matrix Z satisfies $trace(Z) \geq trace(X^{-1})$. Therefore the LMIs in (7.38-7.41) can be solved for all the vertices of the polytopic system and at each vertex the state feedback matrix can be obtained by using the expression $F(\omega_i) = Y(\omega_i)X^{-1}$.

7.4 Simulations

In this Chapter, the control law design is based on the LPV plant of a transport aircraft from [77] and is explained in the next subsection.

7.4.1 LPV model of a transport aircraft

In [77] the nonlinear longitudinal dynamics model of the transport aircraft is approximated by polynomially fitting the aerodynamics coefficients obtained from [83] to create an LPV representation using the function substitution method. The aerodynamic coefficients are polynomial functions of velocity V_{tas} and angle of attack α in the range of $[150,250]$m/sec and $[-2^o,8^o]$ respectively and at the altitude of 7000m [77]. The states of the LPV plant in [77] are $\{\bar{\alpha},\bar{q},\bar{V}_{tas},\bar{\theta},\bar{h}_e\}^T$ which represent *deviation* of the angle of attack, pitch rate, true air speed, pitch angle and altitude from their trim values. The inputs of the LPV plant are $\{\bar{\delta}_e,\bar{\delta}_s,\bar{T}_n\}^T$, which represent deviation of elevator deflection, horizontal stabilizer deflection and total engine thrust from their trim values respectively. The trim values of the states are $\{\alpha_{trim},q_{trim},V_{tas_{trim}},\theta_{trim},h_{e_{trim}}\}=\{1.05^o,0^o/s,227.02m/s,1.05^o,7000m\}$ and the trim values of the LPV plant inputs are $\{\delta_{e_{trim}},\delta_{s_{trim}},T_{n_{trim}}\}=\{0.163^o,0.590^o,42291N\}$. The LPV system matrices are given by

$$A(\rho)=A_0+\sum_{i=1}^{7}\rho_i A_i \quad \text{and} \quad B(\rho)=B_0+\sum_{i=1}^{7}\rho_i B_i \tag{7.42}$$

where $[\rho_1,...,\rho_7]:=[\bar{\alpha},\bar{V}_{tas},\bar{V}_{tas}\bar{\alpha},\bar{V}_{tas}^2,\bar{V}_{tas}^2\bar{\alpha},\bar{V}_{tas}^3,\bar{V}_{tas}^4]$, where $\bar{\alpha}=\alpha-\alpha_{trim}$ and $\bar{V}_{tas}=V_{tas}-V_{tas_{trim}}$. The LPV plant matrices used for the controller design are taken from [77], (and represents the LPV longitudinal axis model of the benchmark aircraft model explained in the Appendix A.1) and has been reordered to have the structure in (7.2). For the controller design the state $\bar{h}_e$ is removed, because normally the altitude can be controlled by controlling the FPA (e.g. this can be seen in [50]) and since the objective in this section is to control the FPA and speed (2 states), therefore altitude is not important while designing the controller. After reordering, the LPV plant states become $\{\bar{\theta},\bar{\alpha},\bar{V}_{tas},\bar{q}\}^T$. The LPV system matrix is given by

$$A(\rho)=\begin{bmatrix} 0 & 0 & 0 & a_{14}(\rho) \\ 0 & a_{33}(\rho) & a_{32}(\rho) & a_{34}(\rho) \\ a_{21}(\rho) & a_{23}(\rho) & a_{22}(\rho) & 0 \\ 0 & a_{43}(\rho) & a_{42}(\rho) & a_{44}(\rho) \end{bmatrix}$$

where

$$\begin{aligned}
a_{14}(\rho) &= 1 \\
a_{33}(\rho) &= -0.5935 - 2.5923\times 10^{-3}\rho_2 \\
a_{32}(\rho) &= -5.2124\times 10^{-4} - 6.2678\times 10^{-7}\rho_2 + 1.1121\times 10^{-11}\rho_4 \\
a_{34}(\rho) &= 0.9914 \\
a_{21}(\rho) &= -9.7851 \\
a_{23}(\rho) &= 5.7733 - 84.5625\rho_1 - 3.5127\times 10^{-2}\rho_2 - 0.7450\rho_3 \\
&\quad -0.7736\times 10^{-4}\rho_4 - 1.6408\times 10^{-3}\rho_5 \\
a_{22}(\rho) &= -6.1168\times 10^{-3} - 2.1091\times 10^{-5}\rho_2 - 2.2374\times 10^{-8}\rho_4 \\
a_{43}(\rho) &= -1.9626 + 3.4170\rho_1 - 0.01729\rho_2 + 0.0301\rho_3 \\
&\quad -0.38081\times 10^{-4}\rho_4 + 6.630\times 10^{-5}\rho_5 \\
a_{42}(\rho) &= -4.9579\times 10^{-4} - 3.8893\times 10^{-6}\rho_2 - 7.6201\times 10^{-9}\rho_4 + 0.19644\times 10^{-11}\rho_6 \\
a_{44}(\rho) &= -0.46087 - 0.00203\rho_2
\end{aligned}$$

and the LPV input distribution matrix is

$$B(\rho)=\begin{bmatrix} 0 & 0 & 0 \\ b_{31}(\rho) & b_{32}(\rho) & b_{33}(\rho) \\ 0 & 0 & b_{23}(\rho) \\ b_{41}(\rho) & b_{42}(\rho) & b_{43}(\rho) \end{bmatrix}$$

where

$$\begin{aligned}
b_{31}(\rho) &= -0.0358 - 1.1877\times 10^{-5}\rho_2 + 1.5311\times 10^{-6}\rho_4 + 3.9135\times 10^{-9}\rho_6 \\
b_{32}(\rho) &= -0.0716 \\
b_{33}(\rho) &= -3.6326\times 10^{-4} - 5.8732\times 10^{-3}\rho_1 + 1.6002\times 10^{-6}\rho_2 + 0.25871\times 10^{-4}\rho_3 \\
b_{23}(\rho) &= 1.3323 - 0.058133\rho_1 \\
b_{41}(\rho) &= -1.7696 - 0.0089\rho_2 + 0.5985\times 10^{-4}\rho_4 \\
&\quad +0.4428\times 10^{-6}\rho_6 + 0.6912\times 10^{-9}\rho_7 \\
b_{42}(\rho) &= -3.9993 - 0.035233\rho_2 - 0.776\times 10^{-4}\rho_4 \\
b_{43}(\rho) &= 0.015328
\end{aligned}$$

7.4.2 Control design objectives

In the simulations scenario it is assumed that the aircraft undergoes over the entire up-and-away flight envelope. This can be achieved by appropriate tracking of FPA and true air speed V_{tas}. The control design

requirements are taken from [50]. The tracking requirements for FPA and V_{tas} are decoupled responses and with settling times of 20sec and 45sec respectively in the fault free scenario. In the case of elevator or horizontal stabilizer failure, the tracking requirement for V_{tas} remains unchanged (because speed is controlled by thrust) but for the FPA response a settling time of 30sec is considered.

The controlled outputs are $[\overline{\gamma},\overline{V}_{tas}]^T$, where $\overline{\gamma}=\overline{\theta}-\overline{\alpha}$, is the flight path angle. For the virtual control the input distribution matrix $B(\rho)$ has been factorized into fixed and varying matrices:

$$B(\rho)=\underbrace{\left[\begin{array}{ccc} 0 & 0 & 0 \\ 0.01 & 0 & 0 \\ \hline 0 & 1 & 0 \\ 0 & 0 & 1 \end{array}\right]}_{B_f}\underbrace{\left[\begin{array}{ccc} b_{31}(\rho) & b_{32}(\rho) & b_{33}(\rho) \\ 0 & 0 & b_{23}(\rho) \\ b_{41}(\rho) & b_{42}(\rho) & b_{43}(\rho) \end{array}\right]}_{E(\rho)} \tag{7.43}$$

In order to introduce the tracking facility in the proposed scheme, the plant states are augmented with the integral action states [97] satisfying

$$\dot{x_r}(t) = r(t) - C_c\overline{x}(t)$$

where $r(t)$ is the reference command to be tracked, and C_c is the controlled output distribution matrix and is given by

$$C_c = \left[\begin{array}{cccc} 1 & -1 & 0 & 0 \\ 0 & 0 & 1 & 0 \end{array}\right]$$

By defining $x_a(t) = col[x_r(t),\overline{x}(t)]$, the augmented system from (7.8) becomes

$$\dot{x}_a(t) = A_a(\rho)x_a(t) + B_{v_a}v(t) + B_r r(t) \tag{7.44}$$

where

$$A_a(\rho) := \left[\begin{array}{cc} 0 & -C_c \\ 0 & A(\rho) \end{array}\right] \quad B_{v_a} := \left[\begin{array}{c} 0 \\ B_v \end{array}\right] \quad B_r = \left[\begin{array}{c} I_l \\ 0 \end{array}\right] \tag{7.45}$$

In the augmented system, the choice of G in (7.10) becomes $G := B_2(B_{f_a}^T B_{f_a})^{-1}B_{f_a}^T$ where

$$B_{f_a} = \begin{bmatrix} 0 \\ B_f \end{bmatrix}$$

and B_2 is the bottom two rows of B_f. In this example for simplicity a fixed gain matrix F is sought, which is valid for all the range of the LPV model. Note that designing a fixed matrix F, also highlights the simplicity of adapting an existing Maltlab LMI multi-model state-feedback synthesis code 'msfsyn' to solve the LMIs (7.38)-(7.41), where the LQR and $\mathscr{L}_2$ objectives can be solved simultaneously by providing appropriate LQR weighting matrices and the tuning parameter γ in (7.40). For designing the state feedback gain F, the Q and R matrices in (7.38) have been chosen as $Q = diag\{500, 50, 20, 20, 0.01, 30\}$, and $R = diag\{4, 8\}$ where the first two states in Q matrix are integral action states. The state feedback gain resulting from the optimization is

$$F = \begin{bmatrix} 1.0380 & 3.5196 & 6.8596 & -3.8666 & -3.2233 & 0.3952 \\ 7.8693 & -0.2319 & -61.8796 & 44.8744 & 0.2072 & -5.8896 \end{bmatrix}$$

The details of the design process are given in the Appendix B.2. Obviously a varying matrix F can also be designed by directly solving the LMIs in (7.38)-(7.41) for all the vertices of the polytopic system.

In the nominal case, the elevator is the primary control surface for FPA tracking and the horizontal stabilizer acts as redundancy. For the V_{tas} tracking engine thrust (T_n) is the only control effector. Therefore in all the simulations it is assumed that the engines are fault free. Based on the condition given in (7.20), for the positive scalar $\varepsilon = 0.197$ using a numerical search the value of $\|\Delta(t,\rho)\|$ by using equation (7.21) is 0.0964. To satisfy the closed-loop stability condition in (7.25), the value of γ_o associated with the operator in (7.24) should satisfy $\gamma_o < \frac{\sqrt{\varepsilon}}{\gamma_1(\sqrt{\varepsilon}+c)} = 10.3734$. The design process for F yields a value of $\gamma_o = 9.7851$, and hence the stability condition in (7.25) is satisfied. During the simulations, the discontinuity associated with the nonlinear control term in (7.32) has been smoothed by using the fractional approximation (equation 3.37) , $\frac{\sigma}{\|\sigma\|+\delta}$ where the value of the positive scalar has been chosen as $\delta = 0.01$.

7.4.3 Simulation Results

In the simulations, the LPV longitudinal axis model of a transport aircraft discussed in Section 7.4.1 is used to demonstrate the efficacy of the proposed FTC scheme. In this Chapter the aircraft operates in an 'up and away' flight envelope [50]. A series of 3^o FPA and 10m/sec V_{tas} commands are given to the controller, in order to ensure the aircraft covers the entire flight envelope.

In [50] only elevator failure (lock and float) are considered. As compared to [50], the FTC scheme proposed in this paper is also tested by considering a stabilizer failure (as well as elevator failure scenarios). In [77] two separate controllers are designed, one for the nominal fault free situation and second if elevator fault occurs so that horizontal stabilizer can be employed in order to achieve FTC. However in case of elevator failure the reallocation to the stabilizer seems ad-hoc and not formally formalized, where as the proposed LPV ISM CA scheme in this Chapter, only requires the nominal fault free model based on the virtual control whereas faults and failures are dealt with naturally through CA.

7.4.3.1 Fault free scenario

In Figures 7.1-7.2, the nominal fault free case is demonstrated, where it can be seen that good tracking performance of FPA and V_{tas} commands according to the control design requirements is achieved. The aircraft undergoes a series of 3^o FPA commands in order to increase the altitude of the aircraft (from 7000 m to 12222 m) and the speed of the aircraft is increased from 150 m/sec to 230 m/sec in steps of 10 m/sec to go through the entire flight envelope.

7.4.3.2 Elevator Lock in place/jam failure

In Figure 7.4 an elevator jam failure (where the elevator jams and stays fixed at some offset position) occurs during the (climb) first FPA command. To counteract this failure, the proposed FTC scheme demands more from the horizontal stabilizer and engine thrust settings without degrading the tracking performance as compared to the nominal as can be seen in Figure 7.3. The sliding motion is maintained in the entire system response even in the presence of elevator failure (Figure 7.4).

7.4.3.3 Elevator float failure

An elevator float failure is considered in Figure 7.6. In order to simulate this failure, at the time of failure, the elevator control signal is replaced with the angle of attack [50], in this way the elevator does not generate the required moment. During the failure when the elevator follows the angle of attack aircraft state, the horizontal stabilizer deflects in the positive direction by 2.8^o to counteract the failure. In the elevator float failure, the effectiveness of the scheme can be seen in Figure 7.5. Both elevator jam and float failures are set to occur during the first FPA command as in [50]. In [50] only elevator failure is considered.

7.4.3.4 Horizontal Stabilizer Lock in place/jam failure

In Figure 7.8 horizontal stabilizer jam failure is demonstrated. To tolerate this failure, the elevator and engine thrust are manipulated by the control allocation scheme to cope with this situation, to maintain the closed-loop performance similar to the nominal one (Figure 7.7). The sliding motion was not destroyed by the failure which shows the efficacy of the FTC scheme against the actuator failure (Figure 7.8).

7.4.3.5 Horizontal Stabilizer hardover/runaway failure

Another hard type of failure which is tested by using the proposed scheme is a hardover/runaway failure, where the horizontal stabilizer runaways to its maximum saturation limit of 3^o with its maximum rate limit and then jams at that position as can be seen in Figure 7.10. The control allocation scheme exploits the available redundancy in an efficient way, and engages the elevator actively together with the engine thrust to maintain the desired performance same as nominal one as can be seen in Figure 7.9. Sliding is maintained in the entire system response which means the closed-loop stability is guaranteed in spite of runaway failure.

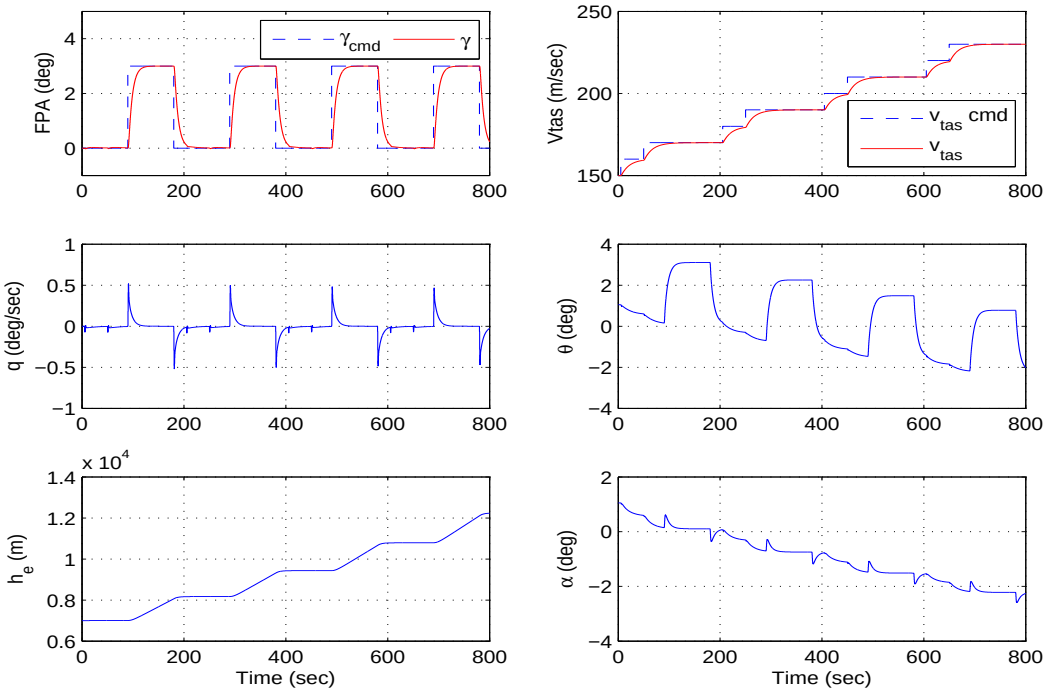

Figure 7.1: nominal scenario: System States

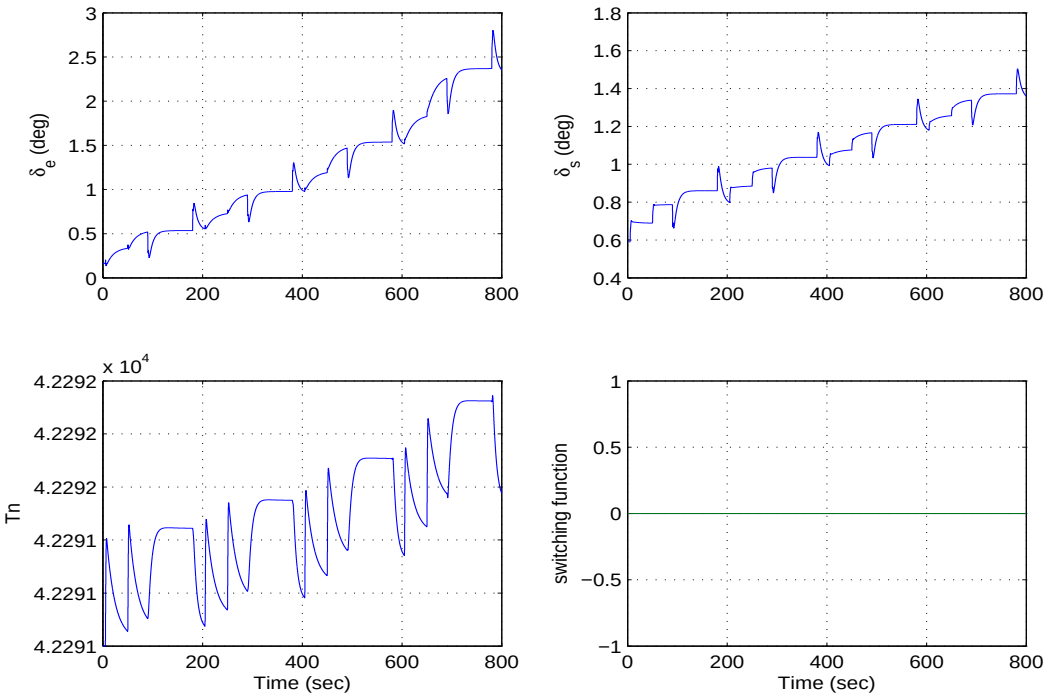

Figure 7.2: nominal scenario: actuators deflection

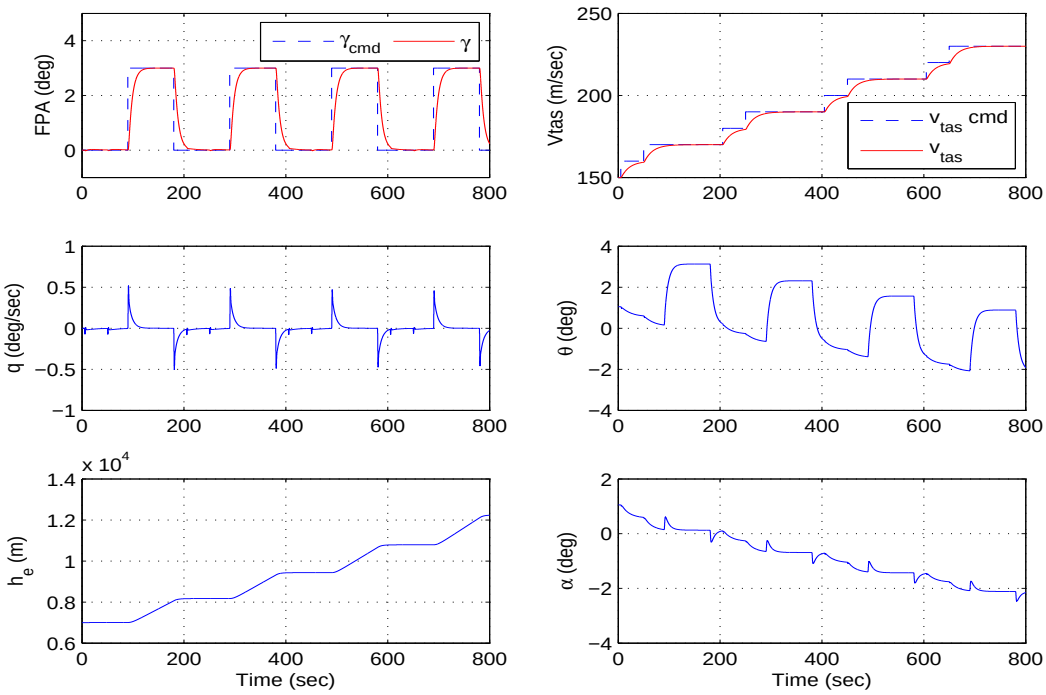

Figure 7.3: Elevator jam failure: System States

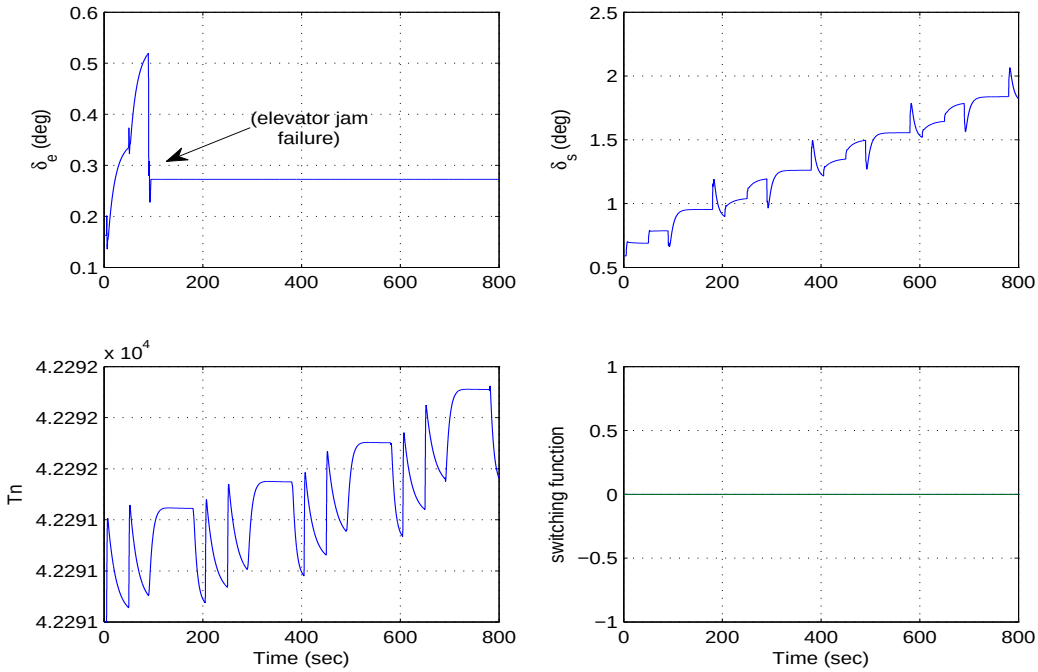

Figure 7.4: Elevator jam failure: actuators deflection

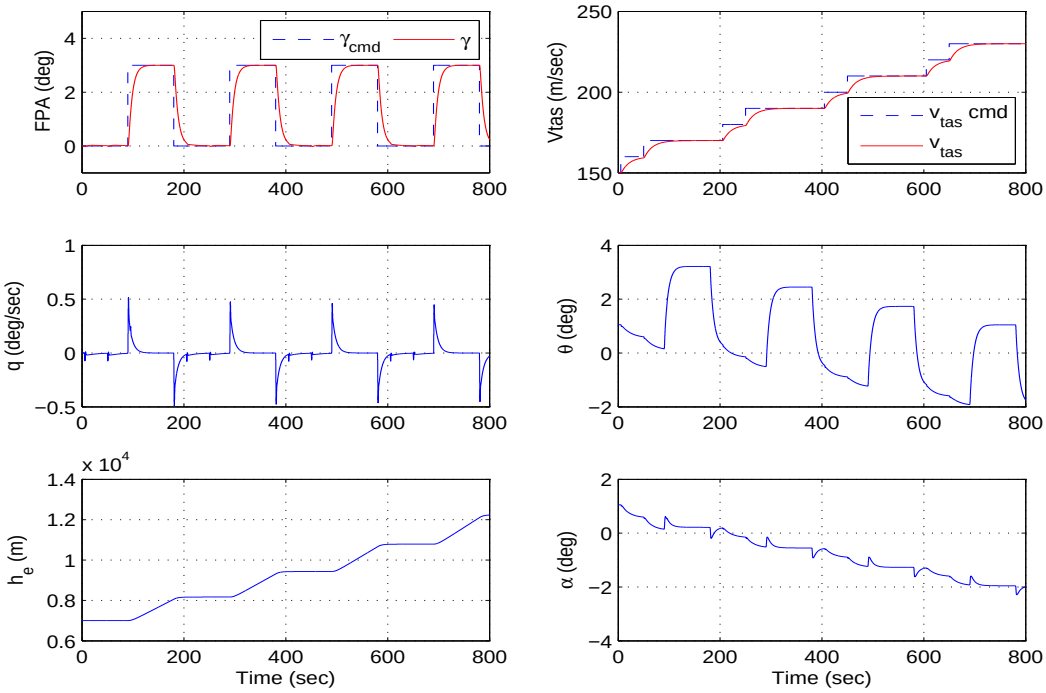

Figure 7.5: Elevator float failure: System States

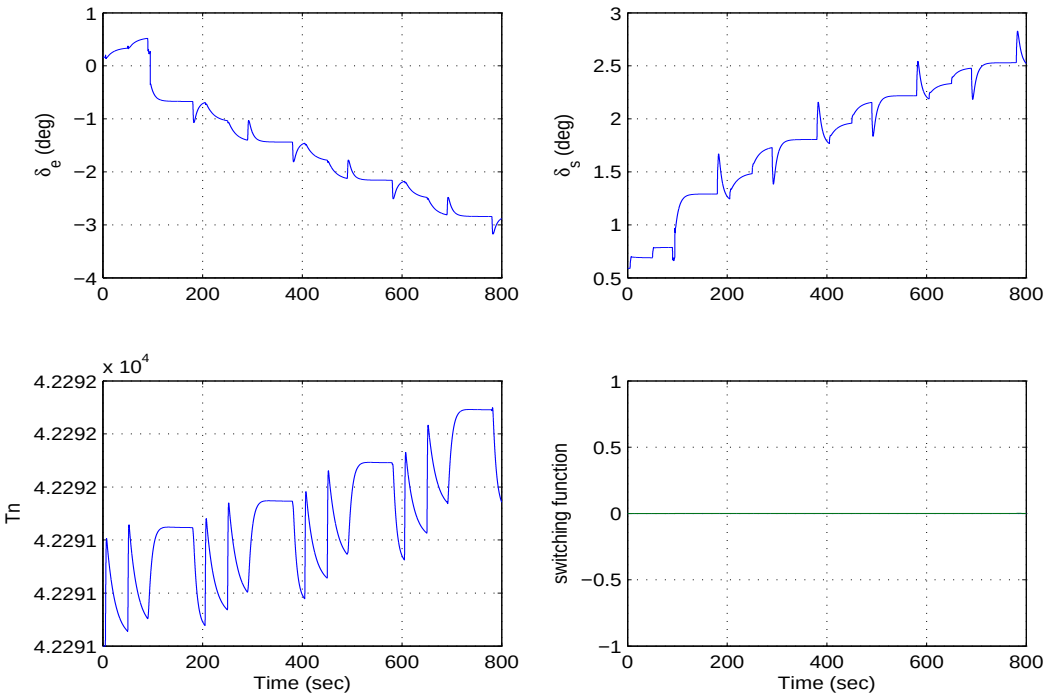

Figure 7.6: Elevator float failure: actuators deflection

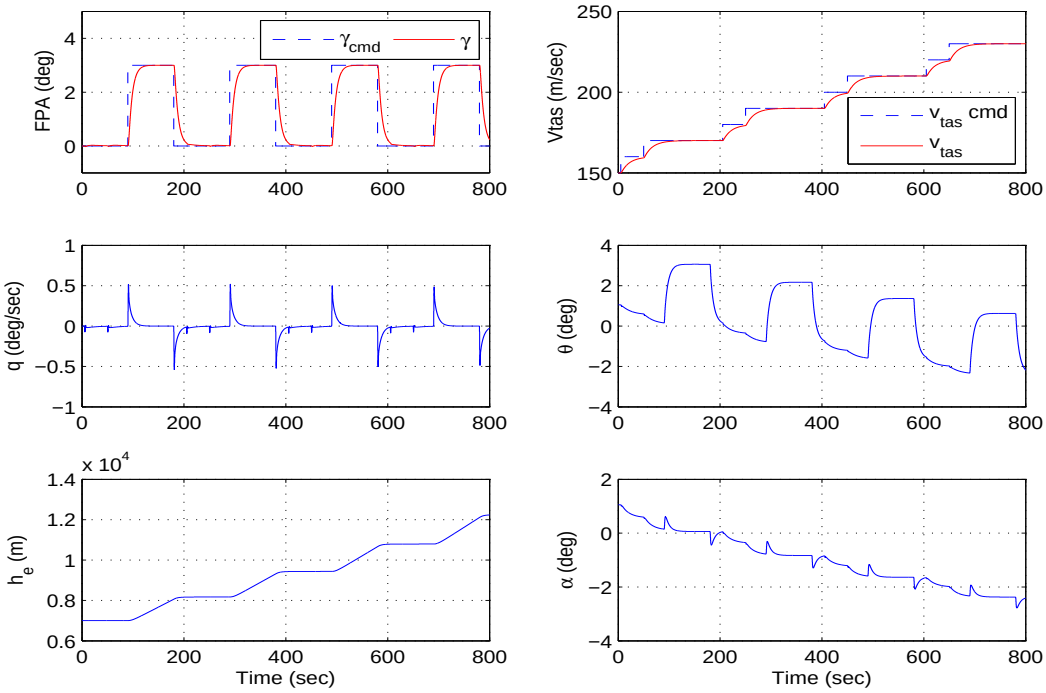

Figure 7.7: Stabilizer jam failure: System States

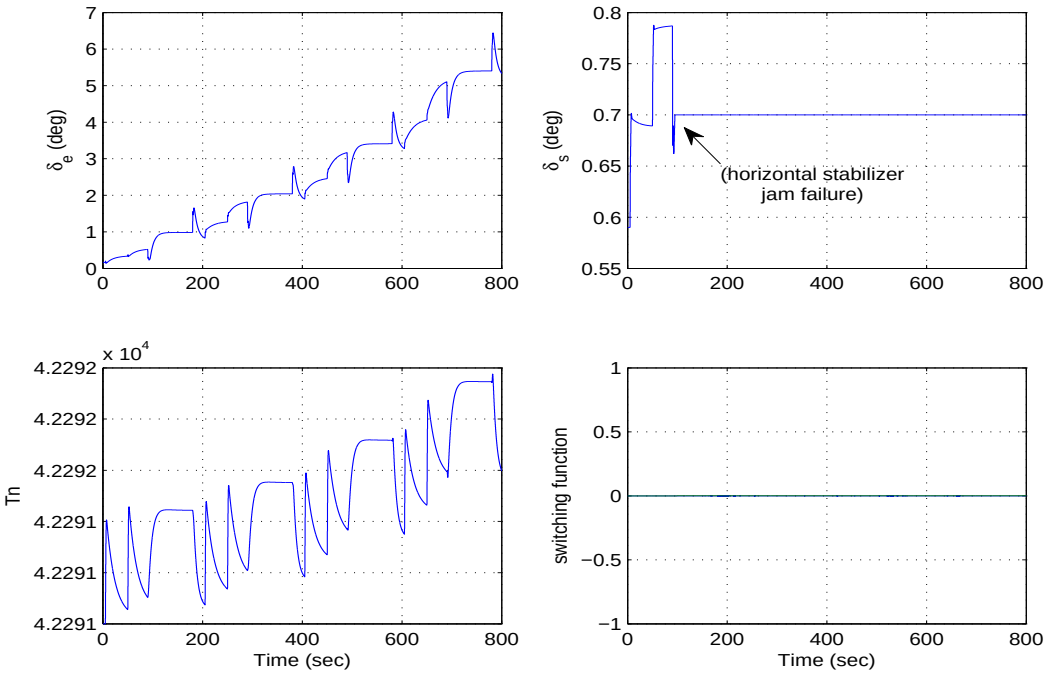

Figure 7.8: Stabilizer jam failure: actuators deflection

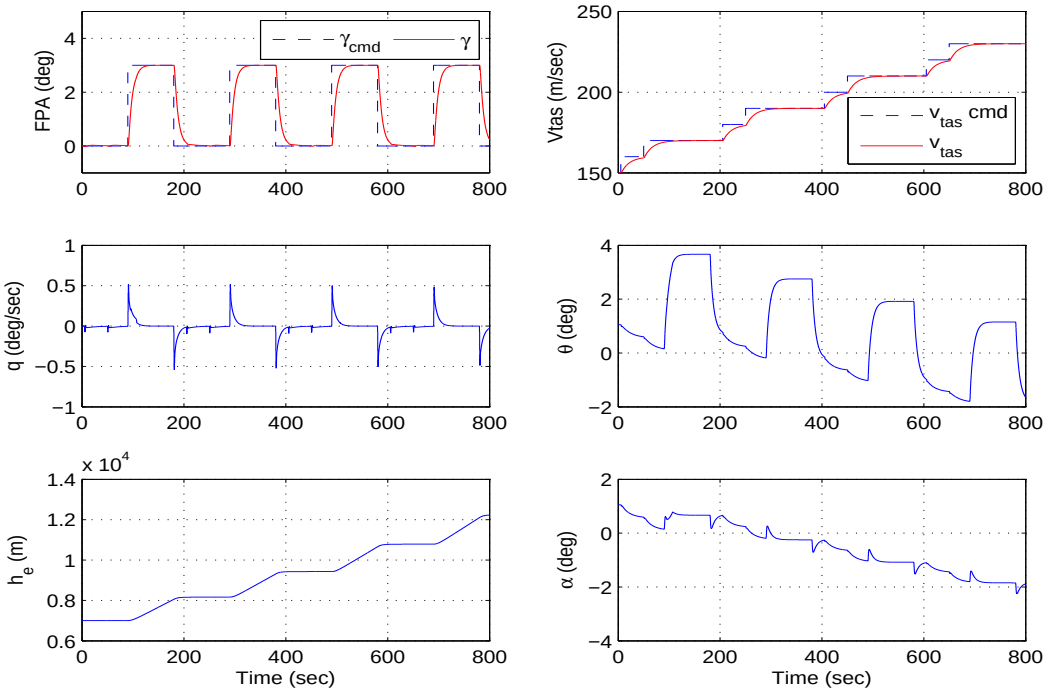

Figure 7.9: Stabilizer runaway failure: System States

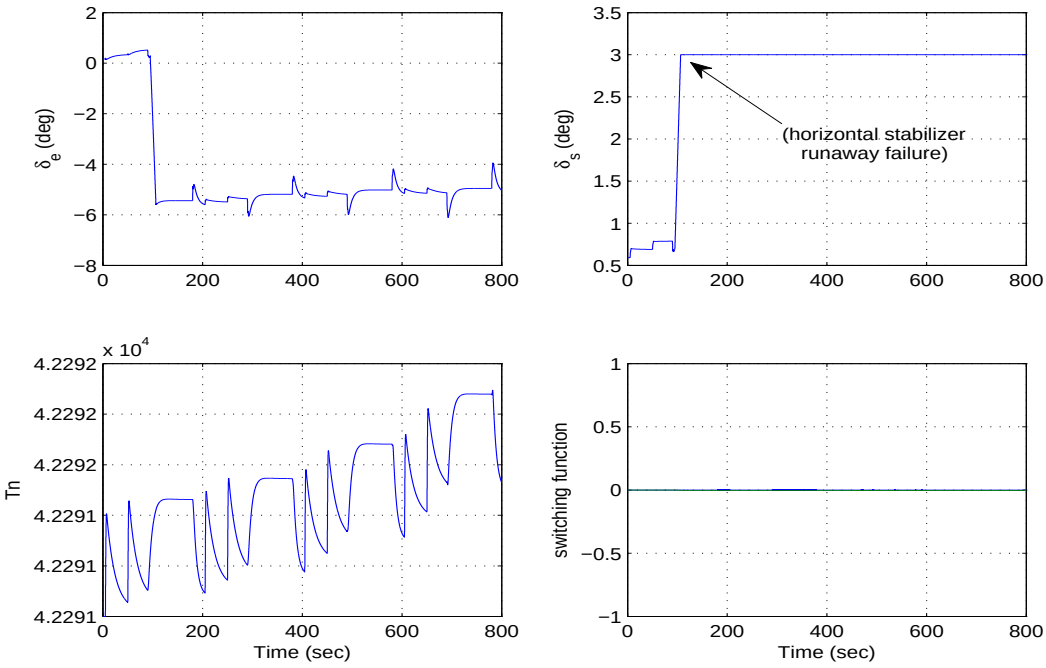

Figure 7.10: Stabilizer runaway failure: actuators deflection

7.5 Conclusion

This Chapter proposed a Fault Tolerant Control scheme for Linear parameter varying systems. The integral sliding mode control was used to maintain nominal performance and robustness in the face of actuator faults or failures. The virtual control signal, generated by the integral sliding mode control law was translated into the physical actuator commands by using the control allocation scheme. The closed-loop stability of the system throughout the entire flight envelope was guaranteed even in the event of a total failure of a certain class of actuators provided redundancy is available in the system. The longitudinal LPV model of a large transport aircraft which has previously been used in the FTC literature was used to show the efficacy of the proposed scheme.

The coming Chapter considers the case where only the output measurements are available and relaxes the requirement of early Chapters that full plant state variables are readily available for the controller design. Also the early FTC schemes in this thesis assume that the information of actuator effectiveness level is known to the control allocation for distributing the control signals among the actuators, but in the coming Chapter this information is also assumed to be unknown. This requires a totally different approach and is explained in the next Chapter.

Chapter 8

An Output Integral Sliding Mode FTC Scheme Using Control Allocation

A fault tolerant control scheme is proposed here for systems where only output information is available. In this Chapter an assumption which is made in early Chapters that the state information is known and available for the controller design is *relaxed* and instead a case is considered where only measured outputs are available. It is also considered that the knowledge of the actuator faults or failures is not available from an FDI scheme. The ideas of integral sliding mode control are used to ensure robustness throughout the entire response of the system, even in certain actuator fault or failure cases. This is accomplished by integrating *fixed control allocation* within the ISM framework. An *unknown input observer* is employed in the proposed scheme to estimate the states. Simulation results on a benchmark civil aircraft model show good tracking of the commanded signals.

8.1 Introduction

In most physical systems, not all system states are measurable and therefore output feedback schemes are more desirable. This also applies for FTC systems. The early work for example [6], [106] and [62] the combination of traditional SMC with CA for fault tolerant control has been previously explored but in all this work it was assumed that the system states are known and that state feedback control schemes could be employed.

The main contribution of this Chapter is to relax the assumption associated with the early Chapters that state information is known, and as compared to the above mentioned papers consider instead the situation

where only measured outputs are available. A full order linear unknown input observer is employed to estimate the system states used in the underlying virtual controller. In this Chapter no attempt is made to estimate the actuator faults or failures (using an FDI scheme), instead, the robustness properties of the UIO coupled with the ISM are relied upon. As compared to the early schemes in this thesis, a fixed control allocation scheme (which does not require actuators effectiveness level $W(t)$) is used to translate the virtual control signals into physical actuator demands. An LMI synthesis procedure is proposed in order to synthesize the observer gains and the controller parameters and a rigorous closed-loop stability analysis is carried out to ensure the stability of the sliding motion in the face of actuator faults and certain failures, provided that redundancy is available in the system. A civil aircraft benchmark model is used to investigate the feasibility of the proposed scheme.

8.2 Problem Formulation

To model the actuator faults or failures same as in early Chapters, actuators effectiveness matrix $W(t)$ is used whereas component faults are modelled as parametric uncertainty in the system matrix. Consider an uncertain system with actuator faults or failures and component faults written as

$$\dot{x}(t) = (A+A^{\delta})x(t)+Bu(t)-BKu(t) \tag{8.1}$$

$$y(t) = Cx(t) \tag{8.2}$$

where $A \in \mathbb{R}^{n\times n}$ is the state matrix, A^{δ} is parametric uncertainty in the system matrix arising from imprecisely known parameters and possible faults at a component level, $B \in \mathbb{R}^{n\times m}$ is the input distribution matrix and $C \in \mathbb{R}^{p\times n}$ is the output distribution matrix where $p \geq m$. The diagonal weighting matrix $K = diag\{k_1,..,k_m\}$, where the scalars $k_1,..,k_m$, models the effectiveness level of the actuators. If $k_i = 0$, the corresponding ith actuator is fault free and is working perfectly, whereas if $1 > k_i > 0$, an actuator fault is present. The value $k_i = 1$ indicates the ith actuator has completely failed.

Remark 8.1: The description of actuator fault or failure apparently looks different from the early Chapters, but in structure is the same because the actuator effectiveness matrix $W(t)$ without loss of generality is defined to be having the structure $W(t) := I_m - K(t)$.

Here it is assumed that the outputs to be controlled are given by $y_c(t) = C_c x(t)$ where $C_c \in \mathbb{R}^{l\times n}$, where

$l < m$. It follows that there is redundancy in the system in terms of the number of control inputs. This will be exploited to achieve fault tolerance. Following the similar discussion as in Chapter 4, to resolve the actuator redundancy, (by permuting the state) it is assumed the matrix B can be partitioned such that

$$B = \begin{bmatrix} B_1^T & B_2^T \end{bmatrix}^T \tag{8.3}$$

where $B_1 \in \mathbb{R}^{(n-l)\times m}$ and $B_2 \in \mathbb{R}^{l\times m}$ is of rank $l < m$. By appropriate scaling of the last l states, it can be ensured $B_2 B_2^T = I_l$, and is assumed that $\|B_1\| \ll \|B_2\| = 1$, so that B_2 reflects that the dominant control action contribution on the system acts in the lower l channels of the system. Using (8.3), the system in (8.1) can be written as

$$\dot{x}(t) = (A + A^{\delta})x(t) + \begin{bmatrix} B_1 \\ B_2 \end{bmatrix} \underbrace{(I - K)}_{W} u(t) \tag{8.4}$$

Notice, by definition $W := I - K$ is a diagonal matrix and its diagonal elements w_i satisfy $0 \leq w_i \leq 1$.

The objective of this Chapter is to develop a control scheme, based on only output measurements, which can maintain closed-loop stability in the face of a class of actuator faults and failures. The physical control law $u(t)$ is realized by a so-called 'fixed' control allocation scheme of the form

$$u(t) = B_2^T \nu(t) \tag{8.5}$$

where $\nu(t) \in \mathbb{R}^l$ is the 'virtual control' effort produced by the control law, which will be described in the sequel. In equation (8.5) the fact that $B_2 B_2^{\mathrm{T}} = I_l$ is exploited.

Remark 8.2: The control allocation structure in (8.5) is different to the one employed in Chapter 4, which require $W(t)$ (or at least a good estimate of $W(t)$ to be known). The fixed CA/ISM scheme developed in this Chapter will be independent of $W(t)$ and will not require an FDI scheme.

By using (8.5), equation (8.4) can be written as

$$\dot{x}(t) = (A + A^{\delta})x(t) + \underbrace{\begin{bmatrix} B_1 W B_2^T \\ B_2 W B_2^T \end{bmatrix}}_{B_w} \nu(t) \tag{8.6}$$

In the nominal case, when there is no fault ($W(t) = I_m$ and $A^{\delta} = 0$), equation (8.6) simplifies to

$$\dot{x}(t) = Ax(t) + \underbrace{\begin{bmatrix} B_1 B_2^T \\ I_l \end{bmatrix}}_{B_v} v(t) \tag{8.7}$$

because $B_2 B_2^T = I_l$ by design. The following assumption will be made and used in the remainder of the Chapter.

*A*1**:** The pair (A, B_v) is controllable.

8.3 ISM Controller Design

In this section the integral sliding mode strategy will be adopted for synthesizing the virtual control signal $v(t)$. The virtual control signal $v(t)$ will use estimated states $\hat{x}(t)$, obtained from an observer, so that only outputs need to be measured. As a first design step, an output and state-estimate dependent integral switching function is proposed of the form

$$\sigma(t) = Gy(t) - Gy(0) + \int_0^t F\hat{x}(\tau)d\tau \tag{8.8}$$

where $G \in \mathbb{R}^{l \times p}$ and $F \in \mathbb{R}^{l \times n}$ are design matrices, selected to specify nominal closed-loop performance. The formulation in (8.8) is similar to that given in equation (3.69) except here both F and G depend on the dimension l rather than the number of control inputs. In order to create the state estimate $\hat{x}(t)$, the full-order unknown input observer UIO developed in [66] is used. The term $BKu(t)$ in (8.1) is treated as an unknown input since by assumption $K(t)$ is unknown. Consequently the distribution matrix associated with the unknown input signal to be rejected is chosen as B. Necessary and sufficient conditions for a linear UIO to exist for the system in (8.1)-(8.2), to provide insensitivity with respect to the term BK(t)u(t), are

*A*2**:** $rank(CB) = rank(B) = m$

*A*3**:** the triple (A, B, C) is minimum phase

The structure of the full-order observer from [66] is,

$$\dot{z}(t) = A_0 z(t) + TBu(t) + Ly(t) \tag{8.9}$$

$$\hat{x}(t) = z(t) + Hy(t) \tag{8.10}$$

where $\hat{x}(t)$ is the estimated state, and A_0, T, L and H are design matrices of appropriate dimension chosen in order to decouple the unknown inputs. The ultimate objective of an UIO is to make the error signal $e(t) = x(t) - \hat{x}(t)$ zero, despite the presence of unknown input $Ku(t)$ so that the estimated states converge to the true states asymptotically. In particular, the matrix $H \in \mathbb{R}^{n \times p}$ must be chosen so that

$$\underbrace{(I - HC)}_{T} B = 0 \tag{8.11}$$

because B is an unknown input direction in this case. As argued in [66], Assumption $A2$ is sufficient to solve (8.11) and $H := B((CB)^T CB)^{-1}(CB)^T$ is an appropriate choice. After computing H, the matrix

$$A_0 := \underbrace{A - HCA}_{A_h} - L_1 C \tag{8.12}$$

can be defined, where $L_1 \in \mathbb{R}^{n \times p}$ is design freedom which is exploited to make A_0 Hurwitz. Finally

$$L_2 := A_0 H \tag{8.13}$$

and the gain $L := L_1 + L_2$.

Remarks 8.3: The ISM scheme in this Chapter can tolerate the presence of stable invariant zeros associated with the triple (A, B, C) (Assumption $A3$) as compared to [15], where it is argued that for the stable sliding motion, it is assumed that the triple (A, B, C) does not have any invariant zeros i.e the pair (C,A) is observable.

If $e(t) = x(t) - \hat{x}(t)$, using the plant equation in (8.1) and the UIO equations in (8.9)-(8.10), the error dynamics can be written as

$$\begin{aligned}
\dot{e}(t) &= Ax(t) + A^{\delta}x(t) + Bu(t) - BKu(t) - A_0 z(t) - TBu(t) - Ly(t) \\
&\quad -HC(Ax(t) + A^{\delta}x(t) + Bu(t) - BKu(t)) \\
&= (I - HC)Ax(t) + (I - HC)A^{\delta}x(t) + (I - HC)Bu(t) - (I - HC)BKu(t) \\
&\quad -A_0 z(t) - TBu(t) - Ly(t) \qquad (8.14)
\end{aligned}$$

where it can be seen that with the choice of $H := B((CB)^T CB)^{-1}(CB)^T$ and using equation (8.11) the error dynamics can be made invariant to unknown input $BKu(t)$. Furthermore using equations (8.10), (8.13) and with the relation $L = L_1 + L_2$, the error dynamics in (8.14) can be further simplified to yield

$$\begin{aligned}
\dot{e}(t) &= TAx(t) + TA^{\delta}x(t) - A_0(\hat{x}(t) - Hy(t)) - L_1 y(t) - L_2 y(t) \\
&= TAx(t) + TA^{\delta}x(t) - A_0\hat{x}(t) - L_1 Cx(t) \\
&= \underbrace{(TA - L_1 C)}_{A_0} x(t) + TA^{\delta}x(t) - A_0\hat{x}(t) \\
&= A_0 e(t) + TA^{\delta}x(t) \qquad (8.15)
\end{aligned}$$

The choice of G in (8.8) suggested in this Chapter is

$$G := B_2\big((CB)^T CB\big)^{-1}(CB)^T \qquad (8.16)$$

where the existence of the inverse is guaranteed by assumption $A2$. As a result of this choice of G, generically $GCB_w(t) = B_2 W(t) B_2^T$ is symmetric. The symmetry is important and simplifies much of the subsequent analysis and avoids the introduction of conservatism. Also nominally, when there are no faults and $W(t) = I$, from the special properties of the matrix B_2, it follows that

$$GCB_w(t)|_{W=I} = B_2 B_2^T = I$$

This means, nominally, G has the pseudo inverse properties which [28] argue as explained in Chapter 3 are optimal from the point of view of minimizing the impact of unmatched uncertainties on the closed

loop dynamics.

Suppose a control law can be designed to force sliding motion for all time. The equivalent control signal $v_{eq}(t)$ necessary to maintain sliding is obtained from equating $\dot{\sigma} = 0$. The derivative of $\sigma(t)$ in equation (8.8) is

$$\dot{\sigma}(t) = G\dot{y}(t) + F\hat{x}(t) \tag{8.17}$$

then substituting from equation (8.6) and equating $\dot{\sigma}(t) = 0$ yields

$$v_{eq}(t) = -(GCB_w)^{-1}\big(F\hat{x}(t) + GC(A + A^{\delta})x(t)\big) \tag{8.18}$$

under the assumption that $\det(GCB_w) \neq 0$. With the choice of G in (8.16) $GCB_w = B_2WB_2^T$, and (8.18) becomes

$$v_{eq}(t) = -(B_2WB_2^T)^{-1}\big(F\hat{x}(t) + GC(A + A^{\delta})x(t)\big) \tag{8.19}$$

Substituting (8.19) into (8.6) the sliding dynamics are given by

$$\dot{x}(t) = (A + A^{\delta})x(t) - B_m\big(F\hat{x}(t) + GC(A + A^{\delta})x(t)\big) \tag{8.20}$$

where

$$B_m := \begin{bmatrix} B_1WB_2^T(B_2WB_2^T)^{-1} \\ I_l \end{bmatrix}$$

Adding and subtracting the term $B_v\big(F\hat{x}(t) + GC(A + A^{\delta})x(t)\big)$ to the right hand side of (8.20) and exploiting the fact that $e(t) := x(t) - \hat{x}(t)$, the sliding dynamics in (8.20) can be written as

$$\begin{aligned}
\dot{x}(t) &= (A + A^{\delta})x(t) - B_v\big(F\hat{x}(t) + GC(A + A^{\delta})x(t)\big) + (B_v - B_m)\big(F\hat{x}(t) + GC(A + A^{\delta})x(t)\big) \\
&= (A - B_vF - B_vGCA)x(t) + A^{\delta}x(t) + B_vFe(t) - B_vGCA^{\delta}x(t) \\
&\quad + \widetilde{B}\Phi(t)\big(Fx(t) - Fe(t) + GC(A + A^{\delta})x(t)\big) \\
&= (A - B_vF - B_vGCA)x(t) + (I - B_vGC)A^{\delta}x(t) + B_vFe(t) \\
&\quad + \widetilde{B}\Phi(t)(GCA + F)x(t) - \widetilde{B}\Phi(t)Fe(t) + \widetilde{B}\Phi(t)GCA^{\delta}x(t)
\end{aligned} \tag{8.21}$$

where

$$\widetilde{B} := \begin{bmatrix} I_{n-l} \\ 0 \end{bmatrix} \tag{8.22}$$

and

$$\Phi(t) = B_1 B_2^T - \underbrace{B_1 W B_2^T (B_2 W B_2^T)^{-1}}_{\psi(t)} \tag{8.23}$$

Combining equations (8.15) and (8.21), the closed-loop system dynamics can be written as

$$\begin{aligned} \begin{bmatrix} \dot{e}(t) \\ \dot{x}(t) \end{bmatrix} &= \begin{bmatrix} A_0 & 0 \\ B_v F & A - B_v F - B_v GCA \end{bmatrix} \begin{bmatrix} e(t) \\ x(t) \end{bmatrix} + B_a \Delta C_a \begin{bmatrix} e(t) \\ x(t) \end{bmatrix} \\ \begin{bmatrix} \dot{e}(t) \\ \dot{x}(t) \end{bmatrix} &= \underbrace{\begin{bmatrix} A_0 & 0 \\ B_v F & A_c - B_v F \end{bmatrix}}_{A_a} \underbrace{\begin{bmatrix} e(t) \\ x(t) \end{bmatrix}}_{x_a} + B_a \Delta C_a \begin{bmatrix} e(t) \\ x(t) \end{bmatrix} \end{aligned} \tag{8.24}$$

where

$$A_c := (I - B_v GC)A \tag{8.25}$$

$$B_a := \begin{bmatrix} (I - HC) & 0 & 0 \\ (I - B_v GC) & \widetilde{B} & \widetilde{B} \end{bmatrix} \tag{8.26}$$

$$C_a := \begin{bmatrix} 0 & I \\ -F & GCA + F \\ 0 & I \end{bmatrix} \tag{8.27}$$

and the uncertainty term $\Delta(t)$ is

$$\Delta(t) := \operatorname{diag} \begin{bmatrix} A^{\delta} & \Phi & \Phi GCA^{\delta} \end{bmatrix} \tag{8.28}$$

It is convenient to analyze (8.24) in the $(e, \hat{x})$ coordinates. Define accordingly

$$\underbrace{\begin{bmatrix} e(t) \\ \hat{x}(t) \end{bmatrix}}_{\hat{x}_a} = \underbrace{\begin{bmatrix} I & 0 \\ -I & I \end{bmatrix}}_{\widetilde{T}} \begin{bmatrix} e(t) \\ x(t) \end{bmatrix} \tag{8.29}$$

which follows

$$\widetilde{A}_a := \widetilde{T}A_a\widetilde{T}^{-1} = \begin{bmatrix} A_0 & 0 \\ A_c - A_0 & A_c - B_vF \end{bmatrix} \tag{8.30}$$

$$\widetilde{B}_a := \widetilde{T}B_a = \begin{bmatrix} (I - HC) & 0 & 0 \\ HC - B_vGC & \widetilde{B} & \widetilde{B} \end{bmatrix} \tag{8.31}$$

$$\widetilde{C}_a := C_a\widetilde{T}^{-1} = \begin{bmatrix} I & I \\ GCA & GCA + F \\ I & I \end{bmatrix} \tag{8.32}$$

then in the new $(e, \hat{x})$ coordinates, equation (8.24) can be written as

$$\dot{\hat{x}}_a(t) = \widetilde{A}_a\hat{x}_a(t) + \widetilde{B}_a\Delta\widetilde{C}_a\hat{x}_a(t) \tag{8.33}$$

Now in order to ensure that the term $\Phi(t)$ in (8.23) is bounded, note that $\Phi(t) = B_1B_2^T - \psi(t)$ and $\psi(t) = B_1B_2^{\dagger,W(t)}$ where $B_2^{\dagger,W(t)}$ is a weighted right pseudo inverse of B_2. Then by using arguments similar to those as given in Chapter 4 as proved in [111] there exists a scalar γ_0 such that

$$\|B_2^{\dagger,W(t)}\| := \|W(t)B_2^T(B_2W(t)B_2^T)^{-1}\| < \gamma_0 \tag{8.34}$$

for all combinations of $(w_1(t), ..., w_m(t))$ such that $\det(B_2W(t)B_2^T) \neq 0$. Therefore $\|\psi(t)\| \leq \gamma_1\gamma_0$ and hence

$$\|\Phi(t)\| \leq \gamma_1(1 + \gamma_0) \tag{8.35}$$

where $\gamma_1 = \|B_1\|$, which is assumed to be small.

*A*4**:** Assume that the parametric uncertainty A^δ in the system matrix A is bounded and therefore since $\Phi(t)$ is bounded, it follows

$$\|\Delta\| < \gamma_a \tag{8.36}$$

for some positive scalar γ_a.

8.3.1 Closed-loop Stability Analysis

In the nominal case, (i.e. when $W(t) = I$, $A^{\delta} = 0$ and $\Delta(t) = 0$), equation (8.33) simplifies to $\dot{\hat{x}}_a(t) = \widetilde{A}_a\hat{x}_a(t)$. From (8.30) it is clear the eigenvalues of $\widetilde{A}_a$ are given by the union of the eigenvalues of A_0 and $A_c - B_vF$. Both these matrices can be made Hurwitz by choice of the design freedom matrices L_1 from (8.12) and F respectively. Consequently, by design, $\widetilde{A}_a$ can be made Hurwitz, and hence nominally the closed loop system is stable. However for the fault or failure cases, stability needs to be proven. Define

$$\gamma_2 = \|\widetilde{G}_a(s)\|_{\infty} \tag{8.37}$$

where

$$\widetilde{G}_a(s) := \widetilde{C}_a(sI - \widetilde{A}_a)^{-1}\widetilde{B}_a \tag{8.38}$$

Proposition 8.1: In fault or failure conditions, for any combination of $(w_1(t),...,w_m(t))$ such that $\det(B_2WB_2^T) \neq 0$, the closed loop system in (8.33) will be stable if:

$$\gamma_2\gamma_a < 1 \tag{8.39}$$

Proof. In order to establish closed-loop stability, the system defined in (8.33) can also be written as

$$\dot{\hat{x}}_a(t) = \widetilde{A}_a\hat{x}_a(t) + \widetilde{B}_a\widetilde{u}_a(t) \tag{8.40}$$

$$\widetilde{y}_a(t) = \widetilde{C}_a\hat{x}_a(t) \tag{8.41}$$

where $\widetilde{u}_a(t) := \Delta(t)\widetilde{y}_a(t)$. In this form, equation (8.33) is the feedback interconnection of the known linear system $\widetilde{G}_a(s)$, and the bounded uncertain gain $\Delta(t)$. According to the small gain theorem (Appendix B.1.2), the feedback interconnection of $\widetilde{G}_a(s)$ and $\Delta(t)$ will be stable if (8.39) is satisfied. ■

Remark 8.4: By hypothesis, $\gamma_1 = \|B_1\|$ is assumed to be small. Basically the size $\|B_1\|$ has a significant impact on the norm of the nonlinearity in the small gain feedback loop, and so if $\|B_1\|$ is small, the gain of the nonlinearity is small, and there is a less stringent requirement on the magnitude of the H_{∞} norm of the linear part. Furthermore if $A^{\delta} = 0$, then $\|\Delta\| \longrightarrow 0$ as $\|B_1\| \longrightarrow 0$ and *Proposition* 8.1 is trivially satisfied.

8.3.2 LMI Synthesis

In this section the observer gain L_1 and the controller gain F are synthesized, so that stability condition (8.39) is satisfied. For the triple $(\widetilde{A}_a, \widetilde{B}_a, \widetilde{C}_a)$, from the Bounded Real Lemma (BRL) $\|\widetilde{G}_a(s)\|_\infty < \gamma_2$ if and only if there exists a s.p.d matrix $X \in \mathbb{R}^{2n\times 2n}$ such that

$$\begin{bmatrix} \widetilde{A}_a X + X\widetilde{A}_a^{\mathrm{T}} & \widetilde{B}_a & X\widetilde{C}_a^{\mathrm{T}} \\ \widetilde{B}_a^T & -\gamma_2^2 I & 0 \\ \widetilde{C}_a X & 0 & -I \end{bmatrix} < 0 \tag{8.42}$$

Here it is assumed that $X = \mathrm{diag}(X_1, X_2)$ where the two sub-blocks $X_1, X_2 \in \mathbb{R}^{n\times n}$ are s.p.d. With this assumption

$$\widetilde{C}_a X = \begin{bmatrix} X_1 & X_2 \\ GCAX_1 & GCAX_2 + Y \\ X_1 & X_2 \end{bmatrix} \tag{8.43}$$

where $Y := FX_2$. The top left sub-block in (8.42)

$$\widetilde{A}_a X + X\widetilde{A}_a^{\mathrm{T}} = \begin{bmatrix} A_0X_1 + X_1A_0^{\mathrm{T}} & X_1A_c^{\mathrm{T}} - X_1A_0^{\mathrm{T}} \\ A_cX_1 - A_0X_1 & \Theta \end{bmatrix} \tag{8.44}$$

where $\Theta = A_cX_2 + X_2A_c^{\mathrm{T}} - B_vY - Y^{\mathrm{T}}B_v^T$. Also write $A_0 = A_h - L_1C$ where A_h is from (8.12). To create a convex representation, define the observer gain

$$L_1 := \beta BE \tag{8.45}$$

where β is a positive scalar and $E \in \mathbb{R}^{m\times p}$ is chosen so that (A_h, B, EC) is minimum phase. This is possible if (A, B, C) is minimum phase (*Assumption* 3). Then as argued in [42] it is possible to find an s.p.d matrix P which has a structure $P = N^{\mathrm{T}}\mathrm{diag}(P_1, P_2)N$ such that $PB = (EC)^{\mathrm{T}}$, where $N \in \mathbb{R}^{n\times n}$ is invertible (and depends on E) and the s.p.d. matrices $P_1 \in \mathbb{R}^{(n-m)\times(n-m)}, P_2 \in \mathbb{R}^{m\times m}$. The matrix N is associated with a change of coordinates to force the triple (A_h, B, EC) into the canonical form proposed

in [42]. Define $X_{11} = P_1^{-1}$ and $X_{12} = P_2^{-1}$. It follows that $L_1C = \beta BEC = \beta BB^{\mathrm{T}}P$ and so if

$$X_1 := P^{-1} = N^{-1}\mathrm{diag}(X_{11}, X_{12})(N^{-1})^{\mathrm{T}} > 0 \tag{8.46}$$

then $L_1CX_1 = \beta BB^{\mathrm{T}}$ and $A_0X_1 = A_hX_1 - \beta BB^{\mathrm{T}}$. It follows that the matrix inequality in (8.42) is affine with respect to the decision variables $X_{11}, X_{12}, X_2, \beta, Y$ and so the synthesis problem is convex.

For the nominal system in (8.7), (i.e. when $W(t) = I$ and $A^{\delta} = 0$), the matrix F must stabilize $(A - B_vF)$. Since (A, B_v) is assumed to be controllable (*Assumption* 1), an LQR formulation will be adopted where F is selected to minimize

$$J = \int_0^{\infty} (x^T Qx + v^T Rv)dt$$

where Q and R are symmetric positive definite design matrices. This problem can be posed as an LMI optimization:

Minimize $trace(X_2^{-1})$ subject to

$$\begin{bmatrix} AX_2 + X_2A^T - B_vY - Y^TB_v^T & (Q_1X_2 - R_1Y)^T \\ Q_1X_2 - R_1Y & -I \end{bmatrix} < 0 \tag{8.47}$$

where $Q_1 = [(Q^{\frac{1}{2}})^T \quad 0_{l\times n}^T]^T$ and $R_1 = [0_{n\times l}^T \quad (R^{\frac{1}{2}})^T]^T$. For a given $\mathscr{L}_2$-gain γ_2, the overall optimization problem proposed in convex form becomes:

Minimize $trace(Z)$ with respect to the decision variables $X_{11}, X_{12}, X_2, \beta, Y$ subject to

$$\begin{bmatrix} -Z & I_n \\ I_n & -X_2 \end{bmatrix} < 0 \tag{8.48}$$

together with (8.42), (8.47), (8.46) and 8.48. The matrix Z is a slack variable which satisfies $Z > X_2^{-1}$ and therefore $trace(Z) \geq trace(X_2^{-1})$. Finally the controller and observer gains can be recovered as $F = YX_2^{-1}$ and $L_1 = \beta BE$.

8.3.3 ISM Control Laws

A control law will be defined to ensure sliding is maintained from $t = 0$. Define the virtual control law in (8.7) as

$$v(t) = v_l(t) + v_n(t) \tag{8.49}$$

where the linear part, responsible for the nominal performance of the system is

$$v_l(t) = -F\hat{x}(t) - GCA\hat{x}(t) \tag{8.50}$$

and the nonlinear part is defined as

$$v_n(t) = -\rho \frac{\sigma(t)}{\|\sigma(t)\|} \qquad \text{for } \sigma(t) \neq 0 \tag{8.51}$$

where ρ is a modulation gain and is defined in *Proposition* 8.2.

Also define the time varying scalar $\varepsilon(t)$ as the solution to

$$\dot{\varepsilon}(t) = -m_0\varepsilon(t) + m_1\|\hat{x}(t)\| \tag{8.52}$$

where m_0 and m_1 are positive scalars to be defined in the sequel and let $V_0 = e^T P_0 e$,[1] where P_0 is the s.p.d matrix obtained from solving $P_0A_0 + A_0{}^T P_0 = -1$. Further suppose that $\|A^\delta\|$ is sufficiently small so that P_0 also satisfies

$$2\|P_0\|\|(I - HC)A^\delta\| < 1 - \mu_o \quad \text{where} \quad \mu_o > 0 \tag{8.53}$$

where $\mu_o > 0$. Then the following Proposition can be proved.

Proposition 8.2: Define the modulation gain from (8.51) as

$$\rho(t) = \frac{\|GCA^\delta\|\|\hat{x}(t)\| + \|v_l\| + \varepsilon(t)(\|GCA\| + \|GCA^\delta\|)/\sqrt{\lambda_{min}(P_0)} + \eta}{(1 - \lambda_0)} \tag{8.54}$$

where η is a positive design scalar, and assume the fault tuple $(k_1, \ldots, k_m)$ belongs to a set

$$\mathscr{D} = \{(k_1, ..., k_m) : \lambda_{max}(B_2 K B_2^T) < \lambda_0 < 1\}$$

[1] Using the Rayleigh-Ritz theorem $V_0 = e^T P_0 e \leq \lambda_{max}\{P_0\}\|e\|^2$.

Also assume that by choice of $\hat{x}(0)$ and $\varepsilon(0)$ the state estimation error at t =0, written $e(0)$, satisfies $\sqrt{e(0)^T P_0 e(0)} < \varepsilon(0)$. Then the integral sliding mode control law defined in (8.50)-(8.51), guarantees that the system trajectories remain on the sliding surface.

Proof. Equation (8.15) can be written as

$$\dot{e}(t) = (A_0 + (I - HC)A^{\delta})e(t) + (I - HC)A^{\delta}\hat{x}(t) \tag{8.55}$$

then the derivative of the positive definite function $V_0 = e^T P_0 e$ is given by

$$\begin{aligned}\dot{V}_0 &= e(P_0 A_0 + A_0^T P_0)e^T + 2e^T P_0 (I - HC)A^{\delta} e + 2e^T P_0 (I - HC)A^{\delta}\hat{x} \\ &\leq -\|e\|^2 + 2\|e\|^2 \|P_0\| \|(I - HC)A^{\delta}\| + 2\|e\| \|P_0\| \|(I - HC)A^{\delta}\| \|\hat{x}\|\end{aligned}$$

and therefore since by assumption $2\|P_0\| \|(I - HC)A^{\delta}\| < 1 - \mu_o$ where $\mu_o > 0$ it follows

$$\begin{aligned}\dot{V}_0 &\leq -\mu_0 \|e\|^2 + (1 - \mu_0)\|\hat{x}\| \|e\| \\ &\leq -\frac{\mu_0}{\lambda_{max}(P_0)} V_0 + \frac{1 - \mu_0}{\sqrt{\lambda_{max}(P_0)}} \|\hat{x}\| \sqrt{V_0}\end{aligned} \tag{8.56}$$

where the Rayleigh-Ritz theorem has been used. Define $\widetilde{V} = \sqrt{V_0}$, then (8.56) implies

$$\dot{\widetilde{V}} \leq -\frac{\mu_0}{2\lambda_{max}(P_0)} \widetilde{V} + \frac{1 - \mu_0}{2\sqrt{\lambda_{max}(P_0)}} \|\hat{x}\| \tag{8.57}$$

which for notational convenience can also be further written as

$$\dot{\widetilde{V}} \leq -m_0 \widetilde{V} + m_1 \|\hat{x}\| \tag{8.58}$$

where the positive scalars m_0, and m_1 are appropriately defined. Comparing (8.58) and (8.52) if $\varepsilon(0) > \tilde{V}(0)$, then it can be shown that $\varepsilon(t) > \tilde{V}(t)$ and consequently

$$\varepsilon(t) \geq \sqrt{\lambda_{min}(P_0)} \|e(t)\| \quad \text{for} \quad t \geq 0 \tag{8.59}$$

Now it will be shown that the control law defined in (8.49) satisfies the standard reachability condition.

Using the relationship $K = I - W$, equation (8.17) can be written as

$$\begin{aligned}\dot{\sigma}(t) &= GC(A+A^{\delta})x(t)+(B_2WB_2^T)\nu(t)+F\hat{x}(t)\\ &= GC(A+A^{\delta})x(t)+\nu(t)-(I-B_2WB_2^T)\nu(t)+F\hat{x}(t)\\ &= GC(A+A^{\delta})x(t)+\nu(t)-(B_2(I-W)B_2^T)\nu(t)+F\hat{x}(t)\\ &= GC(A+A^{\delta})x(t)+\nu(t)-B_2KB_2^T\nu(t)+F\hat{x}(t)\end{aligned} \tag{8.60}$$

Substituting the control law (8.49)-(8.51), into equation (8.60) and exploiting the fact that $e(t) = x(t) - \hat{x}(t)$ yields

$$\dot{\sigma}(t) \quad = \quad GCA^{\delta}\hat{x}(t) + GCA^{\delta}e(t) + GCAe(t) - (B_2KB_2^T)(\nu_l + \nu_n) - \rho\frac{\sigma(t)}{\|\sigma(t)\|}$$

Now consider the time derivative of the candidate Lyapunov function $V = \frac{1}{2}\sigma^T\sigma$. From (8.61) the time derivative

$$\begin{aligned}\dot{V} &= \sigma^T\big(GCA^{\delta}\hat{x}(t) + GCA^{\delta}e(t) + GCAe(t) - (B_2KB_2^T)(\nu_l+\nu_n) - \rho\frac{\sigma(t)}{\|\sigma(t)\|}\big)\\ &\leq \|\sigma\|\big(\|GCA^{\delta}\|\|\hat{x}\| + (\|GCA^{\delta}\|+\|GCA\|)\|e\| + \|B_2KB_2^T\|\|\nu_l\| - \rho(1-\|B_2KB_2^T\|)\big)\\ &\leq \|\sigma\|\big(\|GCA^{\delta}\|\|\hat{x}\| + (\|GCA^{\delta}\|+\|GCA\|)\|e\| + \|B_2KB_2^T\|\|\nu_l\| - \rho(1-\lambda_0)\big)\end{aligned} \tag{8.61}$$

for a fault set $(k_1,\ldots k_m) \in \mathscr{D}$. Then from the definition of $\rho(t)$ in (8.54) and using the fact that $\varepsilon(t) \geq \sqrt{\lambda_{min}(P_0)}\|e(t)\|$, the inequality (8.61) can be written as

$$\dot{V} \leq -\eta\|\sigma\| = -\eta\sqrt{2V} \tag{8.62}$$

which is a standard reachability condition and sufficient to guarantee that a sliding motion is maintained for all subsequent time. ■

Finally the physical control law $u(t)$ is obtained by substituting equations (8.49)-(8.51) into (8.5) to obtain

$$u(t) = B_2^T(-F\hat{x}(t) - GCA\hat{x}(t) - \rho\frac{\sigma(t)}{\|\sigma(t)\|}) \qquad \text{for } \sigma(t) \neq 0 \tag{8.63}$$

8.4 Simulations

The civil aircraft benchmark model as discussed in Appendix A.1 will be used in simulations to demonstrate the effectiveness, and fault tolerant nature of the proposed scheme. The simulation scenario which is considered in this section is that the aircraft undergoes actuator fault or failure during the climb from a straight and level flight. This scenario can be realized by tracking a suitable flight path angle (FPA) while keeping the speed at a constant level. To design the linear component of the controller in (8.50), the flight operating condition considered here is the same as in Chapter 4 and Chapter 5. The linearized state space model is given in Chapter 5 and is reproduced here as

$$A_p = \begin{bmatrix} -0.5137 & 0.0004 & -0.5831 & 0 \\ 0 & -0.0166 & 1.7171 & -9.8046 \\ 1.0064 & -0.0021 & -0.6284 & 0 \\ 1 & 0 & 0 & 0 \end{bmatrix} \quad B_p = \begin{bmatrix} -0.6228 & -1.3578 & 0.0599 \\ 0 & -0.1756 & 5.7071 \\ -0.0352 & -0.0819 & -0.0085 \\ 0 & 0 & 0 \end{bmatrix}$$

The system states are $x(t) = (q, V_{tas}, \alpha, \theta)^T$ where q is the pitch rate (rad/sec), V_{tas} is the true airspeed (m/sec), α is the angle of attack (rad) and θ is the pitch angle (rad). In the simulations, only measured system outputs

$$y = \underbrace{\begin{bmatrix} 1 & 0 & 0 & 0 \\ 0 & 1 & 0 & 0 \\ 0 & 0 & 0 & 1 \end{bmatrix}}_{C_p} \begin{bmatrix} q \\ V_{tas} \\ \alpha \\ \theta \end{bmatrix}$$

are available for use in the control law. The available control surfaces are $\delta_{long} = [\delta_e, \delta_s, \delta_{epr}]^T$ which represent elevator deflection (rad), horizontal stabilizer deflection (rad) and aggregated longitudinal EPR (i.e. the four individual engine pressure ratios (EPRs) aggregated to produce one control input). In the simulations a series of 3-deg flight path angle (FPA) commands are given to increase the altitude of the aircraft, while the true airspeed V_{tas} is held constant by using a separate inner-loop Proportional Integral (PI) controller which creates an auto-throttle manipulating EPR. Throughout the simulations *it is assumed that the engines are fault free*. By splitting the input distribution matrix into matrices which are associated

with $[\delta_e, \delta_s]^T$ and δ_{epr}, the linear model can be written as

$$\dot{x}_p(t) = A_p x(t) + B_s u_1 + B_e \delta_{epr} \tag{8.64}$$

$$y = C_p x(t) \tag{8.65}$$

where $u_1 = [\delta_e, \delta_s]^T$ and matrices $B_s \in \mathbb{R}^{4\times 2}$ and $B_e \in \mathbb{R}^{4\times 1}$. Define a new state associated with the PI controller for V_{tas} as

$$\dot{x}_r(t) = r_1(t) - C_1 x_p(t) \tag{8.66}$$

where $r_1(t)$ is the reference signal for V_{tas} tracking and $C_1 = \begin{bmatrix} 0 & 1 & 0 & 0 \end{bmatrix}$. The inner loop PI control is given by

$$\delta_{epr} = K_p(r_1(t) - C_1 x(t)) + K_i x_r(t)$$

where the PI gains are chosen as $K_p = 0.6$, and $K_i = 0.9$. Now augmenting the plant in (8.64) with $x_r(t)$ yields

$$\begin{bmatrix} \dot{x}_r \\ \dot{x}_p \end{bmatrix} = \underbrace{\begin{bmatrix} 0 & -C_1 \\ B_e K_i & (A_p - B_e K_p C_1) \end{bmatrix}}_{A} \underbrace{\begin{bmatrix} x_r \\ x_p \end{bmatrix}}_{x(t)} + \underbrace{\begin{bmatrix} 0 \\ B_s \end{bmatrix}}_{B} u_1 + \underbrace{\begin{bmatrix} I \\ B_e K_p \end{bmatrix}}_{B_r} r_1 \tag{8.67}$$

Also it is assumed that $x_r(t)$ is available for the controller design, therefore $y = Cx(t)$ where $C = \text{diag}\{1, C_p\}$. In order to introduce the steady state tracking for the controlled output $y_c(t)$, a feedforward term $L_r r_2(t)$ is introduced where

$$L_r := (C_c(A - B_v F - B_v GCA)^{-1} B_v)^{-1} \tag{8.68}$$

and the exogenous constant signal r_2 is the reference to be tracked (by the FPA). From Assumption 1, F can always be chosen to ensure that $(A - B_v F - B_v GCA)$ is Hurwitz and therefore $\det(A - B_v F - B_v GCA) \neq 0$. Consequently the inverse in (8.68) is well defined. In the absence of faults and uncertainty it is easy to see the linear control law $u(t) = -F\hat{x}(t) + L_r r_2 - GCA\hat{x}$ ensures that at steady state $y_c = r_2$. To accommodate this tracking requirement, the control law in (8.63) must be changed to

$$u(t) = B_2^T(-F\hat{x}(t) + L_r r_2(t) - GCA\hat{x}(t) - \rho \frac{\sigma(t)}{\|\sigma(t)\|}) \qquad \text{for } \sigma(t) \neq 0 \tag{8.69}$$

and

$$\sigma(t) = Gy(t) - Gy(0) + \int_0^t (F\hat{x}(\tau) - L_r r_2(\tau))d\tau \tag{8.70}$$

The fault tolerant control will now be designed based on the system in (8.67) governed by the triple (A,B,C) using only the elevator and stabilizer as inputs. A further scaling of the B is required to ensure that $B_2B_2^T = I_l$ (where in this example $l = 1$). It can be verified that $rank(CB) = rank(B) = 2$, and therefore Assumption $A2$ holds. In this aircraft system (A,B,C) has one stable invariant zero. Since the objective is to track an FPA command, the controlled output is $y_c(t) = C_c x(t)$, where $C_c = \begin{bmatrix} 0 & 0 & 0 & -1 & 1 \end{bmatrix}$. The gain G in equation (8.16) is $G = \begin{bmatrix} 0 & 0.6694 & 0 & 0 \end{bmatrix}$. In addition to actuator faults or failures, to introduce potential faults which cause changes to the aerodynamics of the aircraft, a 10% change in the aerodynamic coefficients (due to airframe damage) is considered in the simulation specifically:

$$A^\delta = \begin{bmatrix} 0 & 0 & 0 & 0 & 0 \\ 0 & 0.0514 & 0 & 0.0583 & 0 \\ 0 & 0 & 0.0017 & 0 & 0 \\ 0 & 0.1006 & 0 & 0.0628 & 0 \\ 0 & 0 & 0 & 0 & 0 \end{bmatrix}$$

Choosing

$$E = \begin{bmatrix} -12.4139 & -1.6056 & 12.4139 & -1.6056 \\ 5.6942 & 0 & -5.6942 & 0 \end{bmatrix}$$

gives $ECB = I$, and (A_h, B, EC) is minimum phase with stable zeros at $\{-1.0000, -0.6451, -1.0000\}$. The corresponding value of the observer gain L_1 is

$$BE = \begin{bmatrix} 0 & 0 & 0 & 0 \\ 0 & 1 & 0 & 1 \\ -1 & 0 & 1 & 0 \\ -0.0290 & 0.0566 & 0.0290 & 0.0566 \\ 0 & 0 & 0 & 0 \end{bmatrix}$$

and $A_0 = (A_h - \beta BEC)$ is then stable for any $\beta > 0$. Choosing $Q = \text{diag}(0.02, 0.5, 0.2, 0.1, 10)$ and $R = 1$ in (8.47) the feedback gain matrix F, obtained by solving the LMIs (8.42), (8.47), (8.48) is given by

$$F = \begin{bmatrix} -0.8142 & 9.9401 & -2.2095 & -0.3356 & 8.8802 \end{bmatrix}$$

In the simulations, it is assumed that the engines are fault free. Based on this assumption, using a numerical search, it can be verified using (8.28) that the value of γ_a in (8.36) is $\gamma_a = 0.1597$. To satisfy the closed-loop stability condition in (8.39), the value of γ_2 must satisfy $\gamma_2 < \frac{1}{0.1597} = 6.2621$. This has been satisfied through the designed parameters L_1 and F.

8.4.1 Simulation Results

In this section the performance of the benchmark civil aircraft model is demonstrated by considering the potential failures in the actuators. In the simulations, the discontinuity associated with the control signal in (8.51), is smoothed using a fractional approximation $\frac{\sigma}{\|\sigma\|+\delta}$, where the value of the positive scalar δ is chosen as $\delta = 0.01$. The value of the modulation gain is chosen here as $\rho = 2$. In the simulations the aircraft undergoes a series of 3-deg FPA commands issued in two intervals between (25-50 sec) and between (100-125 sec) in order to increase the altitude of the aircraft, while the true airspeed V_{tas} is kept constant as shown in Figure 8.1. The initial conditions for the plant and observer are taken as $x_0 = [0,0,0,0]^T$, and $x_{0_{obs}} = [0,0,0,0,0.5(\pi/180)]^T$ respectively.

8.4.1.1 Nominal Vs perturbed system matrix

In Figures 8.1-8.2 good tracking performance of the commanded signals is achieved nominally and while perturbing matrix A with A^δ matrix (a 10% change in the aerodynamic coefficients (due to possible airframe damage). The system states and the actuator deflections in both cases are almost overlapping, which shown the robustness of the proposed scheme against the parameter variations.

8.4.1.2 Elevator Lock in place/jam failure

In Figure 8.4 a failure is considered, where the elevator jams at some offset position. To maintain the performance close to the nominal, the proposed FTC scheme invokes the horizontal stabilizer to counter-

act the failure, while maintaining the sliding motion throughout the entire system response (Figure 8.5). There is no performance degradation while comparing the nominal performance (Figure 8.1) with the performance while in the failure (Figure 8.4). In Figure 8.3, it can be seen that the observer output error quickly converges to zero despite the failure scenario.

8.4.1.3 Horizontal stabilizer Hardover/runaway failure

Figure 8.7 demonstrate the situation when the horizontal stabilizer runs-away to a maximum position limit of 3-deg. Due to the availability of the redundant actuator (i.e. elevator) the proposed scheme can still maintain good tracking performance close to nominal as seen in Figure 8.6. The observer output error does not influence with the failure and converges to zero quickly.

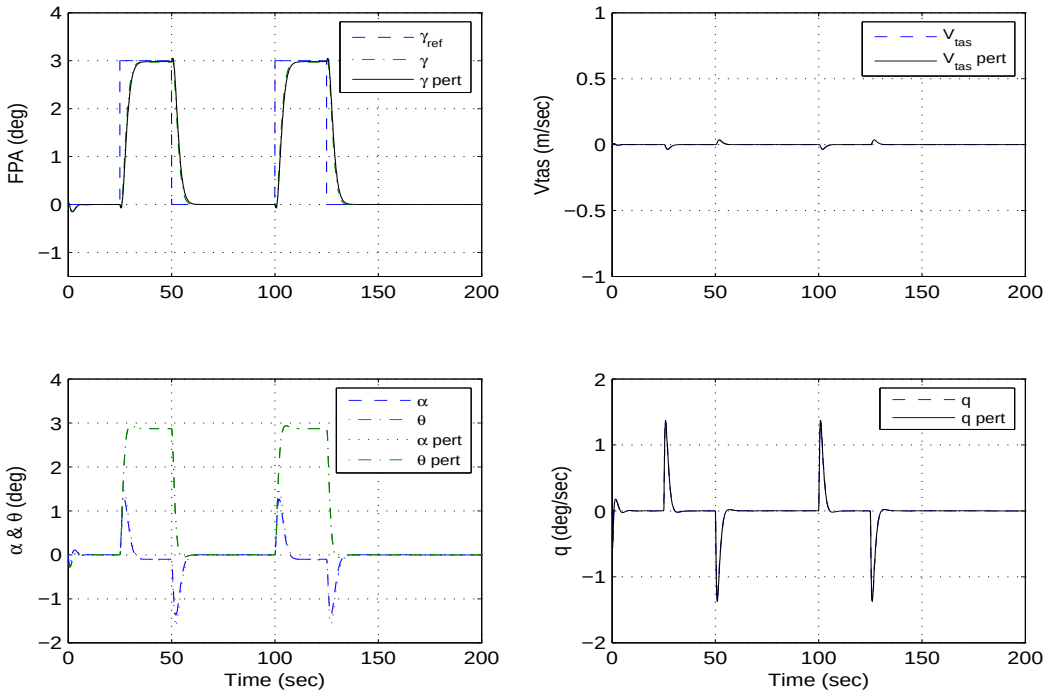

Figure 8.1: No fault Vs perturbation in *A* matrix: states

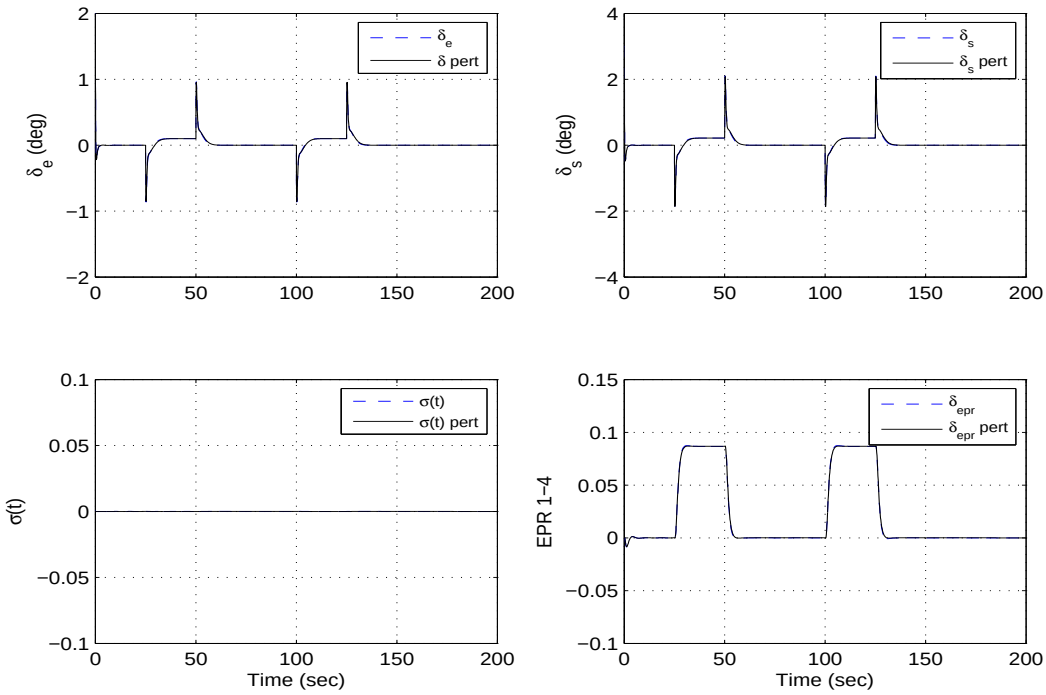

Figure 8.2: No fault Vs perturbation in *A* matrix: surface deflections

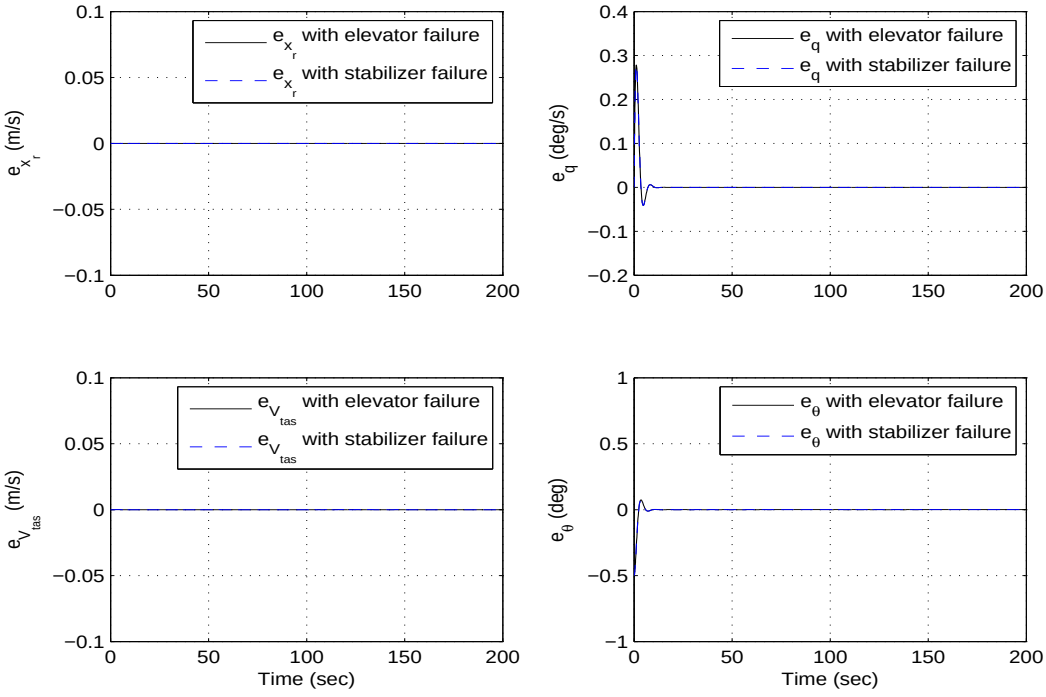

Figure 8.3: State estimation error signals (elevator jam and stabilizer runaway)

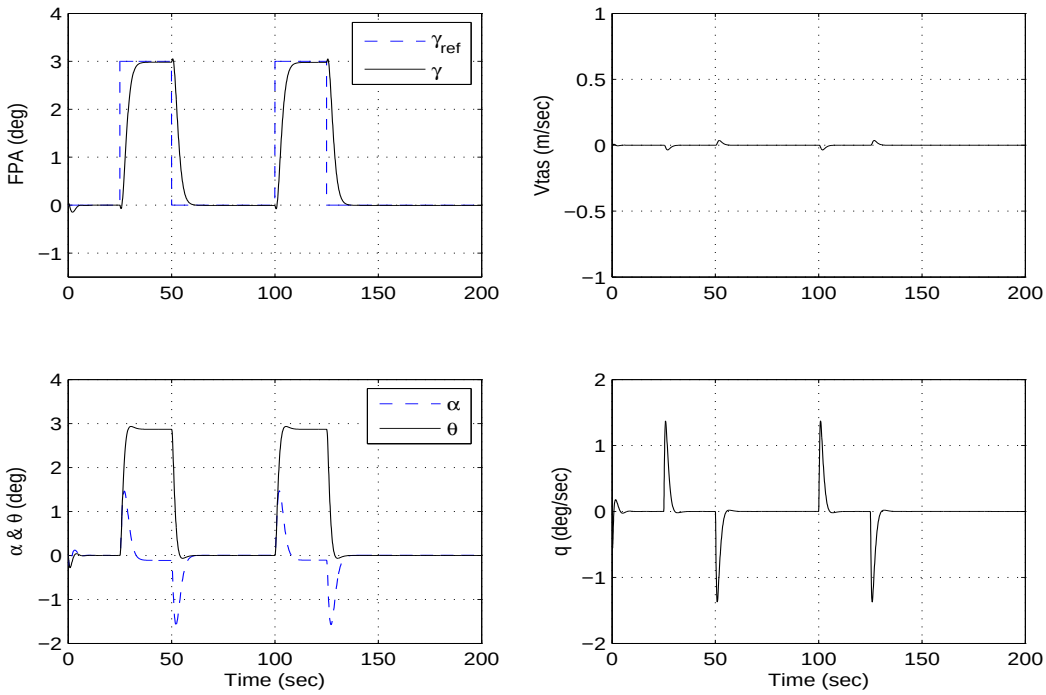

Figure 8.4: elevator Lock in place/jam failure: states

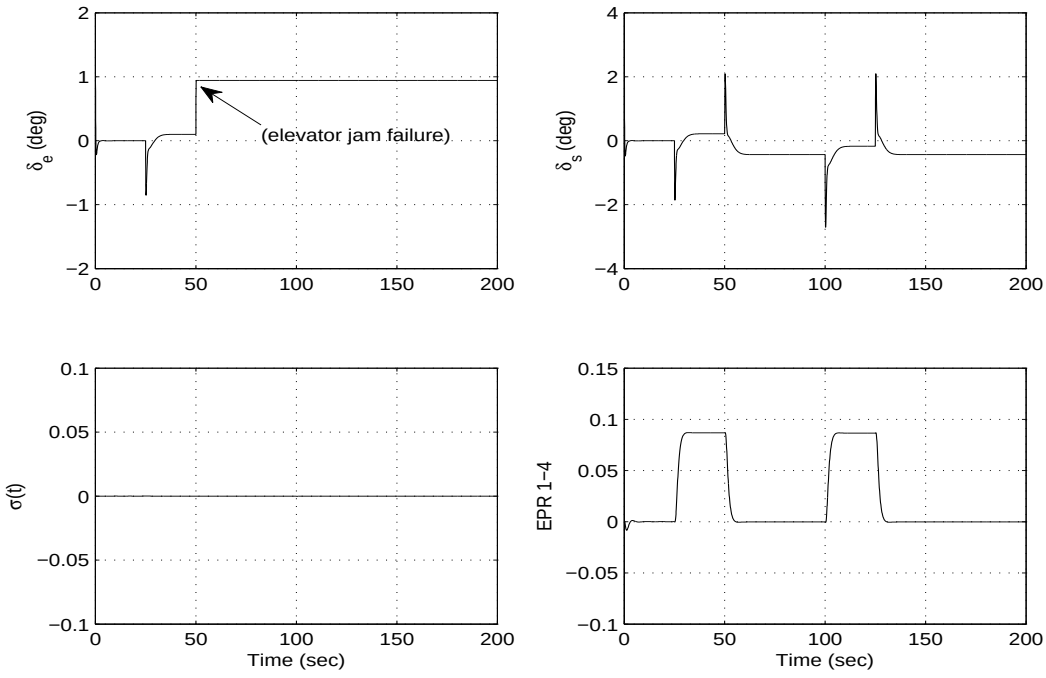

Figure 8.5: elevator Lock in place/jam failure: surface deflections

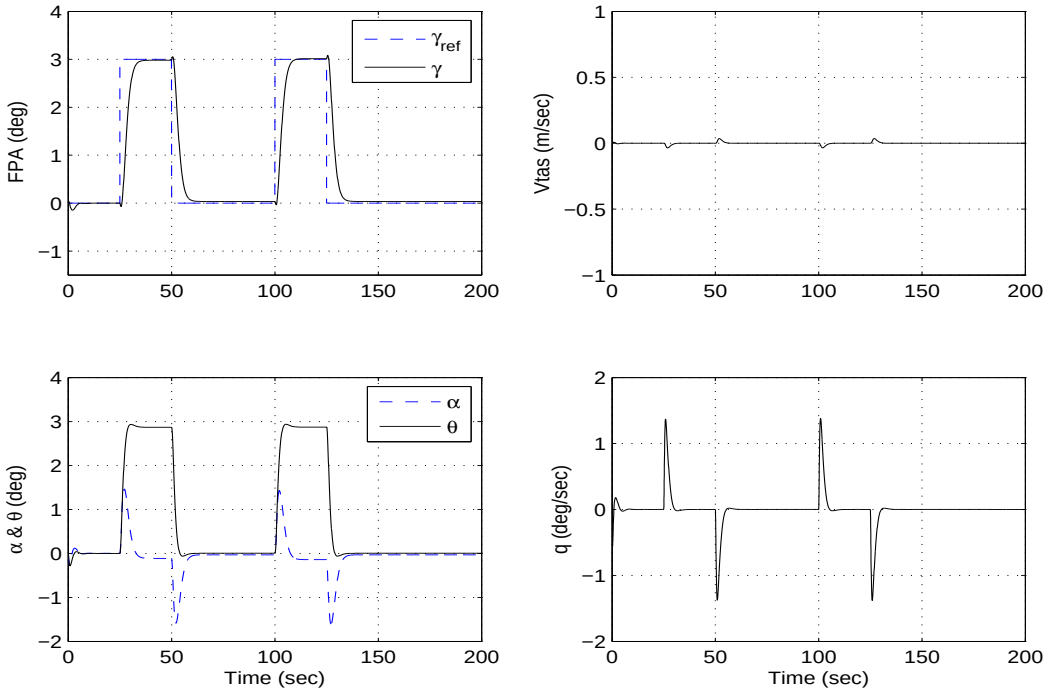

Figure 8.6: stabilizer runaway failure: states

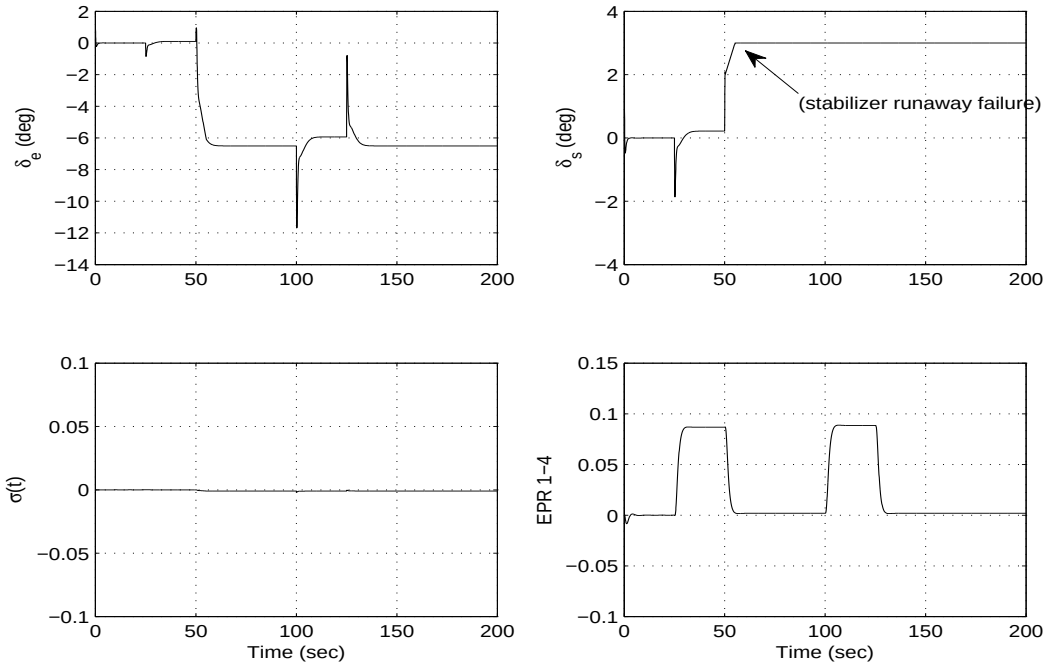

Figure 8.7: stabilizer runaway failure:surface deflections

8.5 Conclusion

In this Chapter, a new fault tolerant control scheme was proposed which assumes only output information is available and no information about the actuator faults or failures is available. To estimate the system states, a linear unknown input observer is employed. The estimated states are used in the virtual control law to produce signals which are then translated into the physical control signals (associated with the actuators) by using a fixed control allocation scheme. The closed-loop stability analysis allows for parameter uncertainty in the system matrix (due to airframe damage for example) in addition to actuator faults/failures. A convex representation of the synthesis problem is established in order to prove closed-loop stability by synthesizing appropriate observer and controller gains. The simulation results on a benchmark aircraft model show fast convergence of the observer output error, and demonstrate good FTC features of the proposed scheme.

Chapter 9

Conclusions and Future work

This Chapter makes some concluding remarks and then ideas for the extension of this research work will be suggested.

9.1 Conclusions

The summary of the thesis is explained as follow: Chapter 4, considers the novel combination of integral sliding mode ideas and control allocation in the framework of FTC to address the issues discussed in Section 3.9: namely that sliding mode schemes cannot directly handle complete actuator failures. This unique combination allows redundant actuators to deal with actuator faults or failures by enforcing a sliding mode during the entire system response without the need to reconfigure the underlying control law. The fault tolerant control scheme uses actuators effectiveness levels provided by a FDI scheme to redistribute the control effort among the healthy actuators. The FTC scheme allows the nominal performance of the system to be considered in the design of the switching function and maintains the performance close to the nominal provided healthy actuators are available. Due to possible uncertainty in estimating the actual actuators effectiveness levels, a bound on the estimation error (i.e. the maximum estimation error which can be coped with) is considered in the rigorous closed-loop stability analysis and an LMI optimization synthesis procedure is employed to compute the parameters associated with the control law such that the closed-loop stability condition is met. The ideas in Chapter 4 are then applied and tested in Chapter 5 on the nonlinear benchmark model, controlling both the longitudinal and the lateral axis

system of the aircraft.

Chapter 6 considers a novel FTC scheme which consider an *a posteri* approach building on an existing state feedback controller designed using only the primary actuators. This approach is quite interesting from an industry viewpoint because it can be retrofitted to almost any existing state feedback control scheme to induce fault tolerance without the need to remove or alter existing control loops. More specifically in the fault free case, the augmented FTC scheme behaves exactly as the existing feedback controller specified using any design paradigm. The FTC scheme uses the estimated effectiveness level of the actuators to distribute the control signals. In fault or failure cases in the primary actuators, the FTC scheme activates the secondary actuators to maintain nominal performance. As in Chapter 4 a rigorous closed-loop stability analysis is carried out in the case of faults or failures, taking into account a bound on error estimation . The integral sliding mode FTC scheme is tested by applying it on the nonlinear benchmark model FTLAB747 software environment where the actuator saturation and rate limits are already embedded by considering severe and even multiple failures on the primary actuators.

Chapter 7 considers a novel fault tolerant control scheme incorporating the ideas of integral sliding modes and control allocation for linear parameter varying systems. This is appealing for nonlinear systems which can be modelled as time varying systems with state dependent parameters. The linear parameter varying FTC scheme allows investigation of the behaviour of the system in the entire operating regime. A single control law is used in the entire operating envelope and the controller automatically schedules according to the varying parameters to maintain the closed-loop stability. The FTC scheme has the potential to mitigate the effects of actuator faults or failures. This was demonstrated by applying it to the benchmark linear parameter varying model of the large civil aircraft. The LMI synthesis procedure is adopted from Chapter 4 and is extended for the polytopic system representation to obtain the controller parameters which satisfy the stability condition.

Chapter 8 considers an FTC scheme for systems where only the measured plant outputs are available and furthermore assumes that information about the actuator faults or failures is not available. To be able to employ the LMI synthesis procedure proposed in Chapter 4, and to address the situation that information about the actuator faults or failures is unknown to the controller, an unknown input observer from the literature is employed to estimate the plant states. To deal with complete loss of actuator effectiveness a direct control allocation scheme, which is quite different form the control allocation schemes proposed

in early Chapters (which require information of actuator effectiveness), is integrated with integral sliding modes. The controller and the observer gains are synthesized by using an LMI synthesis procedure to satisfy the closed-loop stability condition. The efficacy of the output feedback FTC scheme is tested on a benchmark civil aircraft model where the component faults (possible airframe damage) are also considered together with actuator faults or failures. This scheme highlights the fact that the combination of integral sliding modes and direct control allocation can handle the actuator faults or failures without an FDI scheme.

9.2 Future Work

The integral sliding mode FTC schemes proposed in this thesis have only explored how to mitigate the effects of actuator faults or failures. A potential extension of this research work is to look at the option of using integral sliding modes to explore the effects of faults at the sensor level.

The scheme proposed in Chapter 7 extends the ideas of Chapter 4 to linear parameter varying plants. In Chapter 7, the theory developed suggests a controller which is automatically scheduled with the varying parameters, but in the simulations, for simplicity, a fixed state feedback controller is designed for the entire flight envelope using the multi-model state feedback LMI synthesis Toolbox. A fixed state feedback controller for the whole operating envelope may be bit conservative. The next step is to design the controller, using the LMI synthesis procedure proposed in Chapter 7, and the performance can be compared with the fixed design using the LMI synthesis Toolbox. Another direction can be to extend the augmentation FTC scheme in Chapter 6 for linear parameter varying systems.

In Chapter 8 parametric uncertainty is considered in the system matrix arising from imprecisely known parameters and possible faults at a component level, in addition to actuator faults or failures in the output feedback framework. Component faults may also introduce changes to other matrices from the system state space model. A potential extension of the approach in Chapter 8 will be to consider uncertainty in the input distribution matrix, and to investigate the effect of this uncertainty.

List of Publications

Journal Publications

1. M.T. Hamayun, C. Edwards and H. Alwi. Design and Analysis of an Integral Sliding Mode Fault Tolerant Control Scheme. *In IEEE Transactions on Automatic Control* volume 57, number 7, pages 1783-1789 July 2012.

2. M.T. Hamayun, C. Edwards and H. Alwi. An Augmentation Scheme for Fault Tolerant Control using Integral Sliding Modes. *In IEEE Transactions on Control System Technology*, volume pp, issue 99, pages 1-7, 2013.

3. M.T. Hamayun, C. Edwards and H. Alwi. An Output Integral Sliding Mode FTC Scheme Using Control Allocation. *In Automatica Journal of Elsevier*, volume 49, Issue 6, pages 1830-1837, 2013.

Conference Publications

1. M.T. Hamayun, C. Edwards and H. Alwi. Integral sliding mode fault tolerant control incorporating on-line control allocation. *In IEEE International Workshop on Variable Structure Systems*, pages 100-105, Mexico City, Mexico, June 2010.

2. M.T. Hamayun, C. Edwards and H. Alwi. Application of an integral sliding mode FTC for a large transport aircraft. *In IEEE SysTol conference*, pages 38-43, Nice, October 2010.

3. M.T. Hamayun, C. Edwards and H. Alwi. Fault tolerant longitudinal-axis control of a civil aircraft using control allocation. In Proceedings of IBCAST, pages 165-172, Islamabad, January, 2011.

4. M.T. Hamayun, C. Edwards and H. Alwi. An Integral sliding Mode Augmentation Scheme for Fault Tolerant Control. *In IEEE American Control Conference*, pages 3772-3777, San Francisco USA, June 2011.

5. H. Alwi, C. Edwards and M.T. Hamayun. Nonlinear Integral Sliding Mode Fault Tolerant Longitudinal Aircraft Control. *In IEEE MSC*, pages 970-975, Denver USA, September 2011.

6. M.T. Hamayun, H. Alwi and C. Edwards. An Output Integral Sliding Mode FTC Scheme Using Control Allocation. *In 50th IEEE CDC and ECC*, pages 2275-2280, Orlando USA, December 2011.

7. M.T. Hamayun, H. Alwi and C. Edwards. An LPV Fault Tolerant Control Scheme using Integral Sliding Modes. *accepted for publication in 51st IEEE Conference on Decision and Control*, Hawaii USA, 2012.

Appendix A

Benchmark model of Large Transport Aircraft

A.1 Benchmark model FTLAB747 v6.5/v7.1 Release 2.2

FTLAB 747 V6.5/7.1 software environment runs under Matlab/Simulink and was used as the basis for the Group for Aeronautical Research and Technology in Europe Action Group (GARTEUR AG16) benchmark [39]. The purpose of the project AG-16 was to develop new and cutting edge FTC and FDI techniques in Europe for the application to a civil aircraft. This software is an upgraded version of the Delft University Aircraft Simulation and Analysis Tool, DASMAT, and Flight lab 747 FTLAB747 [86]. This high-fidelity nonlinear model contains 77 states and represents a 'real world' model of a B747-100/200 aircraft. The model incorporates realistic actuators, sensors and aero-engine dynamics, where all the control surfaces are modeled using the realistic position and rate limits. The upgraded version FTLAB 747 V6.5/7.1 [109], provides the flexibility to be employed to manipulate the control surfaces independently, which is beneficial to apply FTC schemes in case of faults or failures. The rigid body states of the B747-100/200 aircraft for the longitudinal, lateral and directional axis are

$$x(t) = \{p, q, r, V_{tas}, \alpha, \beta, \phi, \theta, \psi, h_e, x_e, y_e\}^T \tag{A.1}$$

which are determined from the 6-DOF equations. In equation A.1 the states for the longitudinal axis (Figure A.1) are $x_{long} = \{q, V_{tas}, \alpha, \theta, h_e\}^T$, which represent pitch rate q (rad/sec), true air speed V_{tas} (m/sec), angle of attack α (rad), pitch angle θ (rad) and altitude h_e (m). On the other hand the states for the lateral and directional axis (Figures A.2-A.3) are $x_{lat} = \{p, r, \beta, \phi, \psi\}^T$, which represent roll rate p (rad/sec), yaw rate r (rad/sec), sideslip β (rad), roll angle ϕ (rad) and yaw angle ψ (rad). In equation (A.1), the states h_e, x_e, y_e represent the geometric earth position, along the z-axis, x-axis and y-axis respectively.

The typical control surfaces for the longitudinal and lateral axis control are shown in Figure A.4. The

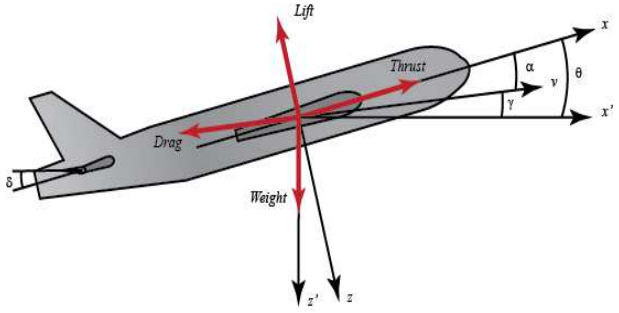

Figure A.1: Longitudinal axis states

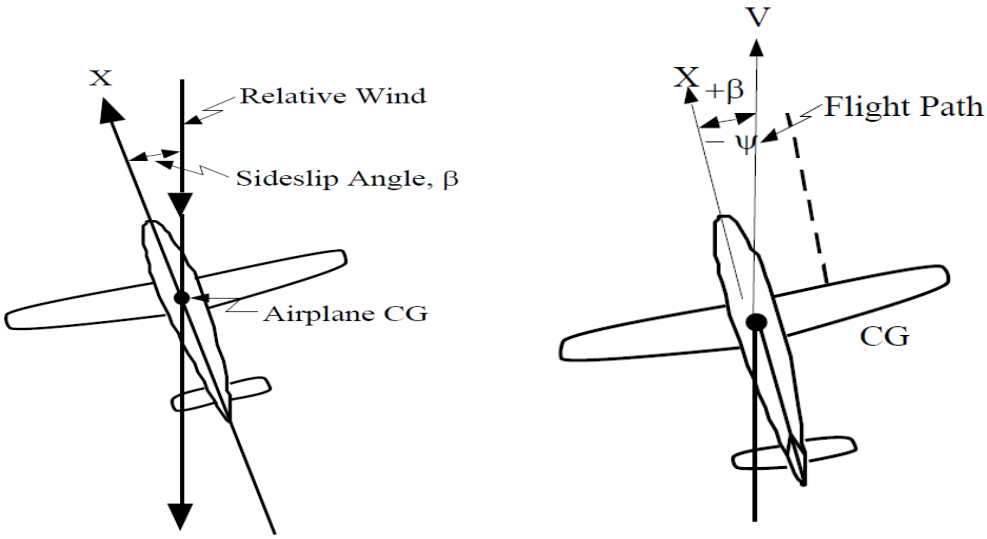

Figure A.2: sideslip and yaw angle (Lateral-Directional Flying Qualities, vmihosting.com)

control surfaces which are typically used for the longitudinal axis control comprise 4 elevators (inner and outer on each elevator), a horizontal stabilizer, 4 engines (two on each wing) thrust, which can be controlled through Engine Pressure Ratio (EPR). For lateral axis control 4 ailerons (inner and outer on

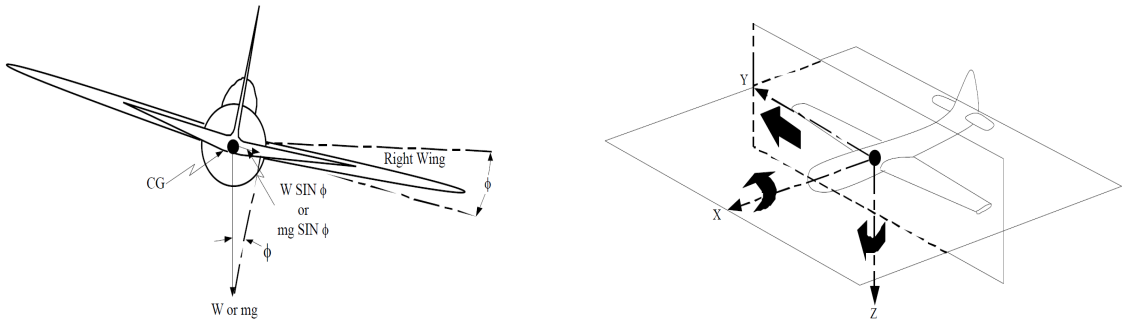

Figure A.3: roll angle and aircraft axis (Lateral-Directional Flying Qualities, vmihosting.com)

each wing), 12 spoilers (2 inner and 4 outer spoilers on each wing), 2 rudders (upper and lower), and 4 engine thrust (controlled through EPR) are used. For designing the linear part of the control law, the

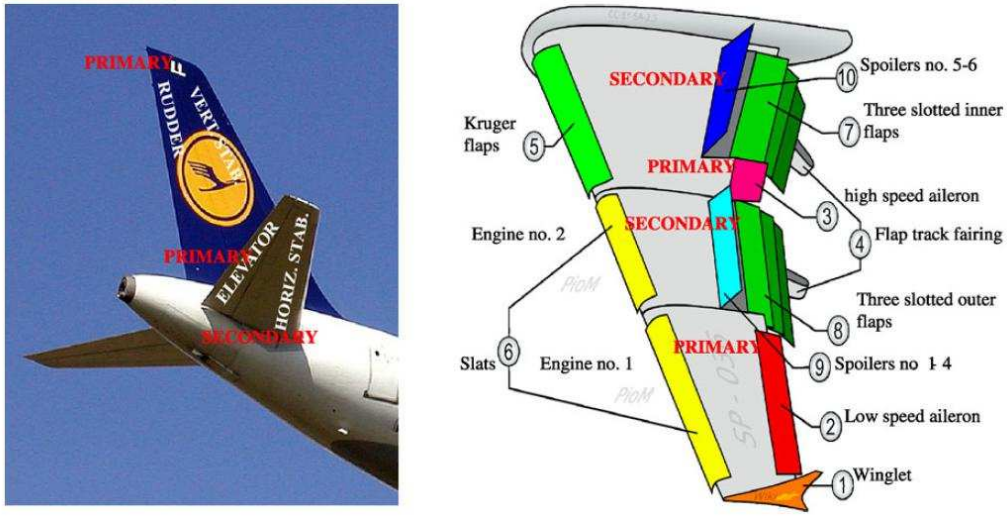

Figure A.4: Primary and secondary control surfaces of a transport aircraft (adopted from [7])

linear state space model of the benchmark nonlinear model can be obtained at the trim point using the FTLAB software. At the trim point, aircraft is in the steady state i.e. straight and level flight. In this thesis longitudinal and lateral axis of the benchmark model at different trim conditions are considered to design the FTC schemes. For example in chapters 4 and 8 the simulations are based around an operating condition of straight and level flight at 263,000 Kg, 92.6 m/s true airspeed, and at an altitude of 600m based on 25.6% of maximum thrust and at a 20 deg flap position. The result is of 12 order linear model, which can be divided into two six order models for longitudinal and lateral axis control. The first four states $x_{long} = \{q, V_{tas}, \alpha, \theta\}^T$ and $x_{lat} = \{p, r, \beta, \phi\}^T$ are used for the controller design. At this trim

condition the state space matrices are:

$$A_{long} = \begin{bmatrix} -0.5137 & 0.0004 & -0.5831 & 0 \\ 0 & -0.0166 & 1.7171 & -9.8046 \\ 1.0064 & -0.0021 & -0.6284 & 0 \\ 1.0000 & 0 & 0 & 0 \end{bmatrix} \tag{A.2}$$

$$B_{long} = \begin{bmatrix} -0.6228 & -1.3578 & 0.0082 & 0.0218 & 0.0218 & 0.0082 \\ 0 & -0.1756 & 1.4268 & 1.4268 & 1.4268 & 1.4268 \\ 0.0352 & -0.0819 & 0.0021 & -0.0021 & -0.0021 & -0.0021 \\ 0 & 0 & 0 & 0 & 0 & 0 \end{bmatrix} \tag{A.3}$$

$$A_{lat} = \begin{bmatrix} -1.0579 & 0.1718 & -1.6478 & 0.0004 \\ 0.1186 & -0.2066 & 0.2767 & -0.0019 \\ 0.1014 & -0.9887 & -0.0999 & 0.1055 \\ 1.0000 & 0.0893 & 0 & 0 \end{bmatrix} \tag{A.4}$$

$$B_{lat} = \begin{bmatrix} -0.0832 & 0.0832 & -0.2285 & 0.2285 & -0.2625 & -0.0678 & 0.0678 \\ -0.0154 & 0.0154 & -0.0123 & 0.0123 & -0.0180 & -0.0052 & 0.0052 \\ 0 & 0 & 0 & 0 & 0.0017 & 0.0006 & -0.0006 \\ 0 & 0 & 0 & 0 & 0 & 0 & 0 \end{bmatrix}$$
$$\begin{bmatrix} 0.2625 & 0.1187 & 0.0246 & 0.0140 & -0.0140 & -0.0246 \\ 0.0180 & -0.2478 & 0.1269 & 0.0724 & -0.0724 & -0.1269 \\ -0.0017 & 0.0174 & 0.0005 & 0.0005 & -0.0005 & -0.0005 \\ 0 & 0 & 0 & 0 & 0 & 0 \end{bmatrix} \tag{A.5}$$

where the control surfaces for the longitudinal axis control are

$$\delta_{long} = \{\delta_e, \delta_s, e1_{long}, e2_{long}, e3_{long}, e4_{long}\}^T$$

which represent elevator deflection (rad) (4 elevators are aggregated to produce one control input), horizontal stabilizer deflection (rad) and four longitudinal engines pressure ratios. For the lateral axis control the control surfaces comprise

$$\delta_{lat} = \{\delta_{air}, \delta_{ail}, \delta_{aor}, \delta_{aol}, sp_{1-4}, sp_5, sp_8, sp_{9-12}, \delta_r, e1_{lat}, e2_{lat}, e3_{lat}, e4_{lat}\}^T$$

which represent aileron inner (right and left) deflection (rad), aileron outer (right and left) deflection (rad), left wing spoilers deflections (rad) (sp_{1-4}, sp_5), right wing spoilers deflections (rad) (sp_8, sp_{9-12}), rudder deflection (rad) (upper and lower rudders are aggregated to produce one control input) and four lateral engine pressure ratios. The spoilers $sp-6, sp-7$ are ground spoilers and not used in the flight.

Further details of the B747-100/200 aircraft model can be found in [86], [39] and the references therein.

Appendix B

Closed loop stability and synthesis of feedback gain

B.1 $\mathscr{L}_2$ gain and small gain theorem

B.1.1 $\mathscr{L}_2$ gain

In case of LTI systems the $\mathscr{L}_2$ gain can be calculated exactly, and to find out the way to calculate it consider a LTI system

$$\begin{aligned} \dot{x}(t) &= Ax(t)+Bu(t) \\ y(t) &= Cx(t)+Du(t) \end{aligned}$$

where it is assumed that matrix A is *Hurwitz*. The above system can be written as $G(s)=C(sI-A)^{-1}B+D$, then according to Theorem 6.4 [75], the $\mathscr{L}_2$ gain of the system $G(s)$ is $\sup_{\omega\in\mathbb{R}}\|G(j\omega)\|_2$, which is induced 2-norm of the system $G(j\omega)$ and is equal to $\sigma_{max}[G(j\omega)]$. The $\mathscr{L}_2$ gain of the system in time domain is equal to the H_∞ norm in the frequency domain [75], which means if $Y(j\omega)=G(j\omega)U(j\omega)$, then in the proof of Theorem 6.4 [75] it is shown that

$$\|y\|_{\mathscr{L}_2}^2 \leq (\sup_{\omega\in\mathbb{R}}\|G(j\omega)\|_2)^2\|u\|_{\mathscr{L}_2}^2 \tag{B.1}$$

where $\|u\|^2_{\mathscr{L}_2} = \int_0^\infty u^T(t)u(t)dt$.

B.1.2 Small gain theorem

The small gain theorem is a systematic approach to investigate the input-output stability of interconnected dynamical systems [75]. To explain the small gain theorem, first the notion of finite gain $\mathscr{L}_2$ stable need

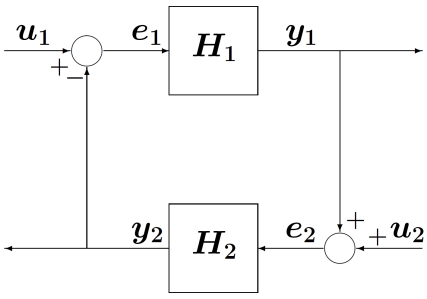

Figure B.1: Feedback interconnection of two systems (adopted from [75])

to be discussed. Suppose that e_1 is the input to a system H_1 and y_1 is the output, then the system H_1 will be finite gain $\mathscr{L}_2$ stable if $\|y_1\|_{\mathscr{L}_2} \leq \gamma_2\|e_1\|_{\mathscr{L}_2}$. Now consider the interconnection of two systems as shown in Figure B.1, then according to the small gain theorem [75], with the assumption that the two systems H_1 and H_2 are finite gain $\mathscr{L}_2$ stable, then the feedback connection will be finite gain $\mathscr{L}_2$ stable if

$$\gamma_2\gamma_1 < 1 \tag{B.2}$$

where γ_2 and γ_1 are the gains of the two systems. The proof of the small gain theorem can be found in [75].

B.2 Matlab LMI multi-model state feedback synthesis

The state feedback gain F for the augmented system in equation (7.44) is obtained by using the Matlab LMI multi-model state feedback synthesis code 'msfsyn' which performs mixed H_2/H_∞ criterion. To be

able to use that code the plant needs to be written in the generalized form as given in [49],

$$\dot{x}_a(t) = A_a(\rho)x_a(t) + B_d w + B_{v_a} v(t) \tag{B.3}$$

$$z_2(t) = C_2 x_a(t) + D_{22} v(t) \tag{B.4}$$

$$z_\infty(t) = C_1 x_a(t) + D_{11} w + D_{12} v(t) \tag{B.5}$$

The matrices $A_a(\rho) = A_{a_0} + \sum_{i=1}^{7} \rho_i A_{a_i}$ and B_{v_a} are given in equation (7.45) and w is the exogenous signal (disturbance). For the simulation example in chapter 7, the above mentioned plant can be written in the matrix form as:

$$P = \left[\begin{array}{c|cc} A_a(\rho) & B_d & B_{v_a} \\ \hline C_2 & D_{21} & D_{22} \\ C_1 & D_{11} & D_{12} \end{array}\right] = \left[\begin{array}{c|cc|c} A_a(\rho) & \widetilde{B} & 0 & B_{v_a} \\ \hline Q^{\frac{1}{2}} & 0 & 0 & 0 \\ 0 & 0 & 0 & R^{\frac{1}{2}} \\ \hline 0 & 0 & 0 & I \end{array}\right] \tag{B.6}$$

The formulation in equation (B.6) is taken from [108], where the matrix $\widetilde{B}$ is defined in equation (7.19) and Q and R are symmetric positive definite matrices. The parameter vector ρ is obtained using the relation $[\rho_1, ..., \rho_7] := [\overline{\alpha}, \overline{V}_{tas}, \overline{V}_{tas}\overline{\alpha}, \overline{V}_{tas}^2, \overline{V}_{tas}^2\overline{\alpha}, \overline{V}_{tas}^3, \overline{V}_{tas}^4]$ where each parameter of the vector has the minimum and the maximum extremal values i.e. $[\underline{\rho}_i, \overline{\rho}_i]$. After getting the range of each parameter the parameter dependent plant can be defined by using the command Matlab command 'psys'.

Here the objective is to obtain the desired H_2 performance objectives while maintaining the closed-loop transfer function w to z_∞ bellow some prescribed value of γ, therefore while using the 'msfsyn' command the optimization option $\left[\begin{array}{cccc} g & 0 & 0 & 1 \end{array}\right]$ is used where g is the value of γ. The details of the 'msfsyn' code can be obtained from [49].

B.3 LMI equivalence of closed-loop stability analysis

To satisfy the stability condition of *Theorem 1* in chapter 4, the closed-loop stability analysis is carried out in an LMI framework in order to find a feedback gain F such that the H_∞ norm of the transfer function $\tilde{G}(s) = F(sI - \tilde{A})^{-1}\tilde{B}$ is less than some predefined scalar γ i.e. $\|\tilde{G}(s)\|_\infty < \gamma$. Two constraints are imposed on the design of feedback gain F which need to be satisfied simultaneously. Firstly to achieve

the performance, an LQR formulation is used, and secondly, to ensure the design of an F to satisfy the stability condition of *Theorem 1*, a Bounded Real Lemma (BRL) formulation is used.

B.3.1 LMI Formulation of LQR

The design of the feedback gain F is based on the nominal system in (4.15). For the LMI formulation of the LQR problem, consider the LTI system

$$\dot{x}(t) = Ax(t) + B_v v(t) \tag{B.7}$$

$$z(t) = Q_1 x(t) + R_1 v(t) \tag{B.8}$$

where Q_1 and R_1 are symmetric positive definite matrices. The LQR problem seeks the control law $v(t) = -Fx(t)$ such that the output energy $\int_0^\infty z^T z$ is minimized. For the Lyapunov function $V(x) = x^T Px$ where $P > 0$ is a Lyapunov matrix, the output energy of z is minimal [21], if the performance index

$$J = \int_0^\infty (\dot{V}(\tau) + z^T z) d\tau \leq 0 \qquad \text{for all } x \text{ and } z \tag{B.9}$$

Taking the time derivative of function $V(x)$ and substituting value of (B.7) into it gives

$$\begin{aligned} \dot{V} &= x^T P(Ax + B_v v) + (Ax + B_v v)^T Px \\ &= x^T (PA + A^T P)x + x^T PB_v v + v^T B_v^T Px \end{aligned}$$

Substituting the value of $\dot{V}$, and (B.8) into (B.9) gives

$$\begin{aligned} J = \int_0^\infty & (x^T (PA + A^T P + Q_1^T Q_1)x + x^T PB_v v \\ & + v^T B_v^T Px + x^T Q_1^T R_1 v + v^T R_1^T Q_1 x + v^T R_1^T R_1 v) d\tau \end{aligned} \tag{B.10}$$

Since $v(t) = -Fx(t)$, (B.10) becomes

$$J = \int_0^\infty (x^T \underbrace{(PA + A^T P + Q_1^T Q_1 - PB_v F - F^T B_v^T P - Q_1^T R_1 F - F^T R_1^T Q_1 + F^T R_1^T R_1 F)}_{\overline{P}} x) d\tau \tag{B.11}$$

To fulfil the condition of (B.9), the matrix $\bar{P}$ should satisfy

$$PA + A^T P + Q_1^T Q_1 - PB_v F - F^T B_v^T P - Q_1^T R_1 F - F^T R_1^T Q_1 + F^T R_1^T R_1 F < 0 \tag{B.12}$$

Inequality (B.12), is clearly not convex [21], and cannot be written as an LMI representation. Define $X = P^{-1}$ then (B.12) is equivalent to

$$AX + XA^T + X^T Q_1^T Q_1 X - B_v F X - X^T F^T B_v^T - X^T Q_1^T R_1 F X - X^T F^T R_1^T Q_1 X + X^T F^T R_1^T R_1 F X < 0 \tag{B.13}$$

With change of variable $Y = FX$, where $Y \in \mathbb{R}^{l \times n}$, the inequality (B.13) can be written as

$$AX + XA^T + X^T Q_1^T Q_1 X - B_v Y - Y^T B_v^T - X^T Q_1^T R_1 Y - Y^T R_1^T Q_1 X + Y^T R_1^T R_1 Y < 0 \tag{B.14}$$

Finally using the Schur's complements [21], the inequality (B.14) can be written as

$$\begin{bmatrix} AX + XA^T - B_v Y - Y^T B_v^T & (Q_1 X - R_1 Y)^T \\ (Q_1 X - R_1 Y) & -I \end{bmatrix} < 0 \tag{B.15}$$

where the matrices X and Y are variables in the inequality (B.15), and the feedback gain F can be recovered as $F = YX^{-1}$. In (B.15), the matrices Q_1 and R_1 are:

$$Q_1 = \begin{bmatrix} Q^{\frac{1}{2}} \\ 0_{l \times n} \end{bmatrix} \qquad R_1 = \begin{bmatrix} 0_{n \times l} \\ R^{\frac{1}{2}} \end{bmatrix}$$

B.3.2 LMI Formulation of BRL

In chapter 4, the closed-loop stability of the sliding motion governed by

$$\dot{x}(t) = (A - B_v F + \tilde{B}\tilde{\Phi}(t)F)x(t) \tag{B.16}$$

which can be represented as

$$\dot{x}(t) = \underbrace{(A - B_v F)}_{\tilde{A}} x(t) + \tilde{B}\omega(t) \tag{B.17}$$

$$z(t) = Fx(t) \tag{B.18}$$

where $\omega(t) = \Phi(t)z(t)$. The $\mathscr{L}_2$ gain from ω to z (which in this case is the H_∞ norm of $\tilde{G}(s)$) is less than γ if there exists a Lyapunov function $V(x) = x^T P x$ where $P > 0$ and $\gamma \geq 0$ for all t [21] such that

$$J = \int_0^\infty (\dot{V}(\tau) + z^T z - \gamma^2 \omega^T \omega) d\tau \leq 0 \qquad \text{for all } x \text{ and } \omega \tag{B.19}$$

holds. Taking the time derivative of the function $V(x)$ and substituting value of (B.17) into it, gives

$$\begin{aligned} \dot{V} &= x^T P(A - B_v F)x + x^T P\tilde{B}\omega + x^T (A - B_v F)^T P x + \omega^T \tilde{B}^T P x \\ &= x^T (P(A - B_v F) + (A - B_v F)^T P)x + \omega^T \tilde{B}^T P x + x^T P\tilde{B}\omega \end{aligned}$$

Substituting $\dot{V}$ and (B.18) into (B.19) gives

$$\begin{aligned} J &= \int_0^\infty (x^T (P(A - B_v F) + (A - B_v F)^T P)x + \omega^T \tilde{B}^T P x + x^T P\tilde{B}\omega + x^T F^T F x - \gamma^2 \omega^T \omega) d\tau \\ &= \int_0^\infty (x^T (P(A - B_v F) + (A - B_v F)^T P + F^T F)x + \omega^T \tilde{B}^T P x + x^T P\tilde{B}\omega - \gamma^2 \omega^T \omega) d\tau \end{aligned}$$

where the function inside the integral can be written in the matrix representation as

$$\begin{bmatrix} x \\ \omega \end{bmatrix}^T \begin{bmatrix} P(A - B_v F) + (A - B_v F)^T P + F^T F & P\tilde{B} \\ \tilde{B}^T P & -\gamma^2 I \end{bmatrix} \begin{bmatrix} x \\ \omega \end{bmatrix}$$

To satisfy the condition in (B.19), it needs to be ensured that

$$\begin{bmatrix} P(A - B_v F) + (A - B_v F)^T P + F^T F & P\tilde{B} \\ \tilde{B}^T P & -\gamma^2 I \end{bmatrix} < 0 \tag{B.20}$$

which can also be written as

$$\begin{bmatrix} P(A-B_vF)+(A-B_vF)^TP & P\tilde{B} \\ \tilde{B}^TP & -\gamma^2 I \end{bmatrix} + \begin{bmatrix} F^T \\ 0 \end{bmatrix} \begin{bmatrix} F & 0 \end{bmatrix} < 0 \tag{B.21}$$

From Schur's complements [21], the system in (B.21) can be written as

$$\begin{bmatrix} P(A-B_vF)+(A-B_vF)^TP & P\tilde{B} & F^T \\ \tilde{B}^TP & -\gamma^2 I & 0 \\ F & 0 & -I \end{bmatrix} < 0 \tag{B.22}$$

From equation (B.22) it is clear that the expression in the top left position is not convex and cannot be written as an LMI representation, therefore multiplying both sides of (B.22) with diag$[P^{-1},I,I]$ gives

$$\begin{bmatrix} (A-B_vF)P^{-1}+P^{-1}(A-B_vF)^TP & \tilde{B} & P^{-1}F^T \\ \tilde{B}^T & -\gamma^2 I & 0 \\ FP^{-1} & 0 & -I \end{bmatrix} < 0 \tag{B.23}$$

Letting $P^{-1}=X$ the inequality in (B.23):

$$\begin{bmatrix} (A-B_vF)X+X(A-B_vF)^TP & \tilde{B} & XF^T \\ \tilde{B}^T & -\gamma^2 I & 0 \\ FX & 0 & -I \end{bmatrix} < 0 \tag{B.24}$$

Finally with the change of variable $Y=FX$, the inequality in (B.24) can be written as

$$\begin{bmatrix} AX+XA-B_vY-Y^TB_v^T & \tilde{B} & Y^T \\ \tilde{B}^T & -\gamma^2 I & 0 \\ Y & 0 & -I \end{bmatrix} < 0 \tag{B.25}$$

where the matrices X and Y are variables in the inequality (B.25). The inequality (B.25) is convex and available LMI tools can be used to find the feasible solution and F can be recovered using the relation $F=YX^{-1}$.

Bibliography

[1] *http://en.wikipedia.org/wiki/uninterruptible power supply*.

[2] J. Ackermann and V. Utkin. Sliding mode control design based on ackermann's formula. *IEEE Transactions on Automatic Control*, 43(2):234–237, 1998.

[3] H. Alwi. *Fault Tolearnt Sliding Mode Control Schemes with Aerospace Applications*. PhD thesis, 2008.

[4] H. Alwi and C. Edwards. Fault Tolerant Control of a Civil Aircraft using a Sliding mode based scheme. In *44th IEEE Conference on Decision and Control, and the European Control Conference*, pages 1011–1016, Seville, Spain, 2005.

[5] H. Alwi and C. Edwards. Sliding mode FTC with on–line control allocation. In *45th IEEE Conference on Decision and Control*, pages 775–795, San Diego, CA, 2006.

[6] H. Alwi and C. Edwards. Fault tolerant control using sliding modes with on-line control allocation. *Automatica*, (44):1859–1866, 2008.

[7] H. Alwi, C. Edwards, and C.P. Tan. *Fault Detection and Fault Tolerant Control using Sliding Modes. Advances in Industrial Control Series*. Springer Verlag, 2011.

[8] P. Apkarian, P. Gahinet, and G. Beck. Self-scheduled H_∞ control of linear parameter varying systems: a design example. *Automatica*, 31(9):1251–1261, 1995.

[9] J. Aravena, K. Zhou, X. Li, and F. Chowdhury. Fault tolerant safe flight controller bank. In *Proceedings of the IFAC Symposium SAFEPROCESS*, pages 807–812, Beijing, 2006.

[10] K. J. Aström and B. Wittenmark. *Adaptive Control*. Addison Wesley, second edition, 1995.

[11] I. Baik, K. Kim, and M. Youn. Robust nonlinear speed control of PM synchronous motor using boundary layer integral sliding mode control technique. *IEEE Transactions on Control Systems Technology*, 8(1):47–54, 2000.

[12] G. J. Balas. Linear parameter-varying control and its application to a turbofan engine. *International Journal of Robust and Nonlinear Control*, 12:763796, 2002.

[13] O. Barambones, A Garrido, and F. Maseda. Integral sliding-mode controller for induction motor based on field-oriented control theory. *IET Control Theory Applications*, 1(3):786–794, 2007.

[14] G. Bartolini, A. Ferrara, and E. Usai. Chattering avoidance by second order sliding mode control. *IEEE Transactions on Automatic Control*, 43(2):241–246, 1998.

[15] F.J. Bejarano, L. Fridman, and A. Poznyak. Output integral sliding mode control based on algebraic hierarchical observer. *International Journal of Control*, 80(3):443–453, 2007.

[16] M. Blanke, M. Kinnaert, J. Lunze, and M. Staroswiecki. *Diagnosis and Fault-Tolerant Control*. Springer-Verlag, 2003.

[17] J. D. Bošković and R.K. Mehra. A multiple model-based reconfigurable flight control system design. In *Proceedings of the 37th IEEE Conference on Decision and Control*, pages 4503–4508, Tampa, FL, 1998.

[18] J. D. Bošković and R.K. Mehra. Stable multiple model adaptive flight control for accommodation of a large class of control effector failures. In *Proceedings of the American Control Conference*, pages 1920–1924, San Diego, California, 1999.

[19] J.D Bošković and R.K Mehra. Control allocation in overactuated aircraft under position and rate limiting. In *American Control Conference*, 2002.

[20] J.D. Bošković and R.K. Mehra. *Fault Diagnosis and Fault Tolerance for Mechatronic Systems: Recent Advances*. Springer-Verlag, 2002.

[21] S.P. Boyd, L. Ghaoui, E. Feron, and V. Balakrishnan. *Linear Matrix Inequilities in System and Control Theory*. 1994.

[22] D. Brire and P. Traverse. Airbus a320/a330/a340 electrical flight controls: A family of fault-tolerant systems. In *Digest of Papers FTCS-23 The Twenty-Third International Symposium on Fault-Tolerant Computing*, pages 616–623, 1993.

[23] J. Buffington. Tailless aircraft control allocation. In *AIAA Guidance, Navigation and Control*, pages 737–747, 1997.

[24] J. M. Buffington and D. F. Enns. Lyapunov stability analysis of daisy chain control allocation. *Journal of Guidance, Control, and Dynamics*, 19:1226–30, 1996.

[25] F.W. Burcham, C.G. Fullerton, and T.A. Maine. Manual Manipulation of Engine Throttles for Emergency Flight Control. Technical Report NASA/TM-2004-212045, NASA, 2004.

[26] J. A. Burton and A. S. Zinober. Continuous approximation of variable structure control. *International Journal of Systems Science*, 17(6):875–885, 1986.

[27] W. Cao and J. Xu. Nonlinear integral type sliding surface for both matched and unmatched uncertain systems. *IEEE Transactions on Automatic Control*, 49(8):1355–1360, 2004.

[28] F. Castanos and L. Fridman. Analysis and design of integral sliding manifolds for systems with unmatched perturbations. *IEEE Transactions on Automatic Control*, 51(5):853–858, 2006.

[29] J. Chang. Dynamic Output Integral Sliding-Mode Control With Disturbance Attenuation. *IEEE Transactions on Automatic Control*, 54(11):2653–2658, 2009.

[30] M.L. Corradini, G. Orlando, and G. Parlangeli. A fault tolerant sliding mode controller for accommodating actuator failures. In *44th IEEE Conference on Decision and Control*, 2005.

[31] J. Vasalek D. Ito, J. Georgie and D.T. Ward. Reentry vehicle flight controls design guidelines: Dynamic inversion. Technical Report 210771, NASA/TP, NASA, 2002.

[32] J.B. Davidson, F.J. Lallman, and W.T. Bundick. Real-time adaptive control allocation applied to a high performance aircraft. In *5th SIAM Conference on Control and Its Application*, 2001.

[33] C. Dorling and A. Zinober. Two approaches to hyperplane design in multivariable variable structure control systems. *International Journal of Control*, 44(1):65–82, 1986.

[34] G. Ducard. *Fault Tolerant Flight Control and Guidance Systems for a Small Unmanned Aeriel Vehicle*. PhD thesis, 2007.

[35] G. Ducard. *Fault-tolerant Flight Control and Guidance Systems: Practical Methods for Small Unmanned Aerial Vehicles, Advances in Industrial Control Series*. Springer, 2009.

[36] G. Ducard and H.P. Geering. Stability analysis of a Dynamic Inversion based pitch rate controller for an unmanned aircraft. In *IEEE/RSJ International Conference on Intelligent Robots and systems*, pages 360–366, Nice, France, 2008.

[37] G.A. Dumont and M. Huzmezan. Concepts, methods and techniques in adaptive control. In *Proceedings of the American Control Conference*, pages 1137–1150, 2002.

[38] W. C. Durham. Constrained control allocation. *Journal of Guidance, Control, and Dynamics,*, 16(4):717–25, 1993.

[39] C. Edwards, T. Lombaerts, and H. Smaili. *Fault Tolerant Flight Control: A Benchmark Challenge*, volume 399. Springer-Verlag, 2010.

[40] C. Edwards and S. Spurgeon. Sliding mode observers for fault detection and isolation. *Automatica*, 36:541–553, 2000.

[41] C. Edwards and S.K Spurgeon. *Sliding Mode control, Theory and Applications*. Taylor and Francis, 1998.

[42] C. Edwards, X. Yan, and S.K. Spurgeon. On the solvability of the constrained lyapunov problem. *IEEE Transactions on Automatic Control*, 52(9):1975–1981, 2007.

[43] J. Eterno, J. Weiss, D. Looze, and A. Willsky. Design issues for fault tolerant-restructurable aircraft control. In *24th IEEE conference on decision and control*, page 900905, 1985.

[44] J. Bin Y. Ming-Kai F. Yan-Ping, C. Yue-Hua. Fault tolerant control with on-line control allocation for flexible satellite attitude control system. In *2nd International Conference on Intelligent Control and Information Processing*, pages 42–46, 2011.

[45] J. Farineau. Lateral electric flight control laws of a civil aircraft based upon eigenstructure assignment technique. American Institute of Aeronautics and Astronautics, 89.

[46] L. Forssell and U. Nilsson. ADMIRE the aero-data model in a research environment version 4.0, model description. Techical report, Swedish defence Agency (FOI), 2005.

[47] L. Fraguela, L. Fridman, and V. Alexandrov. Output integral sliding mode control to stabilize position of a stewart platform. *Journal of the Franklin Institute*, 349:1526–1542, 2012.

[48] G.F. Franklin, J.D. Powell, and A. Emami-Naeini. *Feedback Control of Dynamics Systems*. Pearson Prentice Hall, 5th edition, 2006.

[49] P. Gahinet, A. Nemirovski, A. Laub, and M. Chilali. *LMI Control Toolbox, User Guide*. The MathWorks, 1995.

[50] S. Ganguli, A. Marcos, and G.J. Balas. Reconfigurable LPV control design for boeing 747-100/200 longitudinal axis. In *American Control Conference*, 2002.

[51] Z. Gao and P.J. Antsaklis. Stability of the pseudo-inverse method for reconfigurable control systems. *International Jounrnal of Control*, 53(3):717–729, 1991.

[52] T. Gonzalez, A. Moreno, and L. Fridman. Variable gain Super-Twisting sliding mode control. *IEEE Transactions on Automatic Control*, 57(6), 2012.

[53] M.T. Hamayun, C. Edwards, and H. Alwi. Integral Sliding Mode Fault Tolerant Control Incorporating On-line Control Allocation. In *IEEE Workshop on Variable Structure Systems*, pages 100–105, 2010.

[54] M.T. Hamayun, C. Edwards, and H. Alwi. Design and analysis of an integral sliding mode fault tolerant control scheme. *IEEE Transactions on Automatic Control*, 57(7):1783–1789, 2012.

[55] M.T. Hamayun, C. Edwards, and H.Alwi. Application of an Integral Sliding mode FTC for a Large Transport Aircraft. In *IEEE Conference on Control and Fault Tolerant systems*, pages 38–43, Nice, 2010.

[56] M.T. Hamayun, C. Edwards, and H.Alwi. An integral sliding mode augmentation scheme for fault tolerant control. In *IEEE American Control Conference*, pages 3772–3777, San Francisco, 2011.

[57] M.T. Hamayun, H.Alwi, and C. Edwards. An output integral sliding mode FTC scheme using control allocation. In 50*th IEEE Conference on Decision and Control and European Control Conference*, pages 2275–2280, Orlando, 2011.

[58] M.T. Hamayun, H.Alwi, and C. Edwards. An LPV fault tolerant control scheme using integral sliding modes. In *Proceedings of* 51st *IEEE Conference on Decision and Control*, 2012.

[59] O Harkegard. *Backstepping and Control Allocation for the applications of flight control*. PhD thesis, 2003.

[60] O. Harkegard and S.T Glad. Resolving actuator redundancy - optimal control vs. control allocation. *Automatica*, (41):137–144, 2005.

[61] R.K. Heffley and W.F. Jewell. Aircraft Handling Qualities. Technical Report 1004-1, System Technology Inc., Hawthorne, CA, May 1972.

[62] R.A. Hess and S.R. Wells. Sliding mode control applied to reconfigurable flight control design. *Journal of Guidance, Control and Dynamics*, (26):452–462, 2003.

[63] R. A. Horn and C. R. Johnson. *Matrix Analysis*. Cambridge, 1990.

[64] R. Isermann. Supervision, fault-detection and fault-diagnosis methods - an introduction. *Control Engineering Practice*, 5(5):639–652, 1997.

[65] R. Isermann and P. Ballé. Trends in the application of model-based fault detection and diagnosis of technical processes. *Control Engineering Practice*, 5(5):709–719, 1997.

[66] J.Chen and R. Patton. *Robust model-based fault diagnosis for dynamical systems*. Kluwer Academic Publshers, 1999.

[67] S. Bennani J.F. Magni and J. Terlouw. *Robust flight control: a design challenge*. Springer-Verlag, 1997.

[68] J. Jiang. Fault-tolerant control systems–an introductory overview. *Automatica SINCA*, 31(1):161–174, 2005.

[69] J. Jiang and Y. Zhang. Accepting performance degradation in fault-tolerant control system design. *IEEE Transactions on Control Systems Technology*, 14(2):284–292, 2006.

[70] J. Jiang and Q. Zhao. Design of reliable control systems possessing actuator redundancies. *Journal of Guidance, Control, and Dynamics*, 23(4):709–718, 2000.

[71] D. Joosten, T. van den Boom, and T. Lombaerts. Fault-tolerant control using dynamic inversion and model-predictive control applied to an aerospace benchmark. In *Proceedings of the 17th World Congress IFAC*, pages 12030–12035, Seoul, 2008.

[72] D.A. Joosten and J.M. Maciejowski. MPC design for fault-tolerant flight control purposes based upon an existing output feedback controller. In *Proceedings of the 7th IFAC Symposium on Fault Detection, Supervision and Safety of Technical Processes*, pages 253–258, Barcelona, Spain, 2009.

[73] B. Jung, Y. Kim, and C. Ha. Fault tolerant flight control system design using a multiple model adaptive controller. *Proceedings of the Institution of Mechanical Engineers, Part G: Journal of Aerospace Engineering*, 223:39–50, 2009.

[74] S. Kanev and M. Verhaegen. A bank of reconfigurable LQG controllers for linear systems subjected to failures. In *Proceedings of the 39th IEEE Conference on Decision and Control*.

[75] H.K. Khalil. *Nonlinear Systems*. Prentice Hall, 1992.

[76] A. Khelassi, J. Jiang, D. Theilliol, P. Weber, and Y. M. Zhang. Reconfiguration of control inputs for overactuated systems based on actuators health. In *18th IFAC World Congress*, pages 13729–13734, Milano, 2011.

[77] T. H. Khong and J. Shin. Robustness Analysis of Integrated LPV-FDI Filters and LTI-FTC system for a Transport Aircraft. In *AIAA Guidance, Navigation, and Control Conference and Exhibit, number AIAA 2007-6771*, 2007.

[78] J. Kim, I. Yang, and D. Lee. Accommodation of actuator faults using control allocation with modified daisy chaining. In *11th International Conference on Control, Automation and Systems*, pages 717–720, Korea, 2011.

[79] D. J. Leith and W. E. Leithead. Survey of gain-scheduling analysis and design. international journal of control. *International Journal of Control*, 73(11):10011025, 2000.

[80] A. Levant. Sliding order and sliding accuracy in sliding mode control. *International Journal of Control*, 58(6):1247–1263, 1993.

[81] G.P. Liu and R.J. Patton. *Eigenstructure Assignment for Control Systems Design*. Wiley, 1998.

[82] J. M. Maciejowski and C. N. Jones. MPC fault-tolerant flight control case study: Flight 1862. In *IFAC Symposium SAFEPROCESS*, pages 121–126, Washington DC, 2003.

[83] A. Marcos and G. Balas. Linear Parameter Varying Modeling of the Boeing 747-100/200 Longitudinal Motion. In *AIAA Guidance, Navigation and Control Conference, AIAA-01-4347,*, pages 1–11, 2001.

[84] A. Marcos and G. Balas. Development of linear-parameter-varying models for aircraft. *Guidance, Control and Dysnamics*, 27(2):218–228, 2004.

[85] A. Marcos and G. Balas. Development of Linear-Parameter-Varying Models for Aircraft. *Guidance, Control and Dysnamics*, 27(2):218–228, 2004.

[86] A. Marcos and G.J. Balas. A Boeing 747-100/200 aircraft fault tolerant and diagnostic benchmark. Technical report, Department of Aerospace and Engineering Mechanics, University of Minnesota, 2003.

[87] A. Marcos and G.J. Balas. A robust integrated controller/diagnosis aircraft application. *International Journal of Robust and Nonlinear Control*, 15:531–551, 2005.

[88] A. Marcos, J. Veenman, C. Scherer, G. Zaiacomo, D. Mostaza, M. Kerr, H. Koroglu, and S. Bennani. Application of LPV modeling, design and analysis methods to a re-entry vehicle. In *AIAA GNC/AFM/MST/ASC/ASE Conference*, page pages 118, 2010.

[89] D. Q. Mayne, J. B. Rawlings, C. V. Rao, and P. O. M. Scokaert. Constrained model predictive control: Stability and optimality. *Automatica*, 36:789, 2000.

[90] D. McLean and S. Mir. Reconfigurable flight control systems. In *Proceedings of International Conference on Control*, pages 234–242, 1991.

[91] T. Miksch, A. Gambier, and E. Badreddin. Real-time implementation of fault-tolerant control using model predictive control. In *17th IFAC World Congress*, pages 11136–11141, Seoul, Korea, 2008.

[92] S. Montes, V. Puig, M. Witczak, and L. Dziekan. Fault tolerant strategy for actuator faults using LPV techniques: Application to a two degree of freedom helicopter. *Journal of applied Mathematics and Computer Science*, 22(1):161–171, 2012.

[93] S.K. Mudge and R.J. Patton. Analysis of the technique of robust eigenstructure assignment with application to aircraft control. *Control Theory and Applications, IEE Proceedings D*, 135(4):275 –281, 1988.

[94] K. S. Narendra, O. A. Driollet, M. Feiler, and K. George. Adaptive control using multiple models, switching and tuning. *International Journal of Adaptive Control and Signal Processing*, 17:87–102, 2003.

[95] K. Nonami and S. Sivrioglu. *Variable structure systems, sliding mode and nonlinear control*, volume 247, chapter Sliding mode control with gain scheduled hyperplane for LPV plant, pages 263–279. Springer-Verlag, 1999.

[96] H. Noura, D. Sauter, F. Hamelin, and D. Theilliol. Fault-tolerant control in dynamic systems: application to a winding machine. *IEEE Control Systems magazine*, 20(1):33–49, 2000.

[97] K. Ogata. *Modern Control Engineering*. Prentice Hall, 4th edition, 2002.

[98] M. Oppenheimer, D. Doman, and M. Bolender. Control allocation for overactuated systems. In *14th IEEE conference on Control and Automation MED 06*, pages 1–6, 2006.

[99] A. Page and M. Steinberg. Closed-loop comparison of control allocation methods. In *Prodeedings of AIAA Guidance, Navigation and Control Conference*, pages 1760–1770, 2000.

[100] R.J. Patton. Fault tolerant control systems: The 1997 situation. In *Proceedings of the IFAC symposium SAFEPROCESS'97*, pages 1033–1054, 1997.

[101] R.J. Patton and S. Klinkhieo. LPV fault estimation and FTC of a two link manipulator. In *American control conference*, page 46474652, Baltimore, MD, 2010.

[102] H. E. Rauch. Intelligent fault diagnosis and control reconfiguration. *IEEE Control Systems Magazine*, pages 6–12, 1994.

[103] M. Rubagotti, A. Estrada, F Castanos, A. Ferrara, and L. Fridman. Integral sliding mode control for nonlinear systems with matched and unmatched perturbations. *IEEE Transactions on Automatic Control*, 56(11):2699–2704, 2011.

[104] E. Ryan and M. Corless. Ultimate boundedness and asymptotic stability of a class of uncertain dynamical systems via continuous and discontinuous control. *IMA Journal of Mathematical Control and Information*, 1:223–242, 1984.

[105] D. Shin, G. Moon, and Y. Kim. Design of reconfigurable flight control system using adaptive sliding mode control: actuator fault. *Proceedings of the Institution of Mechanical Engineers, Part G: Journal of Aerospace Engineering*, 219:321328, 2005.

[106] Y. Shtessel, J. Buffington, and S. Banda. Tailless aircraft flight control using multiple time scale re-configurable sliding modes. *IEEE Transactions on Control Systems Technology*, (10):288–296, 2002.

[107] S. Sivrioglu and K. Nonami. Sliding mode control with time-varying hyperplane for AMB systems. *IEEE/ASME Transactions on Mechatronics*, 3(1):51–59, 1998.

[108] S. Skogestad and I. Postlethwaite. *Multivariable Feedback Control Analysis and Design*. John Willey and sons, 1996.

[109] M. Smaili, J. Breeman, T. Lombaerts, and D Joosten. A simulation benchmark for integrated fault tolerant flight control evaluation. In *AIAA Modeling and Simulation Technologies Conference and Exhibit*, 2006.

[110] M. Staroswiecki. Fault tolerant control: The pseudo inverse method revisited. In *Proceedings of the 16th IFAC World Congress*, Prague, 2005.

[111] G.W. Stewart. *On scaled projections and pseudoinverses*, volume 112 of *Linear Algebra and its Applications*. 1989.

[112] S. Sun, L. Dong, C. An, and W. Liu. Fault-tolerant control design for linear systems with input constraints and actuator failures. In *CDC and CCDC conference*, pages 5278 – 5283, 2009.

[113] C.P. Tan and C. Edwards. Sliding mode observers for robust detection and reconstruction of actuator and sensor faults. *International Journal of Roabust and nonlinear control*, 13:443–463, 2003.

[114] G. Tao, S. M. Joshi, and X. Ma. Adaptive state feedback and tracking control of systems with actuator failures. *IEEE Transactions On Automatic Control*, 46(1):78–95, 2001.

[115] D. Theilliol, S. Aberkane, and D. Sauter. Fault tolerant control design for polytopic lpv systems. *International Journal of Applied Mathematics and Computer Science*, 17(1):2737, 2007.

[116] V. Utkin. Variable structure systems with sliding mode. *IEEE Transactions on Automatic Control*, Ac-22(2):212–222, 1977.

[117] V. Utkin. Sliding mode control. In A. Sabanovic, L.M. Fridman, and S. Spurgeon, editors, *Variable Structure Systems: from pronciples to implementation*, IEE Control Series 66, pages 3–17. IEE, London, 2004.

[118] V. Utkin, J. Guldner, and J. Shi. *Sliding Mode control in Electromechanical Systems*. Taylor and Francis, 1999.

[119] V. Utkin and J. Shi. Integral sliding mode in systems operating under uncertainty conditions. In *35th IEEE Conference on Decision and Control*, 1996.

[120] A. Vergas-Martinez, V. Puig, L. Garza-Castanon, and R. Morales-Menendez. MRAC+H_∞ fault tolerant control for linear parameter varying systems. In *Conference on Control and Fault tolerant Systems (SysTol)*, pages 94–99, Nice, 2010.

[121] M. Verhaegen, S. Kanev, R. Hallouzi, C. Jones, J. Maciejowski, and H. Smail. Fault tolerant flight control - a survey. In C. Edwards, T. Lombaerts, and H. Smaili, editors, *Fault Tolerant Flight Control*, volume 399 of *LNCIS*, pages 47–89. Springer, 2010.

[122] T.K. Vetter, S.R. Wells, , and R.A Hess. Designing for damage–robust flight control design using sliding mode techniques. *Proceedings of the Institution of Mechanical Engineers, Part G: Journal of Aerospace Engineering*, 217:245261, 2003.

[123] J. Wang, T. Lee, and Y. Juang. New methods to design an integral variable structure controller. *IEEE Transactions on Automatic Control*, 41(1):140143, 1996.

[124] X. Wei and M. Verhaegen. LMI solutions to the mixed $H2/H_\infty$ fault detection observer design for linear parameter-varying systems. *International Journal of Adaptive Control and Signal Processing*, 25(2):114–136, 2011.

[125] G. Welch and G. Bishop. An introduction to the Kalman Filter. Technical Report TR 95-041, University of North Carolina at Chapel Hill, 2006.

[126] S.R Wells and R.A Hess. Multi-input/multi-output sliding mode control for a tailless fighter aircraft. *Journal of Guidance, Control, and Dynamics*, 26(3):463–473, 2003.

[127] N. Wu, Y. Zhang, and K. Zhou. Detection, estimation, and accommodation of loss of control effectiveness. *Int.J.Adapt. Control Signal Process*, 14(7):775–795, 2000.

[128] J. Xu, Y. Pan, and T. Lee. Analysis and design of integral sliding mode control based on Lyapunov's Direct Method. In *Proceedings of the American Control Conference*, 2003.

[129] Z. Yang and J. Stoustrup. Robust reconfigurable control for parametric and additive faults with fdi uncertainties. In *Decision and Control, 2000. Proceedings of the 39th IEEE Conference on*, pages 4132–4137, 2000.

[130] A. Yetendji, M. Seron, and J. Dona. Robust MPC multicontroller design for actuator fault tolerance of constrained systems. In *18th IFAC World Congress*, pages 4678–4683, Milano, 2011.

[131] Y. Zhang and J. Jiang. Design of integrated fault detection, diagnosis and reconfigurable control systems. In *Proceedings of the IEEE Conference on Decision and Control*, pages 3587–3592, Phoenix, AZ, 1999.

[132] Y. Zhang and J. Jiang. Integrated Active Fault-Tolerant Control using IMM approach. *IEEE Transactions on Aerospace and Electronic Systems*, 37(4):1221–1235, 2001.

[133] Y. Zhang and J. Jiang. Bibliographical review on reconfigurable fault tolerant control systems. In *Proceedings of the IFAC Symposium SAFEPROCESS '03, Washington*, pages 265–276, 2003.

[134] Y. Zhang and J. Jiang. Fault tolerant control system design with explicit consideration of performance degradation. *IEEE Transactions on Aerospace and Electronic Systems*, 39(3):838–848, 2003.

[135] Y. Zhang and J. Jiang. Issues on integration of fault diagnosis and reconfigurable control in active fault-tolerant control systems. In *Proceedings of the IFAC Symposium SAFEPROCESS*, page 14371448, Beijing, China, 2006.

[136] Y. Zhang and J. Jiang. Bibliographical review on reconfigurable fault-tolerant control systems. *Annual Reviews in Control*, 32:229–252, 2008.

[137] Y. Zhang, V.S. Suresh, B. Jiang, and D. Theilliol. Reconfigurable control allocation against aircraft control effector failures. In *16th IEEE International Conference on Control Applications*, 2007.

[138] Y.M. Zhang and J. Jiang. Active fault tolerant control system against partial actuator failures. In *IEE Proceedings of Control Theory and Applications*, volume 149, pages 95–104, 2002.

[139] Q. Zhao and J. Jiang. Reliable tracking control system design against actuator failures. In *SICE '97. Proceedings of the 36th SICE Annual Conference. International Session Papers*, pages 1019–1024, 1997.

[140] Q. Zhao and J. Jiang. Reliable state feedback control systems design against actuator failures. *Automatica*, 34(10):1267–1272, 1998.